COLLETT, TIMOTHY SCOTT

DETECTION AND EVALUATION OF NATURAL GAS HYDRATES FROM WELL LOGS, PRUDHOE BAY, ALASKA

UNIVERSITY OF ALASKA M.S. 1983

DETECTION AND EVALUATION OF NATURAL GAS HYDRATES FROM WELL LOGS, PRUDHOE BAY, ALASKA

A

THESIS

Presented to the Faculty of the University of Alaska

in Partial Fulfillment of the Requirements

for the Degree of

MASTER OF SCIENCE

By

Timothy S. Collett, B.S.

Fairbanks, Alaska

May 1983

DETECTION AND EVALUATION OF NATURAL GAS HYDRATES

FROM WELL LOGS, PRUDHOE BAY, ALASKA

RECOMMENDED:

Chairman, Advisory Committee

Program Head or Department Head

Director, Division of Geosciences

APPROVED:

for Vice Chancellor for Research and Advanced Study

May 16, 1983
Date

ABSTRACT

The purpose of this study is to develop techniques for the detection and evaluation of in-situ gas hydrates from well log data and to determine possible geologic controls on the occurrence of hydrates in the North Slope region of Alaska.

Several new methods of evaluation for subsurface gas hydrate were developed and incorporated with existing techniques. For each of 125 wells examined as part of this study the geothermal gradient was determined and the theoretical stability zone for methane hydrate was calculated. Among these, there were 102 apparent hydrate occurrences in 32 wells.

A subsurface structural-stratigraphic framework was established to a depth of 1,000 meters. This sediment package is characterized by three deltaic depositional sequences.

The high frequency of hydrate occurrences in the structurally up-dip region of the Kuparuk Oil Field suggests that upward migration of free gas preceded hydrate development in the zone of hydrate stability.

TABEL OF CONTENTS

PAGE

LIST OF FIGURES

PAGE

LIST OF PLATES

ACKNOWLEDGEMENTS

I would like to sincerely thank Dr. G. Sharma, my committee chairman, for his guidance and assistance.

This study was supported by a grant from SOHIO Petroleum, made possible by M.H. Marfleet. P. Barker of ARCO Exploration ws very helpful in obtaining well log data and his suggestions and criticisms are gratefully acknowledged.

Keith Mather, Vice Chancellor for Research and Advanced Study, provided financial support during the initial stages of the research. The individual expertise of T. Osterkamp, C.A. Ehlig-Economides and D. Triplehorn was higly appreciated. To Dr. M.W. Payne go special thanks for the development of the original thesis topic.

I would like to thank Richard Veazey, Karen Lundquist and Janis Kara for their help in the preparation of the figures and the final draft.

INTRODUCTION

Objectives and Study Area

A major objective of this study was to develop new techniques for the detection and evaluation of in-situ natural gas hydrates in open hole well log surveys. In addition, new and existing techniques were to be combined in an attempt to identify in-situ natural gas hydrates in the Prudhoe Bay region of northern Alaska and to define their extent. A further objective was the recognition of possible geologic controls on the formation of in-situ natural gas hydrate.

The Prudhoe Bay and Kuparuk oil fields were selected as the study area because the high density of oil wells has provided an extensive data base in a region of potential hydrate stability. The geographic extent of the study area is shown in Figure 1.

Nature of Hydrates

Gas hydrates are crystalline compounds of water and gas in which the ice lattice accommodates the gas molecules in a cage like-structure. A gas hydrate can also be viewed as a solid solution with the water acting as a solvent. Hydrogen-bonded water molecules form a three dimensional shell whose voids can be filled with a wide array of gas molecules, such as methane, ethane and argon. For brevity, the natural gas hydrates will be referred to as gas hydrates or hydrate, which is simply defined as a gas and water mixture in the frozen state.

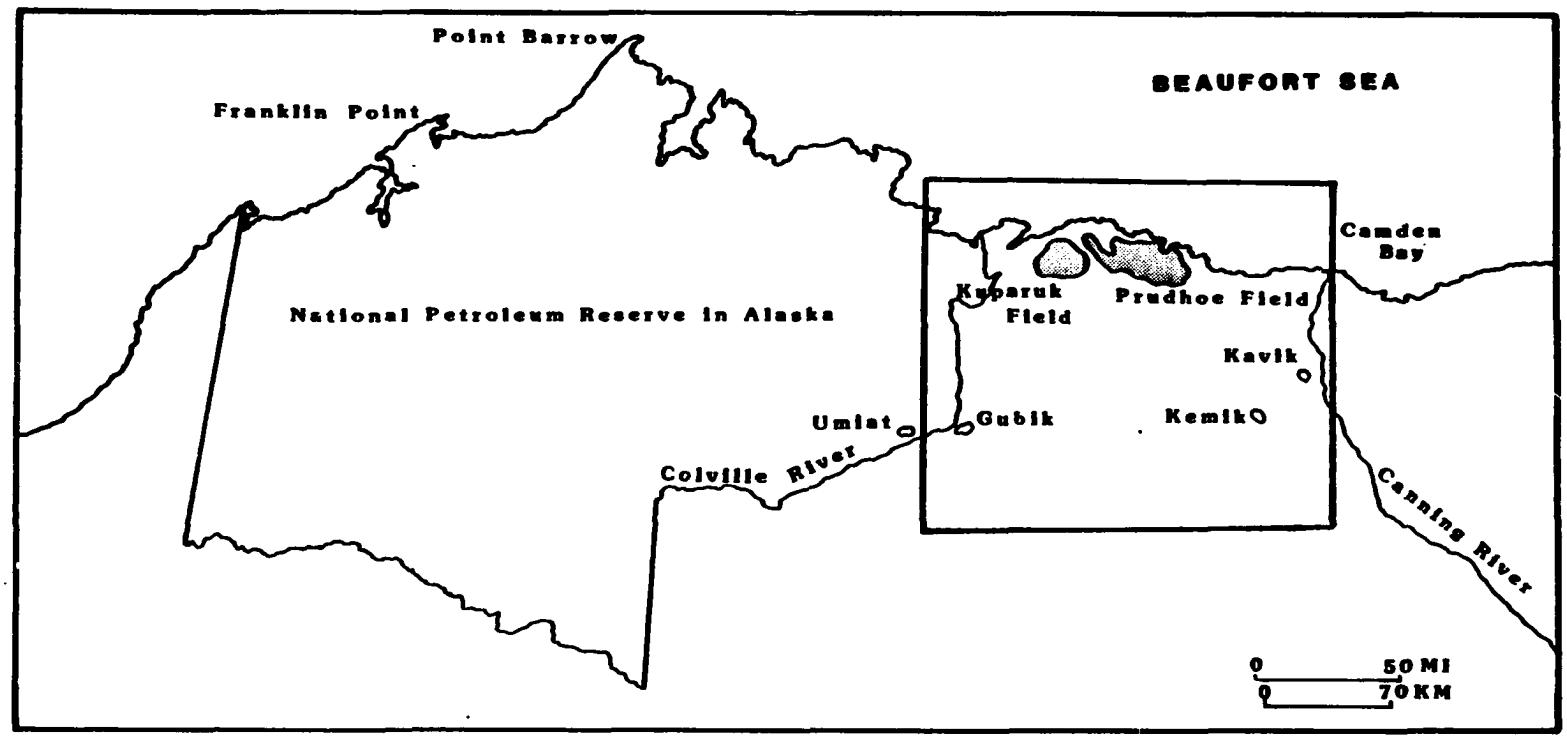

Figure 1-Map of the study area.

The structure of the ice-like framework or lattice depends on the shape and size of the gas molecules which are in contact with the water. The degree of gas saturation within the ice lattice is dependent on temperature and pressure. Typically, more than 90 percent of the available sites in the ice lattice are occupied in a pure methane hydrate.

Hydrates are characterized by two distinct structures known as Hydrate I and Hydrate II. Both hydrates have the same basic structure, a pentagonal dodecahedron. Each unit cell of Hydrate I consists of 46 water molecules which form two small dodecahedral voids and 6 large tetradecahedral voids. The structure of Hydrate I can only hold small gas molecules such as methane and ethane, with diameters not exceeding 5.2 angstroms. The composition of such a hydrate can be expressed as $8(Ar,CH_4,H_2S,CO_2,C_2H_6)46H_2O$ or $(Ar,CH_4,H_2S,CO_2,C_2H_6)\ 5.7H_2O$ (Mackogon, 1981).

The unit cell of Hydrate II consists of 16 small and 8 large voids formed by 136 water molecules, and only the large voids are gas filled. Hydrate II is characterized by gases with dimensions in the range of 5.9-6.9 angstroms, such as propane and isobutane. The composition of hydrate II can be expressed by the formula $8(C_3H_8,C_4H_{10},CH_2Cl_2,CHCl_3)136H_2O$ or $(C_3H_8,C_4H_{10},CH_2Cl_2,CHCl_3)\ 17H_2O$ (Mackogon, 1981).

The formation of hydrate occurs within a limited range of temperature and pressure conditions when sufficient concentrations of the appropriate gases, usually methane, are present (Figure 2). The pressure and temperature conditions suitable for the formation of hydrates occur in regions of permafrost and beneath the sea in outer continental margins and ocean basins (Kvenvolden et al., 1980). The fact that temperature and pressure conditions associated with permafrost

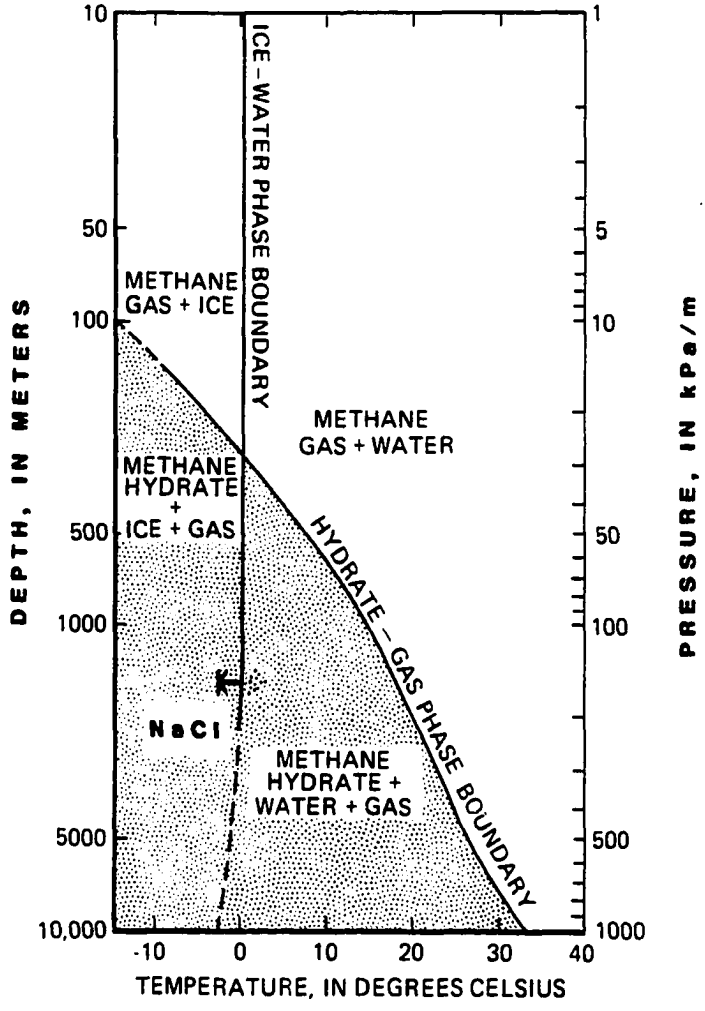

Figure 2-Methane hydrate phase diagram, showing free methane gas and methane hydrate stability fields for a fresh water-pure methane system. Addition of NaCl lowers temperature of the ice-water phase boundary and also lowers temperature of hydrate formation (Kvenvolden et al., 1980).

may fall within the stability field of gas hydrates was recognized by Katz (1945). Hydrates can occur not only in permafrost but also below the base of the permafrost at temperatures above the freezing point of water (Figure 2).

Significant quantities of gas hydrates have been detected in several permafrost regions of the world, including western Siberia, the Mackenzie Delta of Canada, and the North Slope of Alaska (Figure 3). For example, Mackogon (1981) cites a 1970 report that the Messoyakha Field in western Siberia has reserves in the billions of cubic meters of methane frozen as a hydrate. Studies in the Messoyakha Field showed that injections of methanol into the hydrate zones could increase the amount of recoverable gas by 54 percent above that expected in an equal volume of reservoir rocks filled with free gas.

Various mechanisms for hydrate formation have been postulated, as discussed by Pratt (1979). One theory suggests that gas hydrate could be part of a preexisting shallow gas reservoir, later frozen in place. It has also been suggested that a hydrate body could form by flow of free gas into a zone of methane hydrate stability where it becomes frozen (Pratt, 1979). Another theory states that migrating free gas might be trapped at the base of the permafrost and later frozen into hydrate. In addition, gas hydrates are sometimes found closely associated with decaying biomatter, such as coal, which might serve as a source for the methane needed for hydrate development.

There is a great deal of evidence to suggest that extensive gas hydrates exist in many areas beneath the deep seafloors (Kvenvolden et al., 1980). Drilling operations and seismic data have indicated that in-situ natural gas hydrates occur in deep sea sediments even in essentially tropical regions such as the Gulf of Oman and off the northern coast of Colombia and Panama.

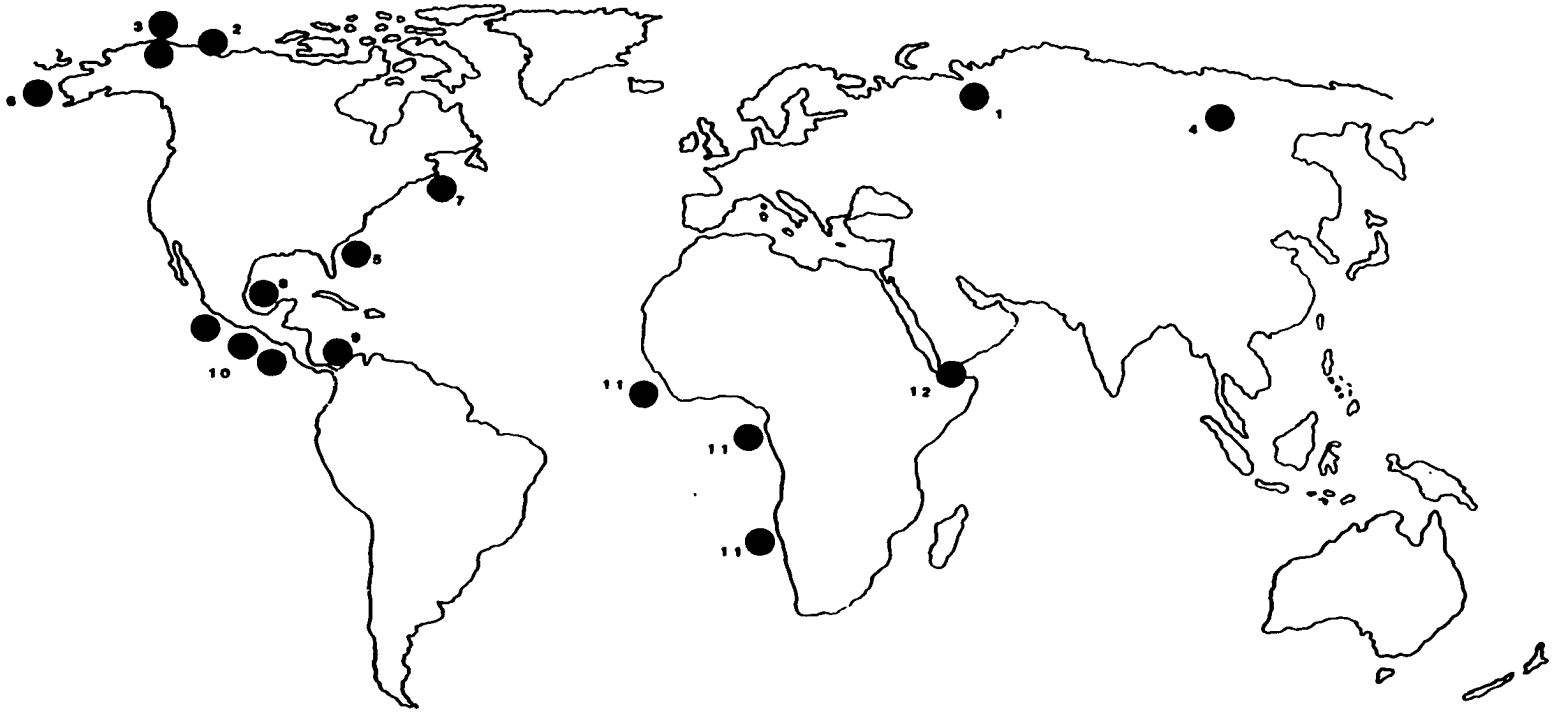

Figure 3-Known and inferred world accumulations of gas hydrate, 1-Messoyakha Field, 2-Mackenzie Delta, 3-North Slope, 4-Vilyuy Basin, 5-Blake Ridge, 6-Bering Sea, 7-North Atlantic, 8-Gulf of Mexico, 9-Colombian Coast, 10-Central America, 11-Western Africa, 12-Gulf of Oman (Kvenvolden et al., 1980).

Previous Work

Frank Howitt (1971) published "Permafrost Geology at Prudhoe Bay", the first and only paper to date describing the upper strata at Prudhoe Bay. He correlated 20 horizon markers identified from the gamma ray logs for the upper 610 meters (2,000 feet) of strata and developed a series of stratigraphic cross sections and isopach maps. Howitt concluded that the main stratigraphic unit is the Sagavanirktok Formation. It lies beneath a thin surface of gravel and was deposited in a steadily subsiding basin, probably during the Miocene. Howitt (1971) suggested that during the deposition of the Sagavanirktok Formation the mean annual temperature was 12°C warmer than the present -9°C (Lachenbruch et al., 1969)

Howitt (1971) described in detail the structural-stratigraphic framework developed from the gamma ray logs. He observed that the Sagavanirktok Formation is characterized by a gentle dip to the north-east, ranging from 20 meters per kilometer to 28 meters per kilometer. In two wells Howitt was able to correlate the gamma ray surveys with well cores to a depth of 300 meters. These cores were characterized by four recurring rock types. Most abundant was poorly-graded well-sorted sand while the dense silt dominated several thick units, and included a great deal of potash-bearing clay minerals. A very small amount of silty sand was recorded and well-graded gravel occurred in small quantities. The mineralogy of individual grains and pebbles includes mostly quartz, quartzite, and chert, with lesser quantities of limestone, limey mud, coal and shale fragments and a trace of talc. All these constituents are from the erosion of the Brooks Range hinterland. According to Howitt, the sediment fabric of the upper strata in

Prudhoe Bay indicates deposition more or less continuously in an aqueous environment. Howitt also suggests that the climate during deposition was temperate, judging from the thickness of the poorly sorted sand units and the angularity of their grains, indicative of high rainfall and swift streams.

The earliest significant studies of gas hydrates occurred in the 1930's when gas hydrates were found in natural gas transmission lines (Kvenvolden et al., 1980). In general, however, the study of in-situ natural gas hydrates has been relatively limited and only several preliminary studies have been published. Bily and Dick (1974) provided the most comprehensive study to date on the detection of in-situ natural gas hydrates. They used well logs, including the dual induction, sonic and mud logs, as potential detection devices for hydrate. Published evidence of the existence of gas hydrates in the Prudhoe Bay region itself is limited to the work of Kvenvolden et al., (1980) and Osterkamp and Payne (1981).

Regional Geology

The primary sedimentary units of concern here were deposited in the Late Cretaceous and Tertiary; they will be described in detail later. Early Cretaceous sediments on the North Slope reflected uplift of the Brooks Range and attendant deposition in a marine basin along the north flank of the range. Sediments that filled this marine basin demonstrate a lateral change from deep to shallow water deposition. Those deposited during the Early Cretaceous include the Torok Formation and Nanushuk Group. Shallow marine Torok shales are succeeded by two river-dominated deltaic sequences of the Nanushuk Group prograding to the north-east.

Post-Nanushuk deposits in northern Alaska are confined to the coastal plain and northern foothills of the central and eastern Arctic Slope. No Late Cretaceous or Tertiary rocks are known on the Arctic Slope west of Point Barrow (Ahlbrandt, 1979). In general, the areal distribution of Tertiary and Late Cretaceous Rocks relative to the distribution of the Early Cretaceous Rocks seems to reflect a continuation of the eastward and northward progradation noted in the Early Cretaceous (Mull, 1979).

Methods of Investigation

To achieve the objectives described earlier it was first necessary to develop a detailed-structural stratigraphic framework for the upper 1,000 meters of strata. Lithologic descriptions of these units based on gamma ray logs were developed and correlated with core samples.

New techniques for the identification of hydrates from well log data were developed and combined with existing methods. Next, the geothermal gradient was calculated for each well and combined with an assumed hydrostatic pressure gradient and a known ground temperature to calculate the thickness of the zone of potential hydrate occurrence.

The remainder of the study dealt with the identification of in-situ natural gas hydrates and the correlation of hydrate occurrences with the structural-stratigraphic framework developed in the study. The frequency and size of the gas hydrate accumulations in the geologic framework was examined in an attempt to assess possible geologic controls on the formation and occurrence of the hydrate.

STRATIGRAPHY

This section is divided into two major parts. The first half, Structural-Stratigraphic Framework, begins with a detailed discussion of stratigraphic relations on the North Slope described by Bird (1982) and concludes with a description of the stratigraphic framework developed within this study. The other half of the stratigraphy portion consists of a detailed description of the depositional environments existing during the Late Cretaceous and Tertiary on the Arctic Slope.

Structural-Stratigraphic Framework

The primary stratigraphic units of concern here range in age from Quaternary to Late Cretaceous. The Quaternary deposits occur as a single formation, the Gubik, a thin mantle of very coarse gravel less than 50 meters thick. The Gubik unconformably overlies the Tertiary Sagavanirktok Formation.

The Sagavanirktok Formation was defined by Gryc et al., (1951) as a marine deposit of shale, sandstone, conglomerate, mudstone and siltstone. Detterman et al., (1975) included within the Sagavanirktok Formation all the beds above the top of the Late Cretaceous Prince Creek Formation of the Colville Group and below the Quaternary Gubik Formation. Because of the uncertainty of the lateral extent of the poorly described lithologic units of the Sagavanirktok Formation, it was redefined by Bird (1982) with a set of informal terms that were descriptive and not acceptable as formation names. Tertiary and Cretaceous stratigraphic relations, including both formal and informal nomenclature, are summarized in

Figure 4.

The "Sagavanirktok-Colville undifferentiated" of Bird (1982) includes all strata assigned to the Colville Group and to the Sagavanirktok Formation. The age is Late Cretaceous and Tertiary and it consists of two parts; an upper "Sagavanirktok-Colville sandstone", and a lower "Colville Group shale".

The "Sagavanirktok-Colville sandstone" consists of interbedded sandstone, shale, coal and conglomerate. The upper boundary is placed at the base of the surficial Gubik deposit, the lower boundary at the base of the lowest continuous sandstone overlying a thick shale section. In Prudhoe Bay, "Sagavanirktok-Colville sandstone" is Late Cretaceous and Tertiary in age and includes the Sagavanirktok Formation and the Colville Group sandstone of Pessel et al., (1978).

The "Colville Group shale" represents the lower shale portion of the "Sagavanirktok-Colville Undifferentiated" (Pessel et al., 1978; Bird, 1982). The "Colville Group shale" near the mouth of the Canning River is Late Cretaceous and Tertiary in age.

A structural-Stratigraphic framework based on 32 key markers picked from gamma ray logs has been established to a depth of 1,000 meters. Each marker represents an abrupt lithologic change that produces a notable response on petrophysical logs; it has no significant thickness. The 32 markers are laterally persistent and were used to define the upper and lower boundaries of 31 stratigraphic units. A lithologic description of each unit was subsequently prepared from gamma ray logs in combination with three complete sets of drill core chips and four petrographic strip logs. Because resistivity and sonic transit time in permafrost are variable, the gamma ray log serves as the only wire line tool available for distinguishing between various lithologies in these upper units.

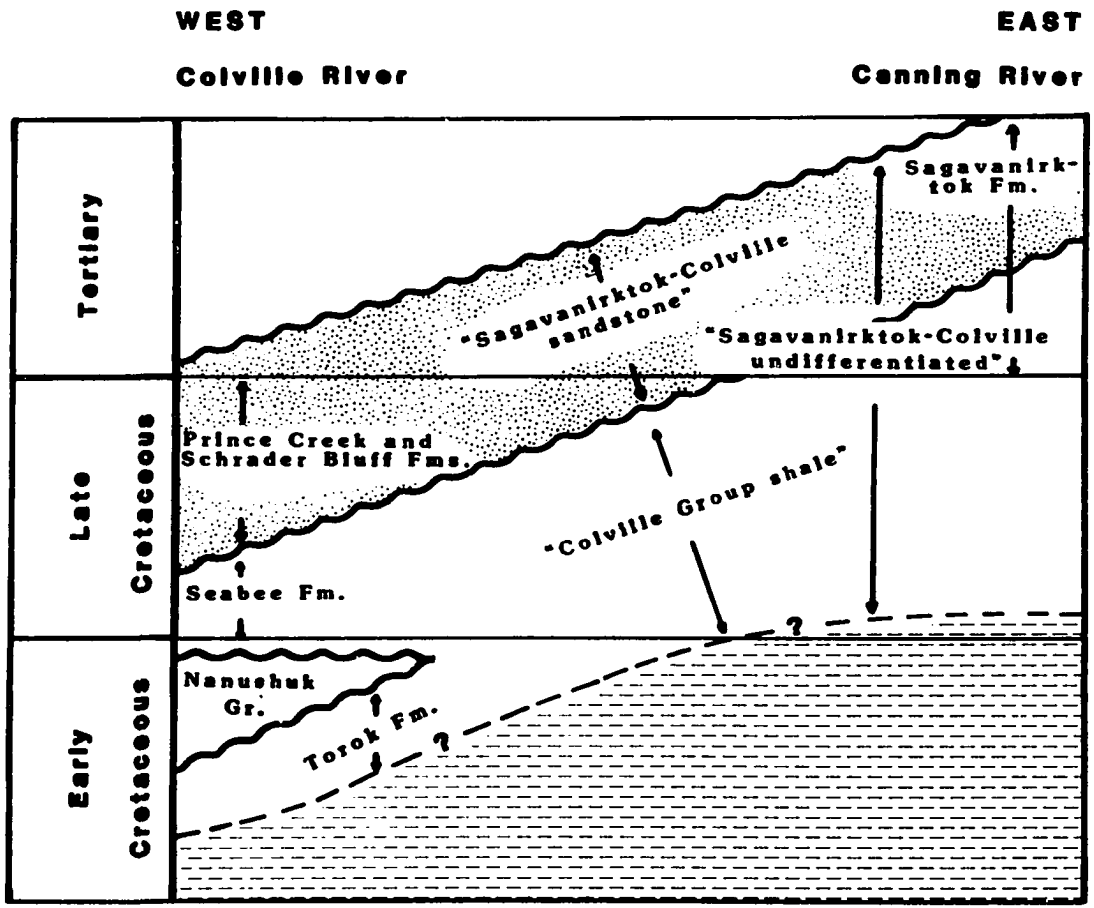

Figure 4-Cross section showing generalized Tertiary and Cretaceous stratigraphic relations and nomenclature, for the Coastal Plain Province and eastern half of the North Slope (Bird, 1982).

One-hundred and twenty-five gamma ray well surveys were correlated to develop the structural framework. Tracing of key markers within the Prudhoe Bay Field itself was not difficult, due to the high well density. However, correlation of markers from the Prudhoe Bay Field to the outlying areas of lesser well control toward the Umiat and Kavik fields proved to be very difficult.

Shown in Figure 5 is a northeast-southwest cross section from Niakuk Island through the center of the Prudhoe Bay Field and ending near the Umiat Field more than 100 kilometers to the south-west. Key stratigraphic markers defined from the gammy ray logs are shown by the numbers, (1, 6, 12, 19, 21 and 26), along with core descriptions and inferred environments of deposition.

The upper 1,000 meters of strata at Prudhoe Bay is characterized by a gentle dip to the north-east, ranging from 20 to 28 meters per kilometer, and is dominated by three large-scale coarsening-upward deltaic sequences, as described later. Marker 21, as used within the present study, coincides with the base of the "Sagavanirktok-Colville sandstone" as described by Bird (1982).

Depositional Environment

The existence of three large-scale coarsening-upward sequences suggests a series of three deltaic systems, each sequence prograding laterally to the north-east. The lateral consistency and broad geographic extent of each unit defined within the stratigraphic framework suggest that deposition took place in a low relief semi-submersed deltaic system, with sea level relatively constant for a long time.

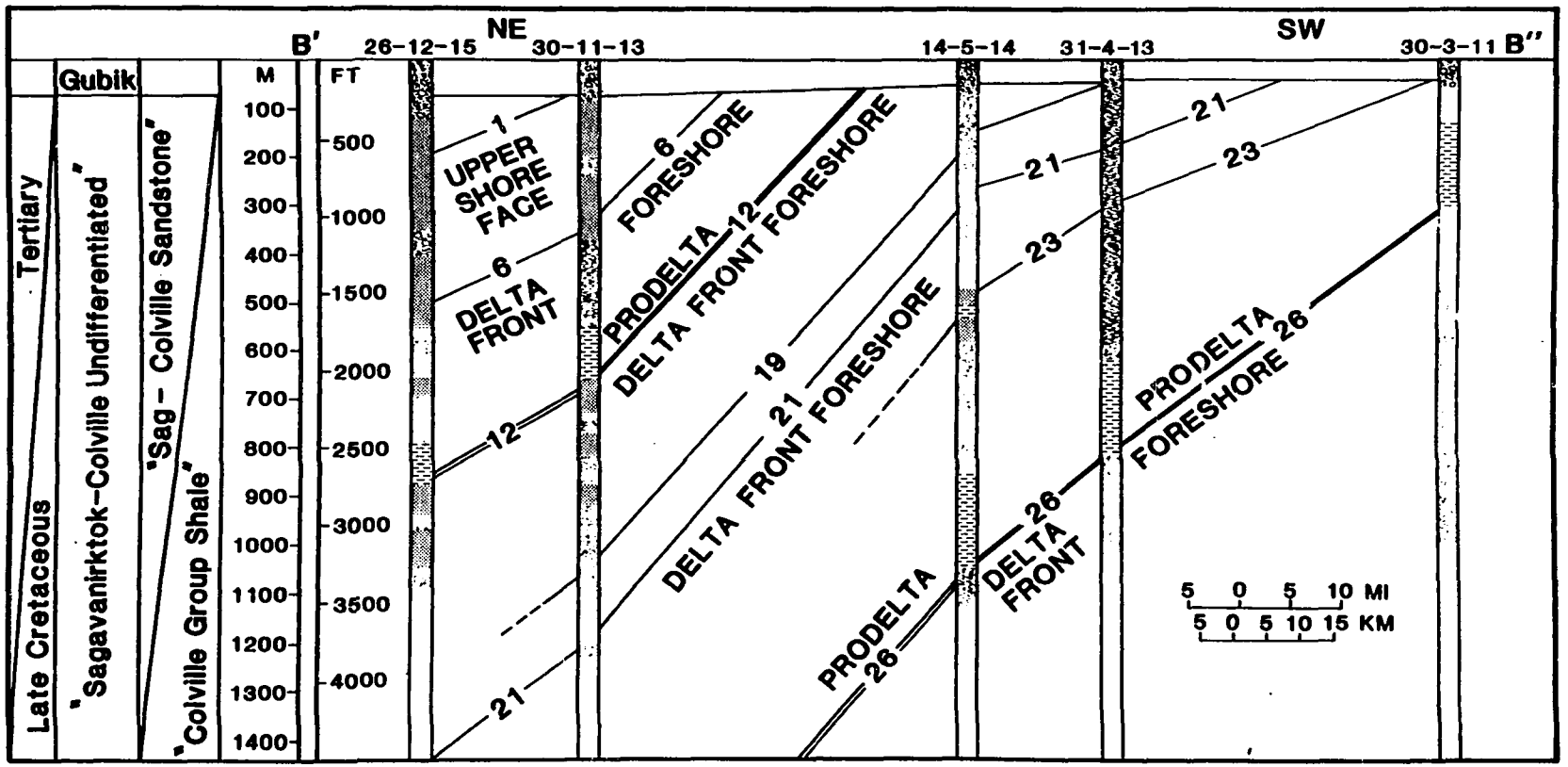

Figure 5-North to south cross section from Niakuk Island to the Umiat Oil Field, along with core descriptions shown by lithologic symbols.

The Late Cretaceous and Tertiary depositional history can be best interpreted from the generalized stratigraphic cross section in Figure 5 and the detailed, local lithologic sections in figures 6, 7, 8 and 9. These figures show lithologic sections from four different wells in the Prudhoe Bay region (locations shown on Plate 1). Each well was selected to represent part of the sequence of 31 units defined by the gamma ray logs; however, there is some overlap. For each section the depth to markers and unit thicknesses are given, along with a description of dominant grain sizes and rock type for every unit. The letters A (youngest) through FF (oldest) have been used to denote the different units, and the horizon markers have been numbered from 1 to 32. Also presented in figures 6, 7, 8 and 9 are inferred environments of deposition as interpreted from well log data, cuttings, and cores. The three deltaic sequences described earlier can be seen as three large-scale coarsening-upward sequences in the four lithologic sections.

The three deltaic sequences also can be identified in the cross section in Figure 5. At Marker 26 in Figure 5 there is an abrupt change in grain size, denoting a facies change from a medium size sand of a deltafront foreshore deposit to that of an overlying prodelta shale, dominated by clays and silt. The lowest delta front foreshore deposit represents the oldest of the three delta sequences noted previously; it will be referred to here as Delta I. The prodelta shale above Marker 26 grades upward into the relatively clean sand of a delta front foreshore environment at Marker 12, representing the beginning of the second deltaic sequence (Delta II). This relatively large-scale coarsening-upward sequence records the passage from a fine grained offshore prodelta depositional facies upwards into a delta front foreshore facies dominated by sand size

Figure 6-Lithologic section from Kemik Number Two, with grain size and inferred environments of deposition (6-1-21).

Key:


shale


conglomerate


sandstone


sandstone & shale

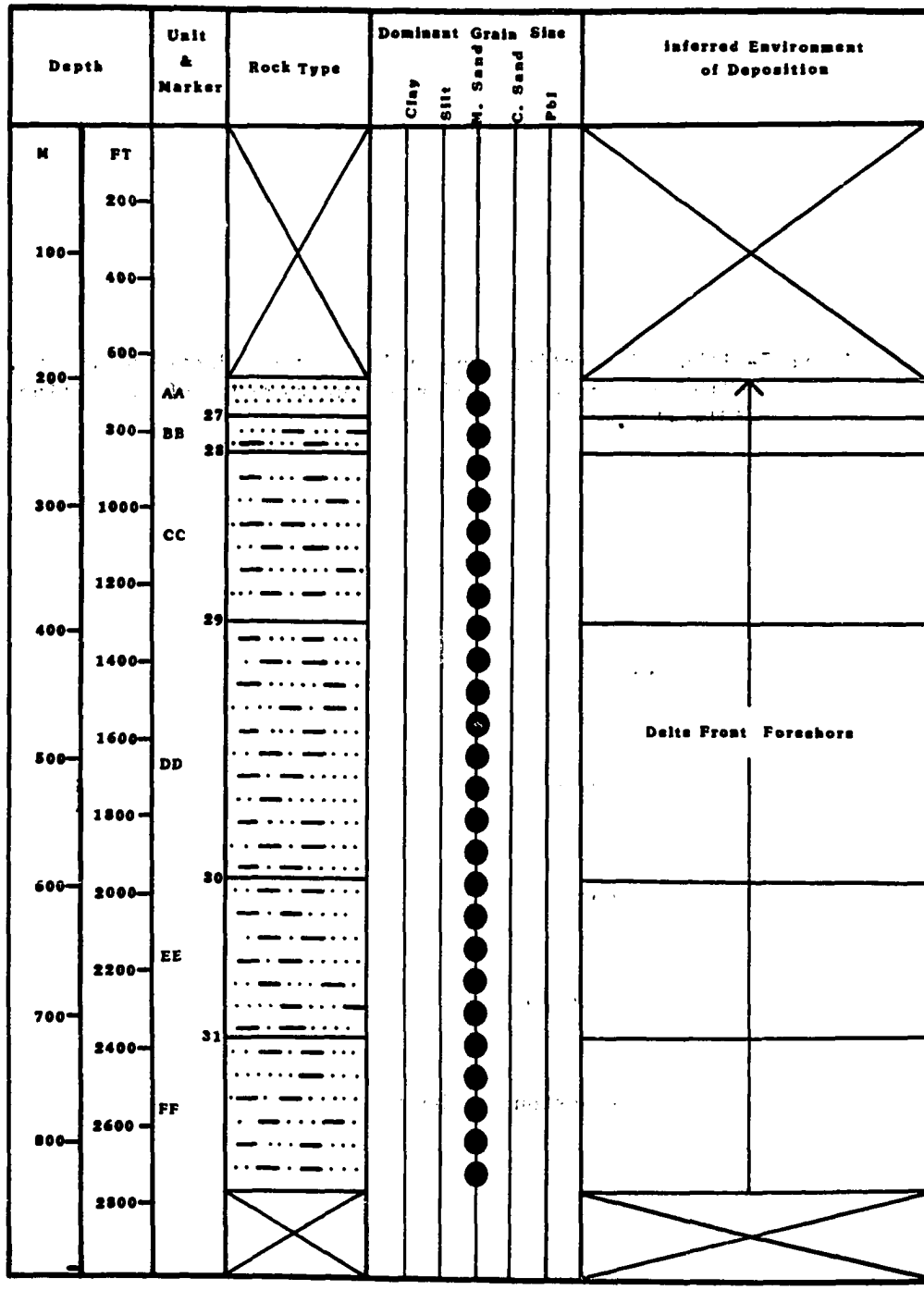

Figure 7-Lithologic section from Bush Federal Federal Number One, with grain size and inferred environments of deposition (31-4-13).

Key:


shale


conglomerate


sandstone


sandstone & shale

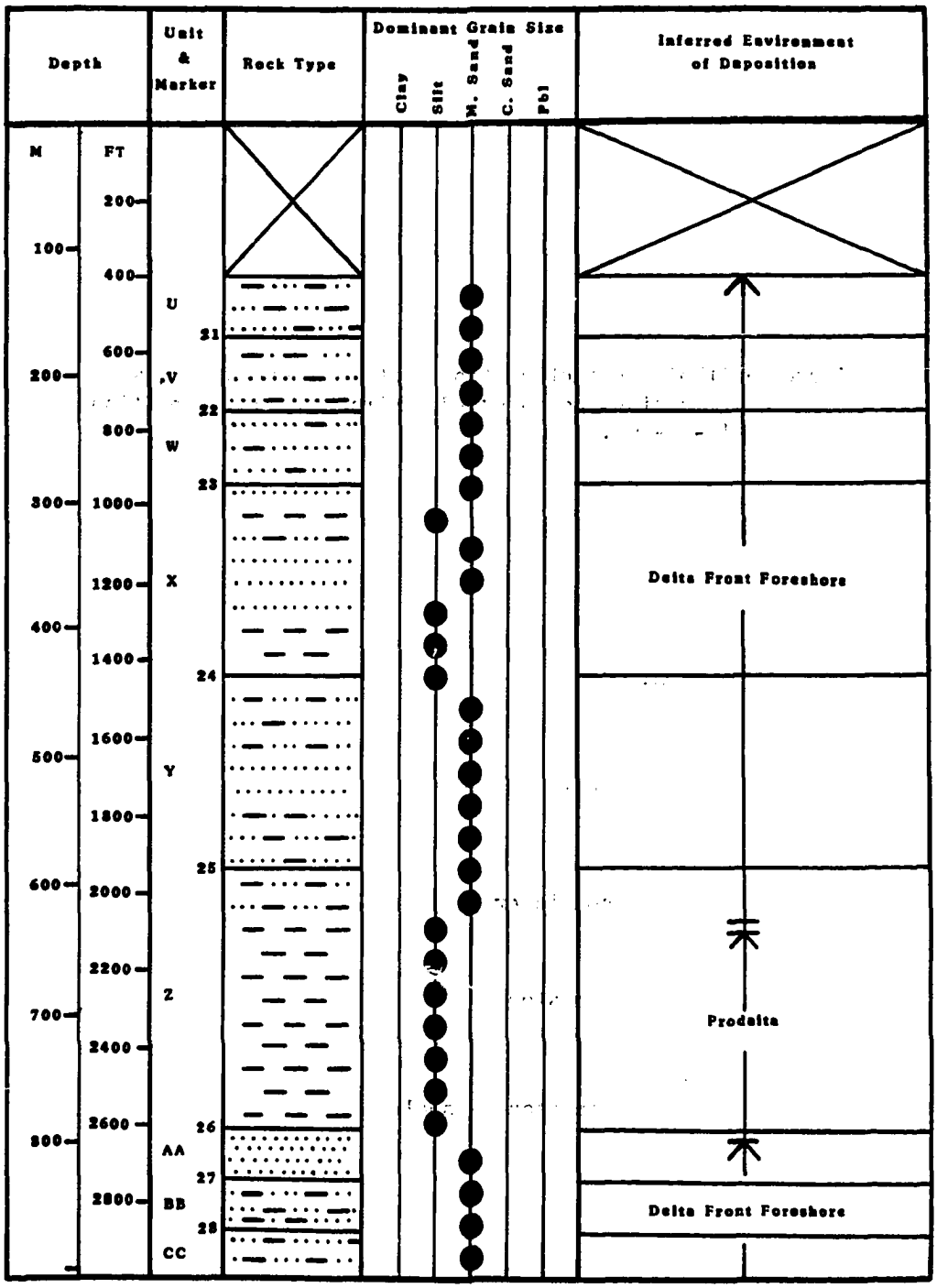

Figure 8-Lithologic section from East Egnu Number One, with grain size and inferred environments of deposition (17-12-10).

Key:


shale


conglomerate


sandstone


sandstone & shale

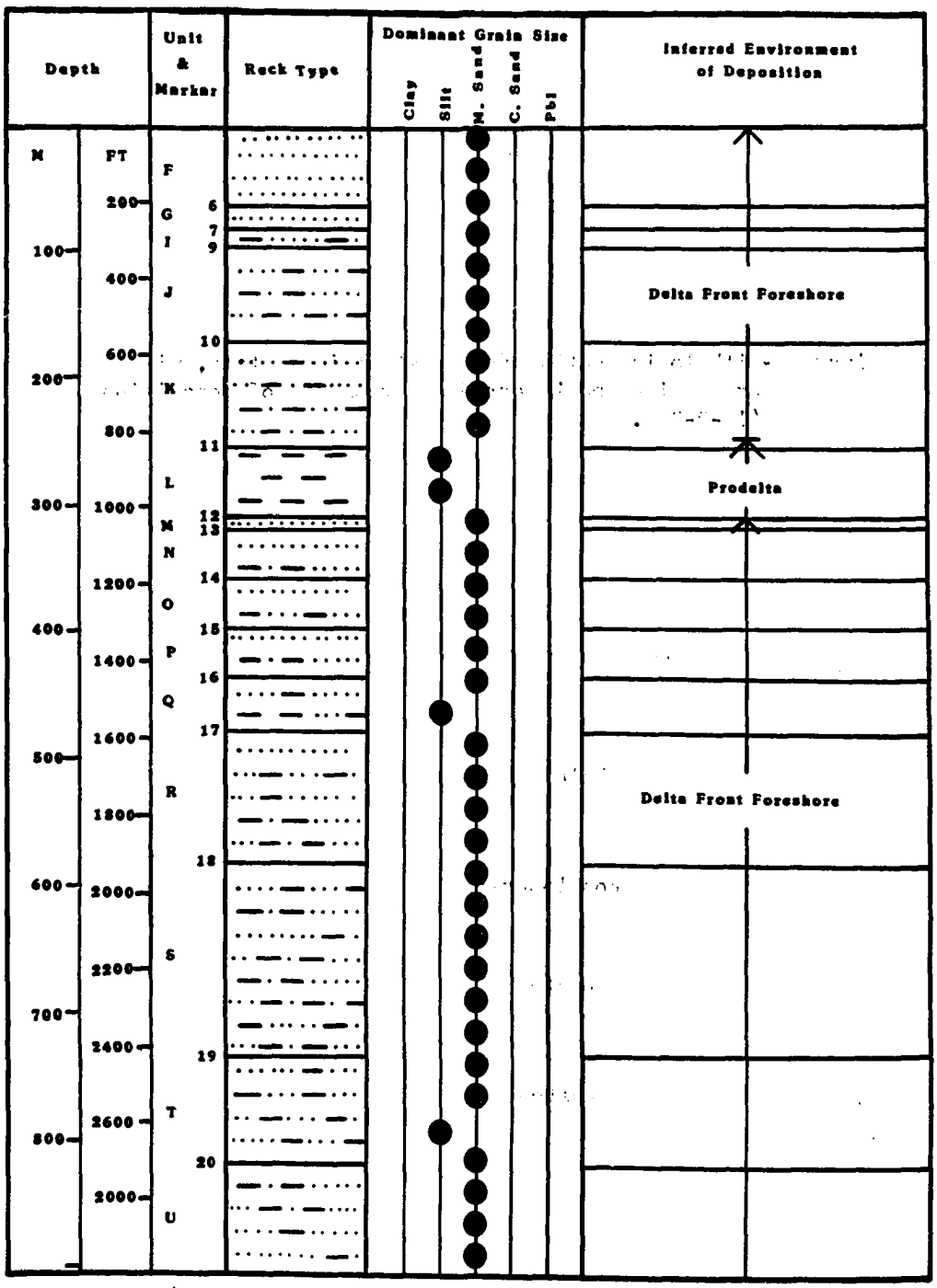

Figure 9-Lithologic section from West Staines State, with grain size and inferred environments of deposition (18-9-23).

Key:


shale


conglomerate


sandstone


sandstone & shale

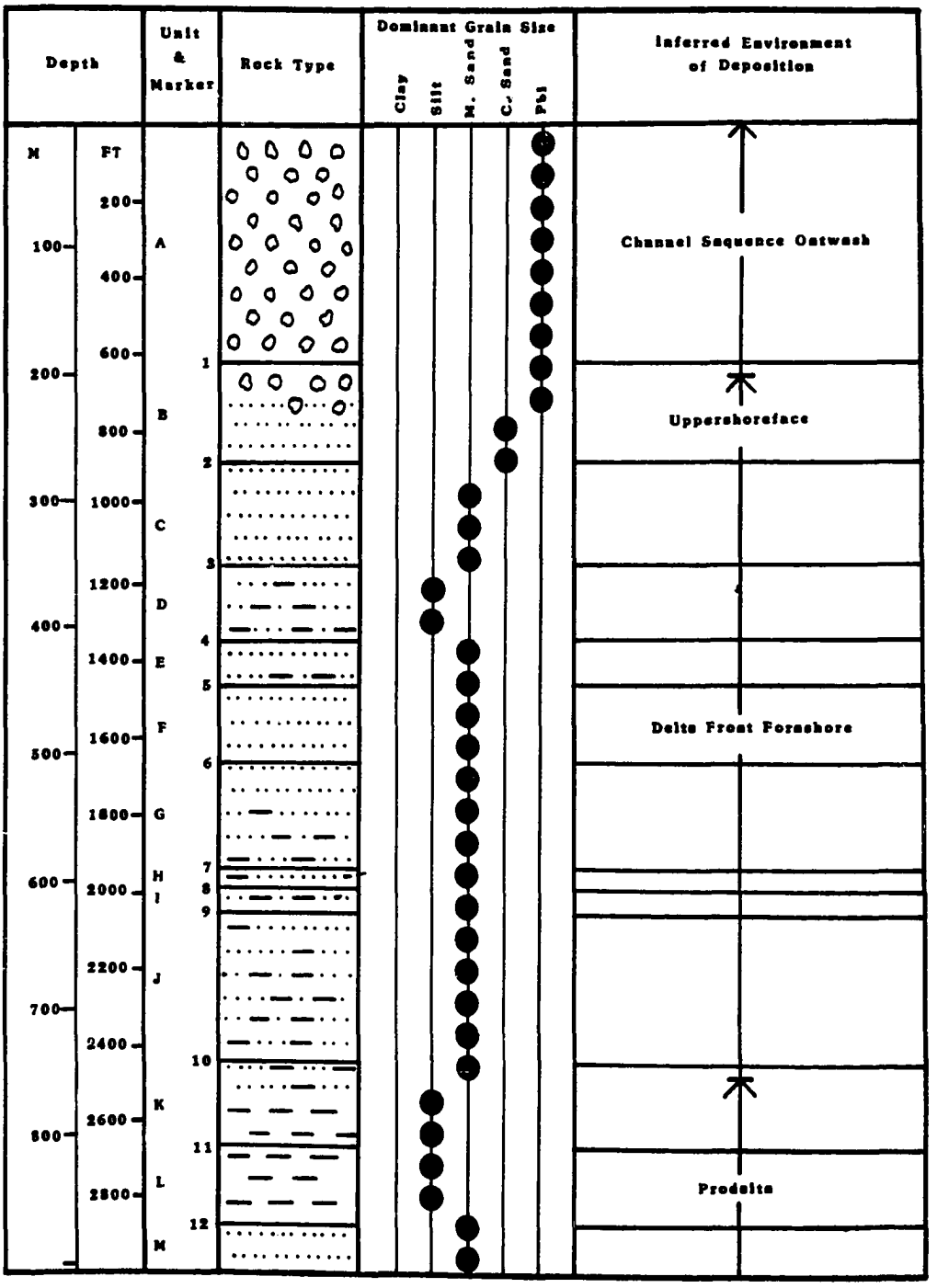

particles. The sand of the delta front deposit below Marker 12 is characterized by medium size sand grains, and is dominated by abundant chert clasts. Between markers 19 and 12 there appear to be several fluctuations in the depositional pattern, marked by interbeds of sand and shale.

Capping the clean sands at Marker 12 is another prodelta shale which in turn coarsens-upward into a coarse clean sand and gravel of an upper-shoreface deposit (Delta III). This is the uppermost part of the exposed Cretaceous-Tertiary sequence. It is overlain by a thin layer of Quaternary Gravel of the Gubik Formation, apparently a fluvial channel deposit.

Further evidence of deltaic deposition appears in the isopach map of unit P (Figure 10), where a prominant feature extending to the north-east can be interpreted as a prograding deltaic lobe. A similar interpretation can be made from the series of three isopach maps shown in Plate 6.

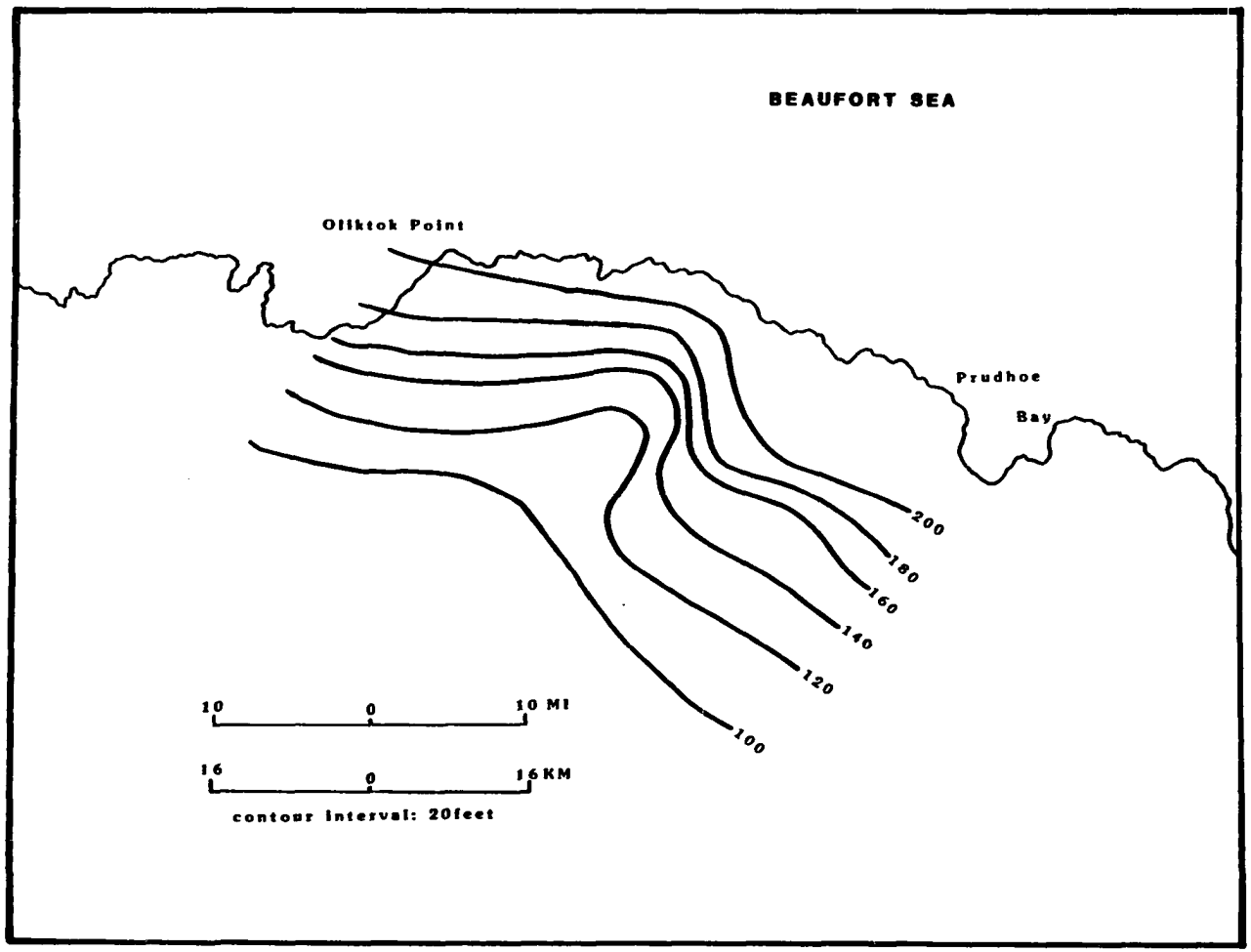

Figure 10-Isopach map of unit P.

CONSIDERATIONS FOR HYDRATE OCCURRENCE

Gas hydrates exist under a relatively limited range of temperature and pressure and only when sufficient concentrations of gas and water are present. The depth and thickness of the zone of potential hydrate stability can be calculated if the extrapolated mean annual temperature, geothermal gradient, hydrostatic pressure gradient and gas density are known.

Determination of the theoretical zone for potential hydrate occurrence establishes constraints on which wells should be studied and on the range of depths that should be examined for each well. In addition, it will be shown later that understanding the theoretical limits on the hydrate formation depths leads to certain conclusions regarding the mechanisms for the original formation of the gas hydrates.

In this section, the parameters necessary for establishing the theoretical hydrate occurrence zone are examined in detail. Previous definitions of the theoretical hydrate stability field are refined to take into account more accurate data on the geothermal gradients and the shallow depth limit of the stability zone.

The presence of biodegradable material such as coal and a number of methane gas shows on the mud logs, as well as detailed gas analysis from drill stem tests, all suggest that methane is the most common gaseous component to be expected in the upper units of Prudhoe Bay. The methane hydrate stability curve needed to calculate the thickness of the zone of potential hydrate development has been defined and described by many investigators (e.g.; Katz, 1971; Bily and Dick, 1974). The methane hydrate stability curve was originally developed many years ago in laboratory studies on clathrate development in gas transmission lines

(Kvenvolden et al., 1980).

The geothermal gradient needed to predict the thickness and the depth to the base of the hydrate stability zone is not easily obtained. Lachenbruch et al., (1982) observed four geothermal gradients from different bore holes along the Alaskan Arctic Coast. The lowest geothermal gradient was 1.6°C/100m (.9°F/100 ft.) at Prudhoe Bay. The highest gradient was 3.3°C/100m (1.8°F/100 ft.) at Cape Simpson. Two intermediate gradients of 2.0°C/100m (1.1°F/100 ft.) and 2.3°C/100m (1.2°F/100 ft.) were recorded at Cape Thompson and Point Barrow, respectively (Lachenbruch et al., 1982). These geographic differences in the geothermal gradients are due to differences in subsurface lithology which in turn alters the thermal conductivity. Because geothermal gradients vary laterally in the Prudhoe Bay region, an average regional gradient cannot be used to calculate the thickness of the zone of potential hydrate occurrence at every location.

A new method had to be developed to measure local geothermal gradients to permit calculation of the thickness of the zone of potential hydrate occurrence with precision. This method involves calculation of an individual geothermal gradient for each well, where depth to the base of permafrost is known and temperature at the interface is assumed to be -1°C with an error of ±.5°C (Lachenbruch et al., 1982). Lachenbruch et al., (1982) noted that the recorded geothermal gradients in the Prudhoe Bay region change abruptly at a depth of about 600± 20 m, where the temperature is approximately -1°C. Lachenbruch et al., believed that this distinct change in the geothermal gradient was due to a discontinuity in the thermal conductivity where pores filled with ice above 600 m changed to pores filled with water below 600 m. This ice/water interface is the base of the permafrost (Figure 11).

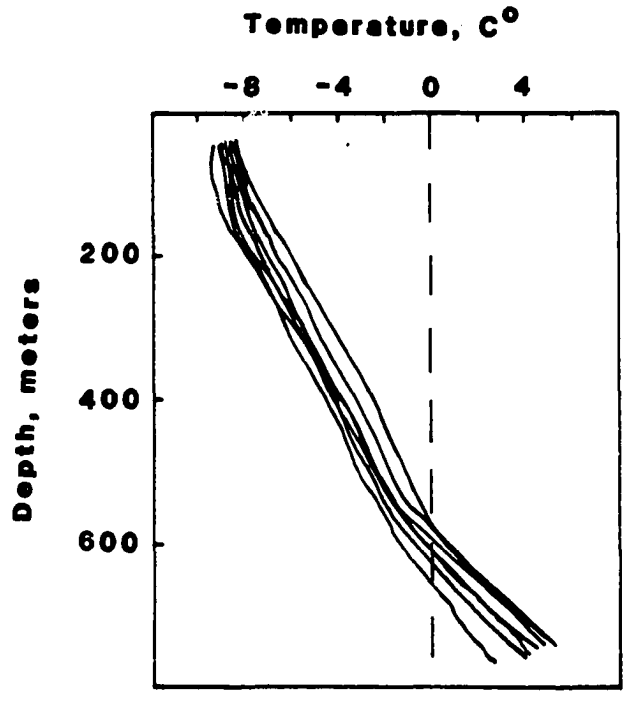

Figure 11-Geothermal gradient profiles from seven holes in Prudhoe Bay, showing gradient change at the base of the permafrost at 600 ± 20m (Lachenbruch et al., 1982).

Formerly, the base of the permafrost was assumed to be in equilibrium at $0^{o}C$, but due to freezing point depression the interface is now believed to be at equilibrium at $-1^{o}C$ with an error of $\pm.5^{o}C$ (Lachenbruch et al., 1982). Freezing point depression is related to several factors that may affect the thermal stability of the phase boundary. These factors include the presence of salt ions in solution, the existence of freeze-back pressure, and variations in the types of solids and fluid saturation levels.

The factors producing freezing point depression are additive and are expressed in the following equation, as stated by Osterkamp and Payne (1981).

$$T_o=0.0100-T_p-T_c-T_s\ ^{o}C$$

The first term T_o represents equilibrium temperature at the base of the permafrost, 0.0100 stands for the triple point of water and T_p, T_c and T_s are the temperature corrections for pressure, chemical composition, and soil particle effects: in this equation air saturation of sub-permafrost water is neglected. Pressure effects (T_p) on the equilibrium of the ice and water phase boundary are assumed to be related to hydrostatic pressure at a given depth, and can be calculated from the following equation, in which B is the Clausius-Clapeyron slope ($0.00751^{o}C\ atmos^{-1}$).

$$T_p = BP$$

The assumption that P represents the hydrostatic pressure at the base of the permafrost is thought to be valid for the North Slope (Osterkamp and Payne, 1981). However, dissociation of a gas hydrate at the base of the permafrost can raise in-situ pressure above normal hydrostatic pressure (Perkins et al., 1974), directly affecting the thermal equilibrium of the permafrost.

The temperature correction for solute concentrations in soil pore water is represented by the term T_c. The predominant salt in the pore water of the North Slope is assumed to be NaCl (Osterkamp and Payne, 1981). If salt concentrations are known, their affect on the equilibrium of the phase boundary can be calculated or obtained from phase diagrams. According to Howitt (1971), salt concentration in permafrost on the North Slope is similar to that of sea water and would account for a freezing point depression at the base of the permafrost of $0^{o}C$ to $-1.8^{o}C$.

The temperature correction for soil pacticle effects (T_s) was reported by Anderson et al., (1973). He simply stated that T_s in a saturated silt or coarse-grained soil would be equal or less than $0.01^{o}C$ while in very fine clay T_s could exceed several degrees Celsius.

The equilibrium of the permafrost phase boundary in Prudhoe Bay appears to be primarily affected by the presence of salt ions (Howitt, 1971). The coarse grained nature of the sediments here suggests only a very slight soil particle effect (T_s). The maximum recorded permafrost depth of 629 meters (Osterkamp and Payne, 1981) would involve a pressure affect on the temperature at the phase boundary of only $0.44^{o}C$. The $-1.8^{o}C$ to $0^{o}C$ variation in the thermal equilibrium at the base of the permafrost attributed to the presence of NaCl ions (Howitt, 1971) is compatible with the observations of Lachenbruch et al., (1982), who theorized that the base of the permafrost is at equilibrium at $-1.0\pm.5^{o}C$.

Depths to the base of the permafrost used here were taken directly from the work of Osterkamp and Payne (1981) on permafrost thickness evaluation from well log data on the North Slope. In their study, the depth to the base of the permafrost was determined from well log data. Specifically, the ice/water interface was identified by electrical resistivity and sonic velocities recorded on the bore-hole compensated sonic and dual induction logs. The dual induction log and the bore-hole compensated sonic logs were found to be particularly sensitive to the presence of ice in the soil pore spaces. Most well logs show what appeared to be a transition zone, involving a mixture of ice and water, at the base of the permafrost.

The base of the permafrost interpreted from well logs (Osterkamp and Payne, 1981) corresponds with the depth of the change in geothermal gradient of Lachenbruch et al., (1982). At the base of permafrost there is a change from interstitial ice to free water. This physical change results in a change in the geothermal gradient. It also controls the electrical resistivity and sonic velocities, the specific log responses used to delineate the base of the permafrost by Osterkamp and Payne (1981). This relationship permits the assumption that the base of the permafrost defined from well logs in Osterkamp and Payne (1981) is at $-1^{o}C$ with an error of $\pm.5^{o}C$.

Obviously it is impossible to make an exact temperature estimate for the base of the permafrost in a well bore without a high resolution temperature log. However, the temperature error in using an assumed regional geothermal gradient in the calculation of the thickness of the zone of potential hydrate occurrence would be more significant than that related to a calculated gradient for each well bore, in which the base of the permafrost is assumed to be at $-1^{o}C$.

Osterkamp and Payne (1981) reported that the ice-bearing permafrost reached a maximum thickness of 629 meters near Prudhoe Bay and Mikkelsen Bay. It thins towards the west and south, with a minimum recorded thickness of 200 meters near Umiat, west of Prudhoe Bay (Osterkamp and Payne, 1981). Using their reported thicknesses of permafrost, the following equation was used to calculate the geothermal gradient to the base of the permafrost for each well:

$$\frac{(T_{BPF} - T_{PMGT})}{\text{(Depth Base Permafrost)}} \times 100 = \text{Geothermal Gradient } (^{o}C/100m)$$

The term T_{BPF} represents the temperature at the base of the ice-bearing permafrost which is assumed to be $-1.0^{o}C$, and T_{PMGT} represents the past mean annual ground temperature which is $-10.9^{o}C$. The mean value of $-10.9^{o}C$ can be viewed as the average surface temperature with which the deep permafrost is presently in equilibrium (Lachenbruch et al., 1982). The difference between the past mean annual ground temperature and the present value of $-9^{o}C$ is due to a recent world-wide warming trend. Using the above values for T_{BPF} and T_{PMGT}, the equation for the geothermal gradient in the permafrost for the Prudhoe Bay region can be rewritten as:

$$\frac{9.9^{o}C}{\text{(Depth Base Permafrost)}} \times 100 = \text{Geothermal Gradient } (^{o}C/100m)$$

To illustrate this method of calculating the geothermal gradients, the North West Eileen State Number Two well is taken as an example. Here the depth to the base of the permafrost is 532 meters and would represent a geothermal gradient within the permafrost of $1.9^{o}C/100m$. By comparison, other areas show a

calculated geothermal gradient within the permafrost ranging from 1.6°C/100m near Mikkelsen Bay to as high as 5.0°C/100m near Umiat. As described by Lachenbruch et al., (1982) the geothermal gradient changes abruptly at the base of the permafrost due to a change in thermal conductivity. Therefore, the geothermal gradient was modified below the base of the permafrost in the calculation of the thickness of the zone of potential hydrate stability. Lachenbruch et al., (1982) were able to calculate the ratio between the geothermal gradient within the permafrost and the geothermal gradient below the base of the permafrost for nine bore holes in the Prudhoe Bay Oil Field. In my calculation of the thickness of the zone of potentially stable hydrates, this ratio was used to compensate for the change in the geothermal gradient at the base of the permafrost. As reported by Lachenbruch et al., (1982) the ratio is:

$$\frac{G_{th}}{G_{fr}} = 1.73$$

The variable G_{th} represents the geothermal gradient within the unfrozen strata, (below the base of the permafrost), while G_{fr} represents the geothermal gradient within the permafrost. For example, if the geothermal gradient within the permafrost is 1.9°C/100m the geothermal gradient below the base of the permafrost would be 3.2°C/100m.

Figure 12 illustrates how the depth to the base of the permafrost and the methane hydrate stability curve can be used to determine the depth and thickness of the zone of potential methane hydrate occurrence. In this example the depth to the base of the permafrost is 532 meters (1,746 feet) with a past mean annual ground temperature of -10.9°C. Assuming that the temperature at the base of the

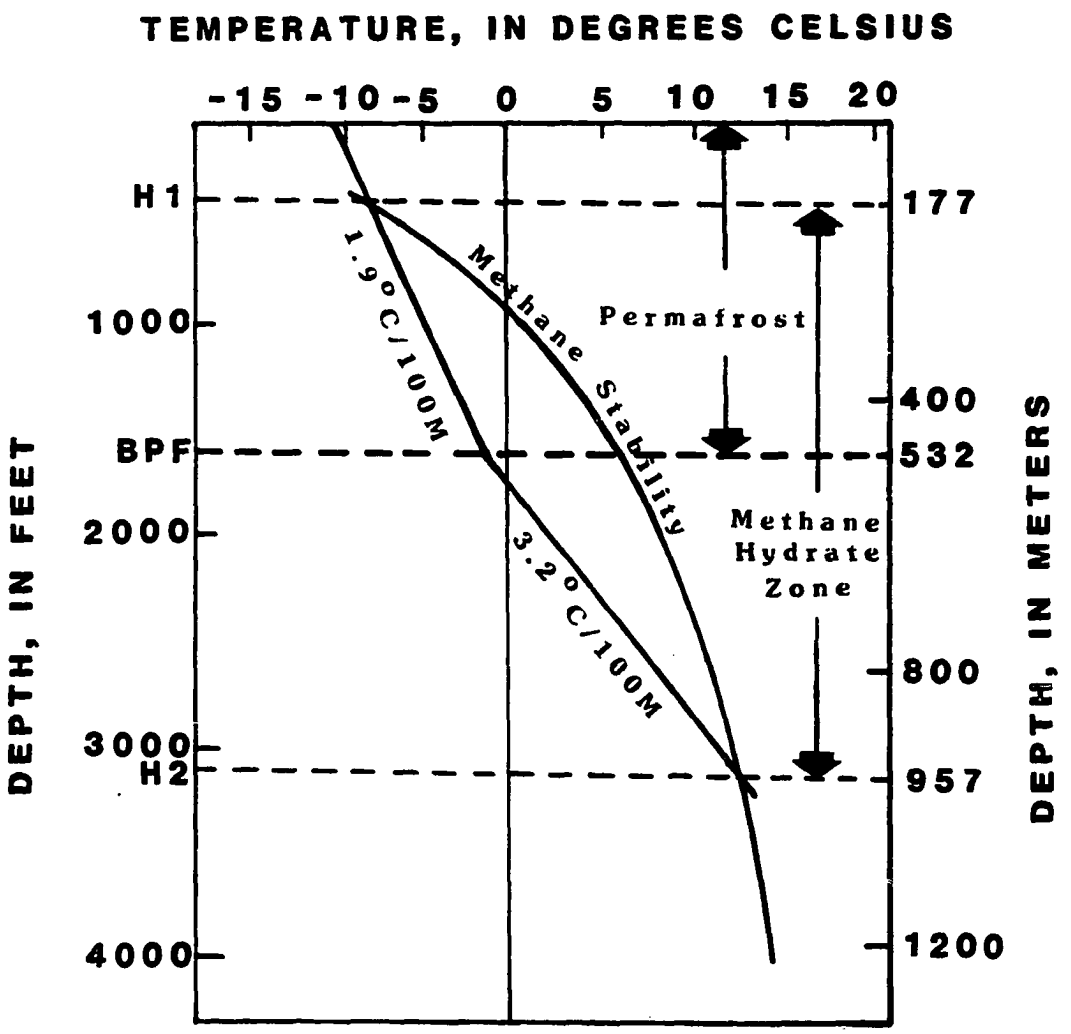

Figure 12-Thickness phase diagram of the methane hydrate stability zone in the Standard Oil 33-29E well in Prudhoe Bay, Alaska.

permafrost is -1°C, the geothermal gradient within the permafrost for this bore hole would be 1.9°C/100m (1°F/100 feet). In Figure 12 a 1.9°C/100m geothermal gradient within the permafrost has been plotted along with a calculated 3.2°C/100m gradient below the base of the permafrost. A methane hydrate stability curve has also been plotted using a hydrostatic pressure gradient of 9.84 kPa/m (.435psi/ft.) (Lachenburch et al., 1982). The lower boundary of the zone of methane hydrate stability is marked by the lower intersection of the geothermal gradient with the methane stability curve. The upper boundary of the zone of methane hydrate stability is defined by the upper intersection of the methane stability curve and the geothermal gradient. In Figure 12 the upper boundary of the zone is marked by H1 at 177 meters (580 feet). While the lower hydrate boundary is marked by H2 at 957 meters (3,140 feet), delineating a zone of potential hydrate occurrence 780 meters (2,560 feet) thick.

The methane hydrate stability curve indicates that the geothermal gradient must be less than 3.7°C/100m (2.1°F/100 feet) for methane gas hydrate to form at Prudhoe Bay. For the geothermal gradient to intersect the methane hydrate stability curve the gradient must be equal to or less than 3.6°C/100m (2.0°F/100 feet), which would correspond with a minimum permafrost depth of 274 meters (900 feet). In other words methane hydrate should not exist at Prudhoe Bay if the depth to the base of the permafrost is less than 274 meters (900 feet). The dashed line in Figure 18 and in Plate 2 represents the 274 meter depth contour on the base of the permafrost. If the above line of reasoning is correct, methane hydrate occurrences should be limited to areas north of this contour. This will be discussed in detail later.

The isopach map of the zone of potential hydrate occurrence in Plate 2 is

very similar to the map showing depth to the base of the permafrost in Osterkamp and Payne (1981). This is not unexpected because there is a direct relationship among geothermal gradient, the thickness of the zone of potential hydrate stability, and permafrost depth. The thickness of the zone of potential hydrate occurrence ranged from nothing at the 274 meter permafrost contour to more than 1,000 meters near Mikkelsen Bay, where the methane hydrate was found to be potentially stable to a depth of 1,119 meters.

It is important to note, however, that hydrate stability can be affected by variations in several different physical and chemical factors; these are very difficult to quantify because the necessary data are not available.

The effects of variations in salinity, gas composition, and grain size will be used to illustrate these difficulties. Salt such as NaCl added to a hydrate system would lower the temperature at which hydrates melt or form (Evrenos et al., 1971). The salinity of the water in contact with the gas during the formation of hydrate can reduce the freezing point about 3^{o} to 5^{o} C per 100,000 ppm of dissolved salt. Figure 13 shows the effect of increasing salt content on the methane stability curves. Minor changes in gas composition can also drastically alter the temperature-pressure conditions under which hydrate is stable. For example, a hydrate of a heavy gas such as butane is stable at greater depths and higher temperatures than a methane hydrate (Evrenos et al., 1971). Due to the lack of heavier gases such as propane, it can be assumed that hydrate stability on the North Slope is only affected slightly by variations in gas composition. Because the salt concentrations reported by Howitt (1971) are highly variable, the effect of salinity changes on the hydrate stability could not be assessed.

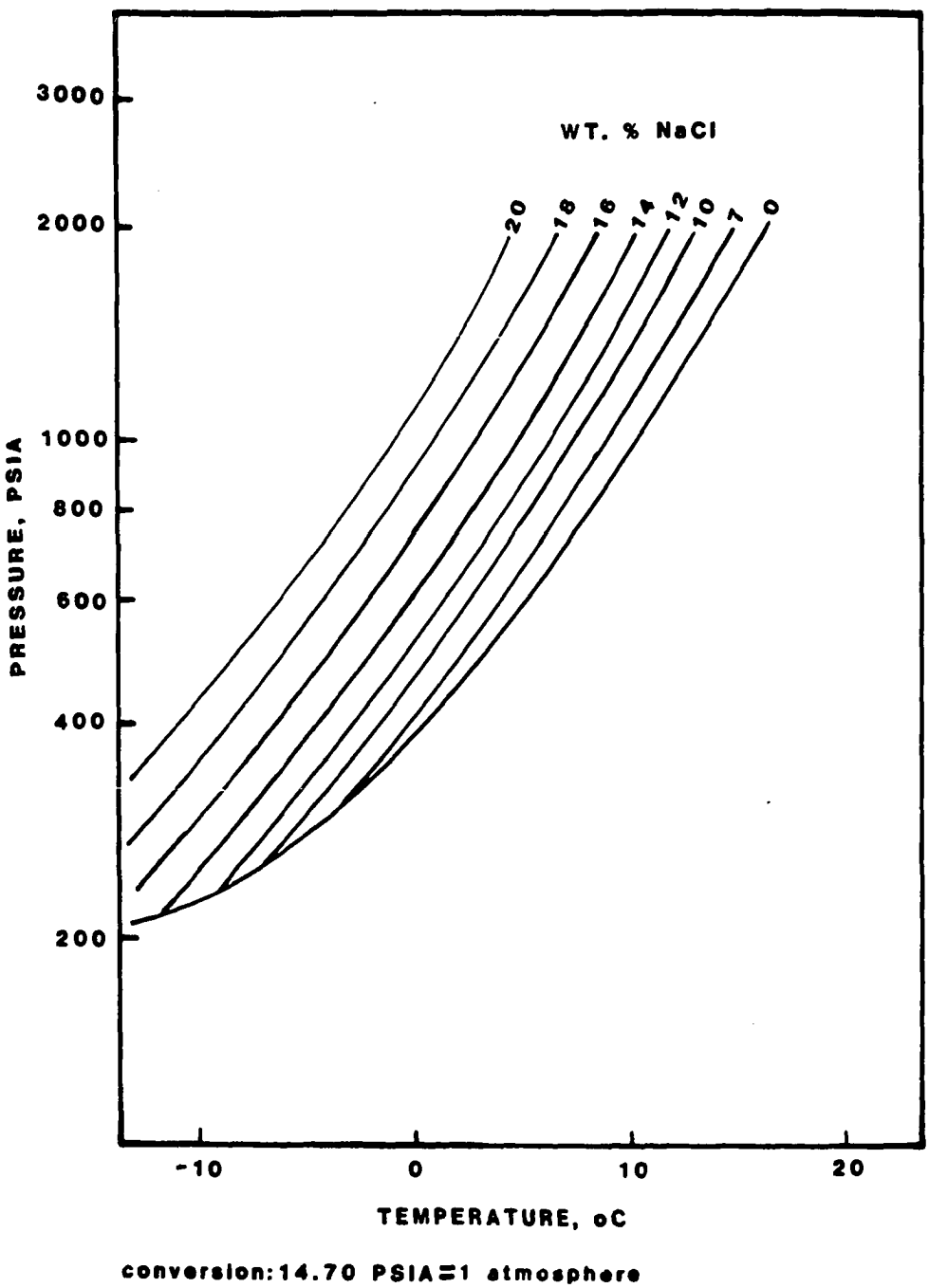

Figure 13-Effect of salt solution on hydrate formation, each curve represents a methane stability curve for a given salt solution (Evrenos et al., 1971).

Variation in grain size can also alter the thermal equilibrium of a given hydrate but the exact effect cannot be easily delineated (Evrenos et al., 1971). Furthermore, thawing hydrate can also alter the pressure conditions of hydrate stability (Evrenos et al., 1971). Within the zone of hydrate stability, two other factors limit the actual occurrence of hydrate. These are 1) the availability of gas and 2) the availability of water. Lack of gas and water presumably is responsible for the absence or failure of the hydrate to occupy all available pore space within the zone of hydrate stability. During the formation of in-situ hydrate all available water may be tied up in hydrates, leaving an excess of free gas in the pore space within the zone of hydrate stability. Similarly, there may be excess water at the end of the hydration process, in which case the free water will remain unfrozen within the zone of hydrate stability.

LOG EVALUATION

The recognition of gas hydrate from well log data was not straightforward; in addition, the zones of potential hydrate occurrence often are not logged or the quality of the logs may be poor. Another limitation is the lack of published information; there is only a relatively small number of prior quantitative studies of hydrate occurrence based on well log data. In this section, the methods used in the study for identifying gas hydrates from well logs are described in detail.

Bily and Dick (1974), evaluated naturally occurring gas hydrate in the Mackenzie Delta, providing one of the few papers dealing with the detection of hydrates on wire line logs. They discovered that when a hydrate zone was penetrated during drilling there was a marked increase in the amount of gas in the drilling mud. These hydrate bearing units produced a relatively high resistivity on the dual induction log and a slight spontaneous potential deflection in comparison to a free gas. In addition, sonic logs indicated an increase in acoustic velocity for hydrate bearing intervals.

The first confirmation of the existence of in-situ natural gas hydrate was not obtained until 1972, when ARCO/EXXON were successful in recovering the first sample of a natural gas hydrate in a frozen state. This was from a depth of 666 meters (2,184 feet) in the North-West Eileen State Number Two well at Prudhoe Bay. The well was drilled with cool drilling muds in an attempt to reduce thawing of the permafrost and hydrate, and the methane hydrate saturated sample was recovered in a pressurized core barrel. The following simple test was devised to check for the presence of hydrate. Pressure within the core barrel was allowed

to equilibrate with the surface pressure after which the barrel was resealed and warmed above in-situ temperature, but not to the degree that the hydrate sample thawed completely. The pressure within the barrel rose, indicating the presence of thawing hydrate; this process was repeated several times with similar results. The hydrate sample had a gas composition of 99.17% methane (P. Barker, personal communication, ARCO Alaska Inc., Anchorage, Alaska).

The confirmed hydrate occurrence in the North-West Eileen Well provides an ideal starting point for the development of log evaluation techniques to detect hydrate bearing zones. There, at a depth of 676 meters just below the recovered hydrate sample, there is a zone that appears to be hydrate saturated, below the base of the permafrost. For the sake of discussion, a detailed description of the log responses within this zone will be presented and compared to other log responses associated with units that are saturated with ice, free gas, fresh water, salt water and any combination of these.

During the drilling of this suspected hydrate zone (658m-683m) there was a marked increase of light gases in the drilling mud, presumably related to thawing hydrate (Figure 14). A very similar mud log response would occur in a zone saturated with free gas. Hence, there is no conclusive method of differentiating hydrate from free gas in the mud log. However, the combination of the gas show on the mud log and corresponding log responses on the dual induction and sonic logs can give more insight into the nature of the gas occupying the pore space.

There is a pronounced resistivity deflection associated with the suspected hydrate zone (658m-683m) on the dual induction log. Within a hydrate the presence of ice in place of a conductive liquid phase would significantly lower the electrical conductivity, corresponding to an increase in the electrical resistivity.

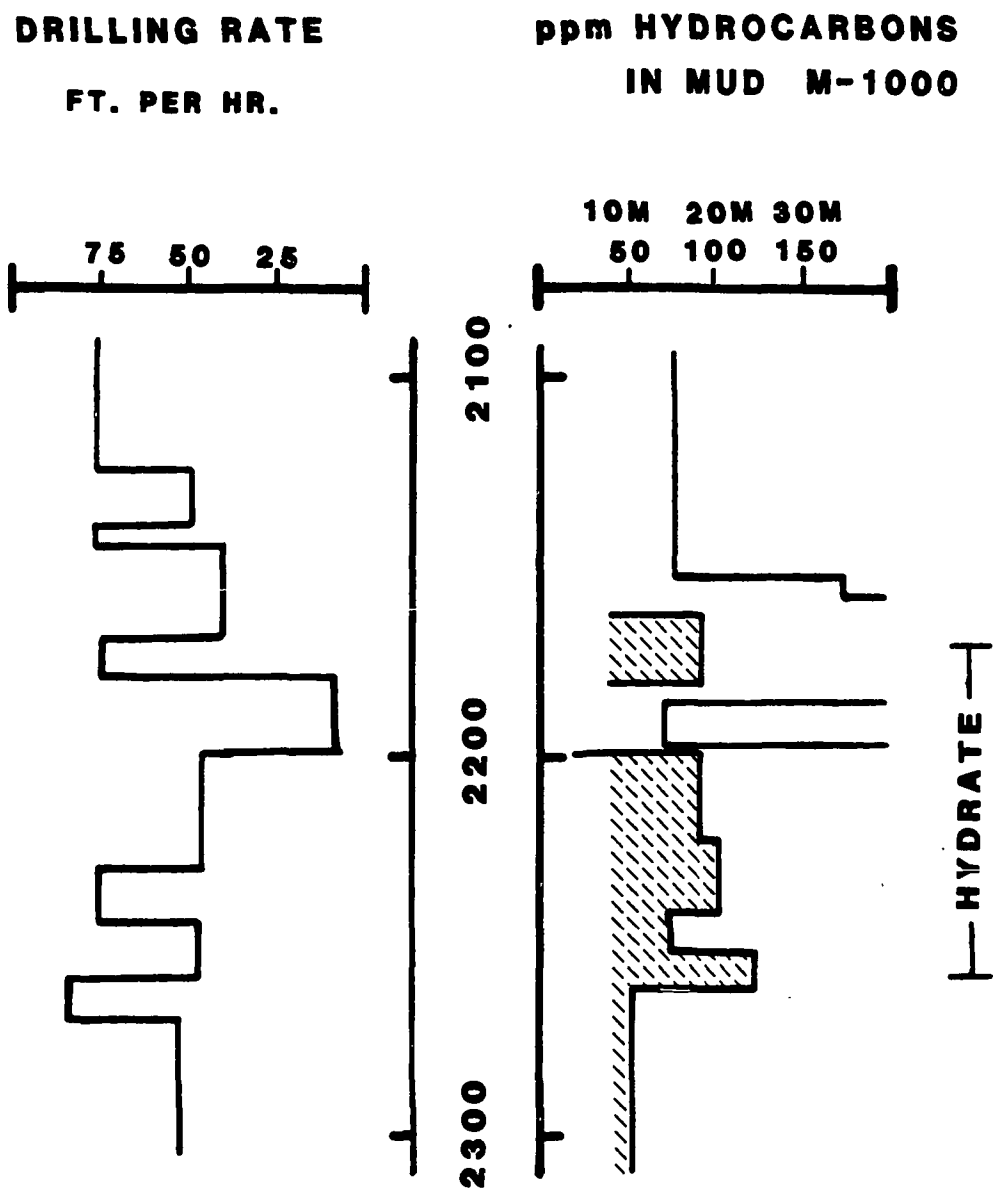

Figure 14-Mud log from N. W. Eileen State Number Two, the suspected hydrate saturated zone has been depiceted from 658 meters to 683 meters (1ft = .3048).

A unit that is saturated with free gas will also exhibit a pronounced resistivity deflection, but due to the solid state of the hydrate the resistivity kick associated with a unit saturated with hydrate would be much more pronounced than a similar unit that is saturated with only free gas.

There is a notable separation of the short normal and the long normal log responses in the hydrate zone. This is due to thawing next to the bore hole (Figure 15). The same response separation is observed for ice-bearing permafrost zones, for the same reason. More commonly, however, the separation between the long and short normal logs is related to invasion by mud filtrate in a hydrocarbon or fresh water zone.

The spontaneous potential survey on the dual induction log can give further distinction between zones saturated with hydrate as opposed to those saturated with free gas. Associated with the pronounced resistivity deflection on the dual induction log within a hydrate zone is an apparent reduced spontaneous potential deflection. The spontaneous potential deflection related to free gas is more pronounced than that related to hydrate. This reduction in the spontaneous potential response in a hydrate zone is associated with the inability of the mud filtrate to penetrate the hydrate.

Within the hydrate zone there is an increase in acoustic velocities, ranging from 3.1 km/s to 4.4 km/s (Figure 16). However, as with the dual induction log, the differentiation of a hydrate saturated unit from ice-bearing permafrost on the bore hole compensated sonic log is impossible. The only tool that is useful in the differentiation of hydrates from ice-bearing permafrost is the mud log.

Other well log devices that suggest the presence of hydrate within this interval were the caliper log and the drilling rate indicator on the mud log. Within

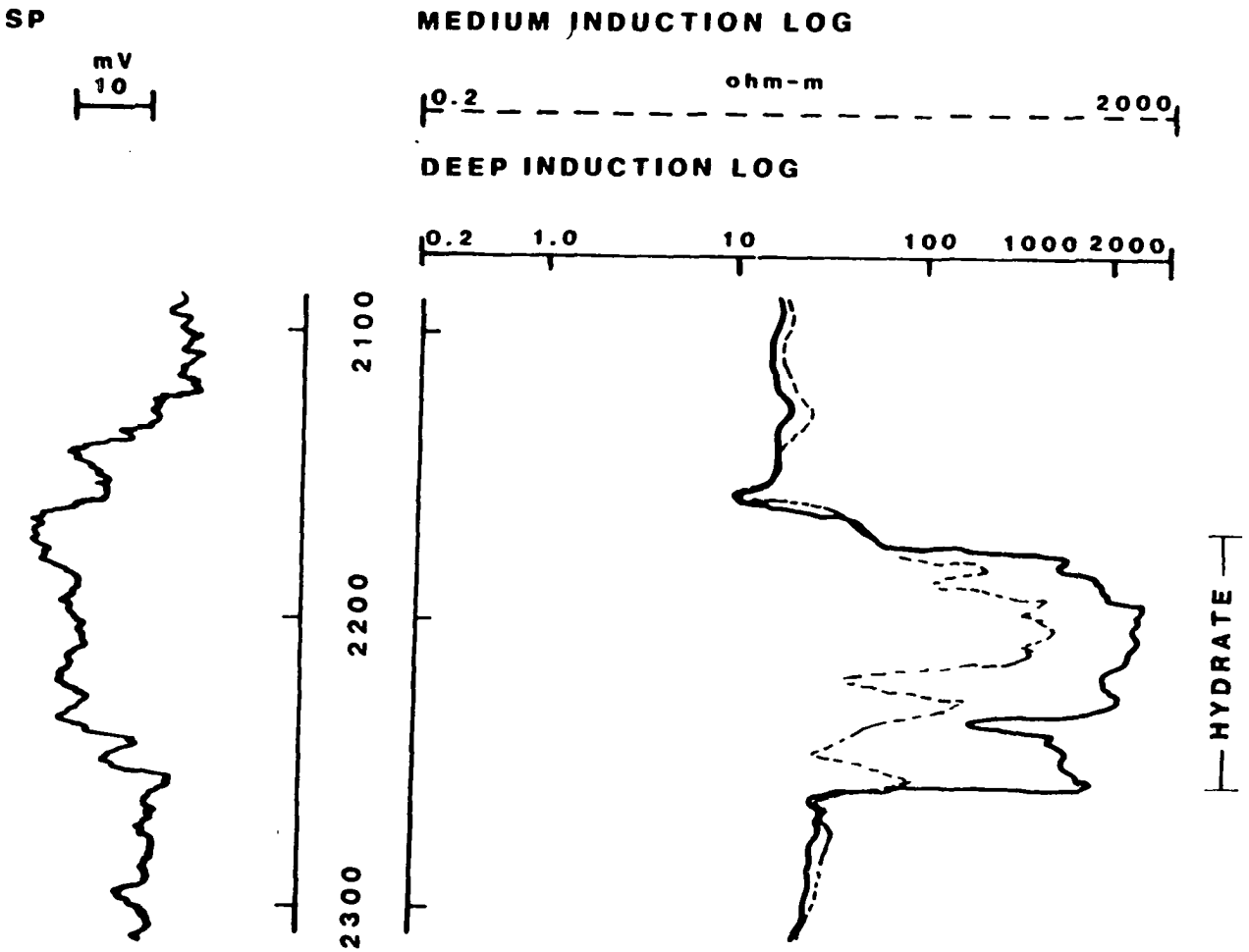

Figure 15-Dual Induction and SP logs from N. W. Eileen State Number Two, the suspected hydrate saturated zone has been depicted from 658 meters to 683 meters (1ft = .3048m).

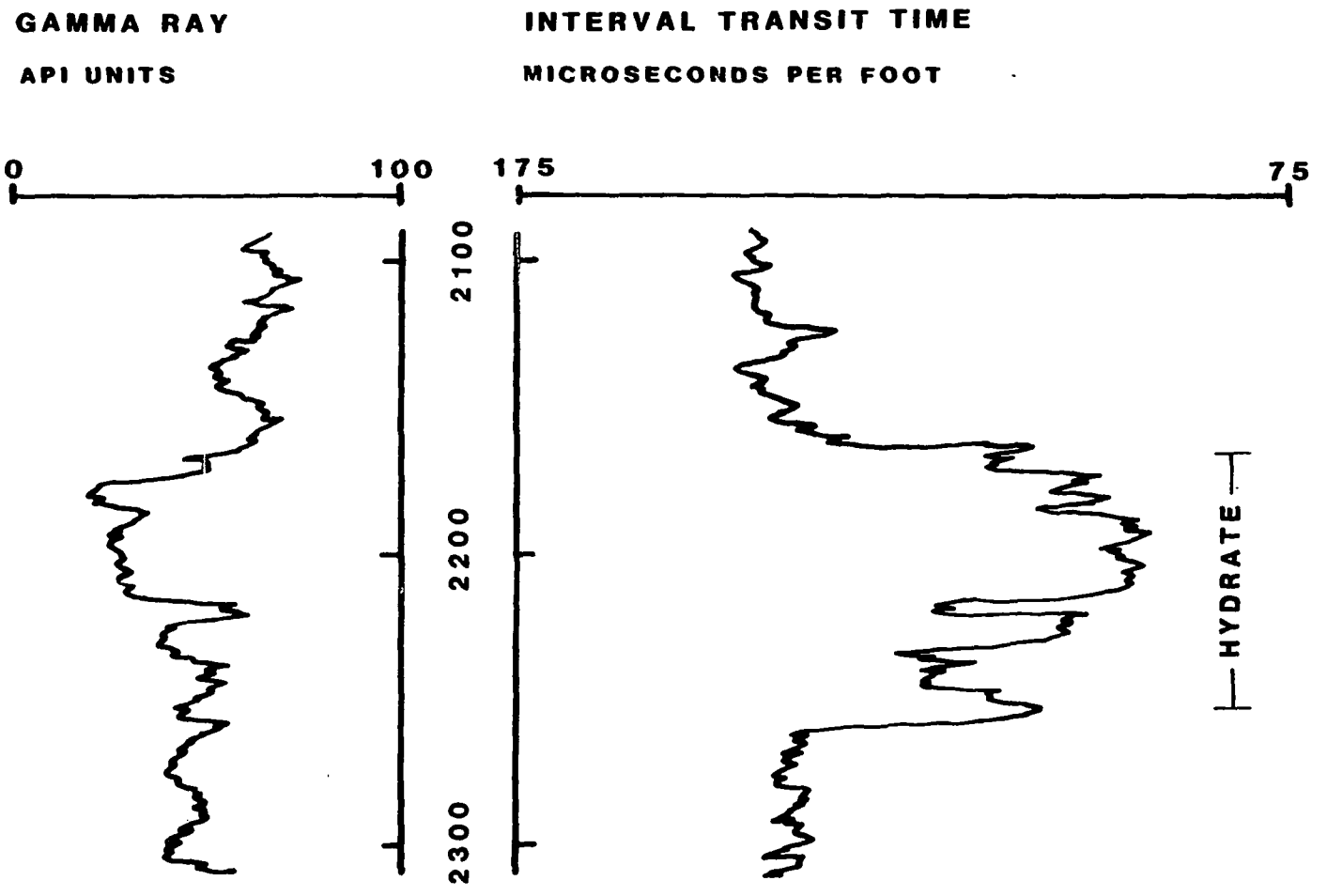

Figure 16-Sonic and Gamma Ray logs from N. W. Eileen State Number Two, the suspected hydrate saturated zone has been depicted from 658 meters to 683 meters (1ft = .3048m).

the hydrate zone, the caliper indicated an enlarged bore diameter due to spalling from the thawing hydrate, and there was a relative reduction in the drilling rate through the hydrate.

The neutron porosity log response was puzzling. In the N.W. Eileen well, the neutron porosity log opposite the hydrate zone showed an increase in apparent porosity. The expected neutron log response in a free gas zone is a deflection towards lower porosity. However, since the neutron log response is related to the number of hydrogen atoms present, the increased neutron porosity reflects the higher density of the hydrocarbon gases in the hydrate state. A somewhat different explanation for this behavior was offered by Hall (1979), who suggested that the increased neutron porosity could be due to a high volume of water in the hydrate zone compared to the small interstitial water volume in a free gas zone.

Complicating the interpretation of the neutron log response was the observation of a decrease in the neutron porosity opposite apparent hydrate zones in several other wells. This could be due to partial thawing near the well bore, which would result in a free gas saturation. Thus, if the neutron porosity log was sensing primarily the thawed region, then the apparent porosity decrease can be explained as a response to free gas. If the well is logged before significant thawing, the neutron log offers some promise as a possible means for estimating the amount of hydrocarbon present in a hydrate zone. Otherwise, the most simple way to recognize a hydrate zone is to examine the sonic log to determine if ice or hydrate is present, and to examine the mud log to detect the release of natural gas due to thawing of the hydrate. The other logs, including the dual induction, drilling rate, spontaneous potential and caliper logs, serve to collaborate the interpretation but cannot by themselves distinguish the hydrate zone.

Cross plots may provide further insight concerning the phase distribution of hydrates, liquid water and free gas in a hydrate zone; in addition they may provide another way to distinguish hydrate zones from non-hydrate zones. Figure 17 is a cross plot showing the deep induction resistivity and the sonic transit time for seventeen intervals from below the base of the permafrost in the N.W. Eileen well. From prior log evaluation techniques, eight of the intervals recorded were theorized to be hydrate saturated. In Figure 17, there is a distinct grouping of intervals with similar constituents in the pore spaces. The grouping of the hydrate saturated units to the lower left shows their similar transit time velocities and resistivities. The non-hydrate saturated units grouped to the upper right corner of the plot showing a reduction in resistivity and transit time. Due to the problems already explained with the neutron log responses, the neutron porosity/resistivity log cross plot was less successful in distinguishing the hydrate zones.

A summary of the log responses for a zone that is hydrate saturated are graphically represented in Figure 18. The following list summarizes various log responses, incorporating the methods developed in this study with the evaluation techniques developed by Bily and Dick (1971) in the Mackenzie Delta. The ability of each log to distinguish hydrates from free gas and ice bearing permafrost is also indicated.

1. Mud Log On a mud log there is a pronounced gas kick associated with a hydrate, due to thawing during drilling. The mud log serves as the best tool available for the differentiation of a hydrate saturated unit from gas-free ice-bearing permafrost. Otherwise, the detection of a gas hydrate in ice-bearing permafrost is very difficult.

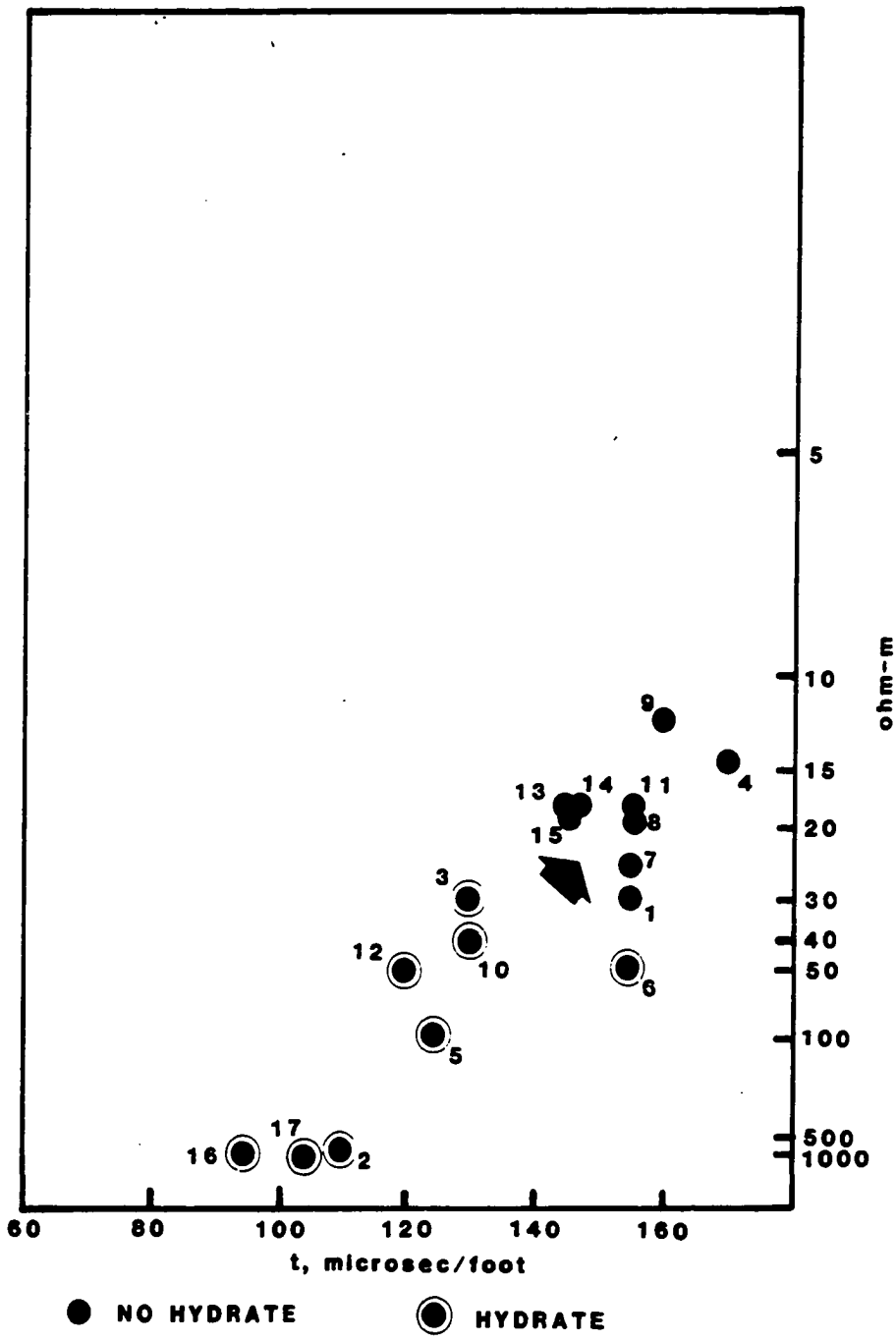

Figure 17-Resistivity-transit time cross plot from N. W. Eileen State Number Two, with reference numbers.

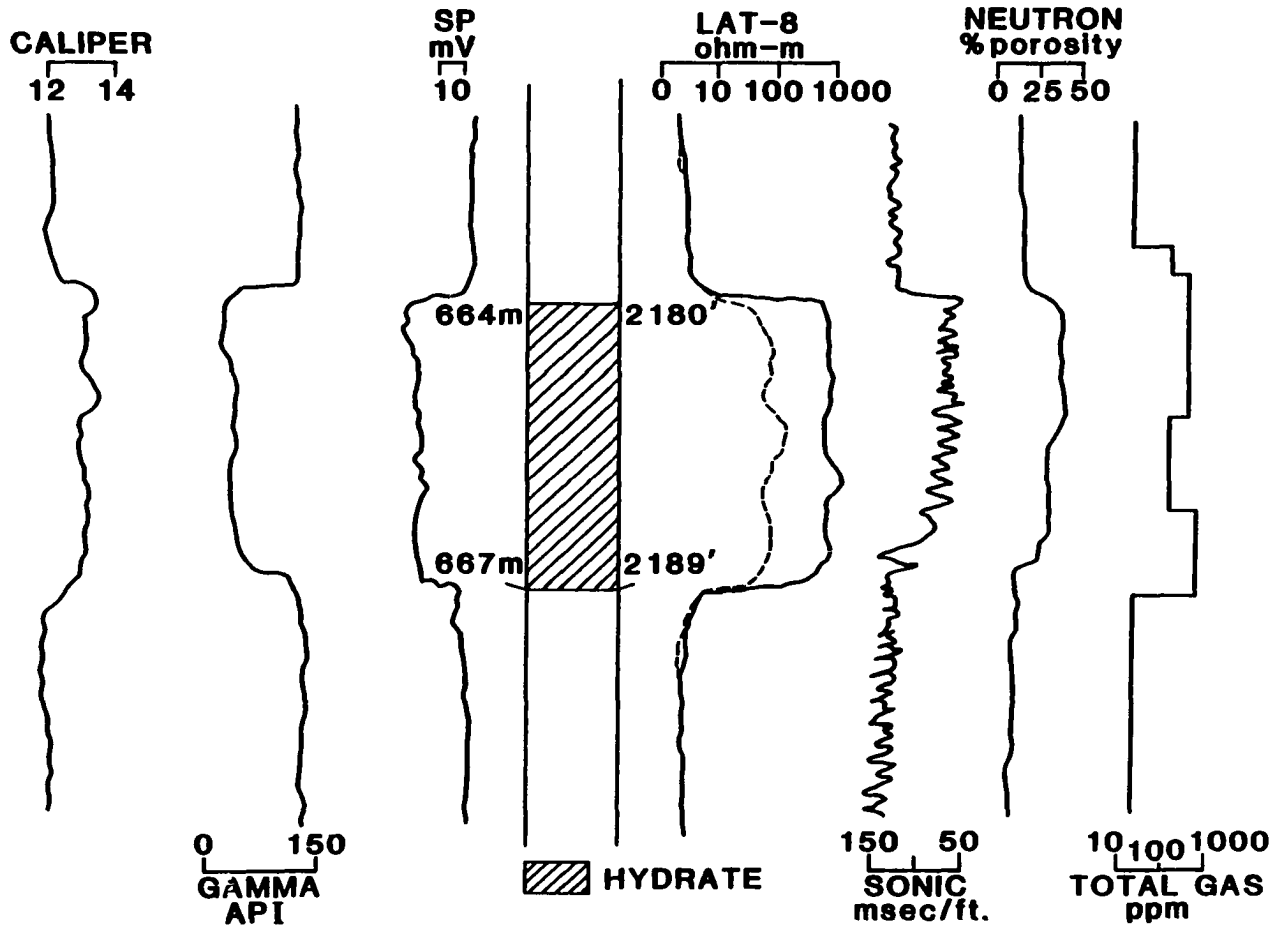

Figure 18-Log responses to the presence of hydrate.

2. Dual Induction Log There is a relatively high resistivity deflection on the dual induction log in a gas hydrate zone, in comparison to that in a free gas zone. The long normal is separated from the short normal due to thawing next to the bore hole. If a unit were hydrate saturated within ice-bearing permafrost, the resistivity response on the dual induction log for the hydrate unit would not be significantly different than the log responses for the surrounding ice-bearing permafrost. Hence, it is impossible without the usage of the mud log to distinguish between hydrate and permafrost. Below the base of the permafrost the high resistivity deflection associated with the hydrate is distinct from the surrounding non ice-bearing zones, but may be similar to that of a free gas.

3. Spontaneous Potential (SP) There is a relatively lower (less negative) spontaneous potential deflection in a hydrate zone when compared to that associated with free gas. The frozen hydrate limits the penetration of mud filtrate thus reducing the negative spontaneous potential. The spontaneous potential for a hydrate saturated unit within permafrost would be similar to that in the surrounding ice-bearing permafrost, where the mud filtrate penetration is similarly limited.

4. Caliper Log The caliper log in a hydrate interval usually indicates an oversized well bore due to spalling associated with the decomposition of a hydrate. Because the caliper log also indicates an enlarged bore

hole in ice-bearing permafrost, it is only useful in detecting hydrates below the base of the ice-bearing permafrost.

5. Sonic Log Acoustic velocities in hydrate are relatively high ranging from 3.1 km/s to 4.4 km/s. Because the sonic velocity of ice-bearing permafrost is very similar to that of gas hydrate, the sonic log cannot be used to detect hydrates within the upper ice bearing permafrost zone, but it is helpful below the base of the ice-bearing permafrost.

6. Neutron Porosity In a hydrate zone there is an increase in the neutron porosity; this contrasts with the apparent reduction in neutron porosity in a free gas zone. If a unit is hydrate saturated and occurs within the ice-bearing permafrost zone the neutron porosity log would theoretically indicate an increased or reduced neutron porosity, depending on the amount of free gas associated with the hydrate in comparison to that of the surrounding ice-bearing permafrost. Below the base of the permafrost a hydrate unit exhibits a relatively higher neutron porosity compared to water saturated or free gas saturated zones. However, thawing near the well bore complicates the neutron log interpretation.

7. Drilling Rate In a hydrate zone the relative drilling rate decreases, due to the cemented nature of the hydrate. There is a very similar drilling rate response within ice-bearing permafrost, and therefore drilling rate change is not useful as a hydrate detector within the permafrost.

8. Cross Plots In a cross plot of the resistivity and transit time for a series of stratigraphic units saturated with either hydrate or free gas and below the base of the ice-bearing permafrost, there is a grouping of units with similar constituents. Hydrate saturated units fall in a region of relatively higher resistivity and faster transit times while free gas saturated units fall in an area of lower resistivity and slower transit times. Differences are relative and not absolute; the cross plots show a simple clustering of similar properties. A resistivity/transit time cross plot of units that are above the base of the permafrost is not useful as a hydrate indicator, due to the similarity in resistivity and transit time velocities in hydrates and in permafrost.

In the Prudhoe Bay wells the dual induction and mud log are the most valuable tools available for the detection of gas hydrates; caliper and sonic logs are helpful but less definitive. The neutron porosity log showed great promise, but the lack of neutron surveys did not allow adequate assessment of it as a hydrate detection device.

Many problems still exist in the evaluation of in-situ hydrates from well log data, and the addition of new evaluation techniques such as the use of cross plots and the addition of the neutron logs has only slightly improved the subjective nature of hydrate detection. For example, during normal drilling activity the warm drilling muds can thaw permafrost and hydrates. If the well is not logged soon after the penetration of a hydrate, it can thaw beyond the maximum sensing depth for normal well logging tools and thus not appear on the log surveys. As

another example, consider the case where the dual induction log suggests hydrate by a sharp resistivity deflection but there is no evidence of gas on the mud log. Such zone could be saturated with fresh water, the gas detection device may not have been operating properly, or it simply may not have been engaged during the penetration of the hydrate.

HYDRATE OCCURRENCES AT PRUDHOE BAY

One-hundred and twenty-five wells were examined for potential hydrate occurrence, with 102 occurrences in 32 different wells. Hydrates occurred in relative porous discrete units. Many wells had multiple zones of hydrate occurrence, with individual occurrences ranging from 2 to 28 meters thick. In this section, the locations of the hydrate occurrences are described. Then some preliminary conclusions are offered concerning the source of the gas and the mechanism for the formation of the hydrates.

Most hydrate occurrences appear to be geographically restricted to the Kuparuk Field to the west of Prudhoe Bay, as shown in Figure 19. There were four laterally continuous hydrate-saturated units and two less extensive units. The lateral extent of each hydrate-saturated unit is shown in the block diagram in Figure 20. Figure 21 is a east to west cross section through the Kuparuk Oil Field showing individual hydrate accumulations and infrerred environments of deposition of the associated sedimentary rocks. The location of this cross section is shown in Figure 19. The distribution of all the hydrate occurrences have been plotted in a series of thirteen cross sections in plates 7 through 9.

The presence of structual-stratigraphic control on the occurrence of hydrate was apparent upon close examination of all hydrate zones. With only a few exceptions all hydrate occurrences were below Marker 12, which is the base of a non-porous prodelta shale. Hydrates were found exclusively in units M, N, O, P, Q and R all of which were interpreted as a delta front foreshore deposits of shaly sand with thick interbeds of shale and clean sand. Within this 300-meter thick sediment interval there are several impermeable shale beds which serve as

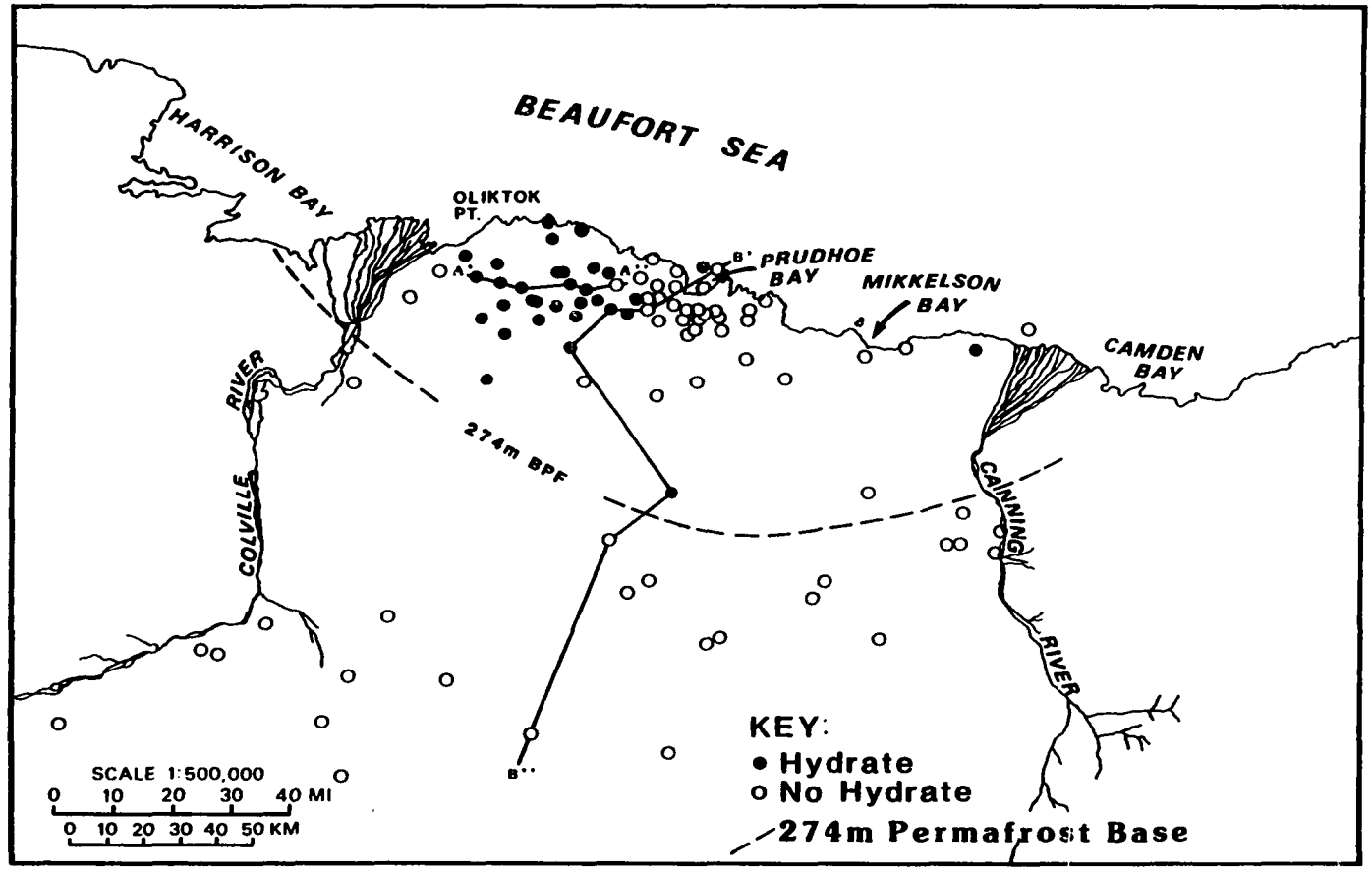

Figure 19-Geographic distribution of hydrate occurrences.

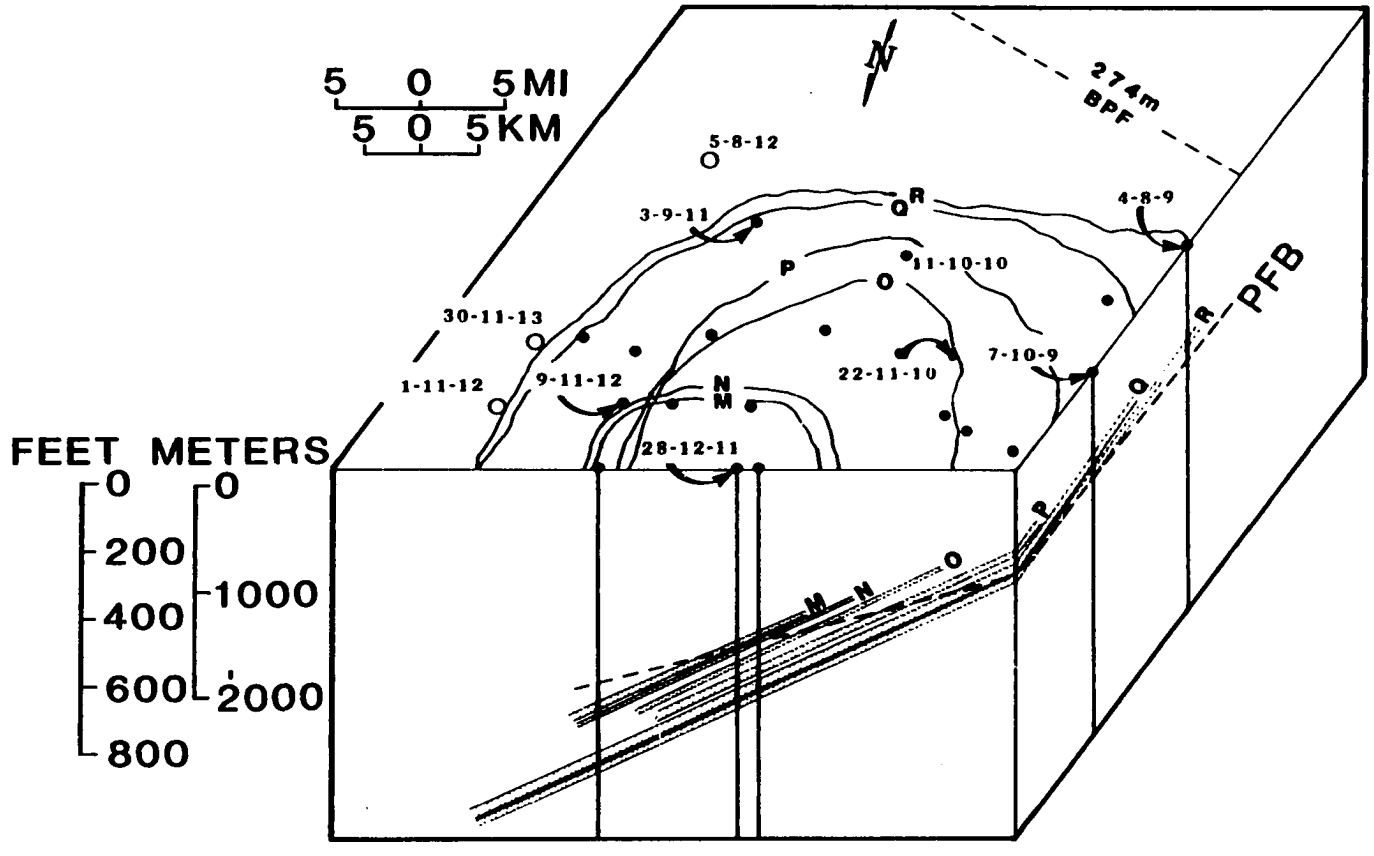

Figure 20-Block diagram showing hydrate occurrence in the Kuparuk Oil Field, and lateral extent of hydrate saturation in units M, N, O, P, Q and R.

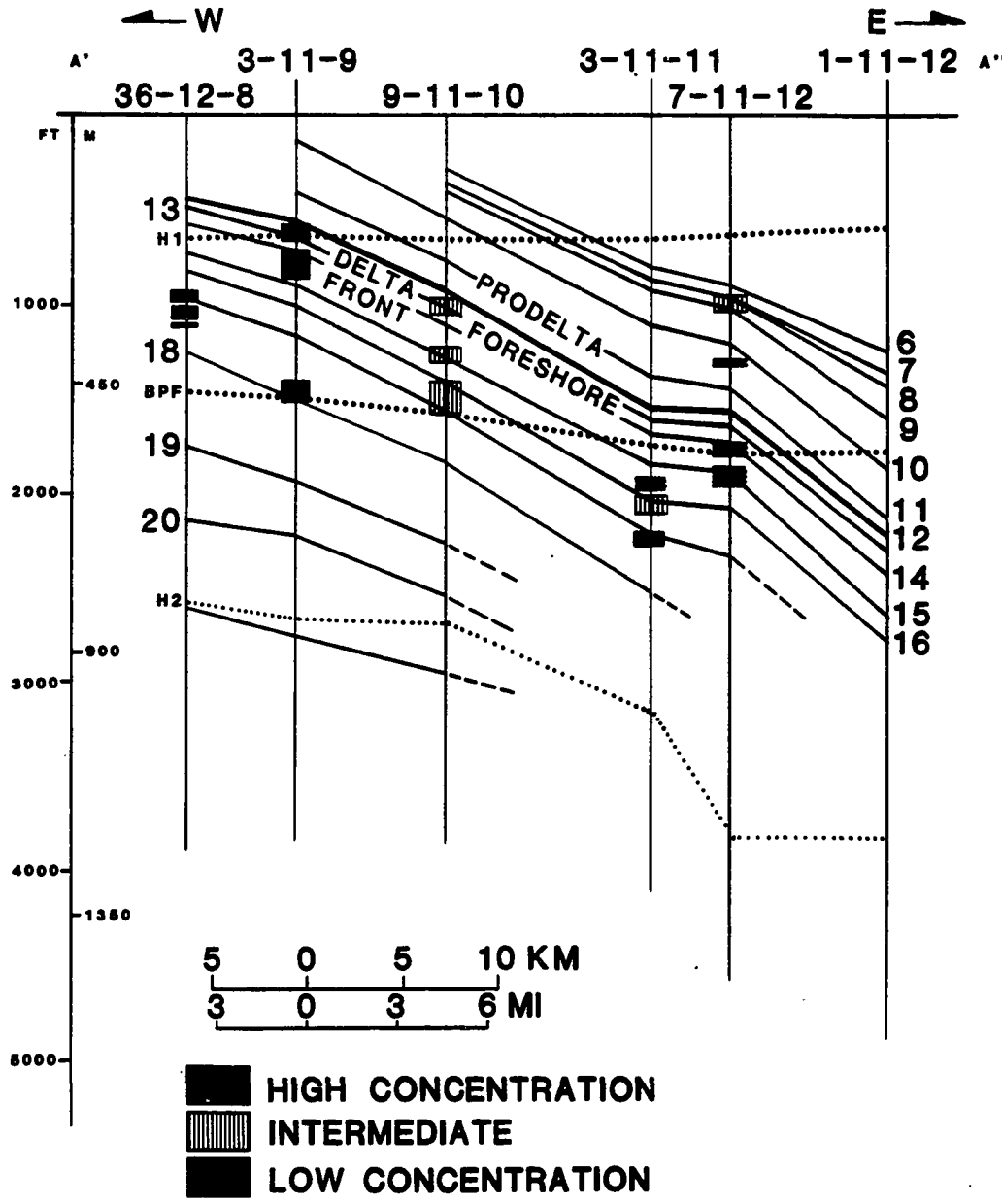

Figure 21-East to west cross section through the Kuparuk Oil Field, showing hydrate occurrences and degree of saturation.

caps for the relatively porous underlying sand units which appear to be hydrate-saturated. Due to the interbedded nature of porous and non-porous sediments the hydrate occured in multiple discrete units. For example, within a single well there were as many as eight different hydrate-saturated porous units separated by impermeable intervals free of hydrates.

A subjective ranking of A (high), B (intermediate) and C (low) has been assigned to each hydrate occurrence in an attempt to quantify the degree of hydrate saturation. This is based mainly on the magnitudes of the resistivity deflection and the gas show associated with each hydrate occurrence. If a hydrate occurence is within the permafrost, the dual induction log cannot be used to quantify the degree of hydrate saturation due to the similar electrical resistivity of permafrost and hydrate. Therefore, above the base of the permafrost the intensity of the gas show on the mud log was the only method of determining the degree of hydrate saturation. A unit with an "A" ranking had a resistivity on the deep induction log between 500 ohm-m and 1,000 ohm-m. A unit with "B" ranking, exhibited a resistivity between 100 ohm-m to 500 ohm-m while the resistivity of a "C" unit fell below 100 ohm-m. Note that these resistivity values are for hydrates occurring below the base of the permafrost.

In the cross section shown in Figure 21, the hydrate appears to be concentrated in the westward up-dip direction with a decrease in hydrate saturation down-dip to the east. The geographic restriction of hydrate to the Kuparuk Region along with its increase in the up-dip direction suggest that the free gas necessary for hydrate development may have migrated into place. Further evidence of up-dip migration of free gas into the zone of potential hydrate stability is found in the stratigraphic isopach map of unit P (Figure 22).

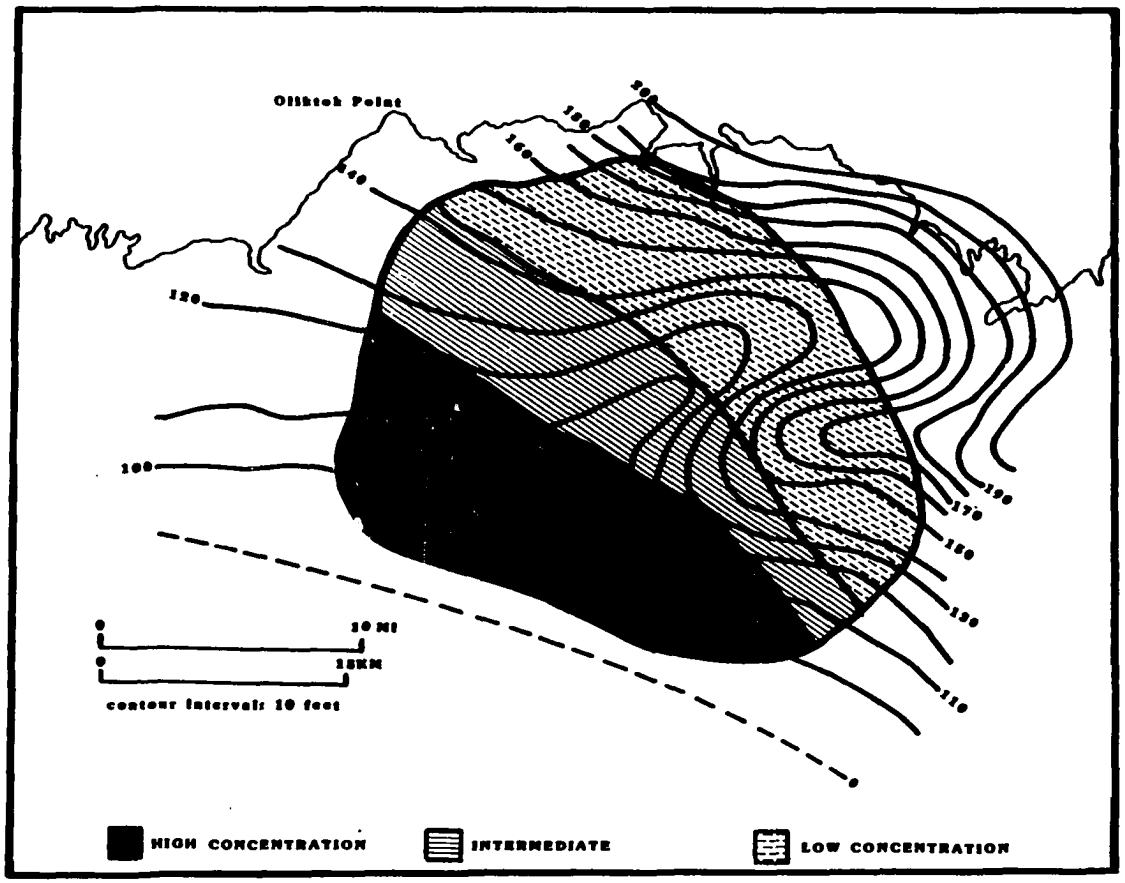

Figure 22-Isopach map of unit P showing varying degree of hydrate saturation.

The highest concentration of hydrate occurs in the south-west up-dip section of unit P; this unit thins in the up-dip south-west direction and is erosionally truncated to the south and west. In other words, there is a relative decrease in the hydrate saturation as unit P thickens in the down-dip direction; similar patterns exist in units M, N, O, Q and R. The dominance of methane gas in the hydrate on the North Slope does not permit conclusive identification of the source of the gas. Methane may have been produced in the upper units by biological decay of coal or it could have migrated from a deep gas deposit, perhaps associated with petroleum. However, the lack of heavier gases such as ethane in these shallow units suggests that the gas source for the hydrates may not have been a deep gas related to oil production here because the latter contains notable amounts of ethane as well as minor amounts of heavier gases. The high methane content also reduces the likelihood that the gas originated from the shallow oil occurrences reported by Holder et al., (1976).

One possible scenario for the formation of hydrate in the North Slope would begin with free gas migration from either local diagenesis or from depth through a relatively permeable sand unit along the base of an impermeable prodelta shale. This shale would act as a cap, preventing further vertical gas migration. Within the permeable sand, the migrating methane gas could be blocked in the up-dip direction by several different causes, such as a self forming hydrate seal, impermeable permafrost, porosity/permeability wedge-out, or a fault.

Porosity/permeability wedge-outs or fault traps for the migrating free gas is unlikely. The physical characteristics controlling the rate of free gas migration and the existence of possible porosity/permeability traps in the hydrate saturated sands are not easily delineated due to the lack of data. The only data available

on porosity and permeability are from stratigraphic logs prepared by the American Stratigraphic Company. These logs show the porosity within the hydrate saturated sands to be fairly uniform, ranging from 38 to 46% (American Stratigraphic Company, 1982, personal communication). The lack of lateral variation in porosity reduces the likelihood of porosity/permeability wedge-outs. Lack of evidence for significant faulting of these sediments after their deposition in the Early Cretaceous reduces the likelihood of fault traps.

It is possible that the free gas formed a trap by freezing in place as it entered the hydrate stability field, thereby forming a seal impermeable to further free gas migration (Evrenos et al., 1971). The occurrence of frozen hydrate more than 1,000 meters above the base (denoted by H2 in Figure 21) of the zone of hydrate stability indicates that there must have been a significant change in the mean annual temperature at some time in the past. Also, there are a number of hydrate occurrences within the permafrost, such as those shown above the dotted line indicating the base of the permafrost in Figure 21. The occurrence of hydrate within the permafrost places a time restraint on the formation of hydrate: because permafrost is impermeable to gas migration the hydrate must have developed in the upper intervals before the formation of permafrost to the present depth. It is possible that free gas may have been present at an early stage in the shallow strata and later became hydrate as the permafrost formed during a cooling period.

The presence of hydrate within the permafrost and the occurrence of hydrate above the base of the zone of potentially stable hydrate indicates that during the past the climatic conditions were such as to allow gas movement within the now frozen units. The mean annual ground temperature during the

implacement of the free gas must have been significantly higher than today, and can be determined as follows. In Figure 23, the geothermal gradients and the methane stability curve from Standard Oil 33-29E has been plotted in a similar fashion to Figure 12. In Figure 23, a 1.9°C/100m geothermal gradient has been constructed from intersection of the methane hydrate stability curve and the -1°C horizon, which would represent the hypothetical base of the permafrost at a warmer period in the past. Even though the mean annual ground temperature was higher during this interstadial period, geothermal gradients would not change within the permafrost or below the base of the permafrost, because these gradients are controlled by the thermal conductivity of the strata. So it is possible to project a temperature of the hypothetical warmer period when the free gas could migrate and there would be no hydrate formation. The intersection of the 1.9°C/100m gradient with the temperature axis at the surface would represent the minimum mean annual ground temperature during this theorized warmer period, which would be -5.5°C (22°F).

There have been many temperature fluctuations over the last 150,000 years (Figure 24) and there may have been several interstadial warmer periods. A good example of a significantly warmer period is the Emian Interglacial event, approximately 125,000 years ago (GARP, 1977). During the Eemian, the mean annual temperature may have been warm enough to allow gas migration within the upper presently frozen strata, which is hydrate saturated today.

There are several hydrate occurrences approximately 300 meters above the present base of the permafrost. By using the Stefan formula (given below) it is possible to calculate the approximate time required for the permafrost to advance

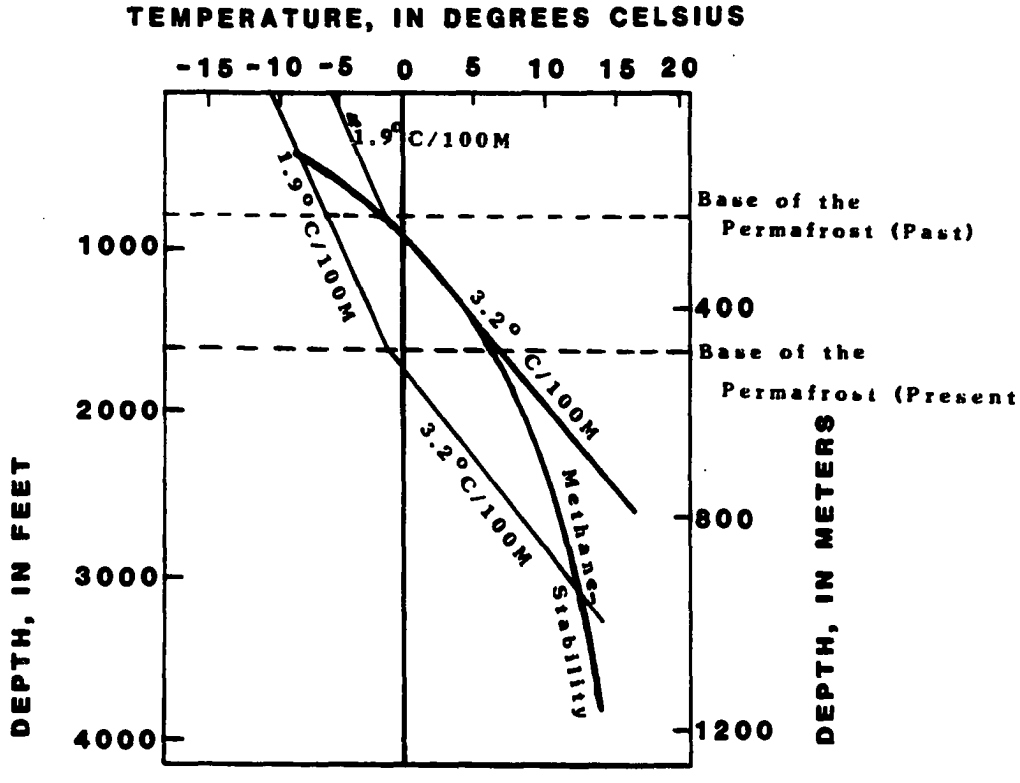

Figure 23-Methane hydrate phase diagram for a probable warm period in the past, compared to the thickness phase diagram of the methane hydrate stability zone in the Standaed 33-29E well in Prudhoe Bay Alaska, it is assumed that the permafrost is ice-bearing.

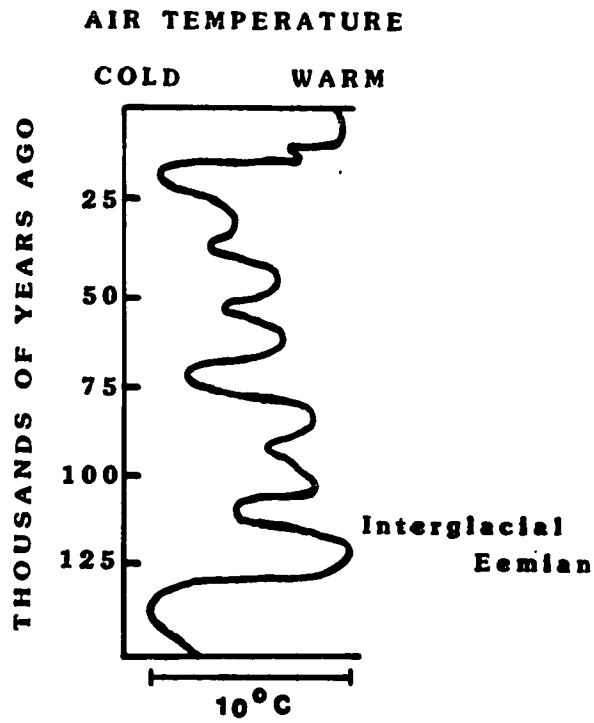

Figure 24-Generalized northern hemisphere air-temperature trends (GARP, 1977).

from the upper hydrate occurrences to the present depth of the permafrost base.

$$X = \sqrt{\frac{2K_f}{L\rho}\,(T_b - T_s)\,t}$$

In this equation K_f is the thermal conductivity of the permafrost and is assumed to be 10.6×10^7 J(ma°C)$^{-1}$ and $L\rho$ is equal to 1.2×10^8 J-m^{-3} for the Prudhoe Bay region. X represents the thickness of the permafrost which formed and t is the amount of time required to develop a given thickness of permafrost. Assuming that the melting temperature for the permafrost T_b is equal to -1.0°C and that the temperature during this cooling period could have been as cold as -10.9°C, it would have taken 5,145 years for the base of the permafrost to advance from the upper hydrate occurrences to the present depth. Since the Eemian, over 125,000 years ago, there have been many periods in which the temperature was warm enough to account for the 5,145 years needed for the permafrost to advance the 300 meters from the upper most hydrate occurrences to the present permafrost depth.

During this interstadial warmer period when the gas was mobile the permafrost would not have been deeper than 274 meters or may not have existed at all. The shallowest present-day occurrences of hydrates are at a depth of 128 meters well above the shallowest depth at which hydrates could form during this interstadial warm period. Hence, it is apparent that the free gas migrating along the bedding plane during this interstadial warm period was trapped at the base of a thin layer of impermeable ice-bearing permafrost. Trapping of free gas and oil below the base of the permafrost is known from the Umiat wells drilled in the 1940's. Due to the significantly higher mean annual ground temperature of at

least -5.5°C at that time, any free gas trapped at the base of the permafrost would not form hydrate. Later there was a decrease in the mean annual ground temperature and the permafrost began to thicken and the upper stable free gas zone underwent hydration. The gas hydrate and permafrost continued to thicken as the temperature decreased until the temperature stabilized or some other factor controlling hydrate formation was altered, such as the availability of free gas or water, as discussed earlier. The self forming hydrate trapping model and the permafrost trapping model are not totally independent. Once formed, hydrate would always have the potential of creating its own trapping mechanisms.

Formation of hydrate would be favored by a driving pressure behind the migrating gas. A scenario in which free gas necessary for hydrate development was migrating under a driving pressure would be an ideal mechanism for hydrate formation. As the migrating free gas entered the zone of hydrate stability under initial pressure the gas would react with the interstitial water and begin hydration. It is possible the hydrate would form as a freezing front similar to permafrost, and as the migrating free gas encountered the advancing hydrate base the free gas would be incorporated into hydrate as long as the necessary pressure was maintained and there was a significant source of water and gas.

SUMMARY AND CONCLUSIONS

The upper 1,000 meters of strata at Prudhoe Bay is characterized by a gentle dip to the north-east, ranging from 20 to 28 meters per kilometer, and is dominated by three distinct coarsening-upward deltaic sequences. The upper units were characterized by four recurring rock types. Most abundant was poorly-graded well-sorted sand while dense silt dominated several thick units, and included a great deal of potash-bearing clay minerals. Silty sand and well-graded gravel occurred in small quantities.

The thickness of the zone of potential hydrate occurrence ranged from nonexistent at the 274 meter permafrost depth contour to more than 1,000 meters near Mikkelsen Bay, where the methane hydrate was found to be potentially stable to a depth of 1,119 meters.

In the Prudhoe Bay area wells the dual induction and mud log are the most valuable tools available for the detection of gas hydrates while the caliper and sonic logs are of secondary value. Many problems still exist in the evaluation of in-situ hydrates from well log data and the addition of new evaluation techniques such as the use of cross plots and the addition of the neutron logs have improved the subjective nature of hydrate detection.

Methane gas hydrate occurs in six discrete units in the Kuparuk Oil Field on the North Slope of Alaska, immediately west of the Prudhoe Bay Oil Field. The hydrates are found in a series of porous sand units that were deposited in a delta-front environment and capped by pro-delta muds, now compacted to relatively impermeable shale.

Free gas necessary for hydrate development originated either by biological

decay within coal or escaped from a deeply buried gas zone. Free gas migrated up-dip through relatively porous and permeable sand units until it encountered a impermeable barrier at the base of ice-rich permafrost or pre-existing hydrate accumulations. If conditions fall within the stability field of hydrate, such gas would be converted to in-situ hydrate.

The major findings of this study are:

1. Several well logs have been found to be indicative of the presence of hydrate. Although no single log is definite by itself, used in combination they permit at least a subjective evaluation of hydrate occurrences. For example, the development of new evaluation techniques such as the use of cross plots and the addition of the neutron porosity log as a hydrate detector has reduced the subjective nature of the hydrate evaluation. Hydrate occurrences were identified by a variety of different well logs. The internal consistency of their determination, and their application in a large number of wells, indicate the validity of the method.

2. The recognition of the primarily structural-stratigraphic control on the up-dip gas migrational model for the hydrate accumulations was a significant contribution. The correlation of the actual hydrate occurrences identified in well log data with the structural-stratigraphic framework has allowed the development of a conceptual model for hydrate formation in the North Slope region.

3. The method for determining the zone of hydrate stability was refined to take into account both the difference in thermal conductivity between ice bearing and water bearing strata and the shallow depth limit of the stability zone. The method used for estimating the local geothermal gradients allows estimation of temperature profiles during warmer periods in the Earth's history which, in turn, has provided insight concerning the original formation and accumulation of the actual gas hydrate occurrences.

4. The structural-stratigraphic framework developed in the course of the research has contributed substantially to the existing data on the depositional history of the Cretaceous and Tertiary Strata of the North Slope. The addition of more subdivisions within the upper strata and an increased number of well log markers in comparison to previous work has improved the general geologic understanding.

Further research on quantitative log evaluation procedures should be undertaken in which factors such as saturation levels and porosity characteristics are known and controlled. Subsurface in-situ formation of hydrate is poorly understood due to the lack of data, and there is a need to refine the basic understanding of the hydrate formation processes. Detailed examination of possible geologic factors controlling the occurrence of gas hydrate should be undertaken. And finally, evaluation of hydrates as a potential energy resource should be pursued, including development of methods for the production of hydrate on a commercial scale.

APPENDIX

Hydrate Occurrences in Prudhoe Bay

Key

Supporting Evidence

1-increase in acoustic velocity

2-resistivity deflection

3-small spontaneous potential deflection

4-gas show on mud log

5-oversized caliper

6-increase in the neutron porosity recorded

7-long normal separates from the short normal

8-decrease drilling rate

Degree of Hydrate Saturation

A-high

B-intermediate

C-low

Well Name, location	Depth(m)	Evidence	Sat.
N.W. Eileen State #2	472-503	1 2 3 4 5 7 8	A
28-12N-11E ARCO	512-521	1 2 3 4 5 7 8	A
	530-536	1 2 3 4 5 6 7 8	A
	570-591	1 2 3 4 5 6 7 8	B
	610-616	1 2 3 4 5 7 8	B
	658-683	1 2 3 4 5 6 7 8	A
Kuparuk #1			
21-11N-12E ARCO	552-562	1 2 3 5 7	A
	585-604	1 2 3	B

BP (H1)41-28-11-13 21-11N-13E BP	506-515	1 2 3 7	C
S.E. Eileen State #1 35-11N-12E ARCO	739-768 808-831 846-861	1 4 8 1 4 8 1 4 8	B B B
Toolik Red #2 4-8N-9E ARCO	658-672 701-722	2 3 4 8 2 3 4 8	C C
Beechey Point State #1 20-12N-12E ARCO	762-892 960-975 1075-1090	4 6 8 4 6 8 4 6 8	B C C
Gull Island State #2 28-12N-15E ARCO	128-139 143-162 347-363 418-424 433-442	2 3 7 2 3 7 2 3 7 2 3 7 2 3 7	B B C C C
Highland State #1 24-11N-11E ARCO	527-549 860-872	1 2 3 7 1 2 3 4 7 8	C C
West Sk River #3 26-11N-9E ARCO	360-378 415-436	1 2 3 4 5 7 8 1 2 3 4 5 7 8	A A
West Sak River #5 11-10N-10E ARCO	363-372 329-335 517-527	1 2 3 4 5 7 8 1 2 3 4 5 7 8 1 2 3 4 5 7 8	B B B
Kuparuk (7-11-12) 7-11N-12E Mobil	293-320 399-402 533-543 568-593	1 4 5 8 1 4 5 8 1 4 5 8 1 4 5 8	B C C C
W. Kuparuk State #1 3-11N-11E Mobil	582-591 625-643 678-692	1 2 3 4 7 8 1 2 3 4 7 8 1 2 3 4 7 8	C A A
33-29E (29-12-11) 29-12N-11E Standard	448-463 472-512 567-576 619-671	1 2 3 4 8 1 2 3 4 8 1 2 3 4 8 1 2 3 4 8	A B B B
Colville Delta State #1 9-13N-6E Gulf	338-344 439-451	1 2 3 4 7 8 1 2 3 4 7 8	B C
Hurl State #1 5-10N-13E Mobil	582-591	1 2 3 5	B

Milne Point 18-1	494-521	1 2 3 4 5 7 8	C
11-13N-10E Contin.	643-649	1 2 3 4 5 7 8	C
	735-750	1 2 3 4 7 8	C
N. Kuparuk State #1	719-741	1 2 3 4 5 7 8	B
26-12N-12E Mobil			
W. Kadleroshilik Unit #1	482-491	1 2 3 4 5 7 8	B
14-5N-14E Mobil	549-555	1 2 3 4 5 7 8	C
W. Staines State #1	527-549	1 2 3 4 7 8	C
18-9N-23E Mobil	576-582	1 2 3 4 7 8	C
Hemi State #1	457-472	1 2 3 5 7	B
3-9N-11E Mobil	492-506	1 2 3 5 7	A
Kalubik Creek #1	158-195	2 3 4 7 8	C
10-12N 8E Union	207-242	2 3 4 7 8	C
	578-590	2 3 4 7 8	B
Kaverak Pt. 32-25	512-552	1 4 8	B
25-13N-10E Standard	646-690	1 4 8	A
Ugna #1	318-320	4 8	B
22-12N-9E Sinclair	832-835	1 4 5 7 8	C
	853-863	1 2 3 4 5 7 8	B
W. Sak #7	287-305	2 3 4 7 8	B
9-11N-10E ARCO	367-383	2 3 4 7 8	B
	427-436	2 3 4 7 8	B
	443-471	2 3 4 7 8	B
W. Sak #1	436-451	2 3 7	A
2-10N-11E ARCO	472-451	2 3 7	A
	497-509	2 3 7	A
	518-533	2 3 7	A
Kuparuk A-8 (W. Sak)	174-186	2 3 4 7 8	A
5-11N-10E	395-411	2 3 4 7 8	A
	471-482	2 3 4 7 8	A
W. Sak #2	297-314	2 3 7	A
22-11N-10E ARCO	450-454	2 3 7	A
	552-567	2 3 4 7 8	A
W. Sak #9	165-169	2 3 4 8	A
3-11N-9E SOHIO	174-198	2 3 4 8	A
	215-265	2 3 4 8	A
	427-451	2 3 4 8	A

W. Sak #8	207-235	2 3 4 6 7 8	A
23-11N-10E ARCO	320-326	2 3 4 7 8	A
	402-415	2 3 4 6 7 8	A
	433-446	2 3 4 6 7 8	A
	466-469	2 3 4 6 7 8	A
	491-509	2 3 4 6 7 8	A
W. Sak #4	213-241	2 3 6 7	A
7-10N-9E SOHIO	311-332	2 3 6 7	A
	457-469	2 3 6 7	A
W. Sak #10	290-305	2 3 4 7 8	A
23-10N-9E ARCO	311-320	2 3 4 7 8	A
	323-338	2 3 4 7 8	A
	354-372	2 3 4 7 8	A
	378-393	2 3 4 7 8	A
	395-411	2 3 4 7 8	A
	415-457	2 3 4 7 8	A
	463-488	2 3 4 7 8	A
W. Sak #6	366-418	2 3 7	A
29-11N-11E ARCO	466-488	2 3 4 7 8	A
W. Sak #11	282-296	2 3 4 7 8	A
36-12N-8E SOHIO	305-326	2 3 4 7 8	A
	332-335	2 3 4 7 8	A

REFERENCES

Ahlbrandt, T.S., 1979: Introduction to Geologic Studeis of the Nanushuk Group, North Slope, Alaska, in T.S. Ahlbrandt, ed., Preliminary Geologic, Petrologic, and Paleontologic Results of the Study of Nanushik Group Rocks, North Slope, Alaska: U.S. Geologic Survey Circular 794, p. 1-4.

Anderson, D.M., Tice, A.R. and McKim, H.L., 1973: The unfrozen water and the apparent specific heat capacity of frozen soils, in Proc. of the Second International Conference on Permafrost, Yakutsk, U.S.S.R., National Academy of Sciences, Washington, D.C.

Bily, C., and Dick, J.W.L., 1974: Naturally Occurring Gas Hydrates in the Mackenzie Delta, N.W.T.: Bulletin of Canadian Petroleum Geology, v. 22, no. 3, p. 340-352.

Bird, K.J., 1982: Rock-Unit Reports of 228 Wells Drilled on the North Slope, Alaska: U.S. Geological Survey Open-File Report 82-278, 106 p.

Detterman, R.L., Reiser, H.N., Brosage, W.P., and Dutro, J.T., Jr., 1975: Post-Carboniferous Stratigraphy, Northeastern Alaska: U.S. Geological Survey Professional Paper 886, 46 p.

Evrenos, A.I., Heathman, J., and Ralstin, J., 1971: Impermeation of porous media by forming hydrates in-situ: Journal of Petroleum Technology, v. 23, p. 1059-1066.

GARP (Global Atmospheric Research Program), 1977: Panel on Climatic Variation: National Academy of Science, no. 19, p. 12.

Gryc, G., Patton, W.W., Jr., and Payne, T.G., 1951: Present Cretaceous Stratigraphic Nomenclature of Northern Alaska: Washington Academy of Science Journal, v. 41, no. 5, p. 159-167.

Hall, G.H., 1979: Recognition of Hydrates by Use of Open Hole Logs of NPRA Wells, in A.L. Bowsher, ed., Proceedings of a workshop on Clathrates (Gas Hydrates) in the National Petroelum Reserve in Alaska, July 16-17, 1979 Menlo Park California: U.S. Geological Survey Open-File Report No. 81-1298, p. 40-43.

Holder, G.D., Katz, D.L., and Hand, J.H., 1976: Hydrate Formation in Subsurface Environments: American Association of Petroleum Geologists Bulletin, v. 60, no. 6, p. 981-994.

Howitt, F., 1971: Permafrost Geology in Pudhoe Bay, Alaska: World Petroleum, September, p. 28-34.

Katz, D.L., 1971: Depths to Whick Frozen Gas Fields (Gas Hyudrates) may be expected: Journal of Petroleum Technology, v. 23, p. 419-423.

Katz, D.L., 1945: Prediction of Conditions for Hydrate Formation in Nautral Gases: Trans. AIME, v. 160, p. 140-149.

Kvenvolden, D.A., and McMenamin, M.A., 1980: Hydrates of Natural Gas: A Review of Their Geologic Occurrence: U.S. Geological Survey Circular 825, 11 p.

Lachenbruch, A.H., Sass, J.H., Marshall, B.V., and Moses, T.H., 1982: Permafrost, Heat Flow, and the Geothermal Regime at Prudhoe Bay, Alaska: Journal of Geophysical Research, v. 87, no. B11, p. 9301-9316.

Lachenbruch, A.H., and Marshall, B.V., 1969: Heat Flow in the Arctic: Arctic, v. 22, p. 300-311.

Mackogon, Y.F., 1981: Hydrates of Natural Gas: PennWell Publishing Company, Tulsa, Oklahoma, 237 p.

Mull, C.G., 1979: Nanushuk Group Deposition and the Late Mesozoic Structural Evolution of the Central and Western Brooks Range and Arctic Slope, in T.S. Ahlbrandt, ed., Preliminary Geologic, Petrologic, and Paleontologic and Paleontologic Results of the Study of Nanushuk Group Rocks, North Slope, Alaska: U.S Geologicl Survey Circular 794, p. 5-13.

Osterkamp, T.E., 1983: Thermal Models for Estimating the Potential Impact of a Warmer Climate on Permafrost in Alaska: Interim Report to the Alaska Council on Science and Technology for Grant W-81-03, 14 p.

Osterkamp, T.E., and Payne, M.W., 1981: Estimates of Permafrost Thickness from Well Logs in Northern Alaska: Cold Regions Science and Technology, v. 5, p. 13-27.

Perkins, T.K., Rochon, J.A., and Knowles, C.R., 1974: Studies of Pressures Generated upon Refreezing of Thawed Permafrost Around a Wellbore, Journal of Petroleum Technology, (October), p. 1159-1166.

Pessel, G.H., Tailleur, I.L., and Bird, K.J., 1978: Generalized Isopach map of Sandstone Within the Colville Group, Eastern North Slope Petroleum Province Alaska: U.S. Geological Survey Miscellaneous Field Studies Map MF-928D.

Pratt, R.M., 1979: Gas Hydrate Evaluation and Recommendations, National Petroleum Reserve, Alaska: U.S. Geological Survey Special Report TC-7916, 27 P.

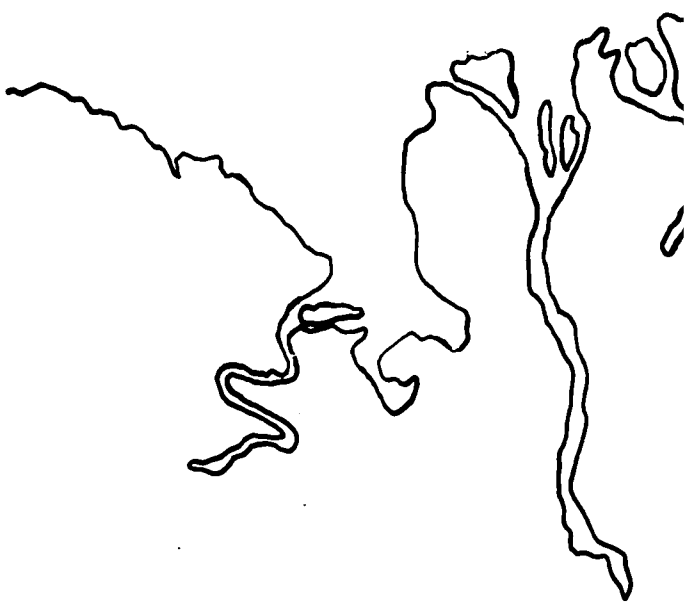

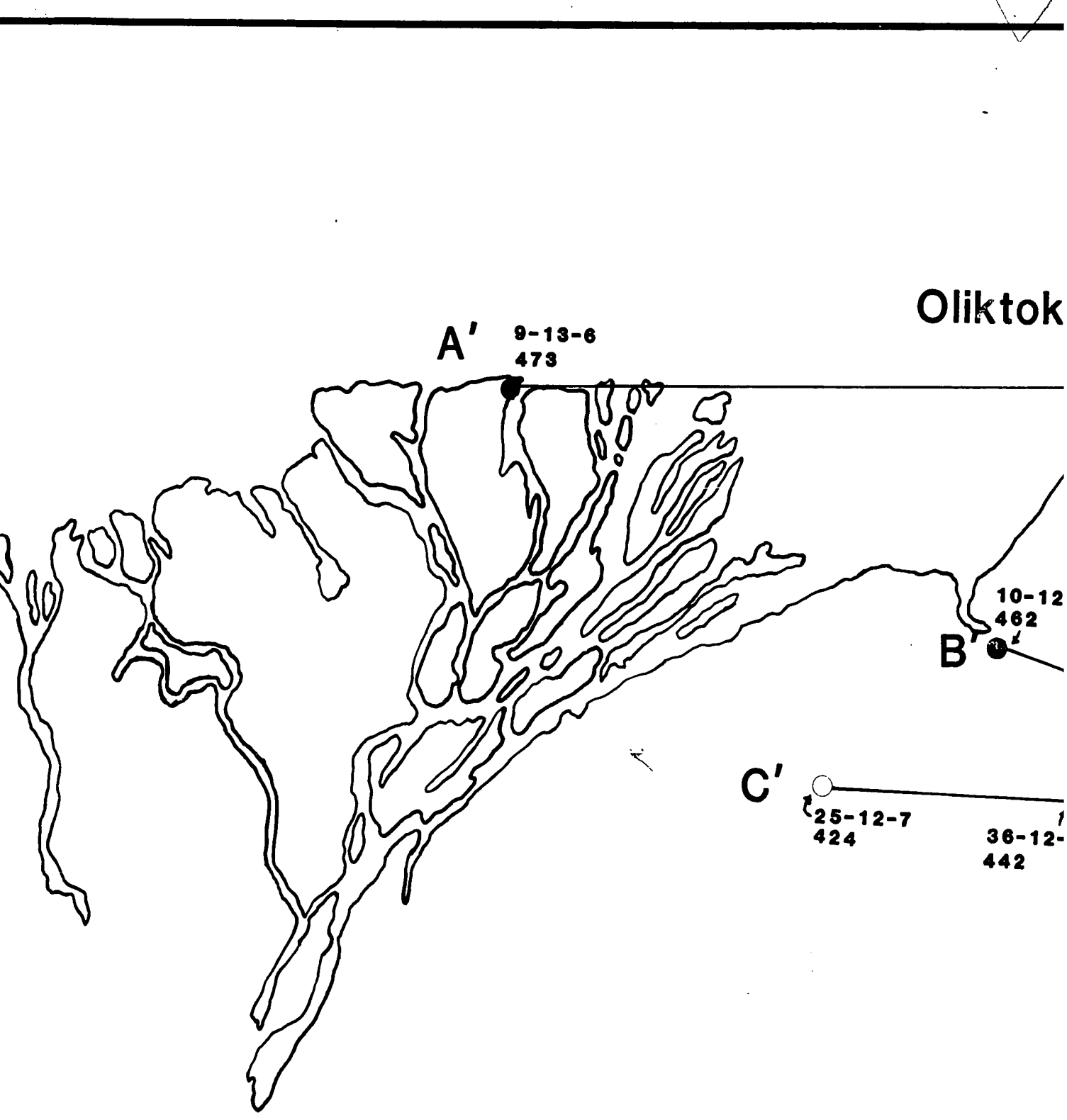

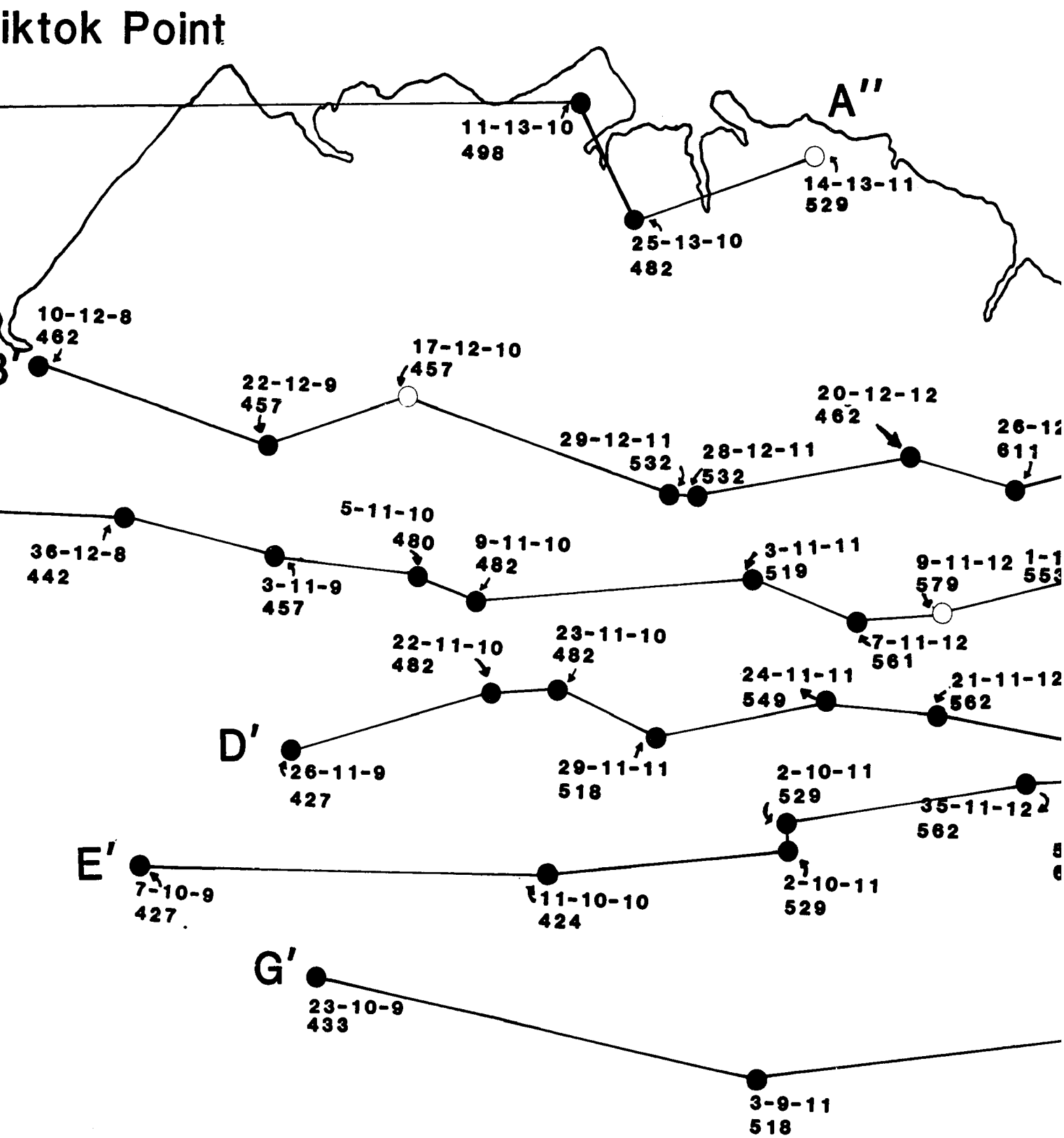

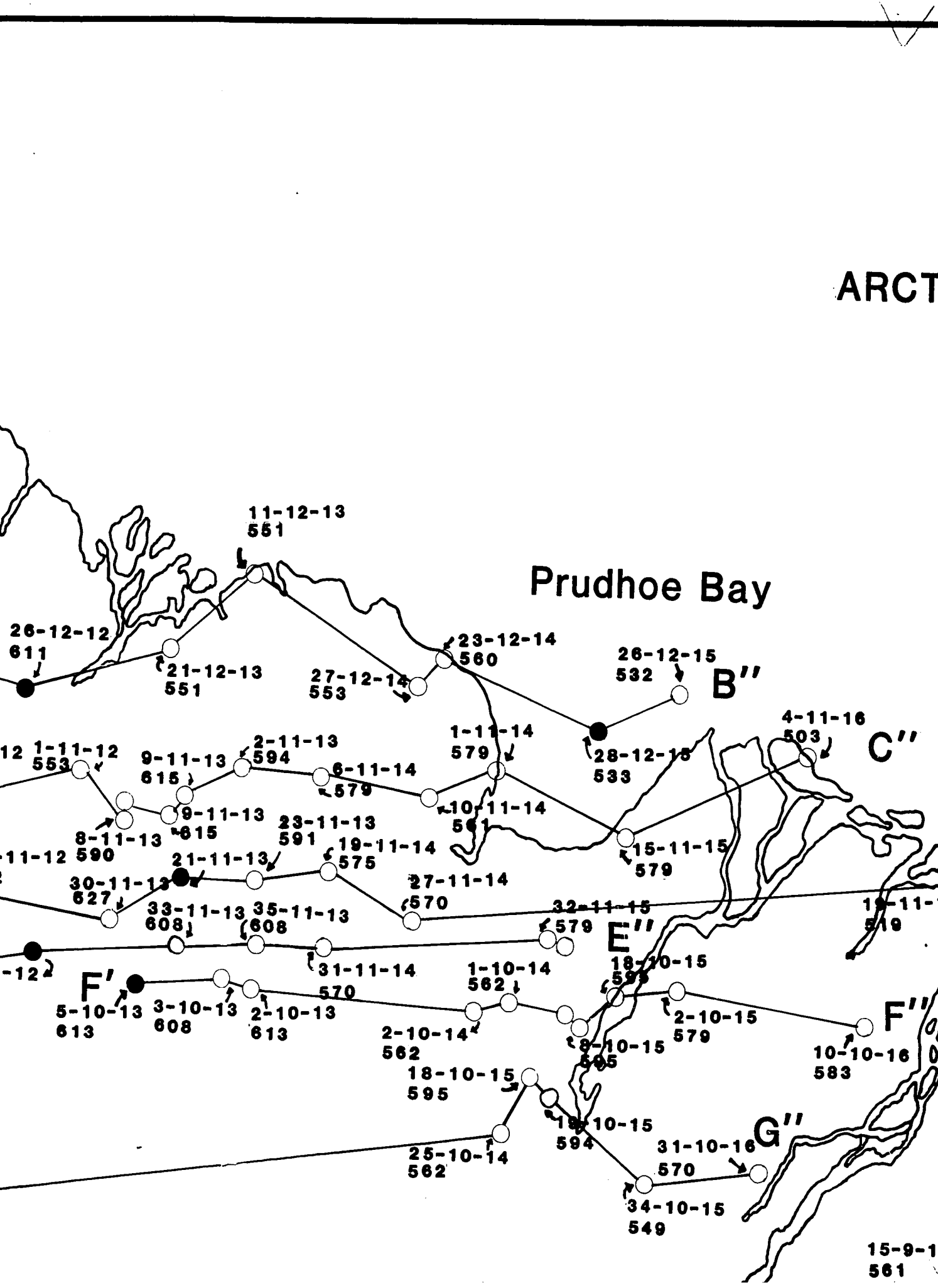

RCTIC OCEAN

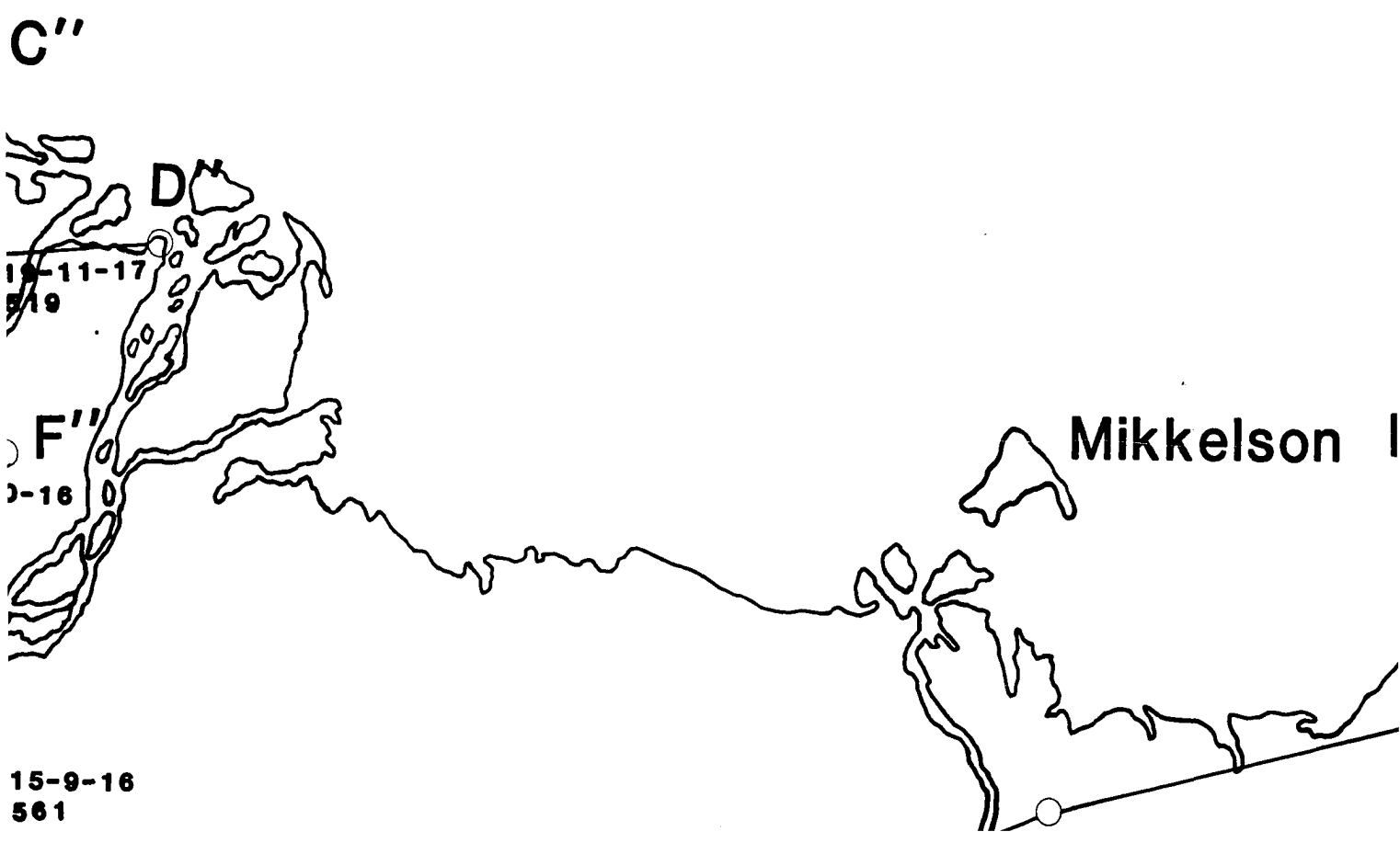

15-9-16
561

on Bay

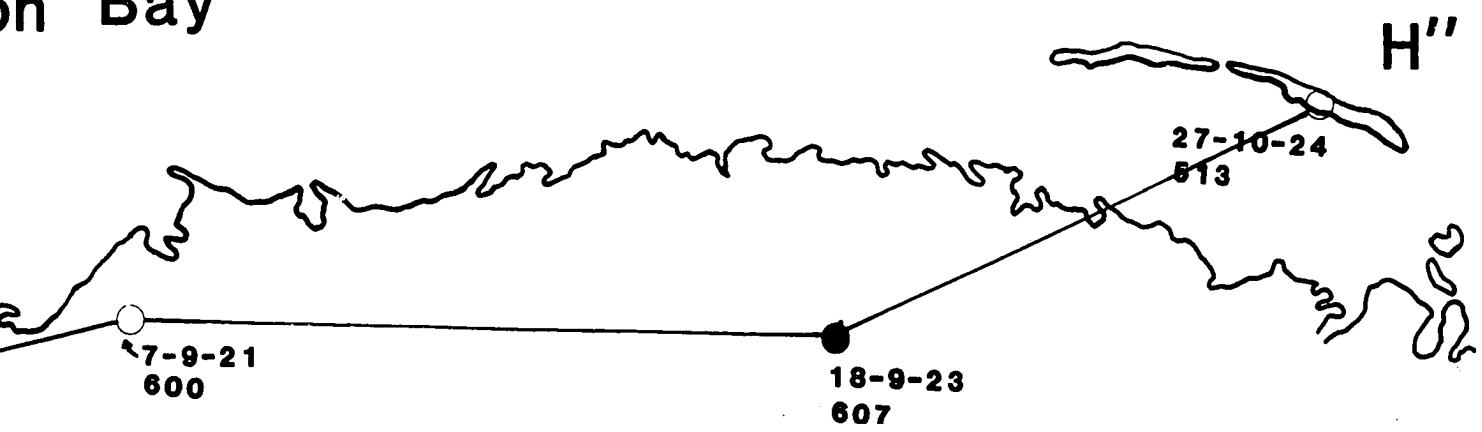

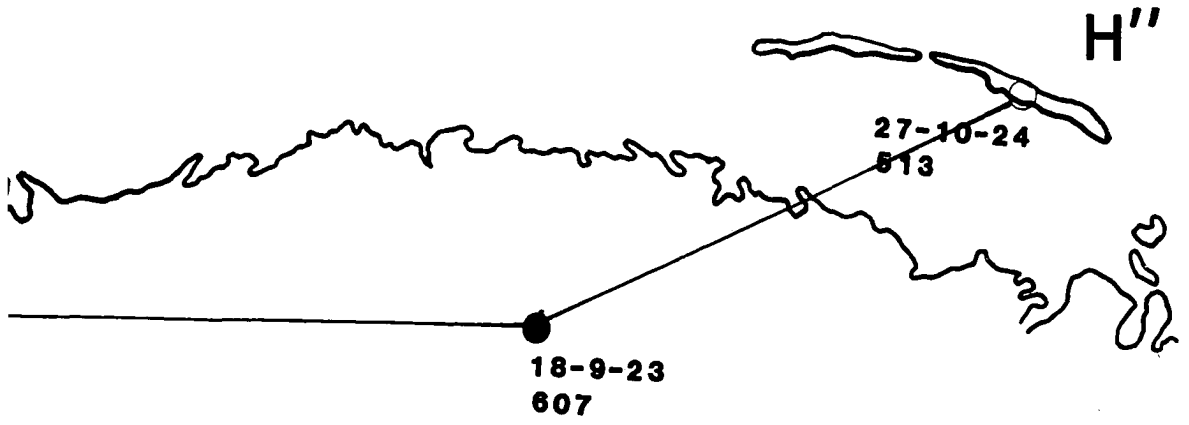

10-8-5
335

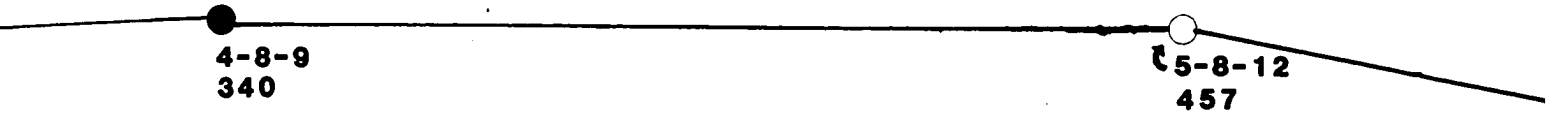

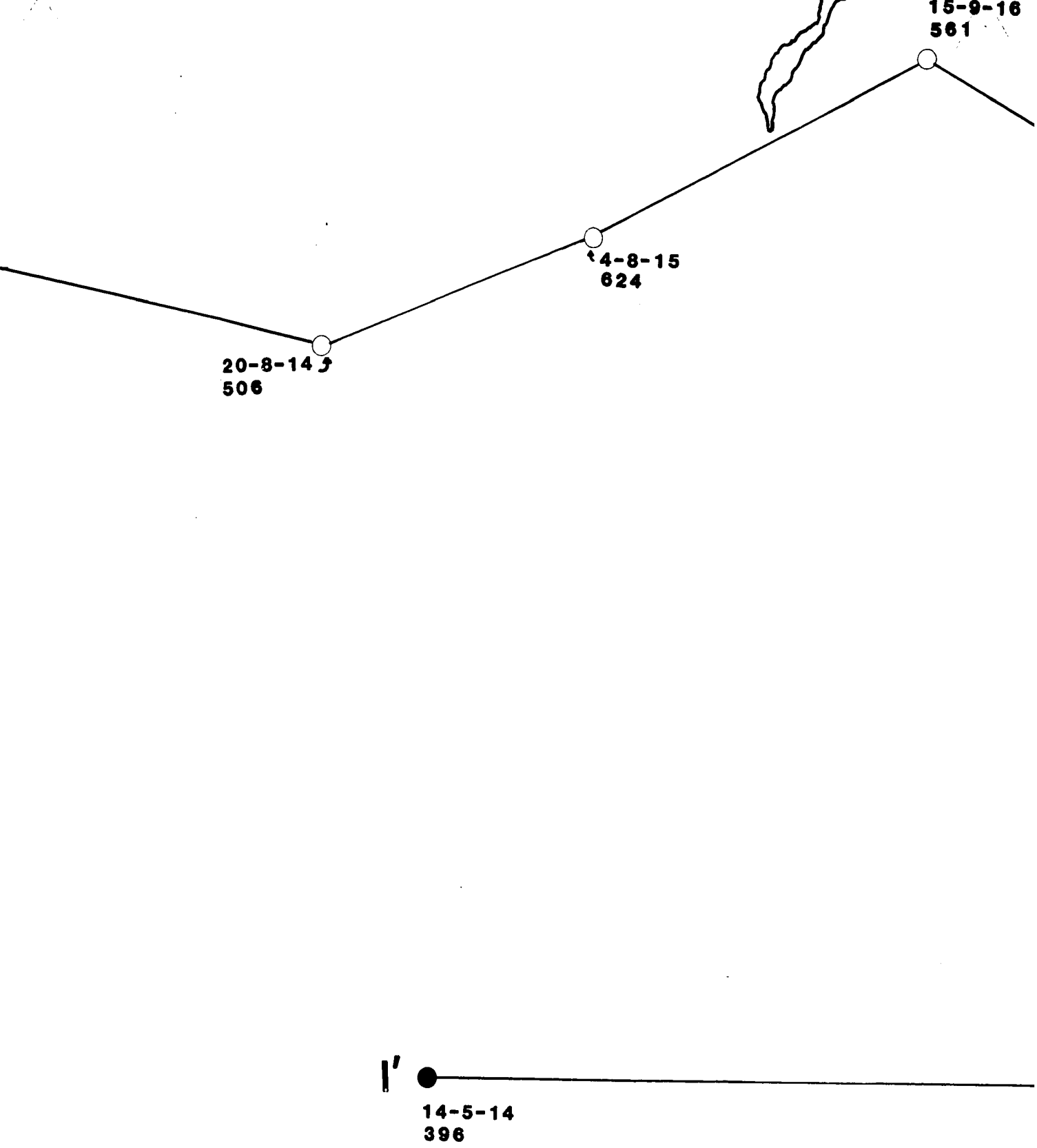

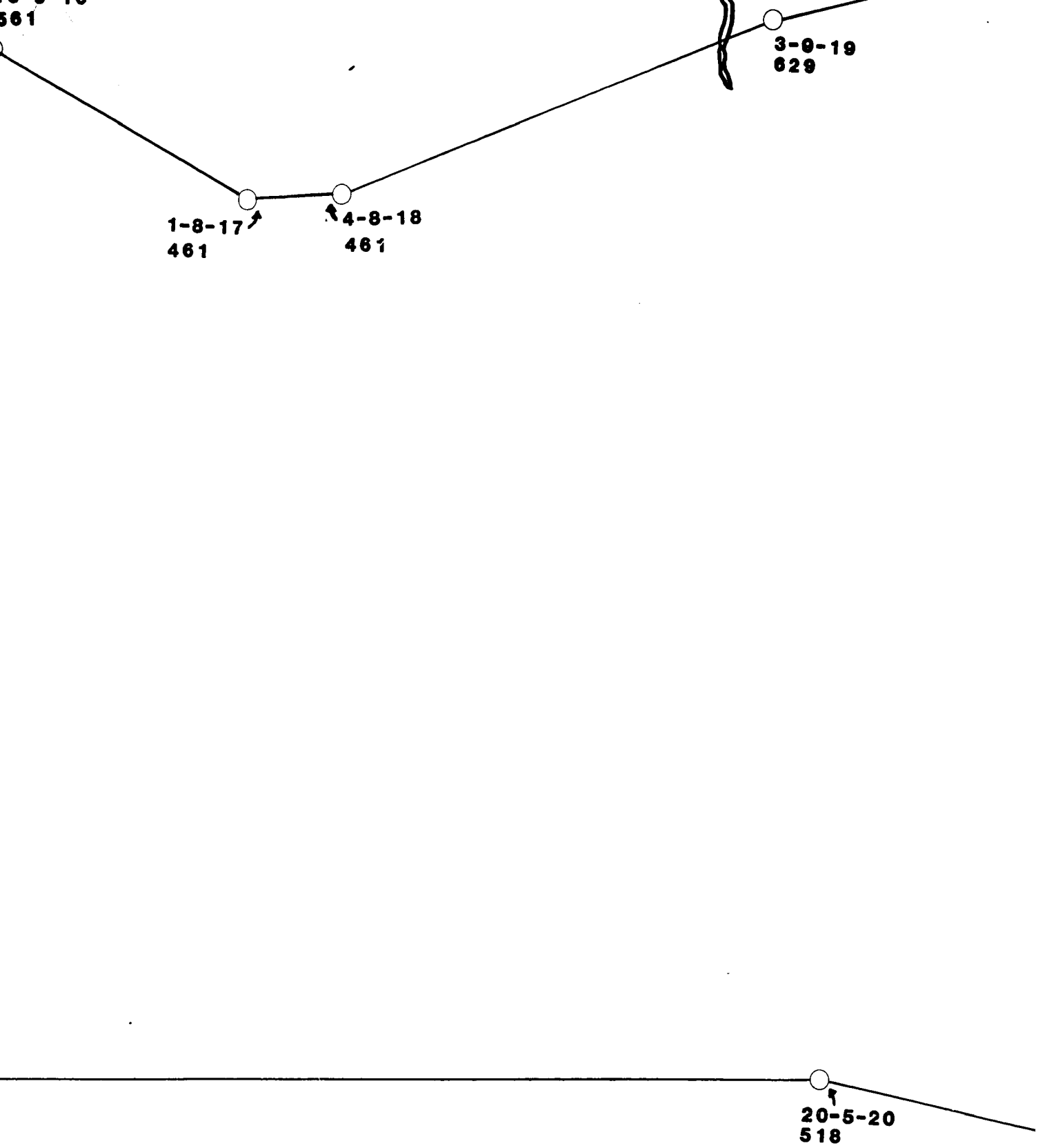

18-9-23
607

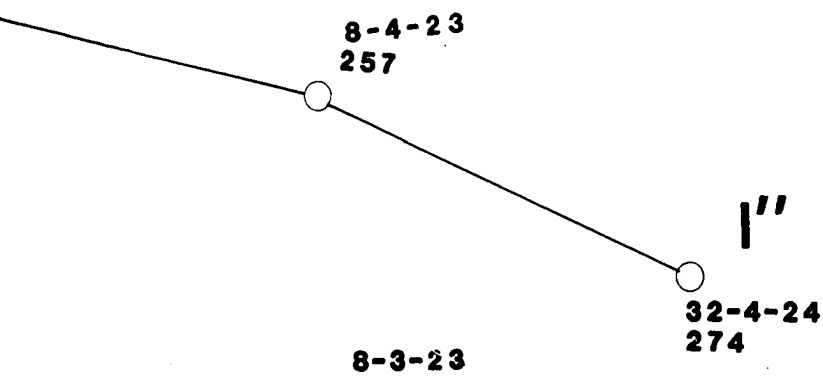

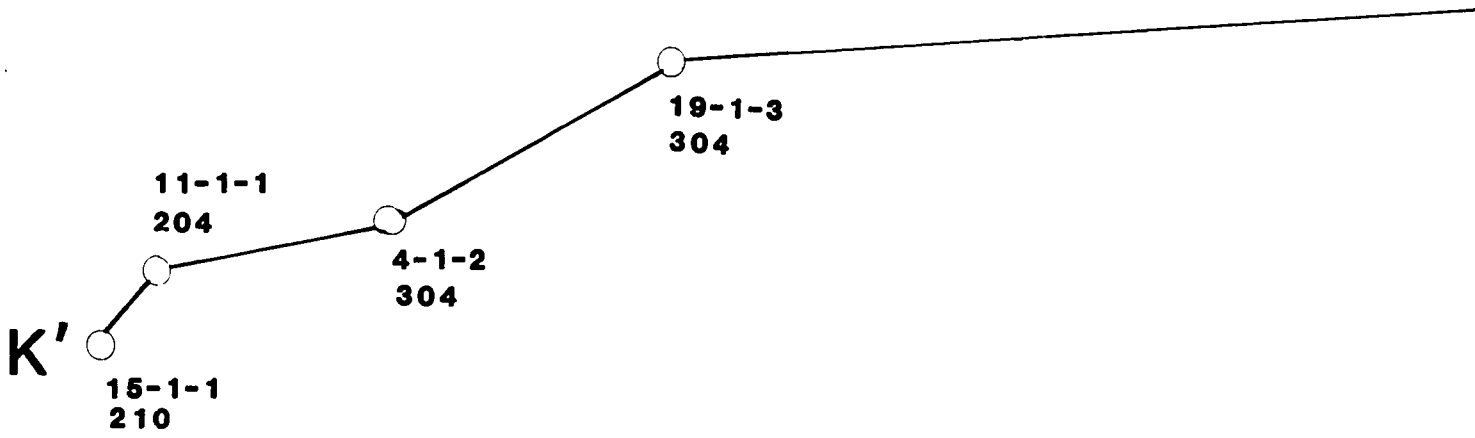

4-3-5

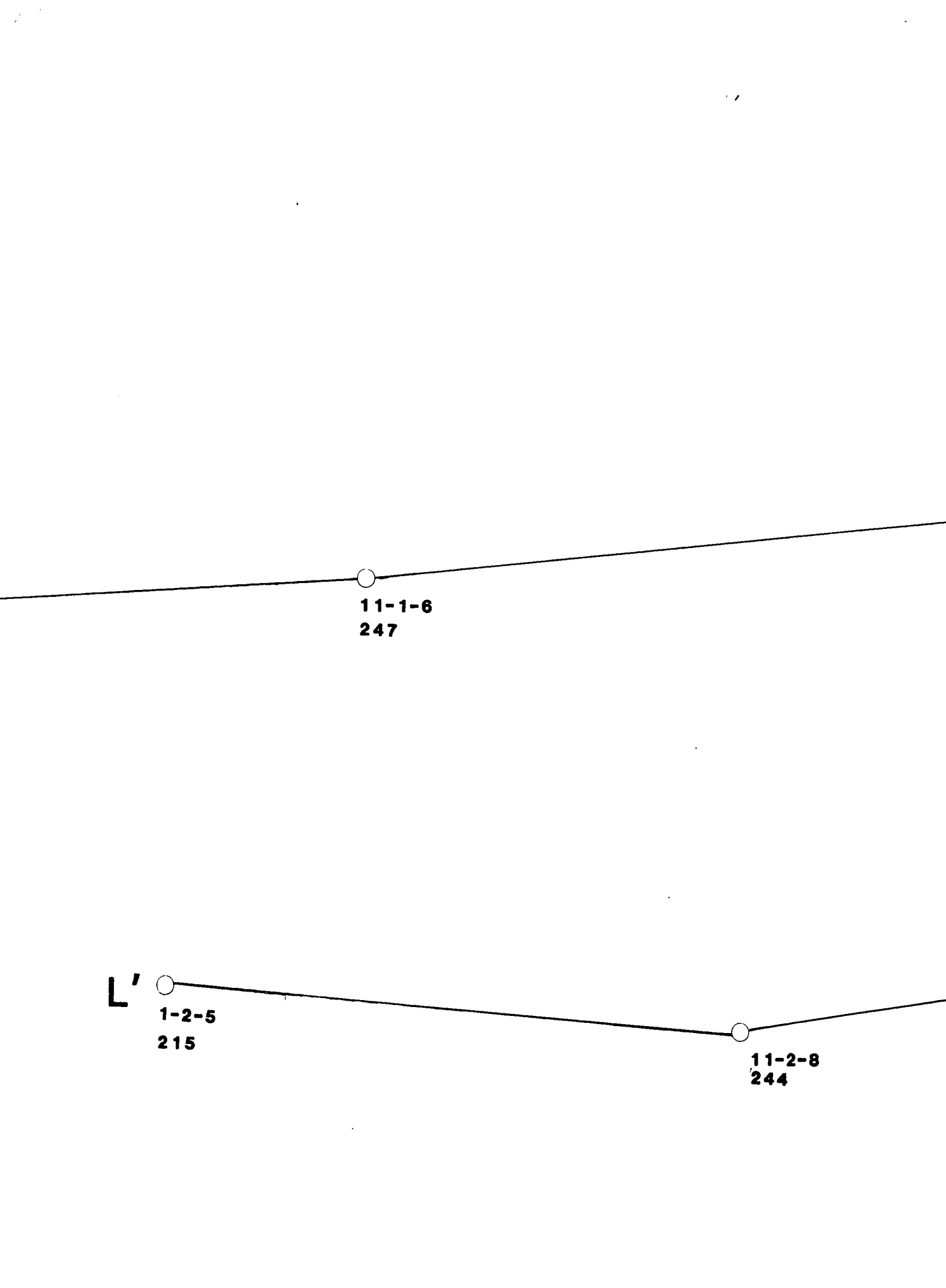

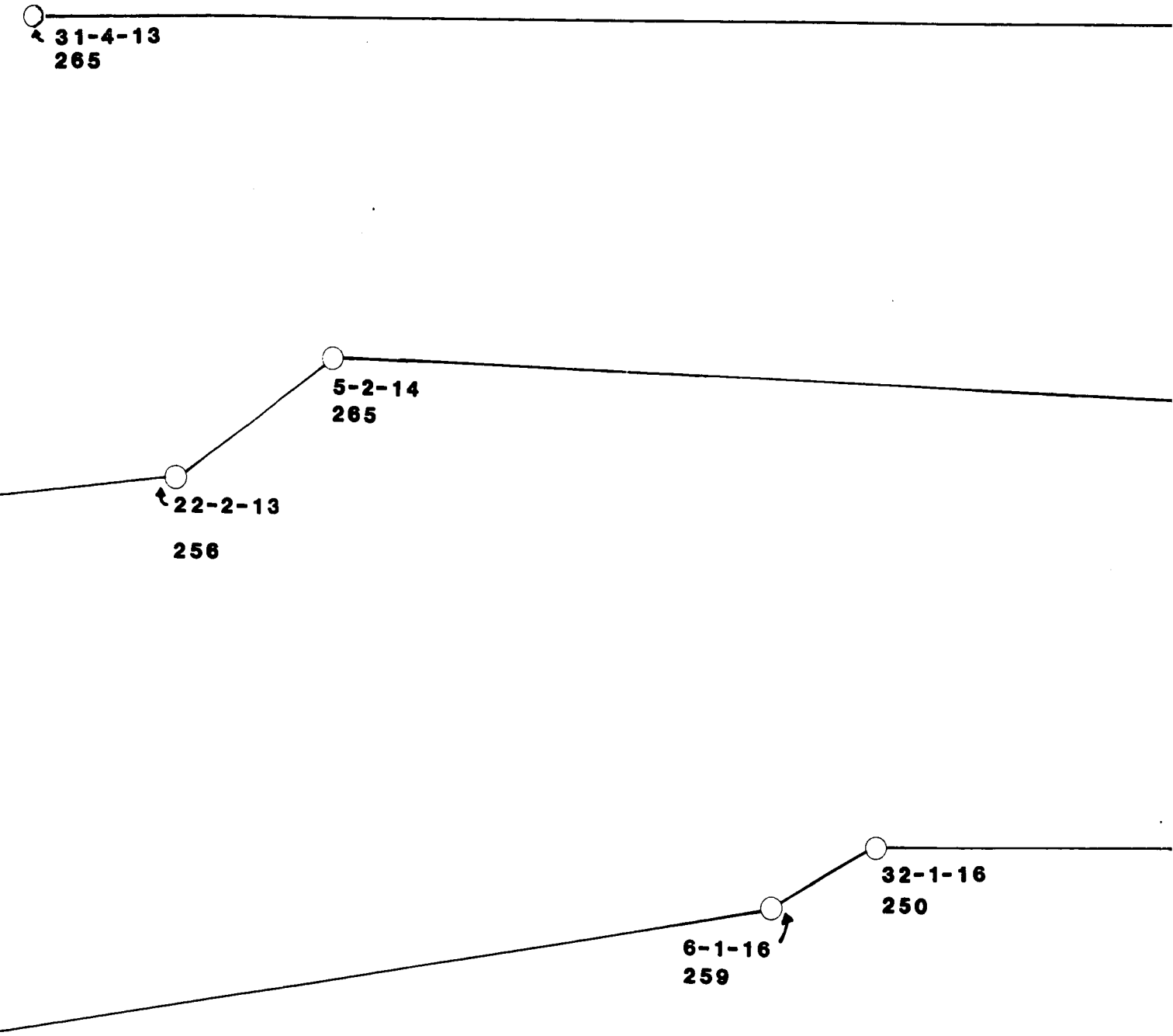

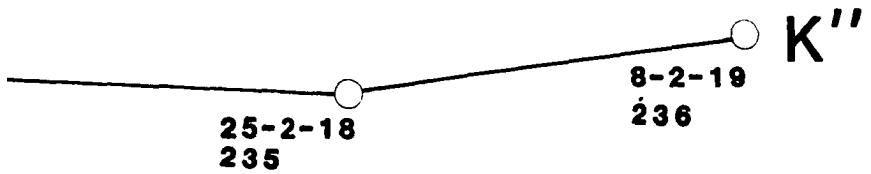

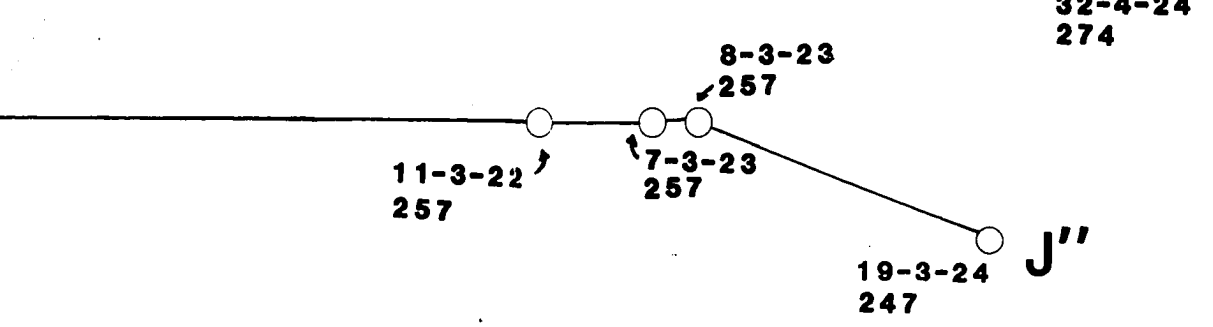

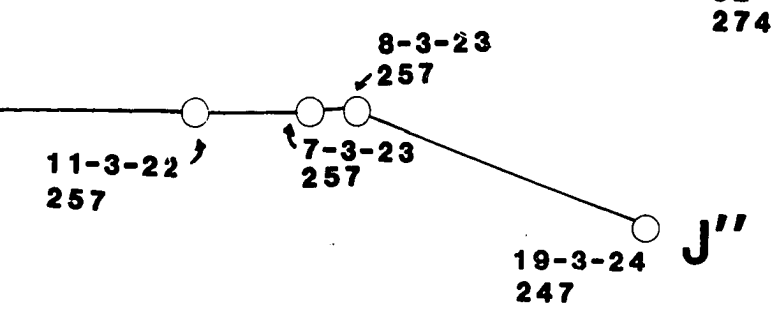

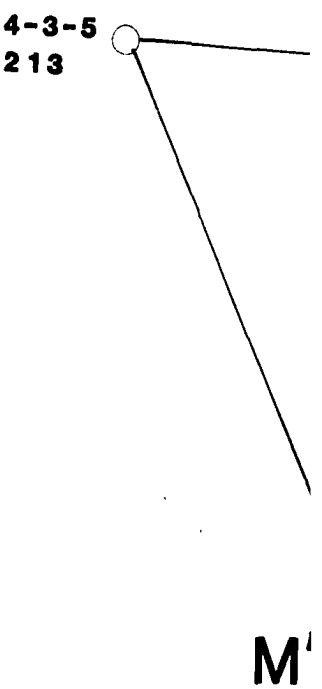

M

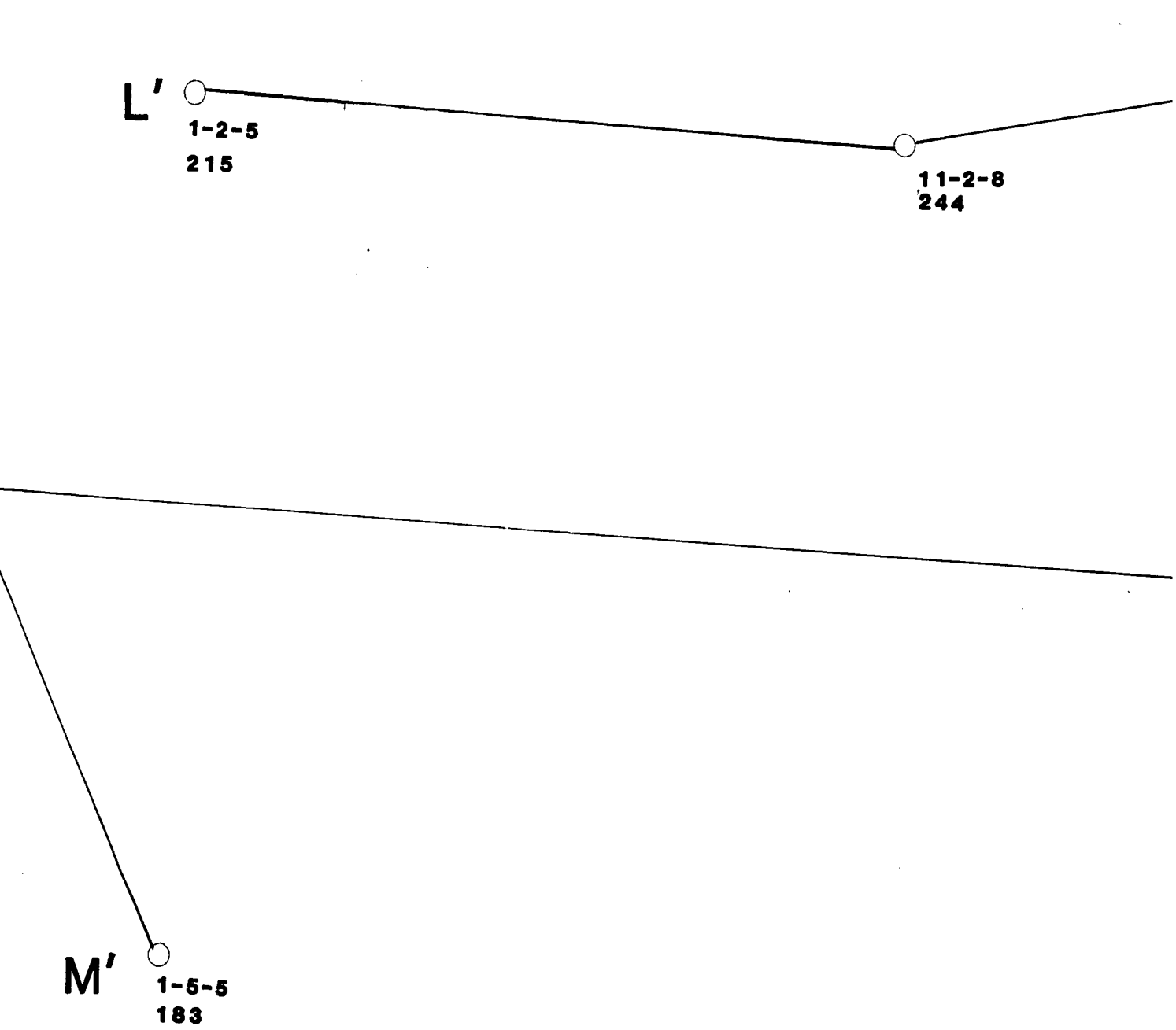

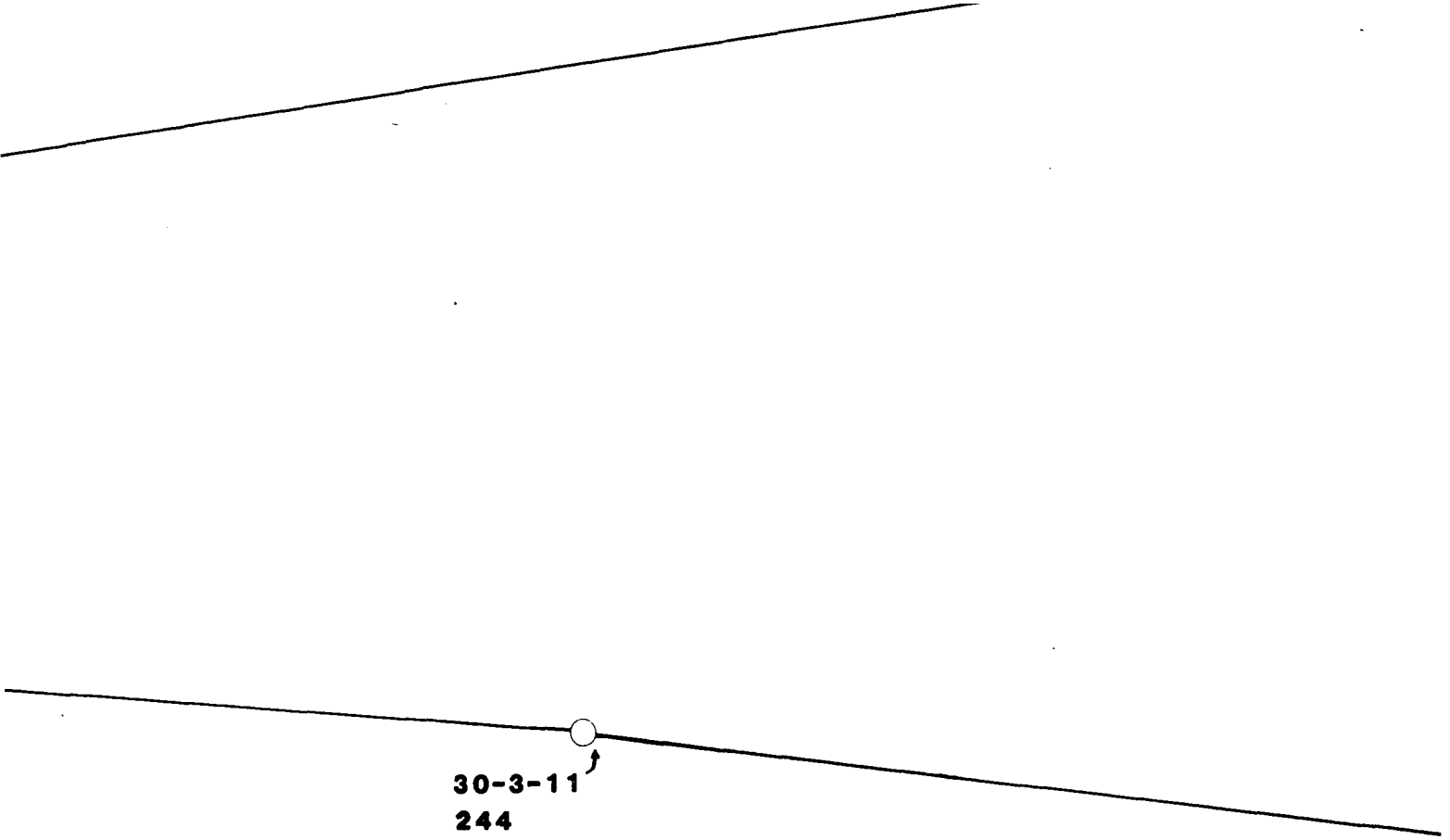

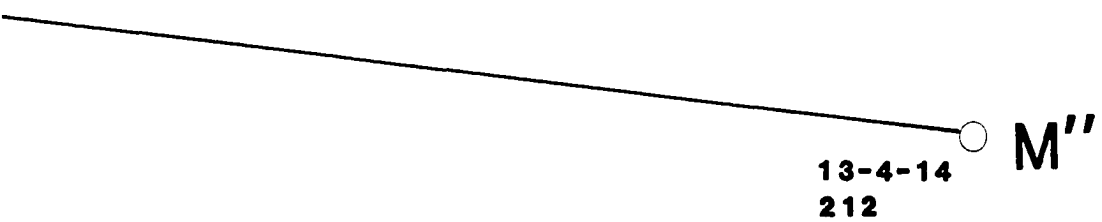

PLATE 1
BASE MAP

Key:

● **Hydrate**

○ **No Hydrate**

4-6-8 Location

346 Depth to the base of the permafrost

(Units in Meters)

Scale

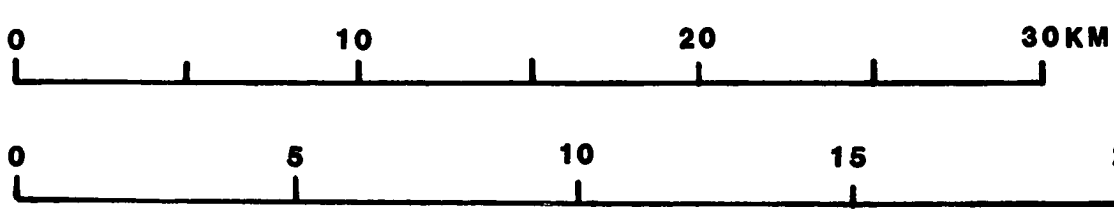

PLATE 1
BASE MAP

ey:

Hydrate

No Hydrate

-6-6 Location

146 Depth to the base of the permafrost

Units in Meters)

Scale

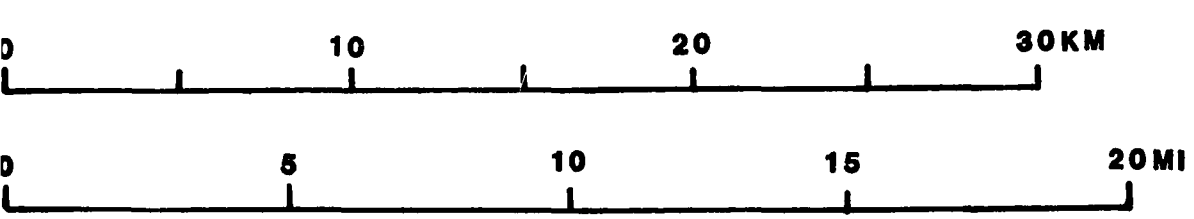

PLATE 1

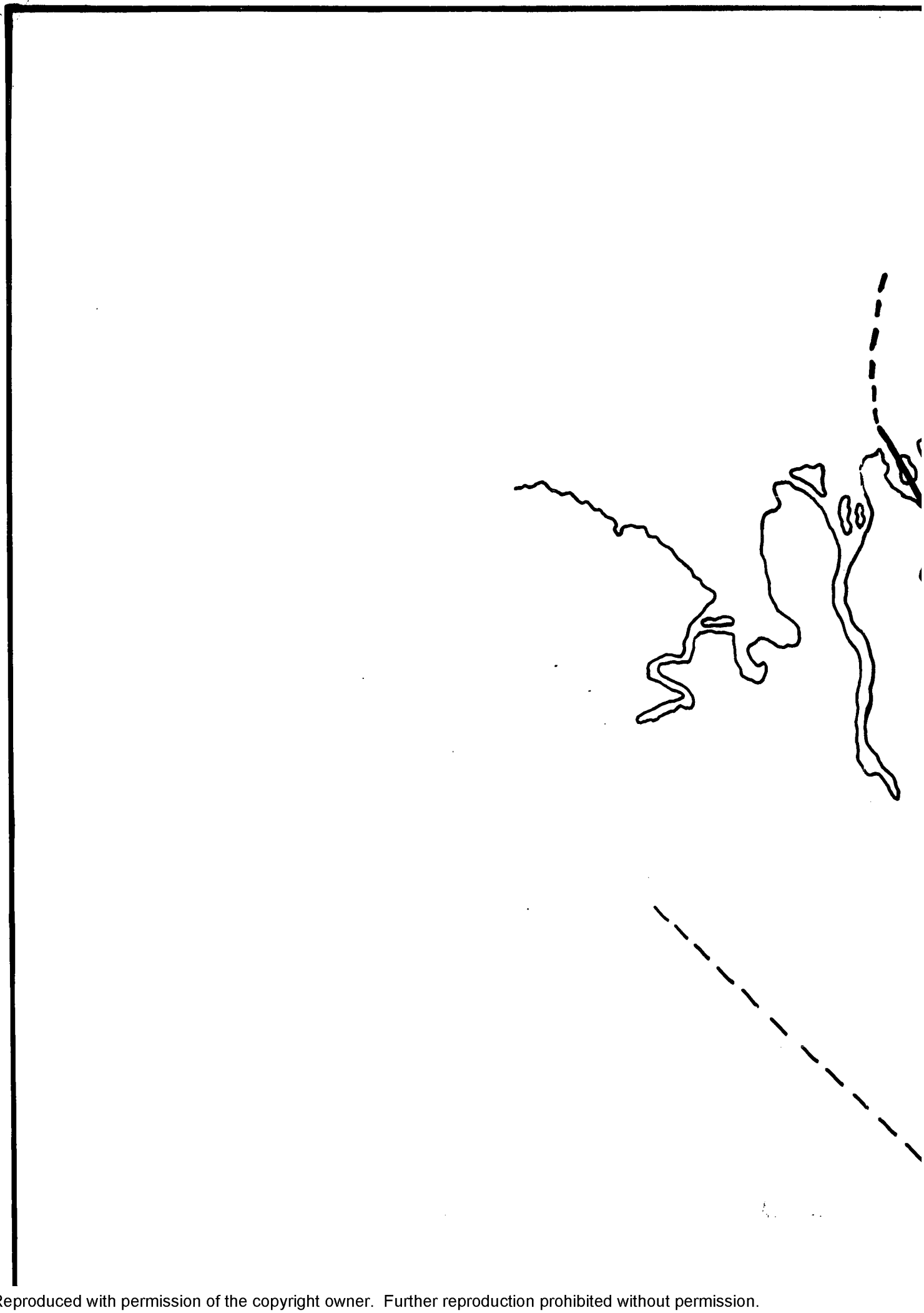

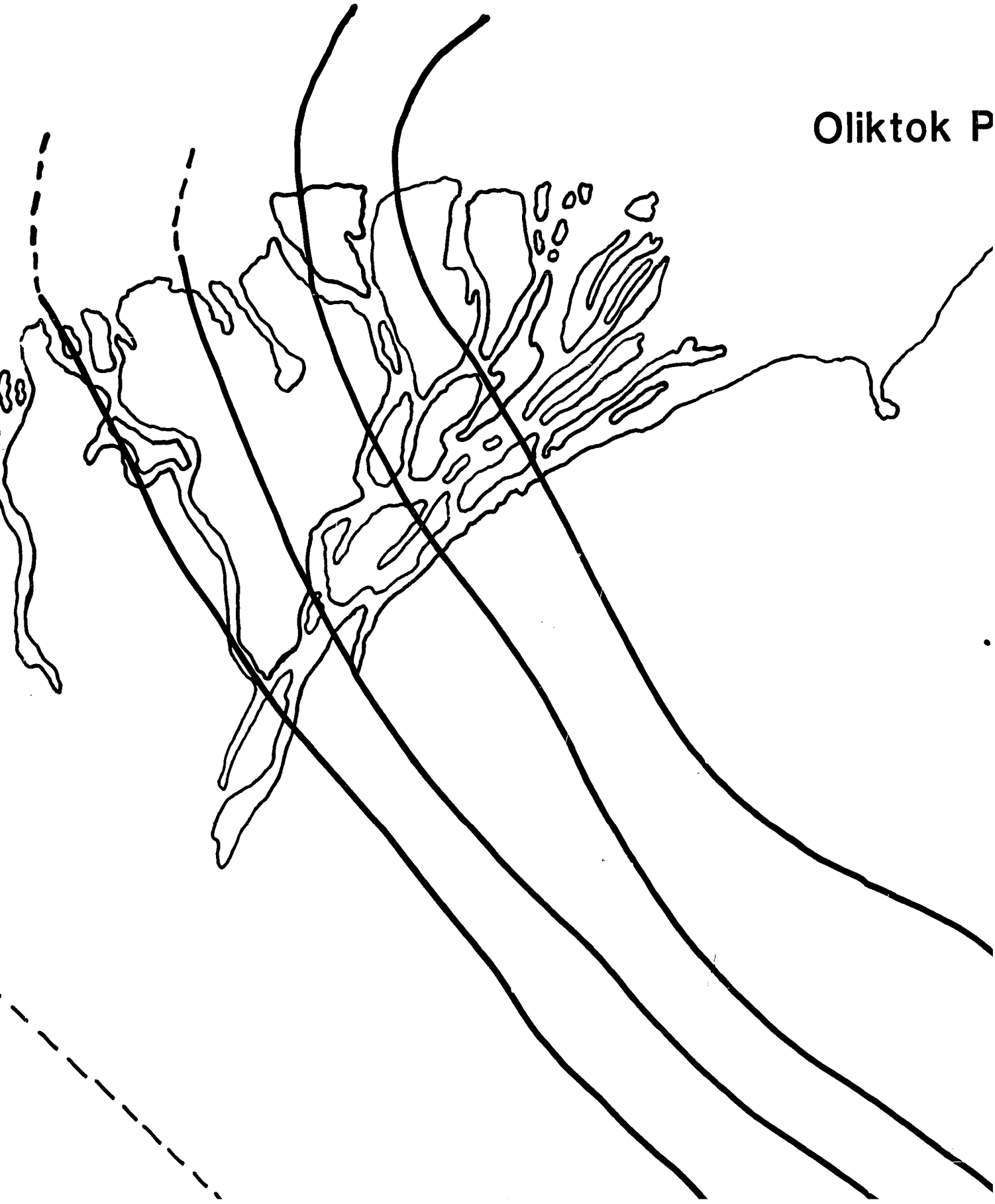

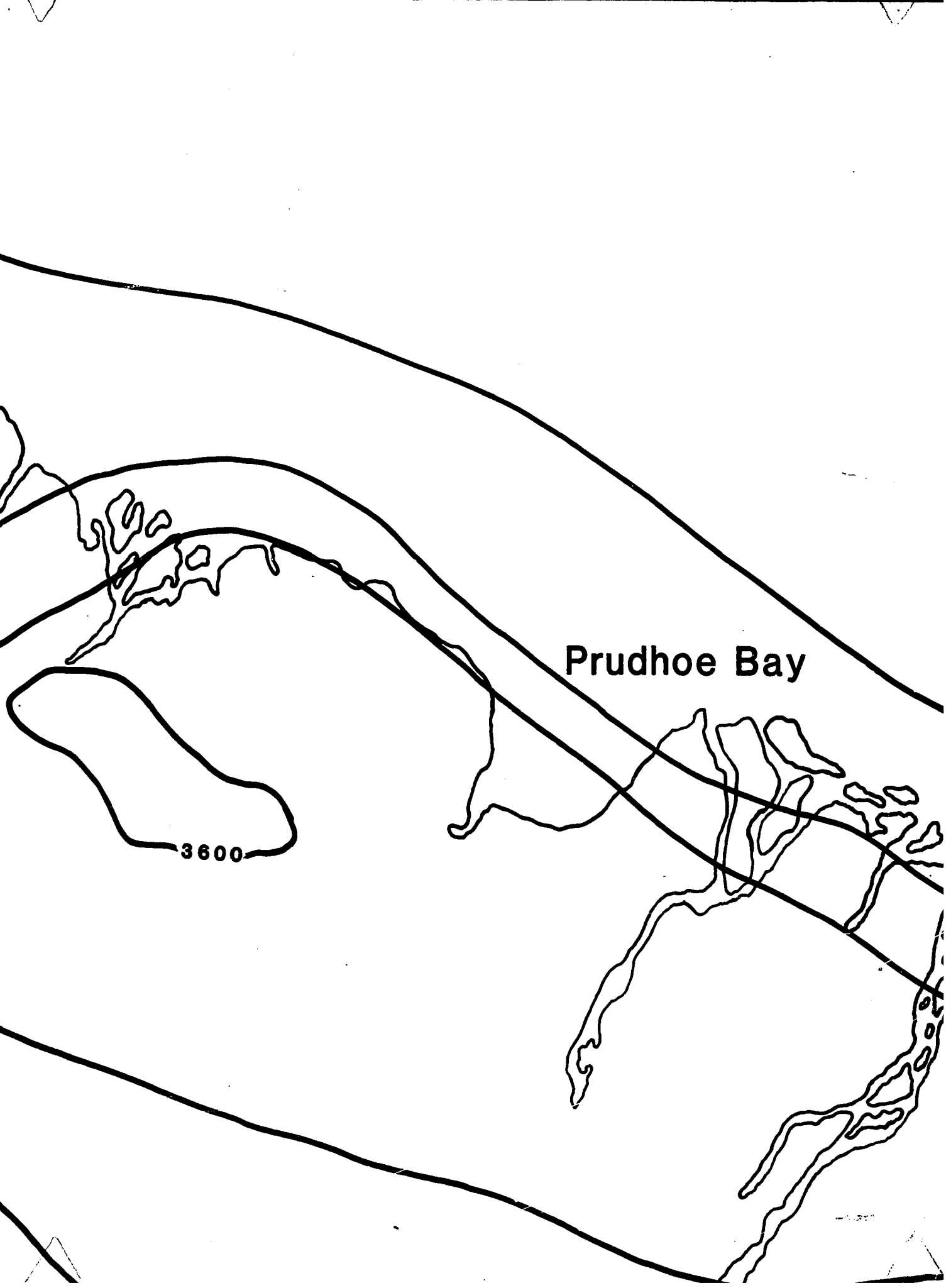

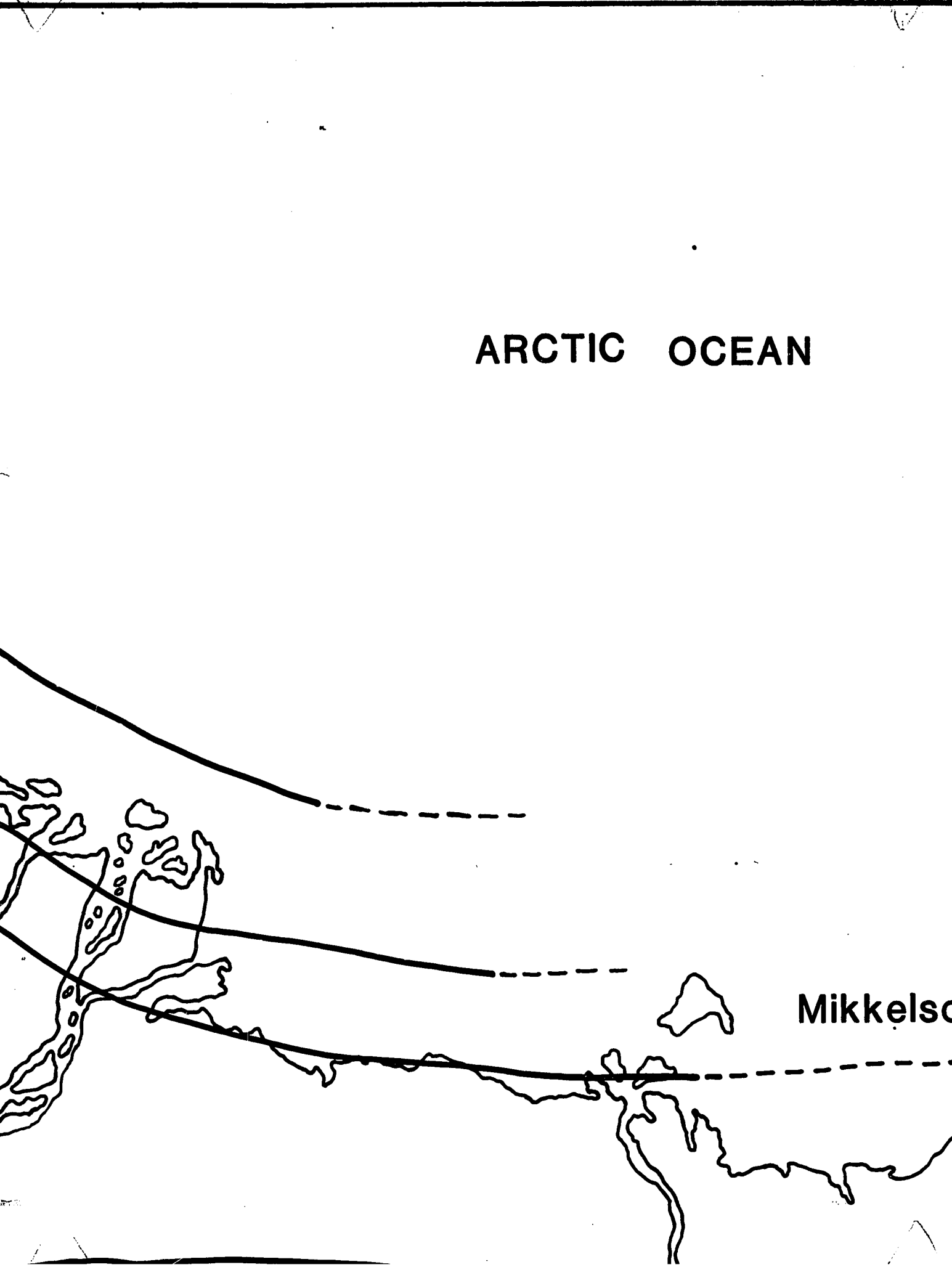

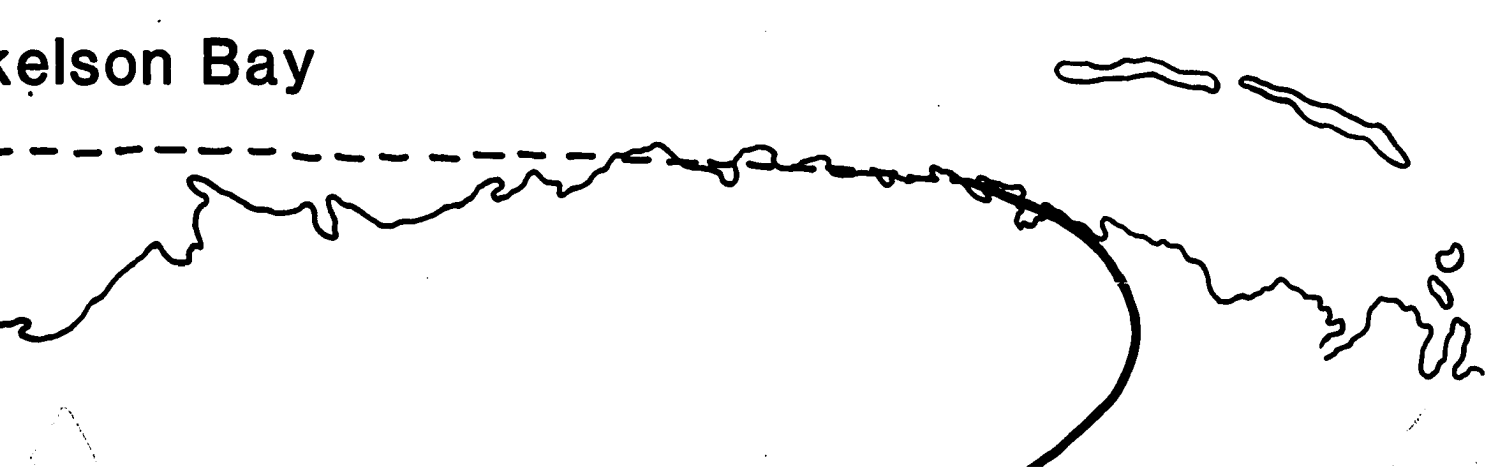

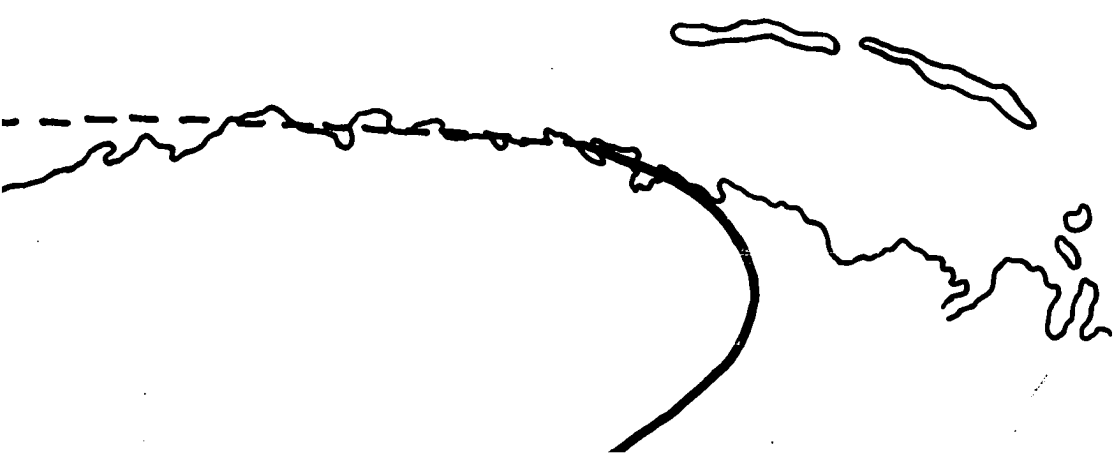

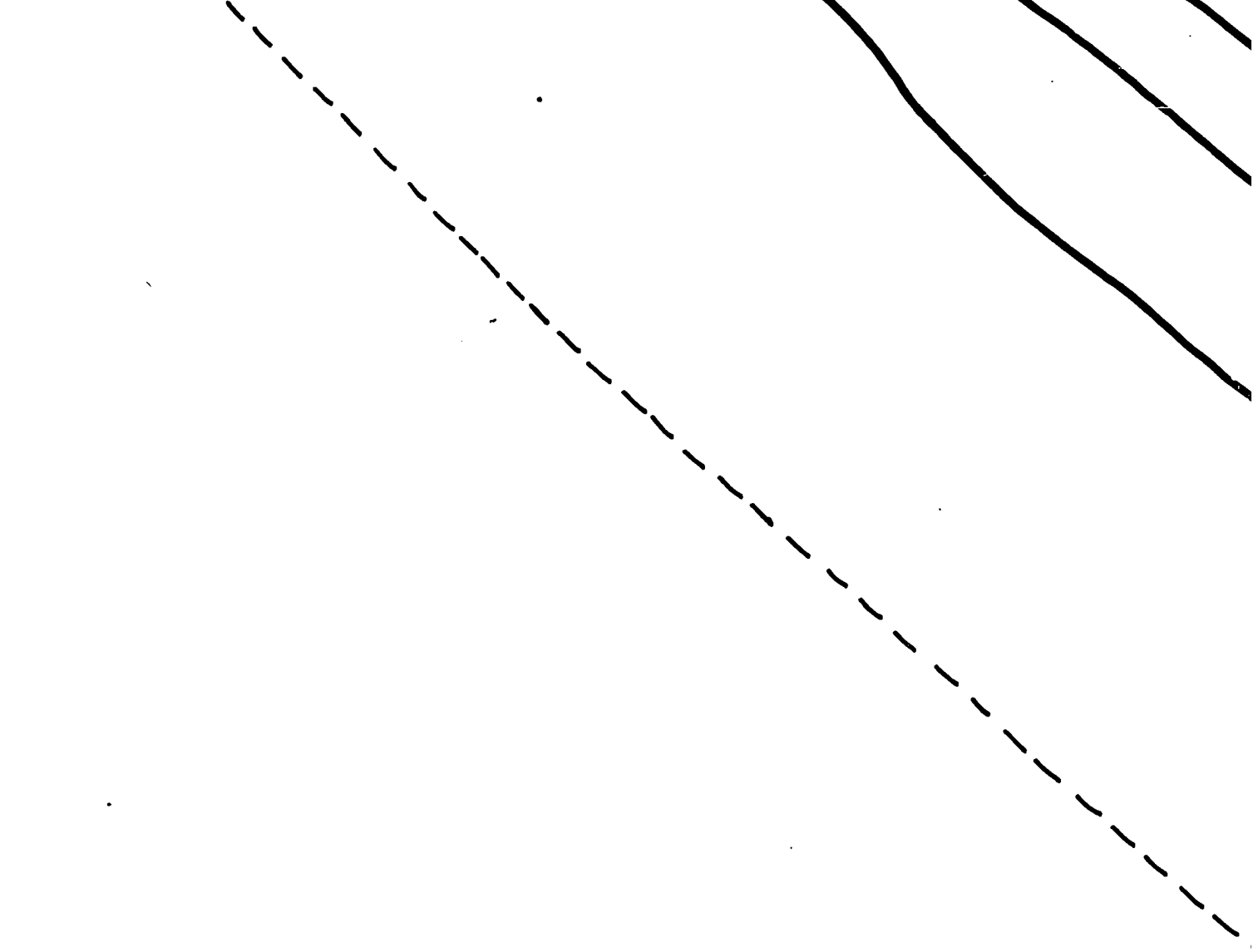

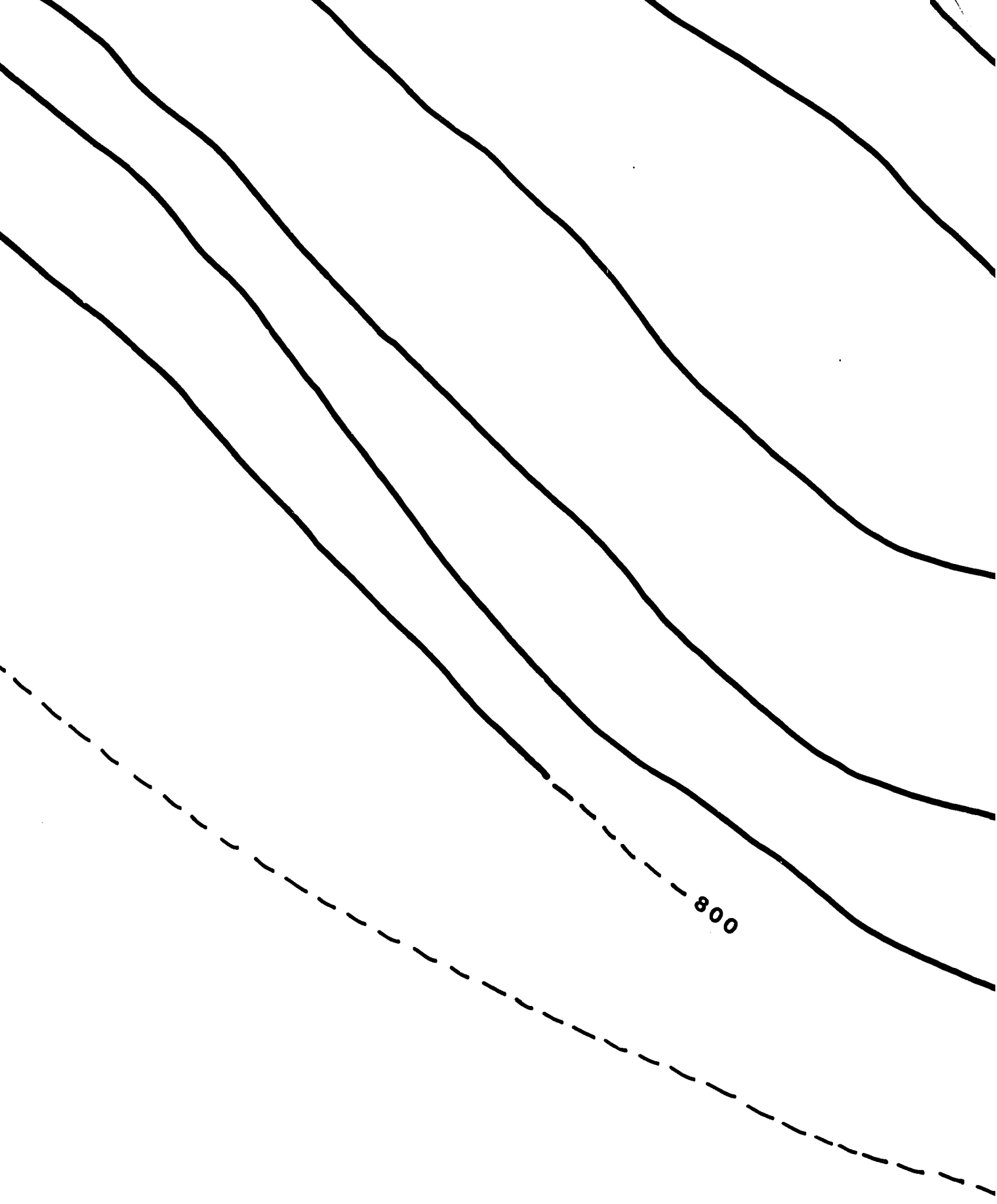

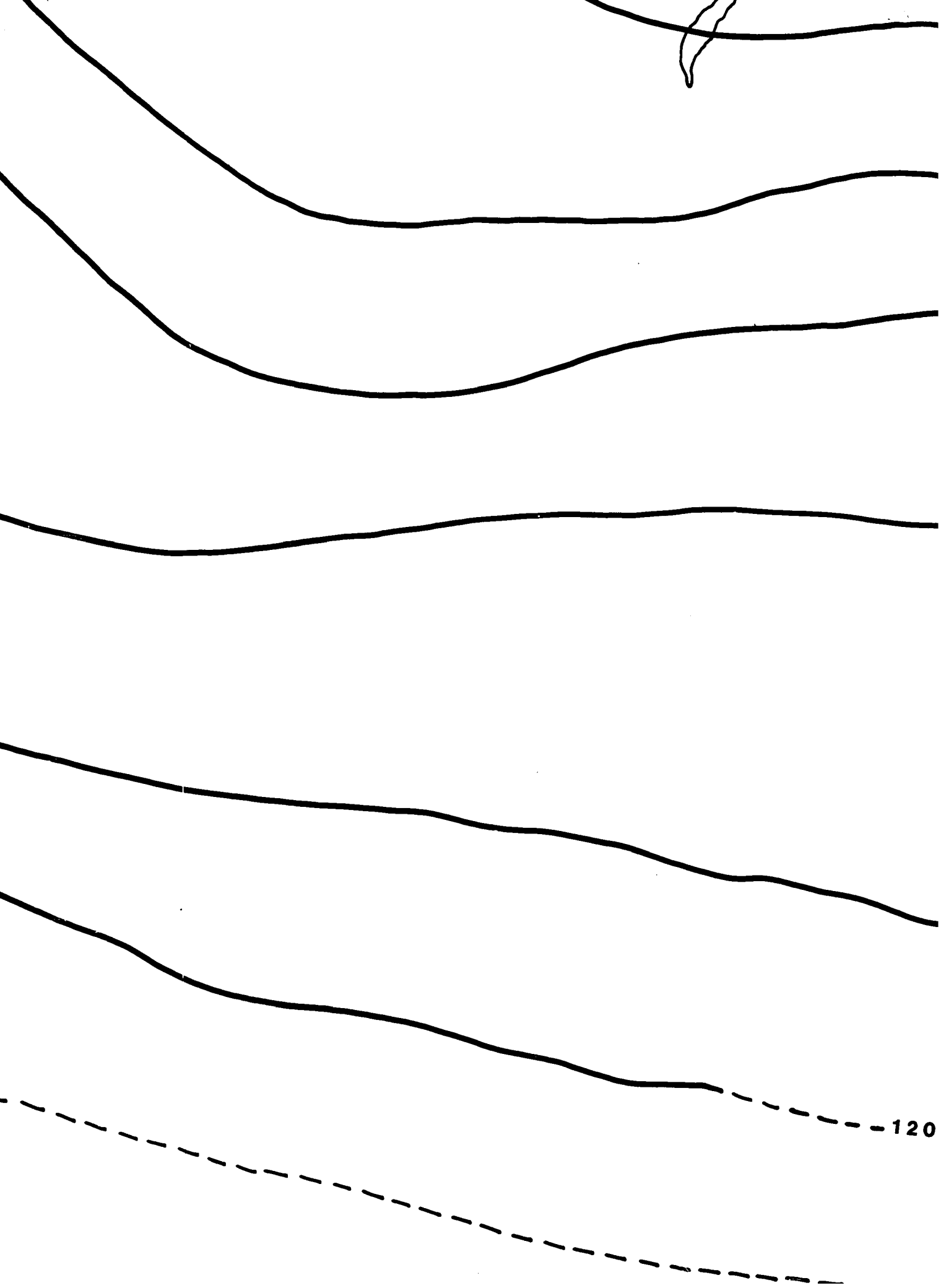

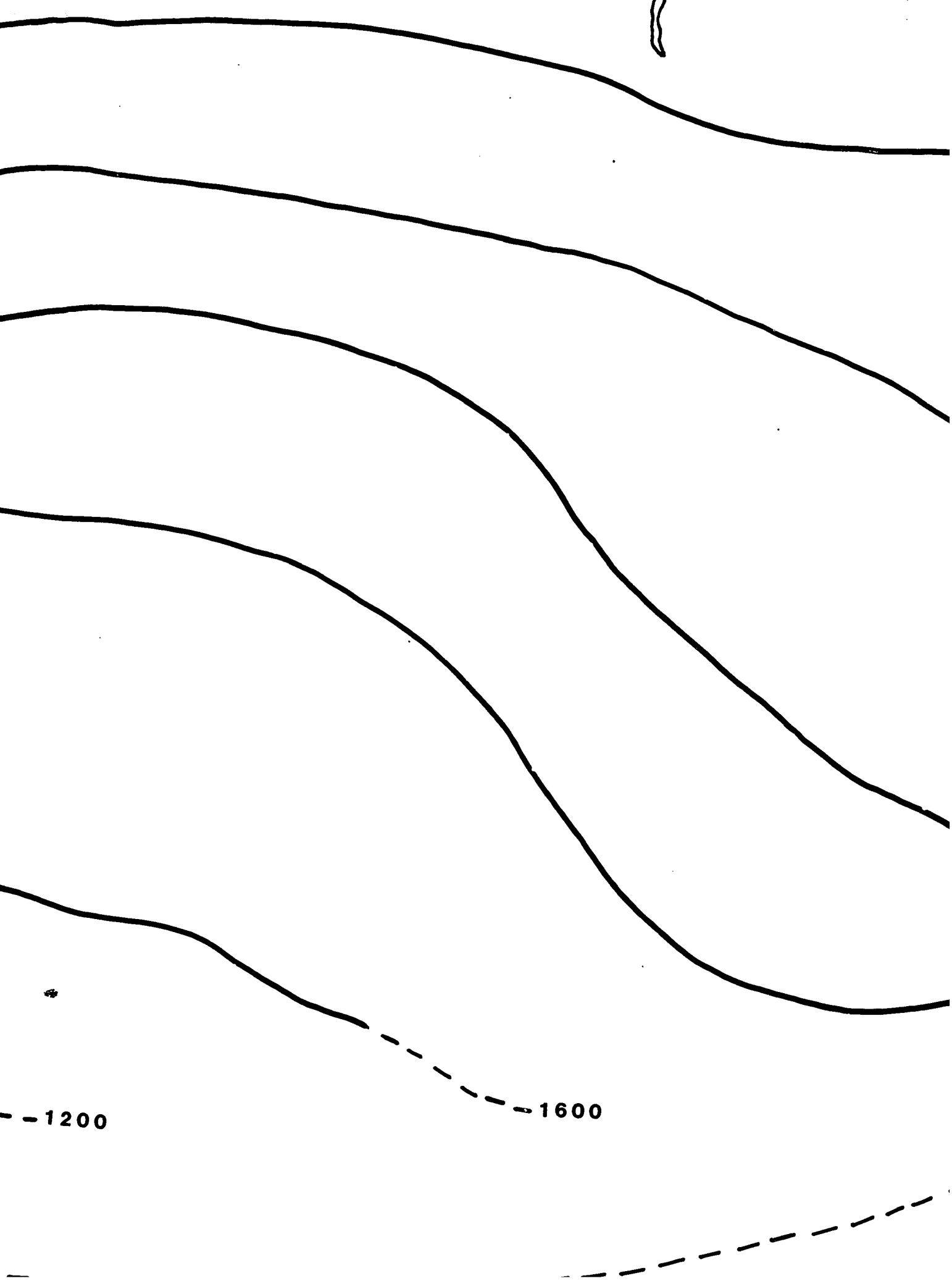

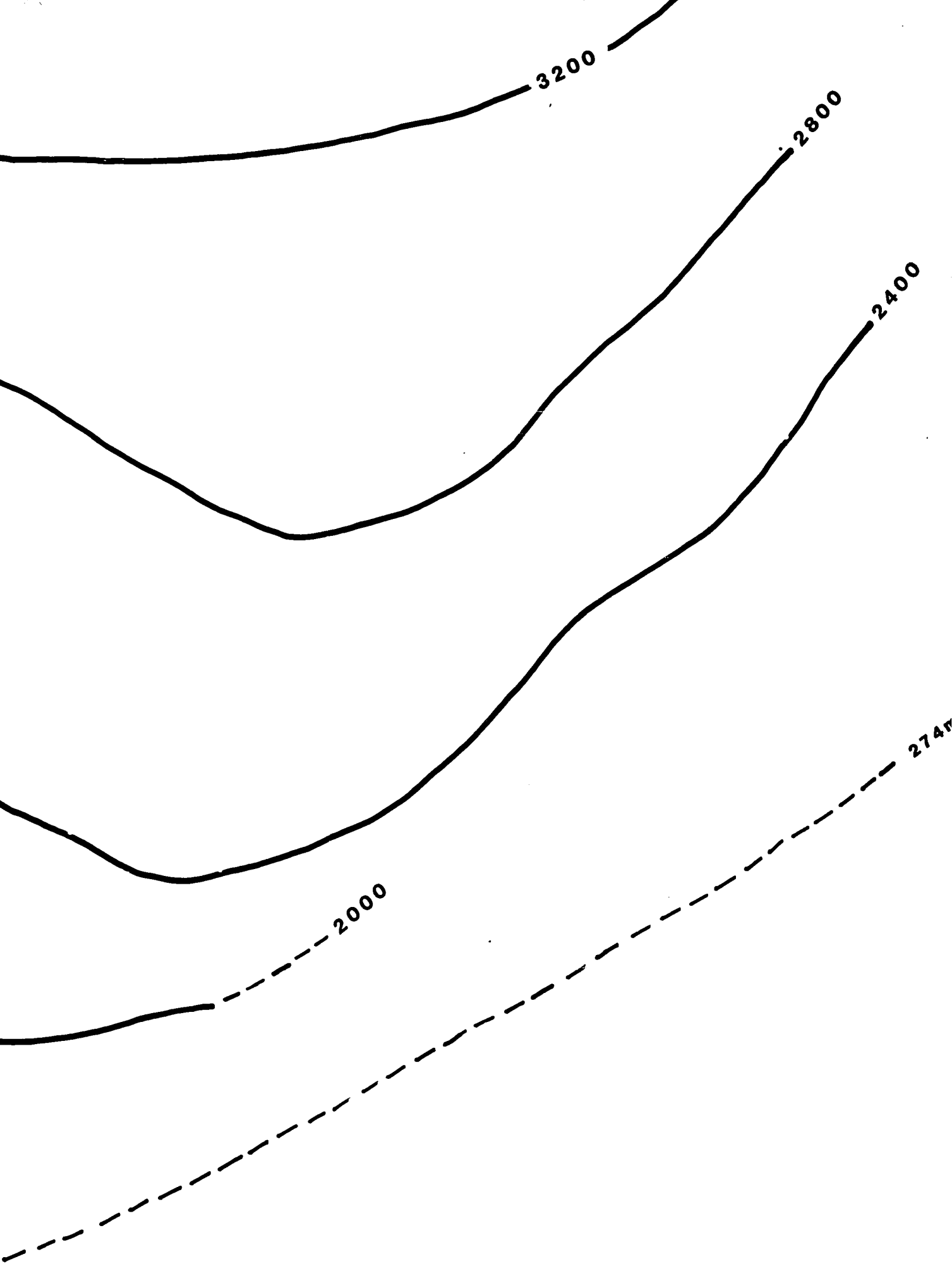

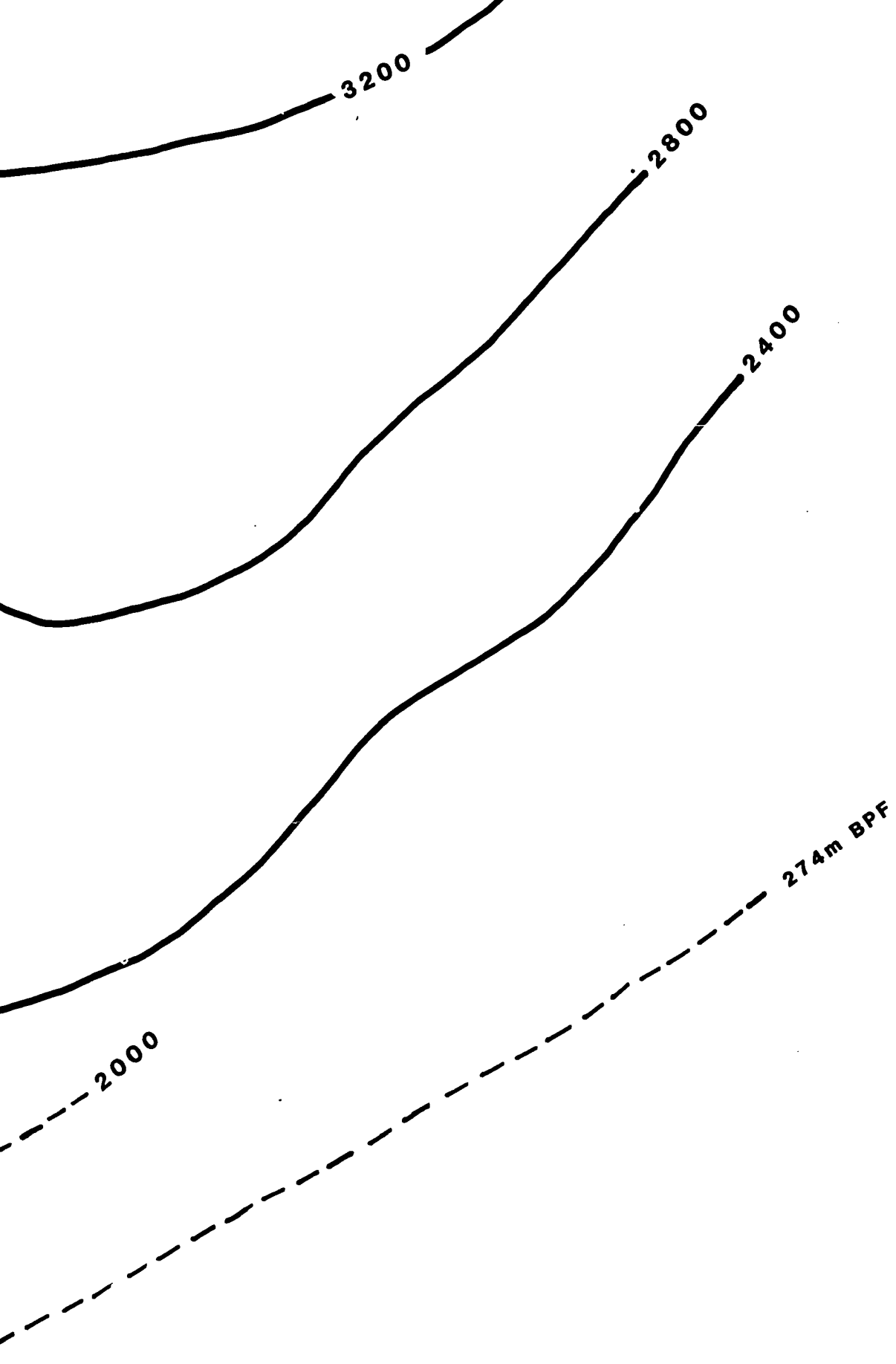

PLATE 2

ISOPACH OF THE THEORETICAL HYDRATE STABILITY FIELD

contour interval:400 feet

Scale

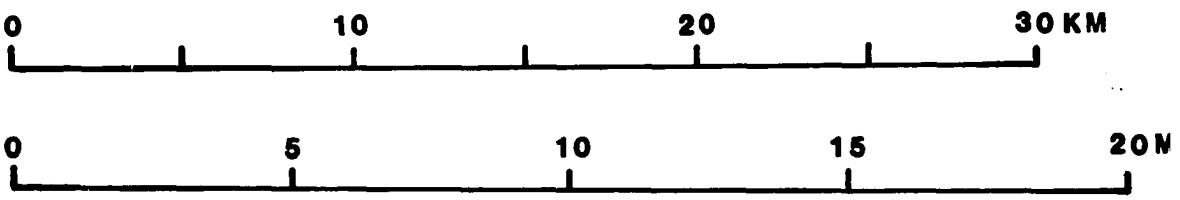

PLATE 2

ISOPACH OF THE THEORETICAL HYDRATE STABILITY FIELD

contour interval:400 feet

Scale

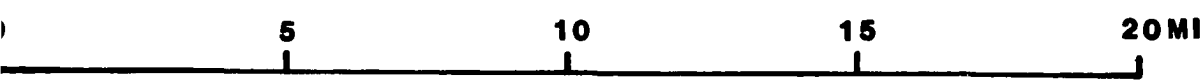

PLATE 2

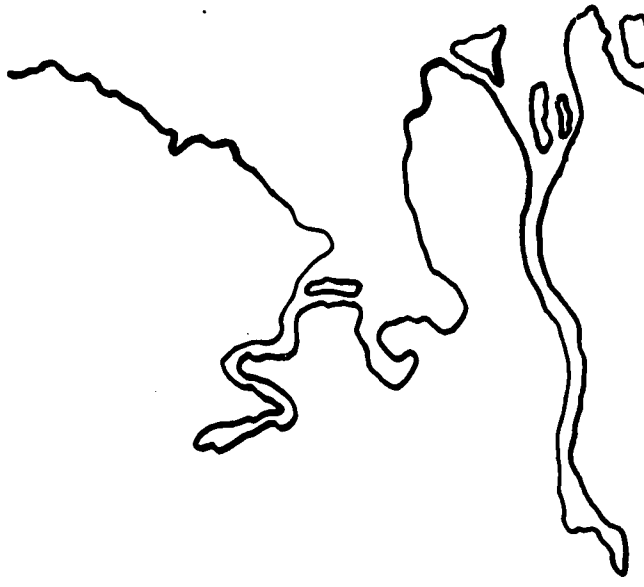

Oliktok

ktok Point

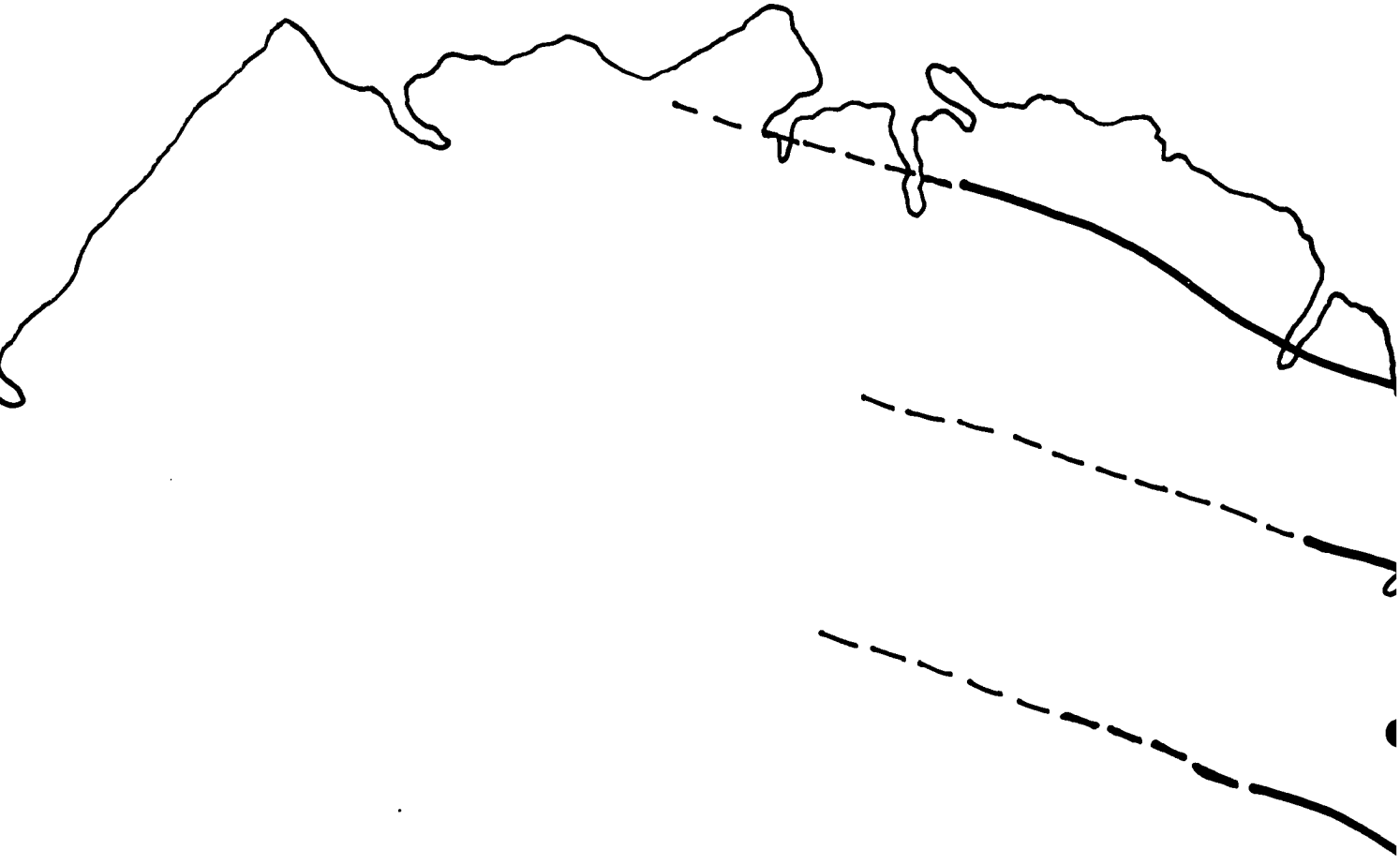

HORIZ

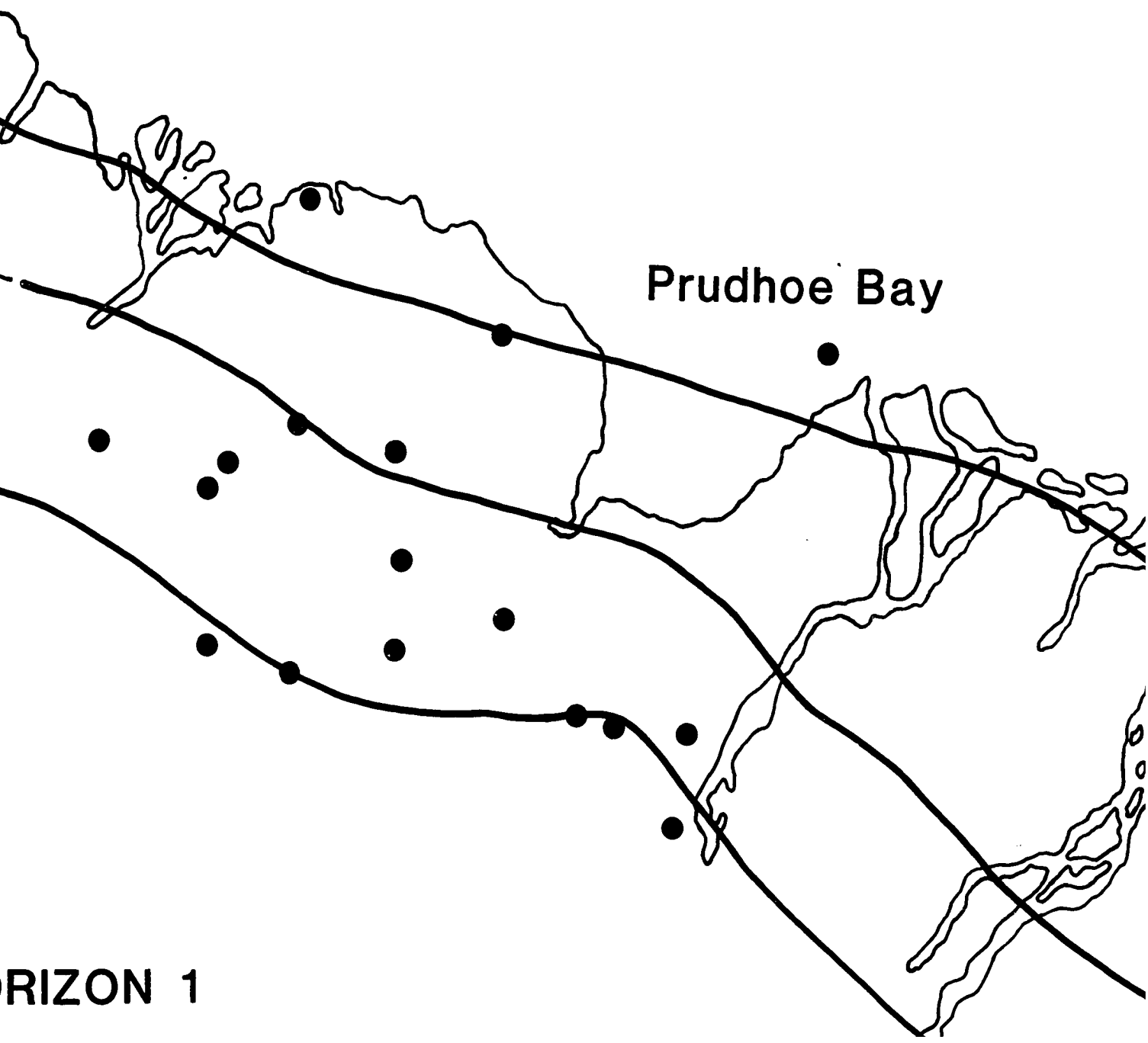

RIZON 1

ARCTIC OCEAN

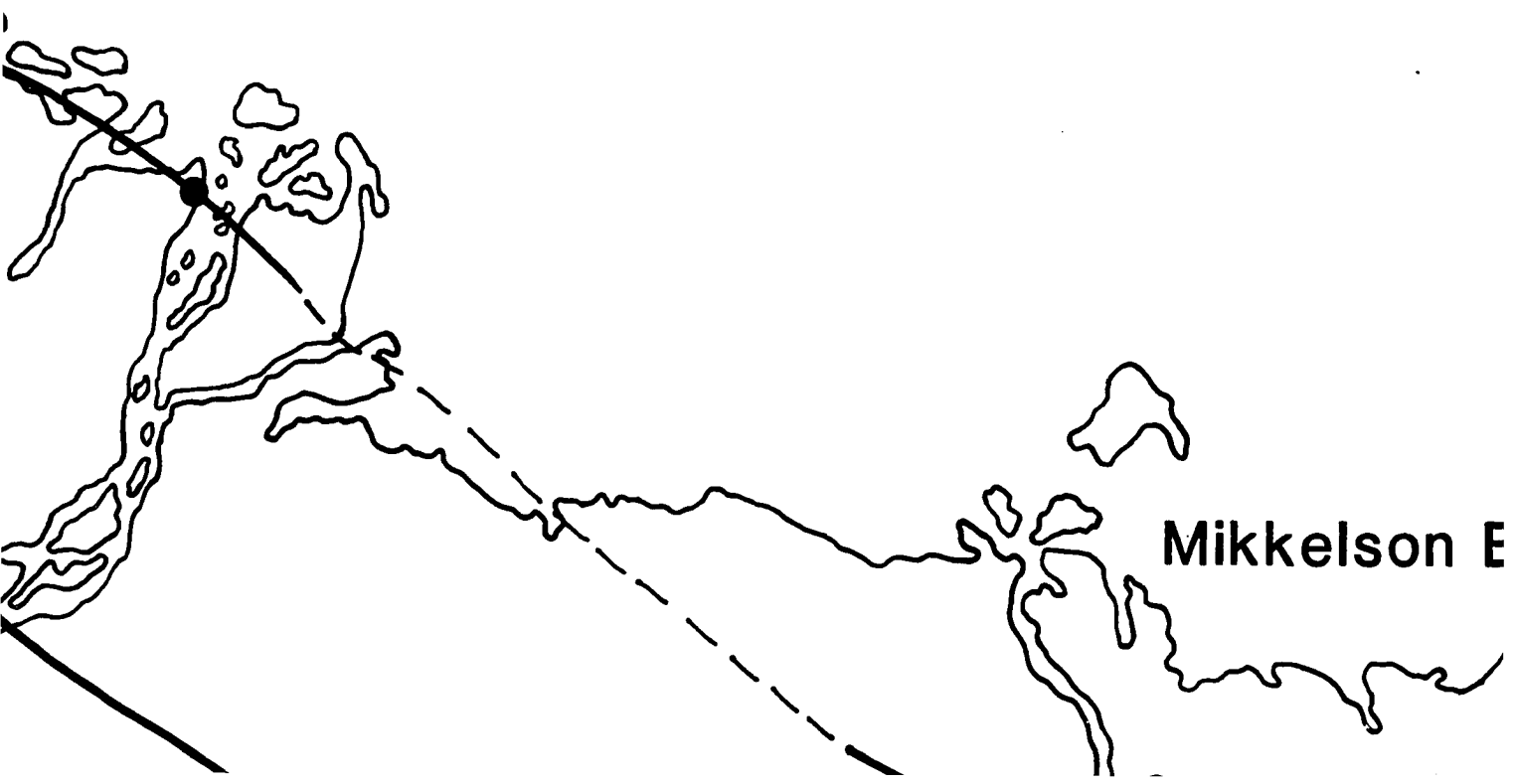

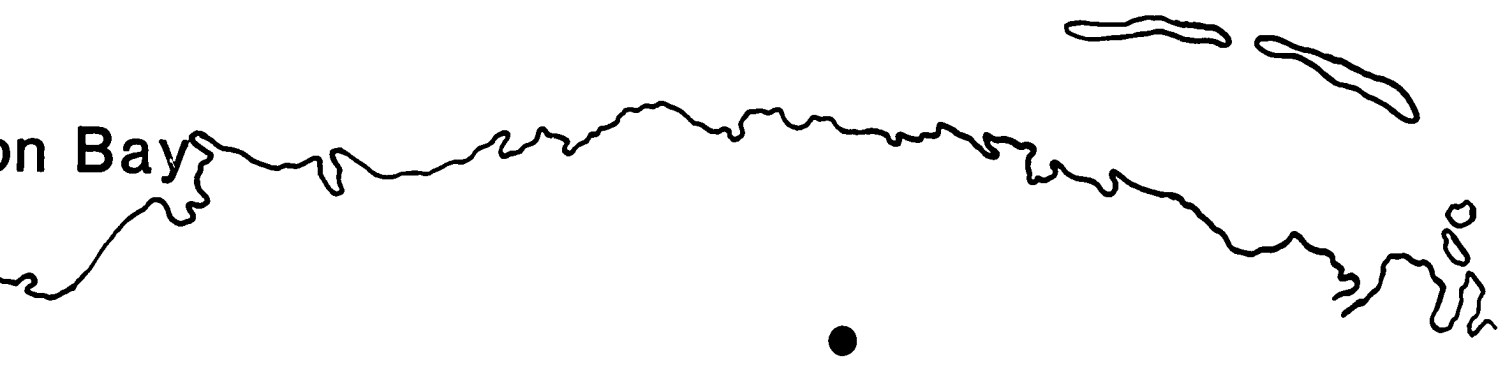

Oliktok P

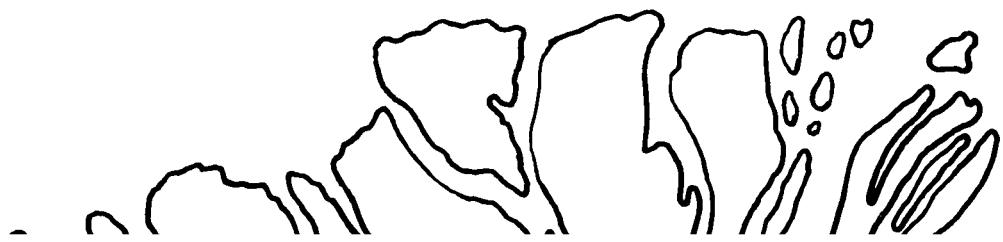

ok Point

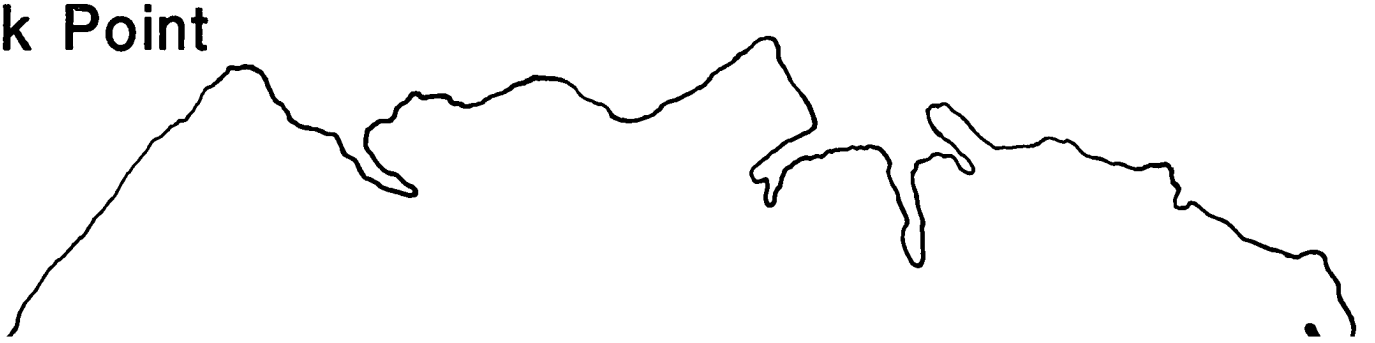

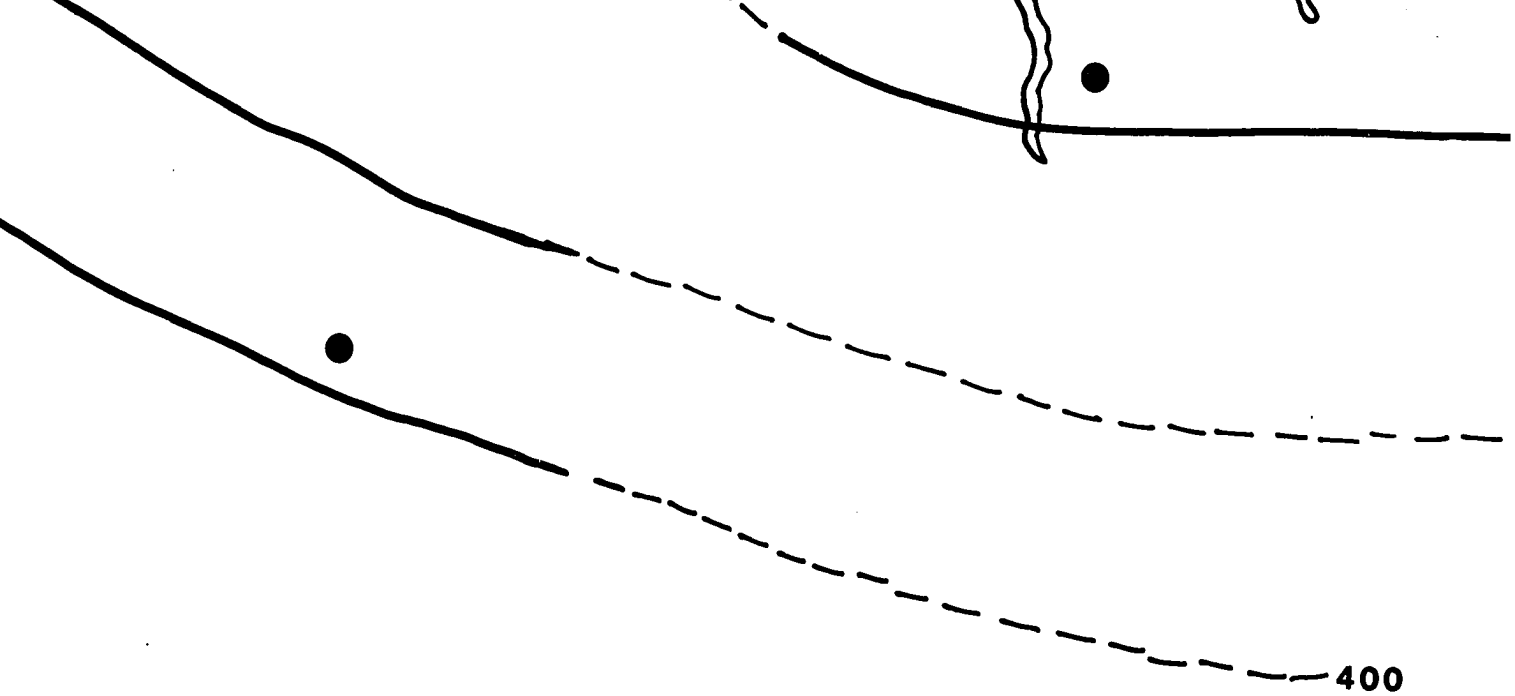

ARCTIC OCEAN

00

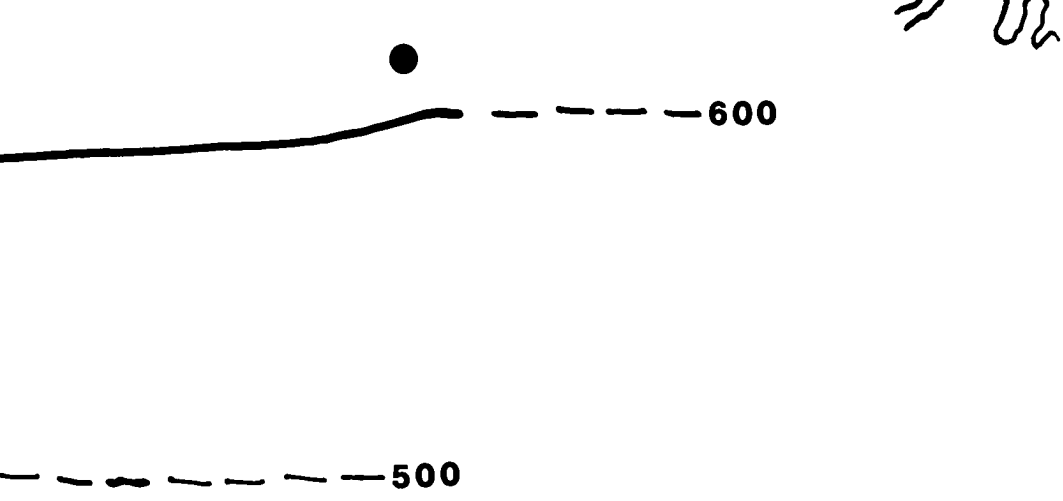

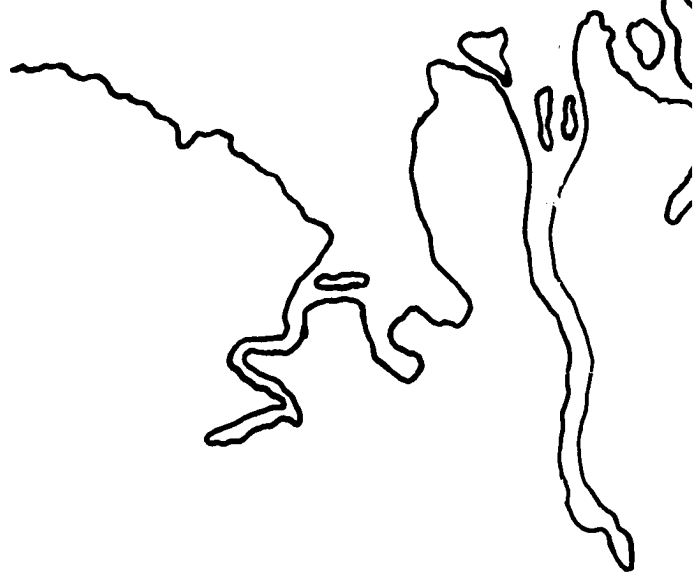

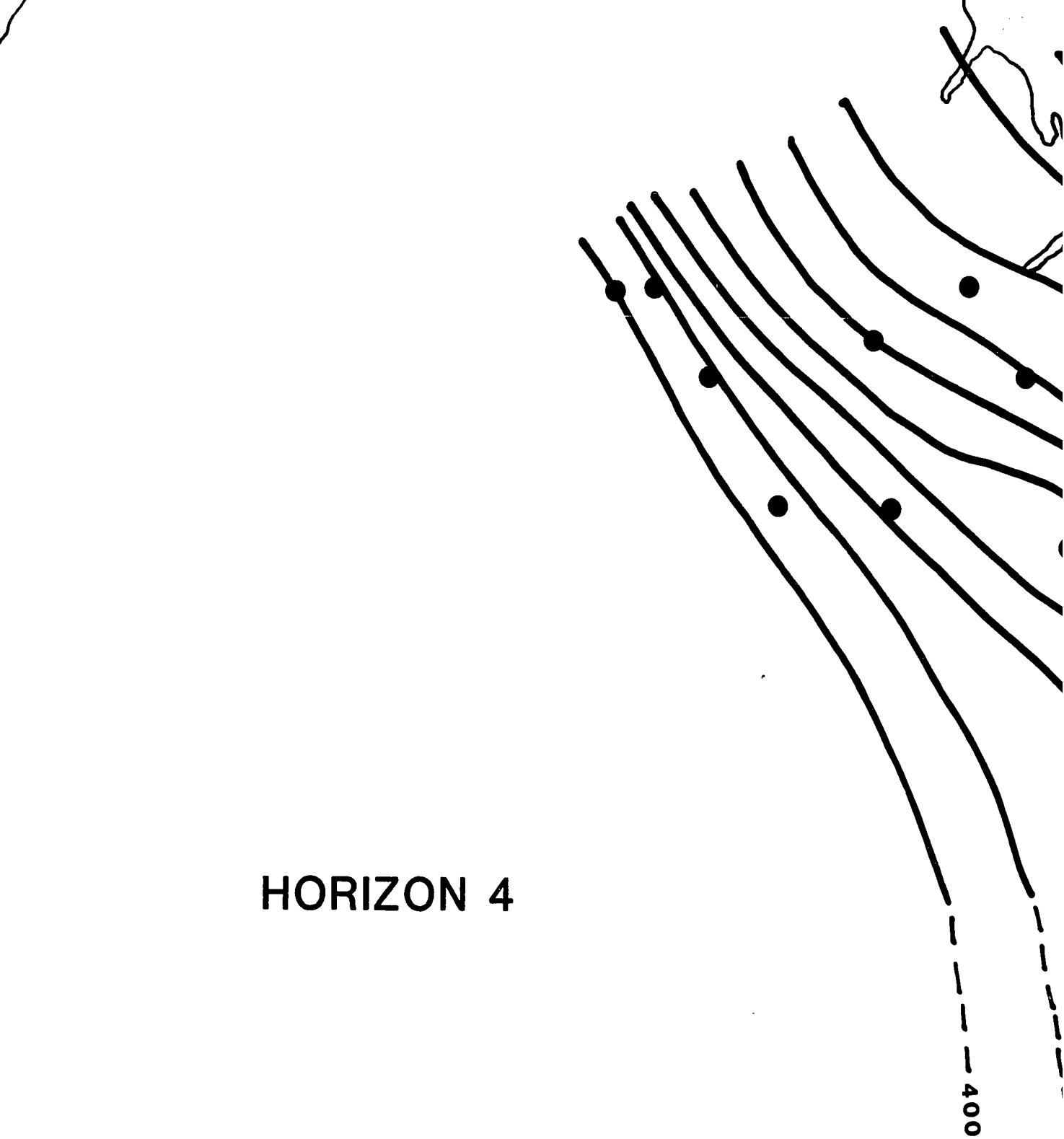

HORIZON 4

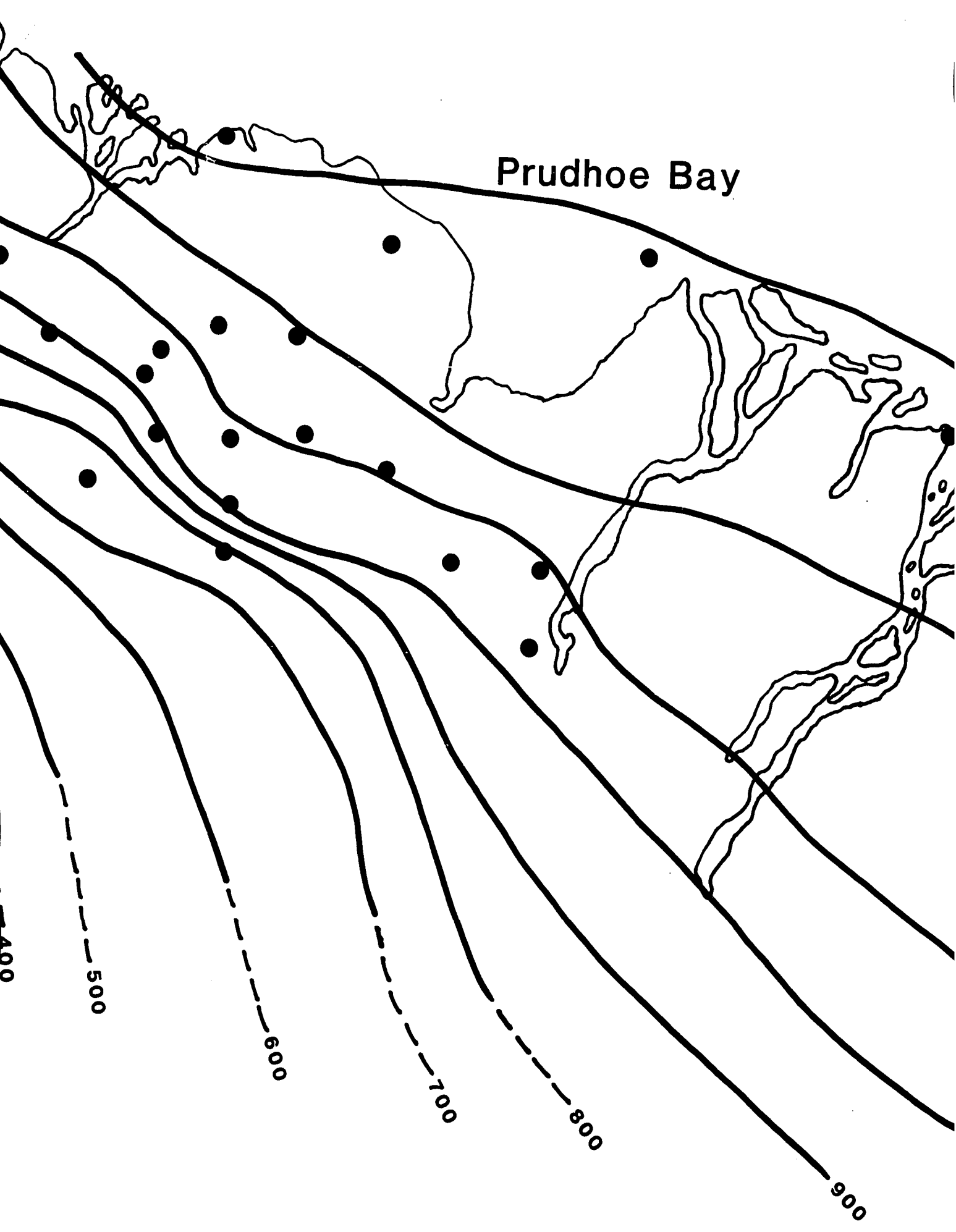

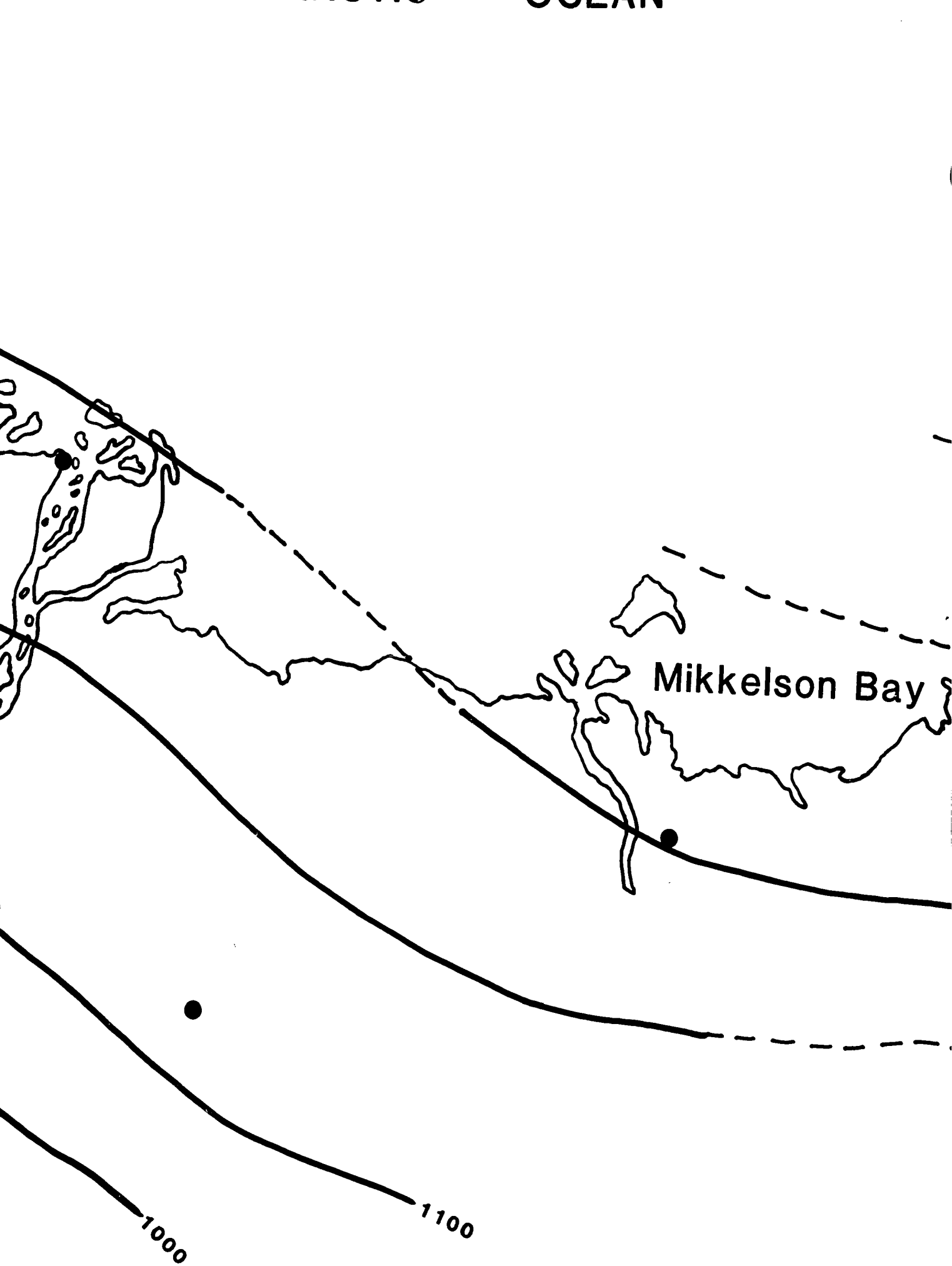

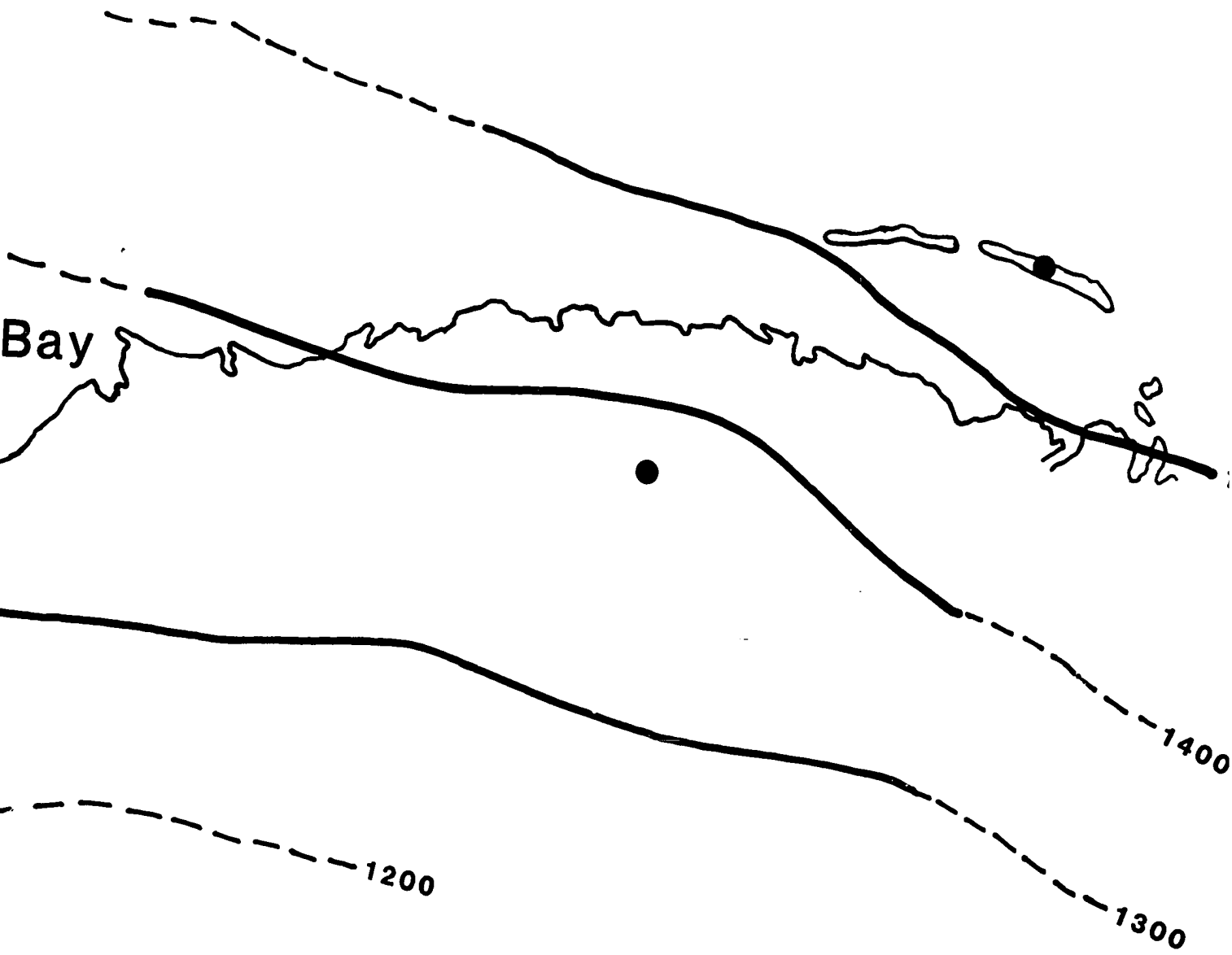

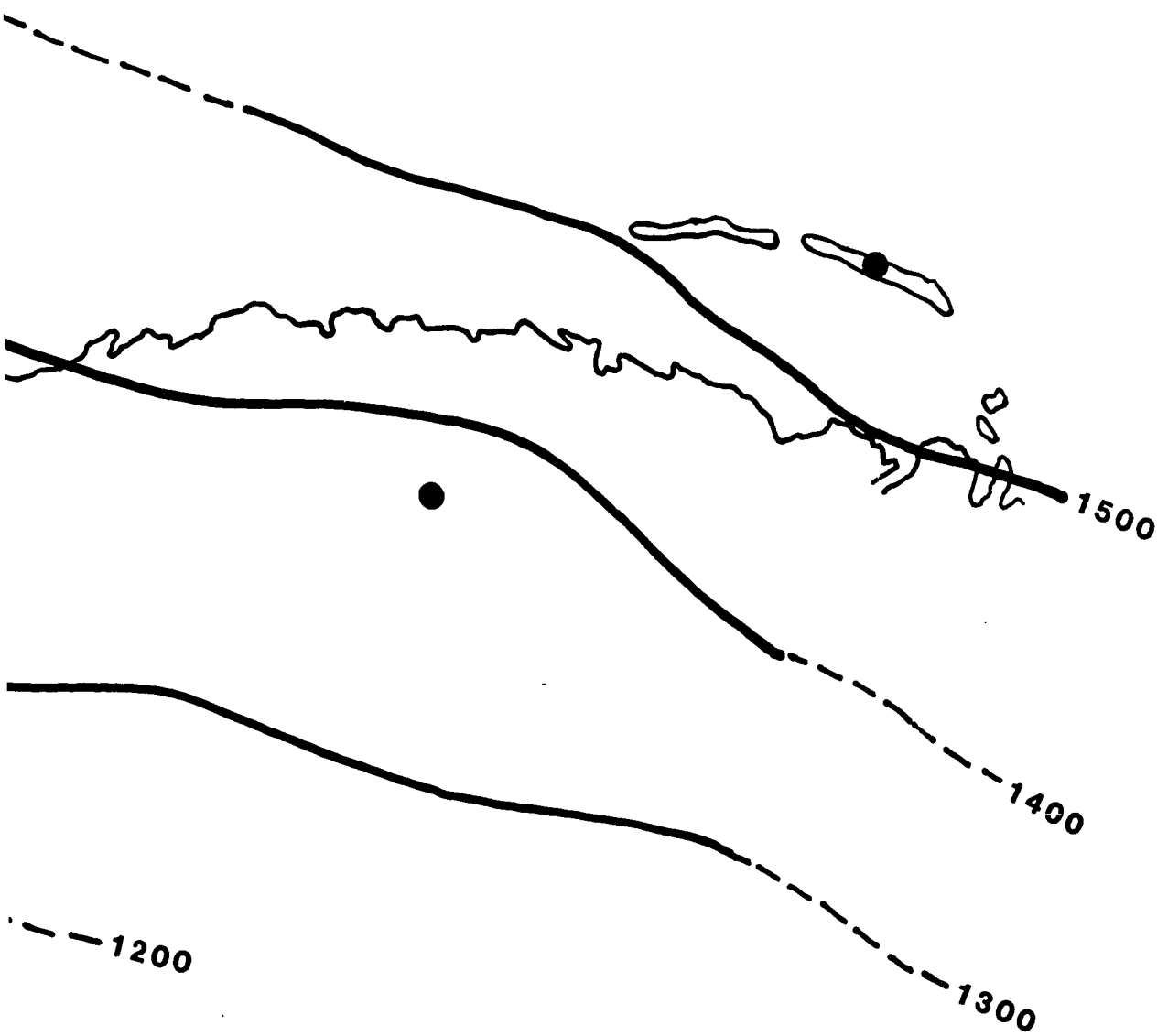

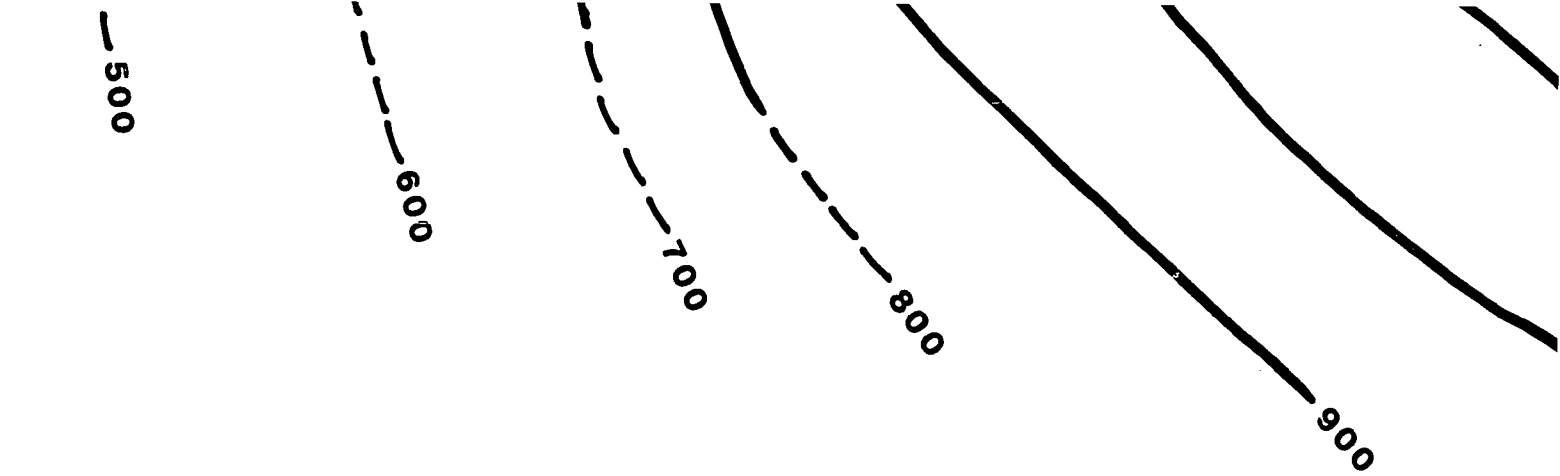

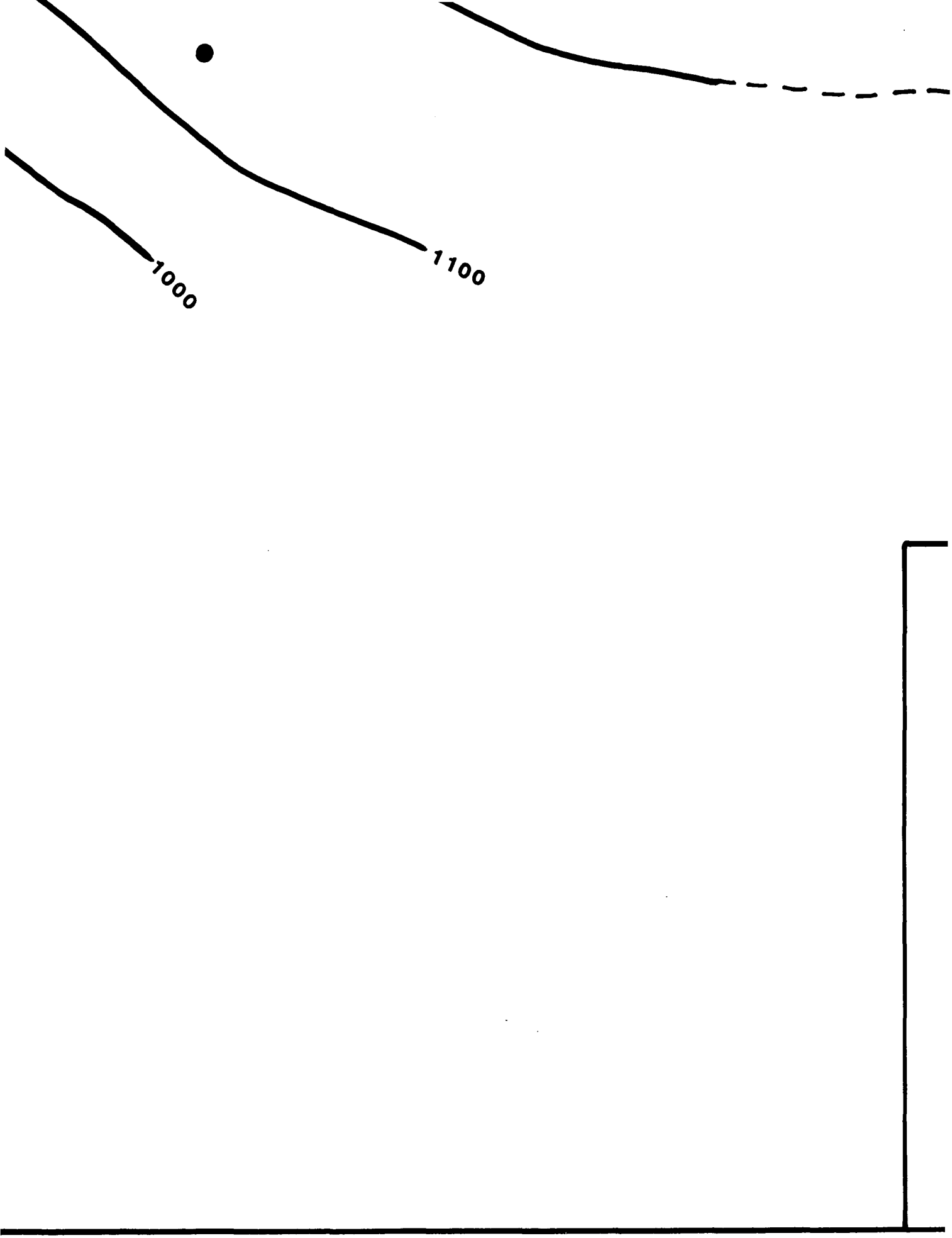

PLATE 3

MAPS OF DEPTH TO HORIZON 1 & 4

contour interval:100 feet

Scale

0 10 20 30KM

0 5 10 15 20M

● **Data Point, Well Location**

PLATE 3

APS OF DEPTH TO HORIZON 1 & 4

contour interval:100 feet

ile

10 20 30KM

5 10 15 20MI

Data Point, Well Location

PLATE 3

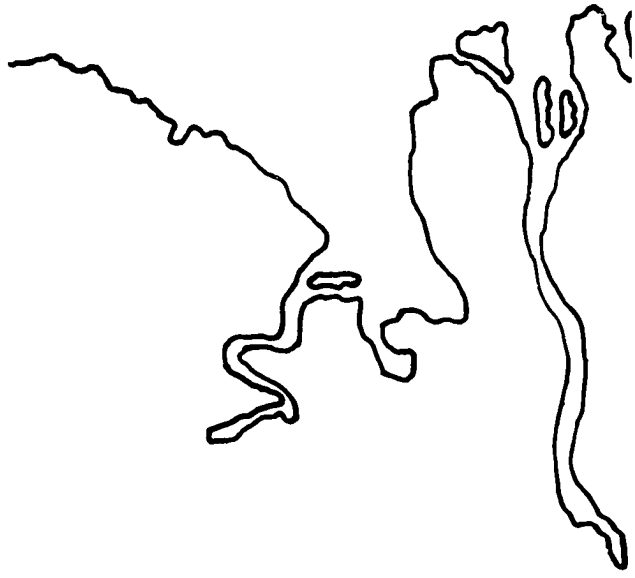

Oliktok F

HORIZO

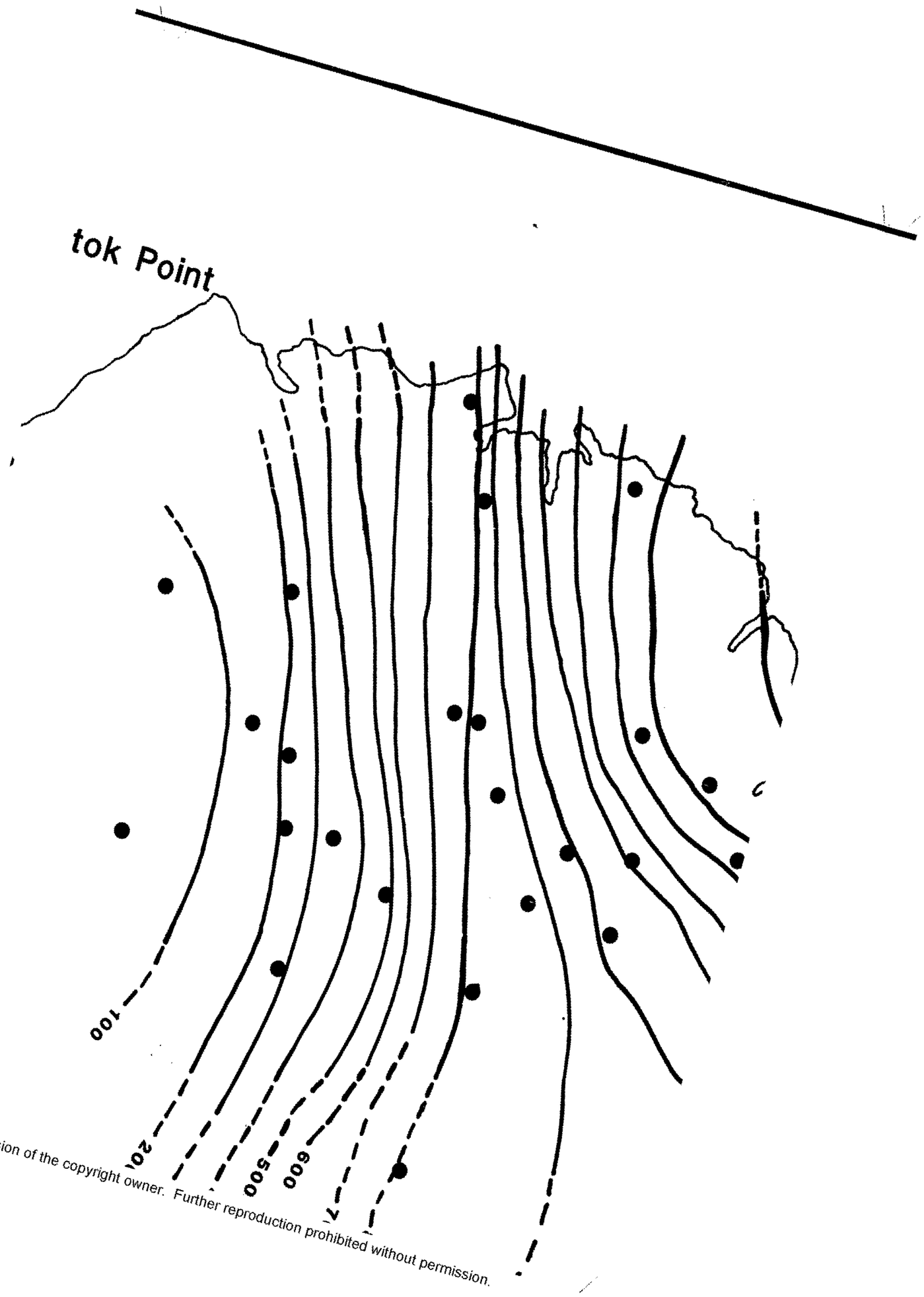

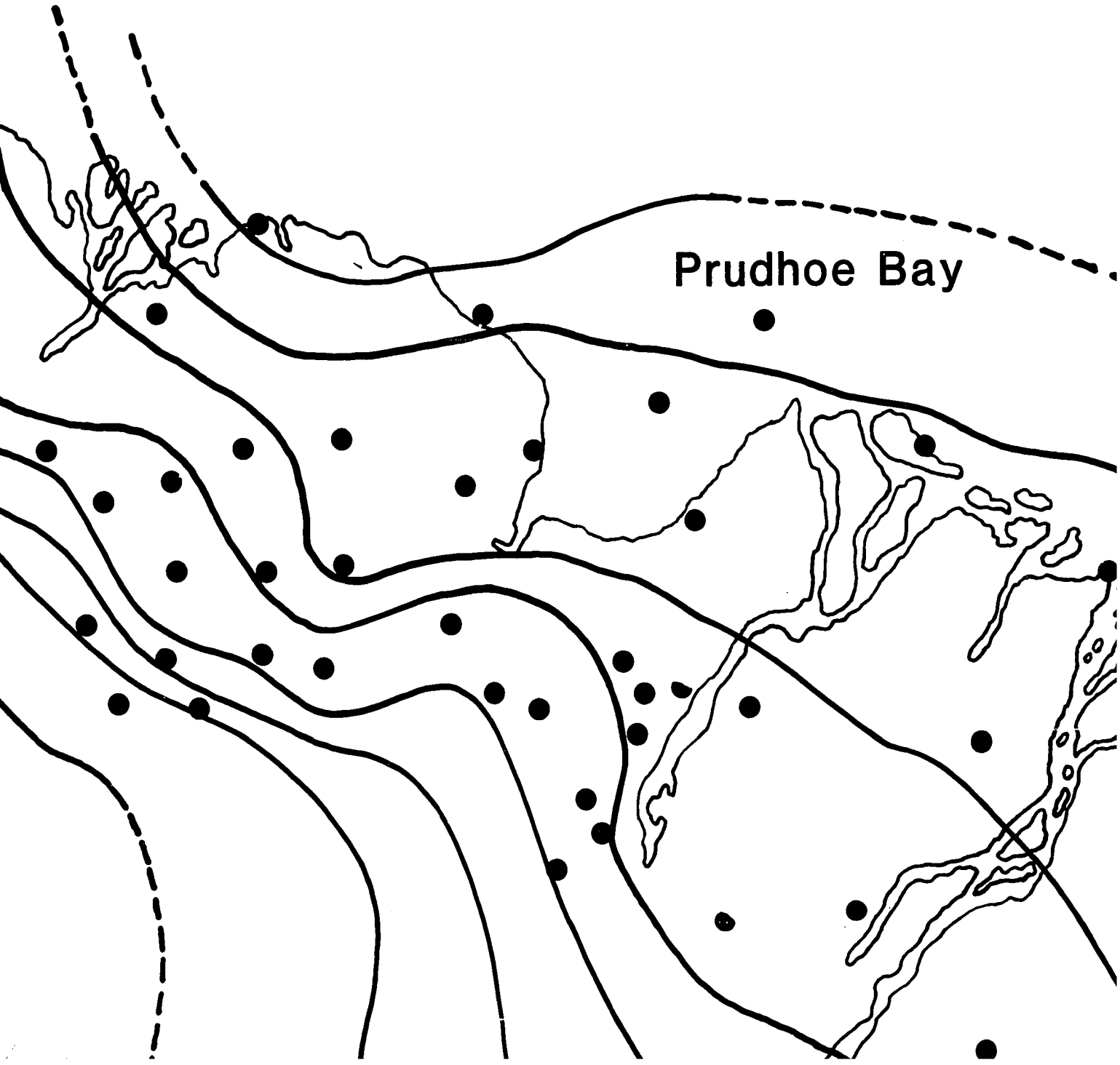

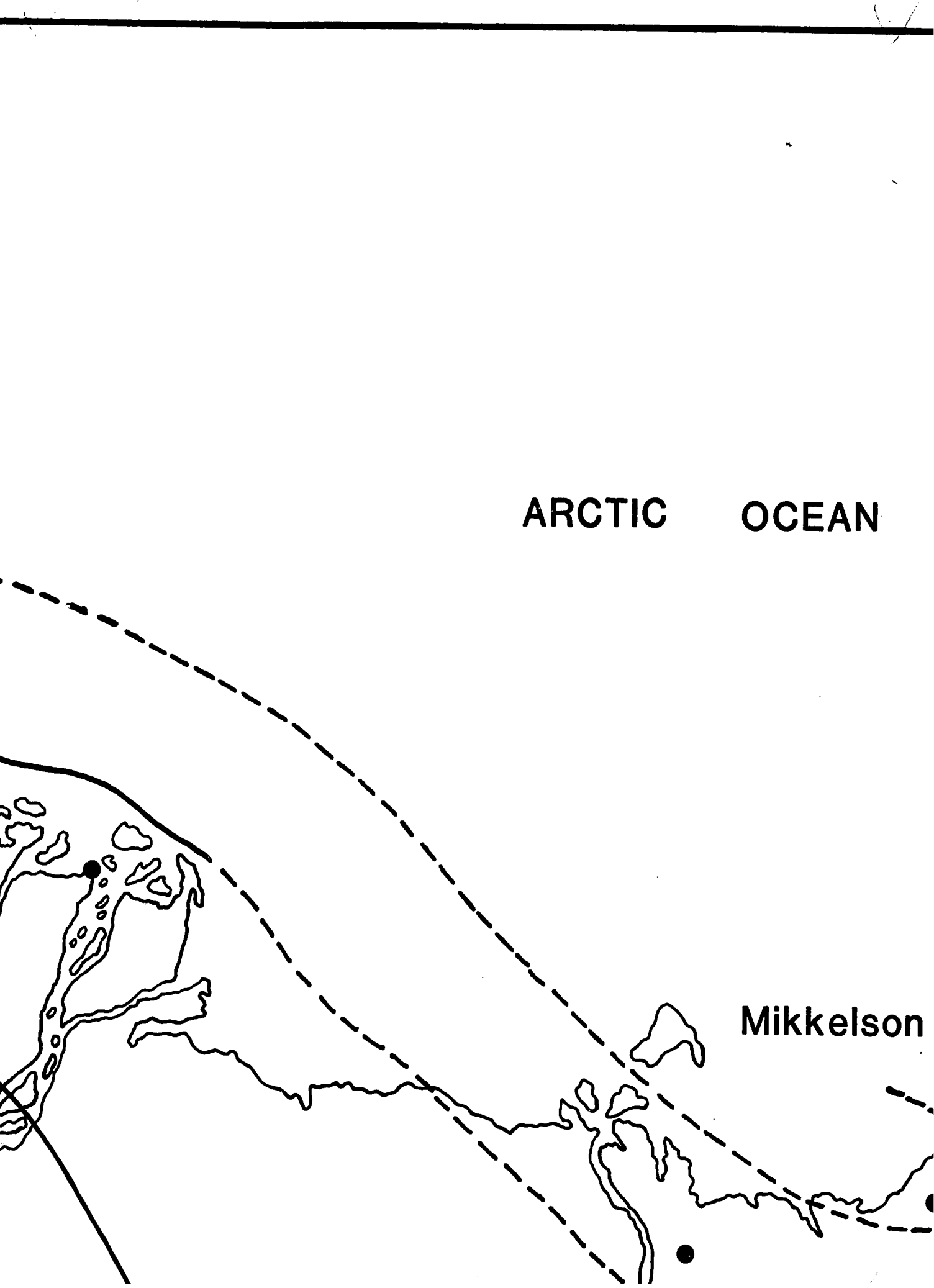

N

elson Bay

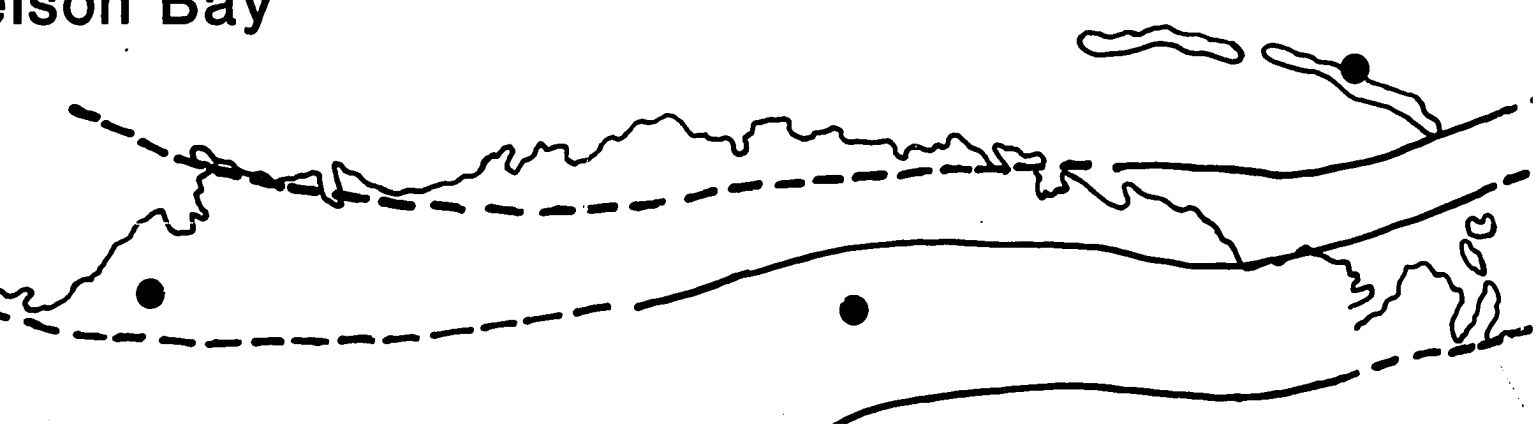

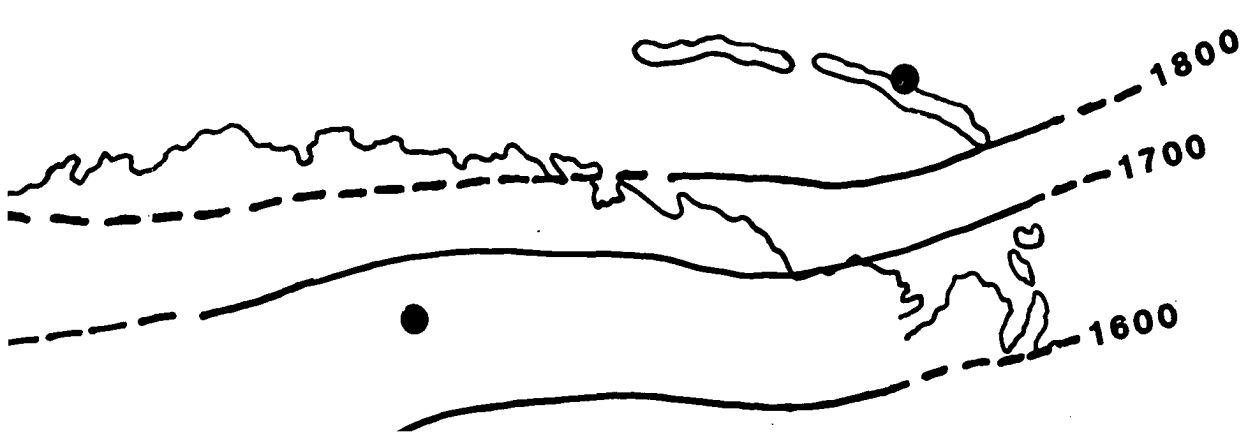

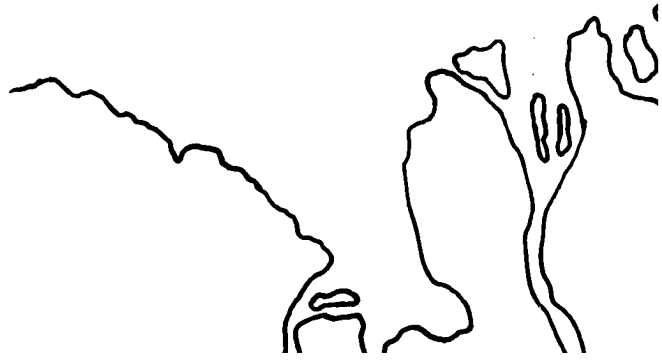

HORIZO

Oliktok

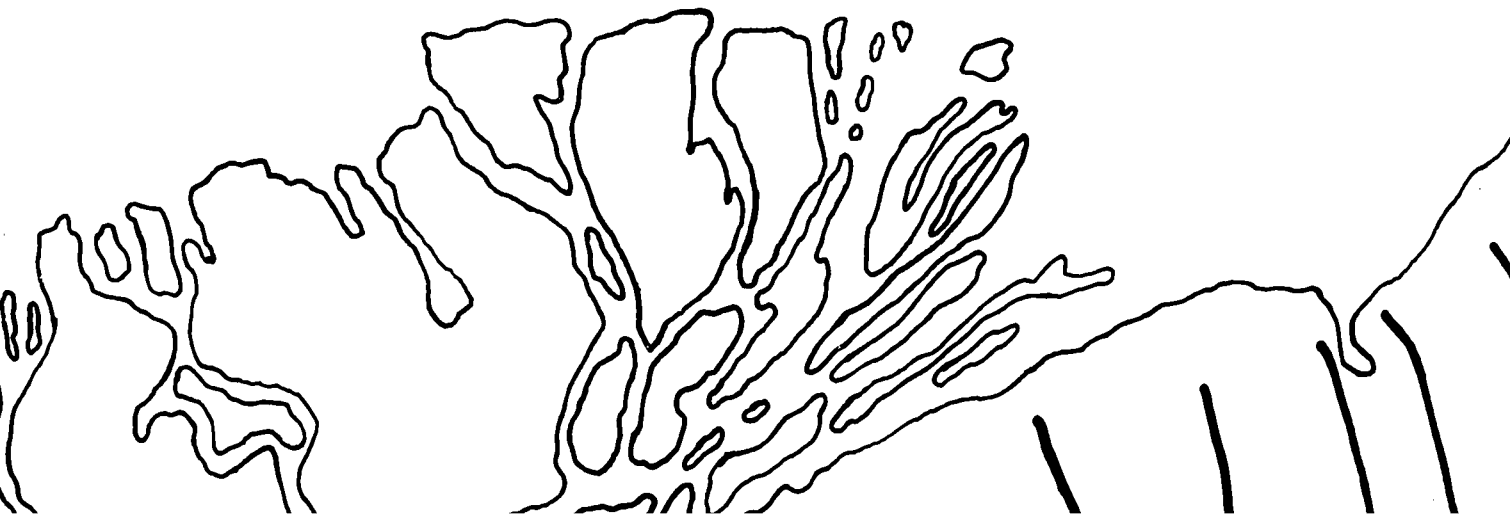

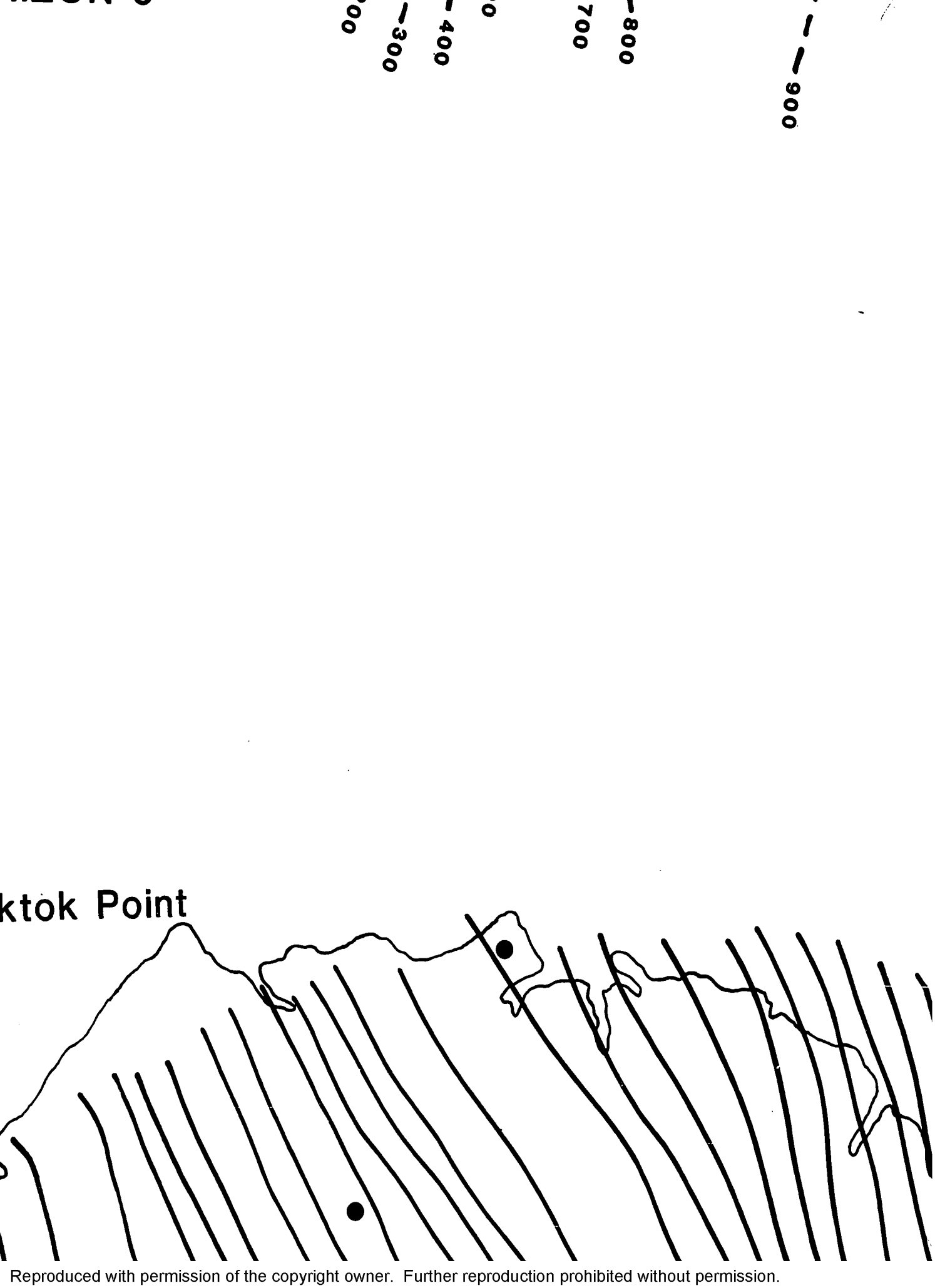

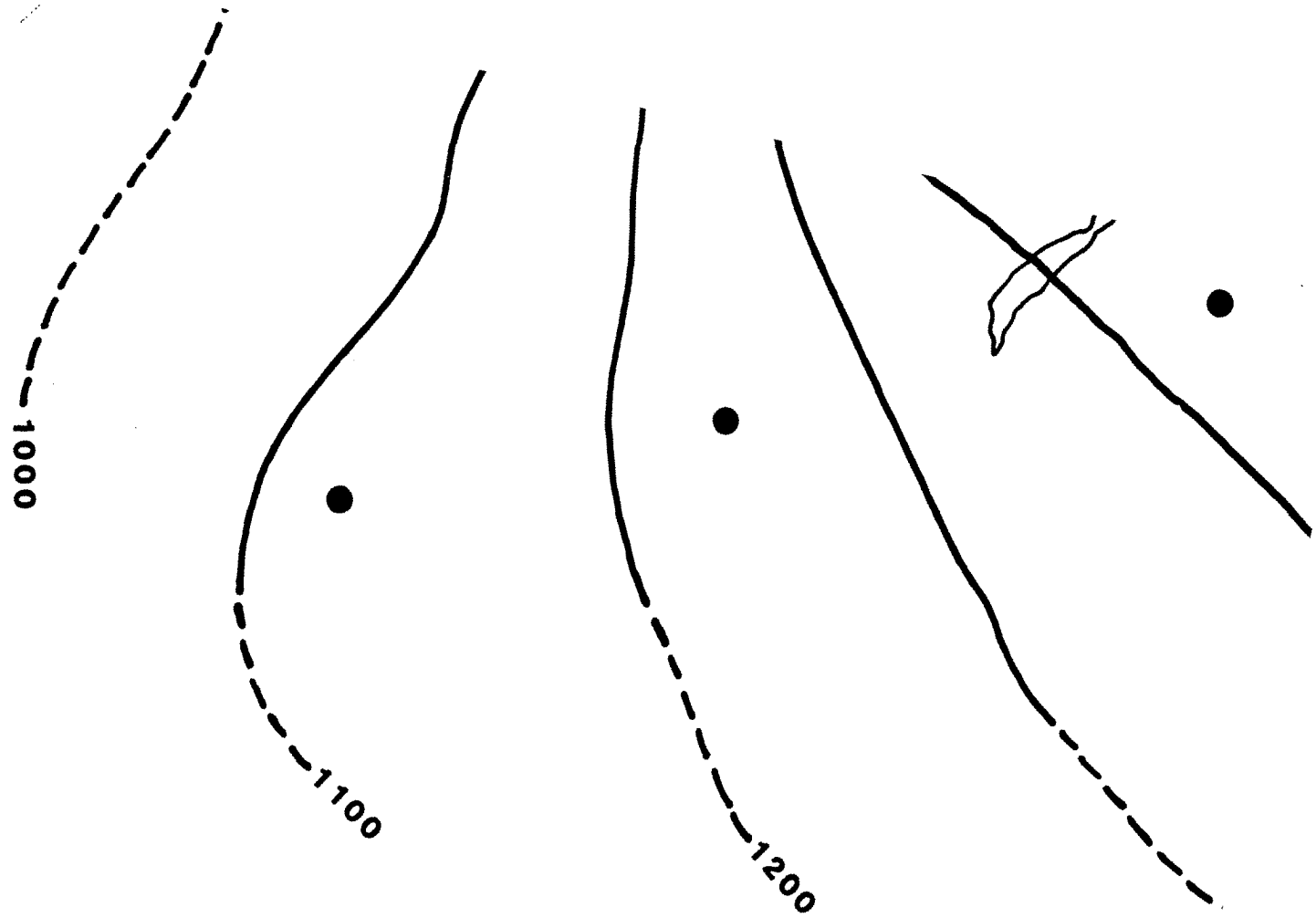

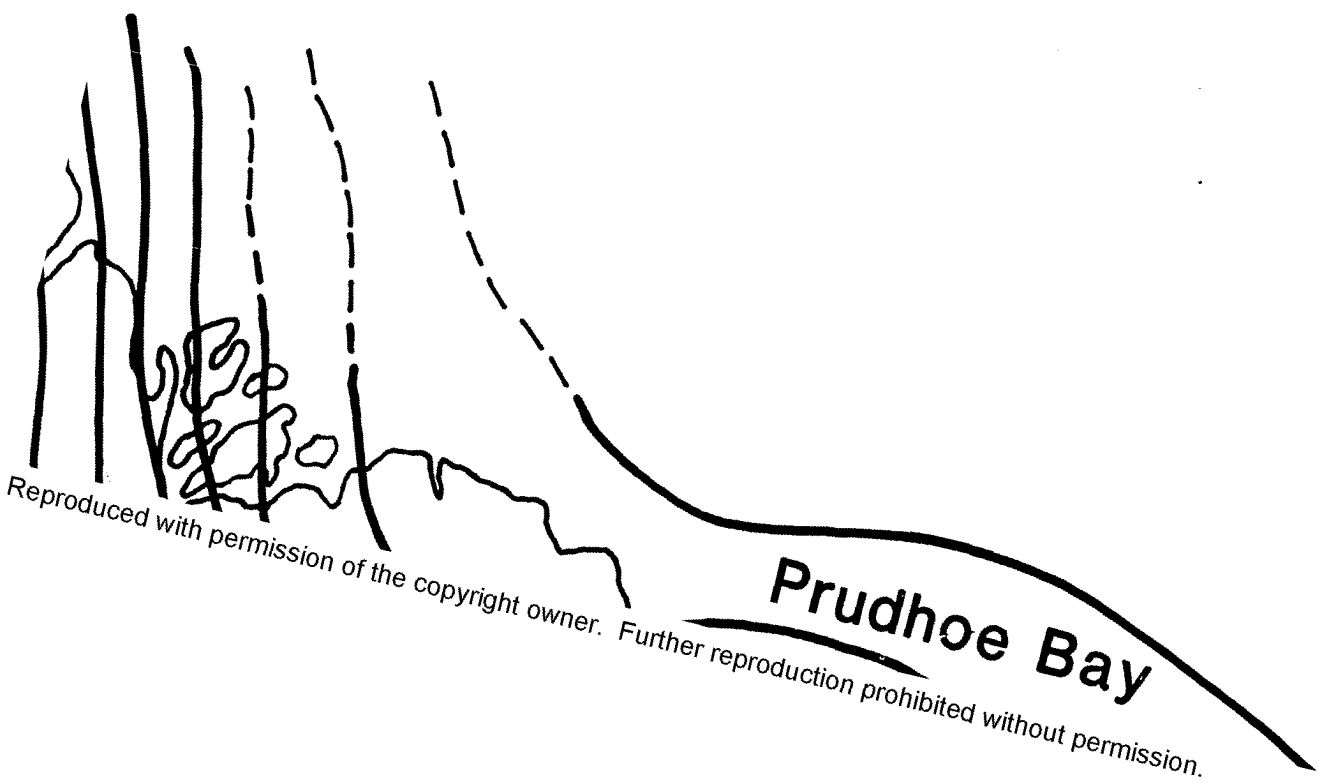

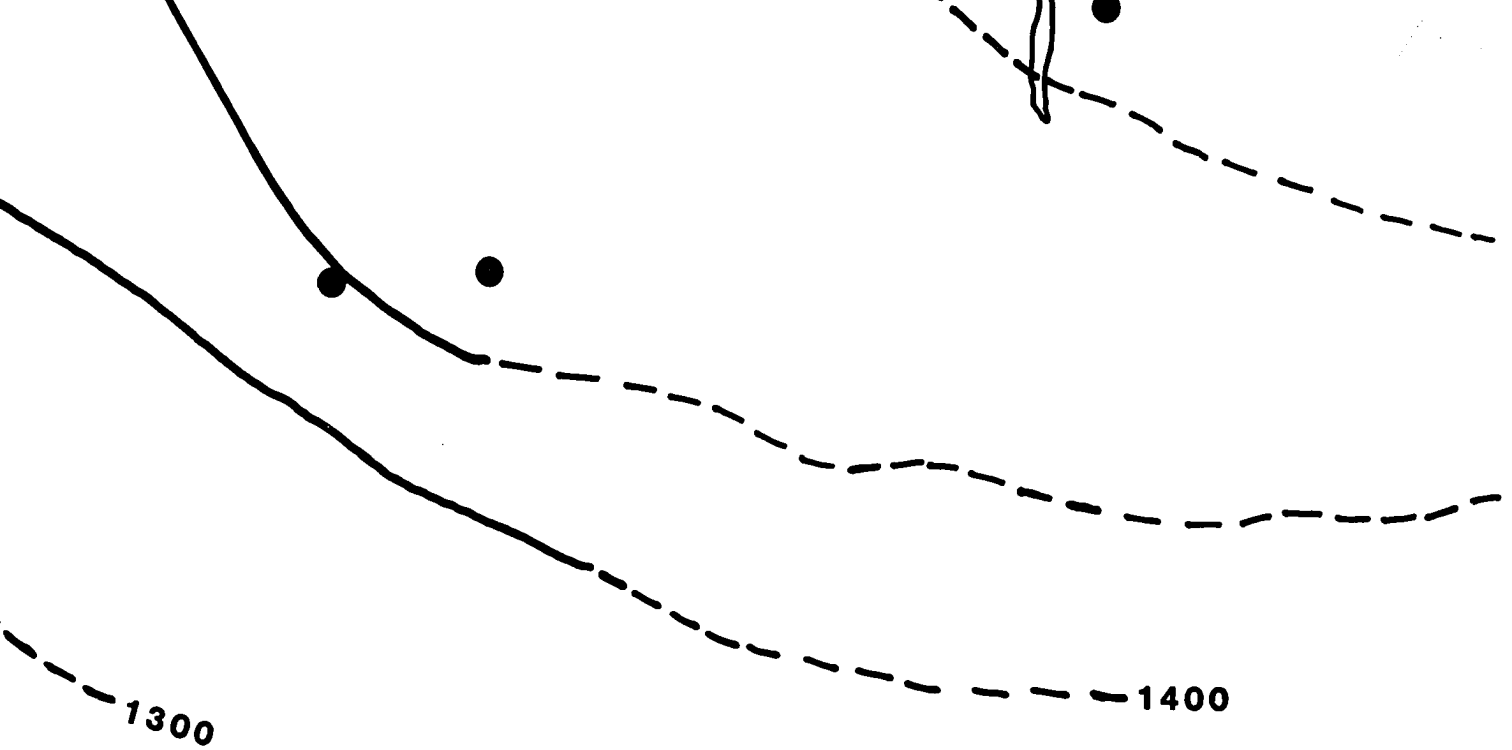

ARCTIC OC

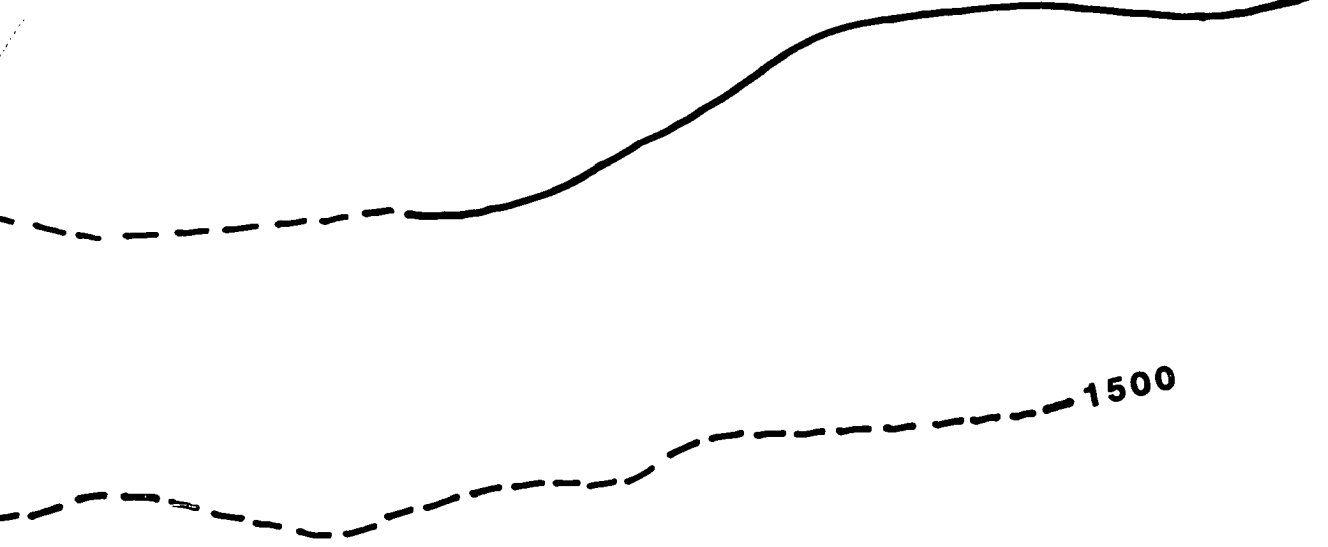

OCEAN

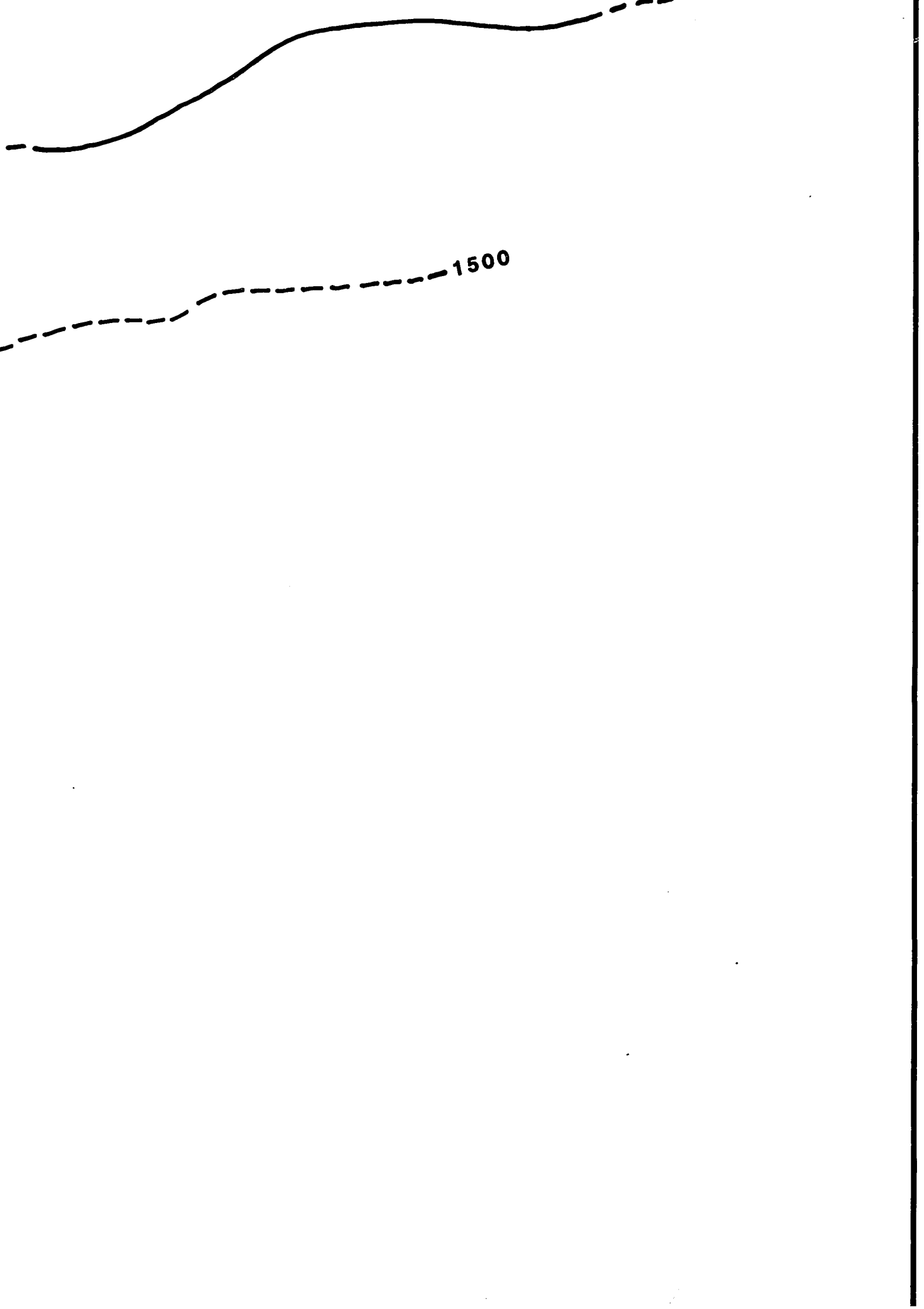

HORIZON 12

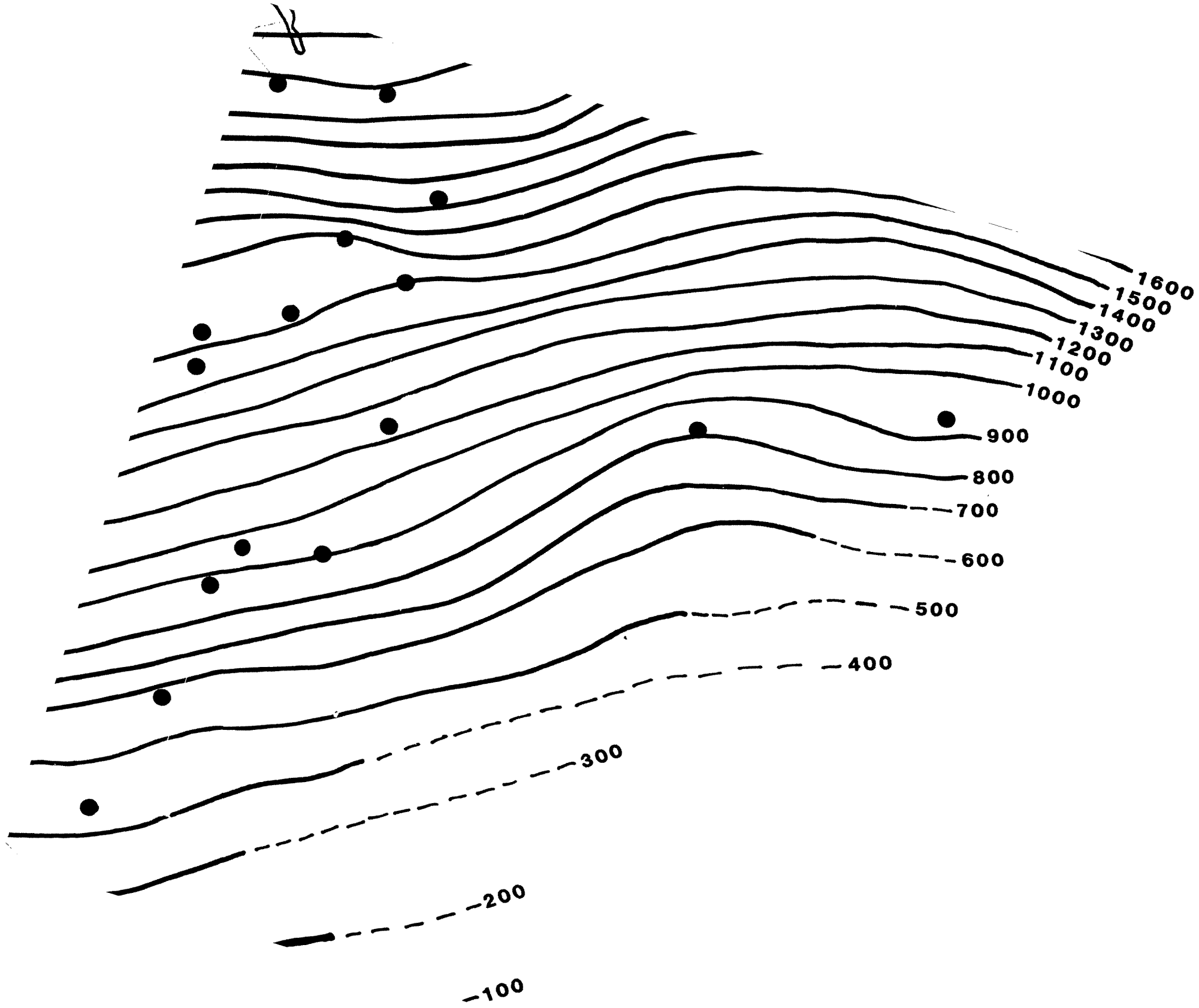

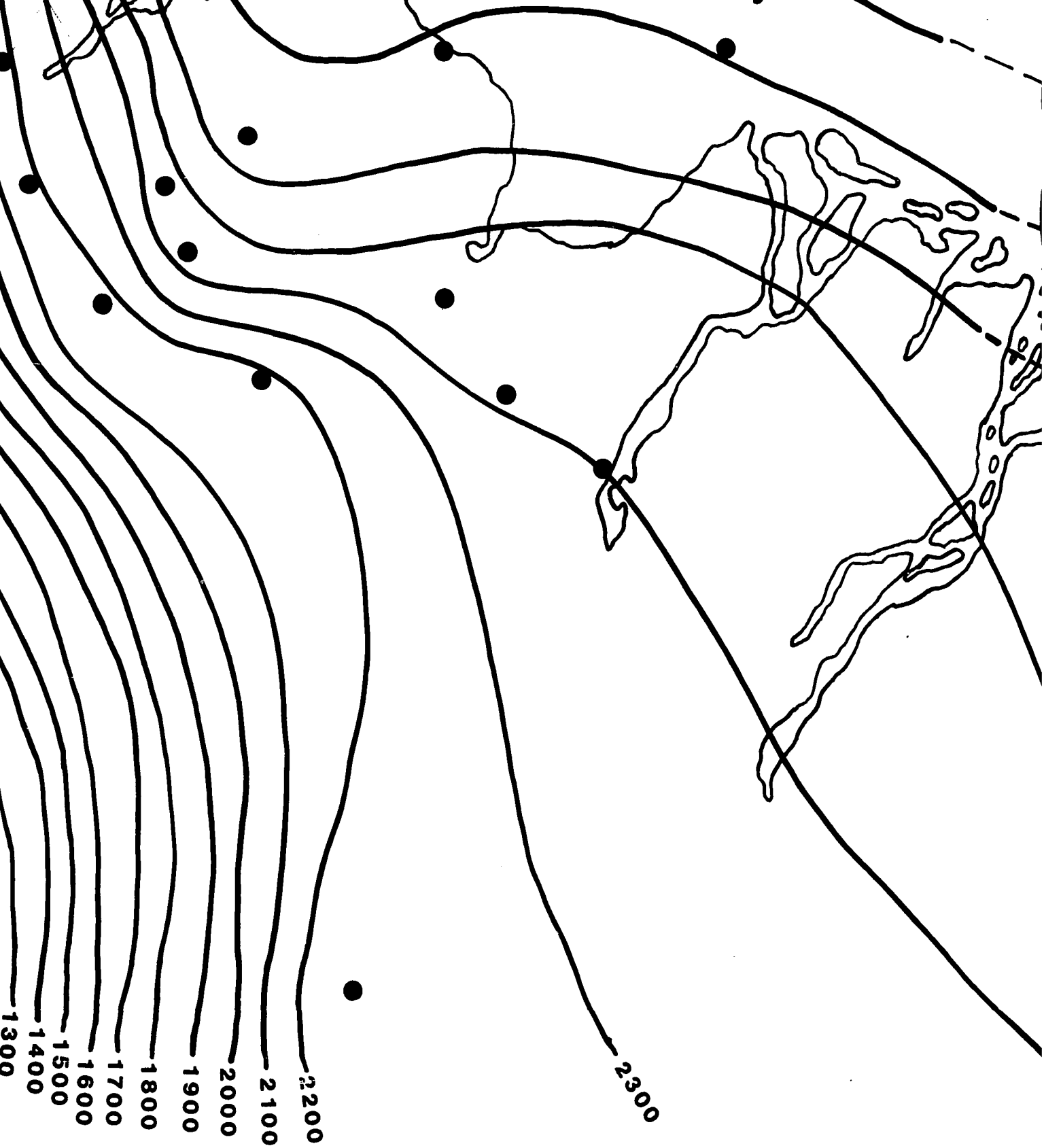

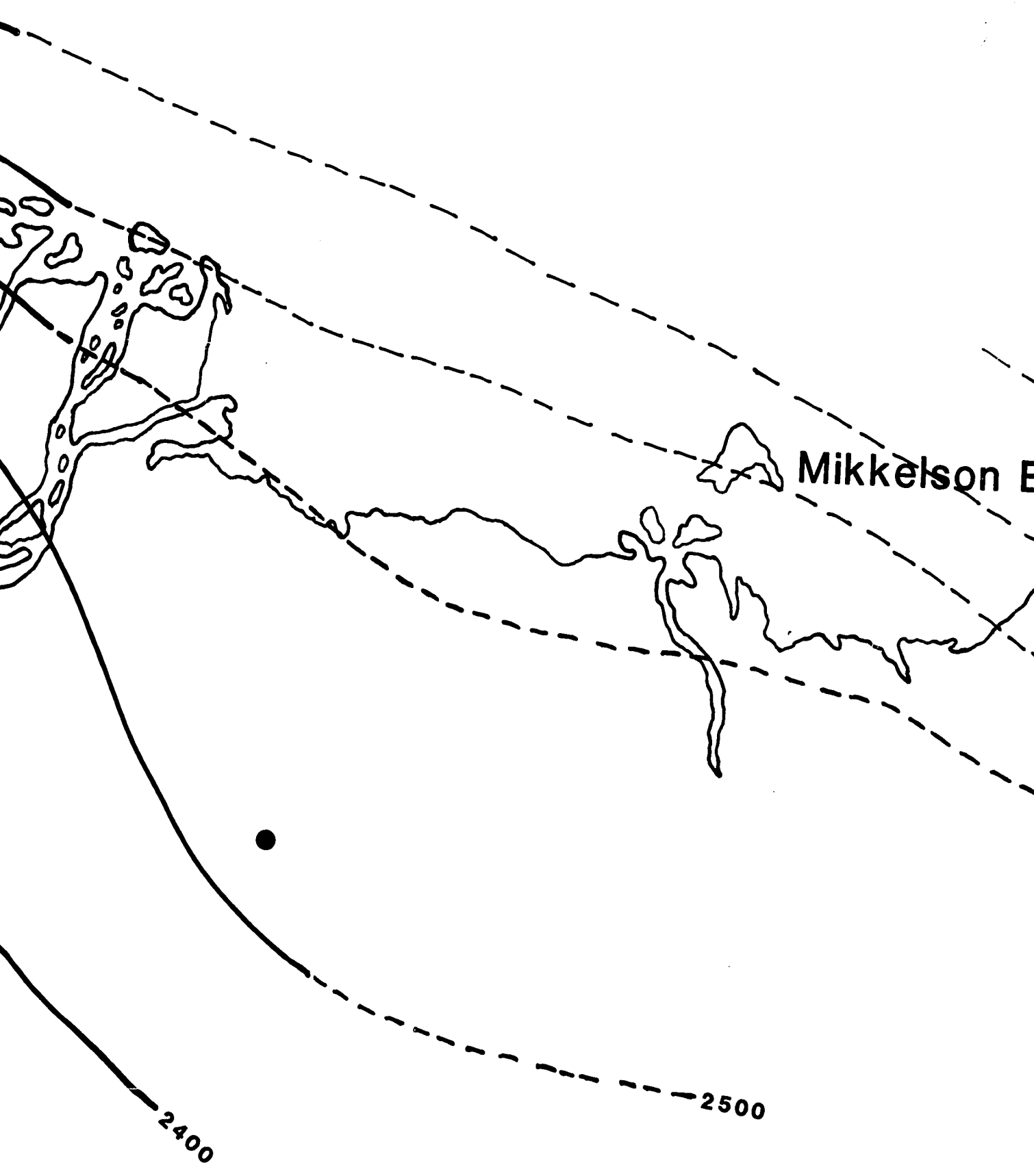

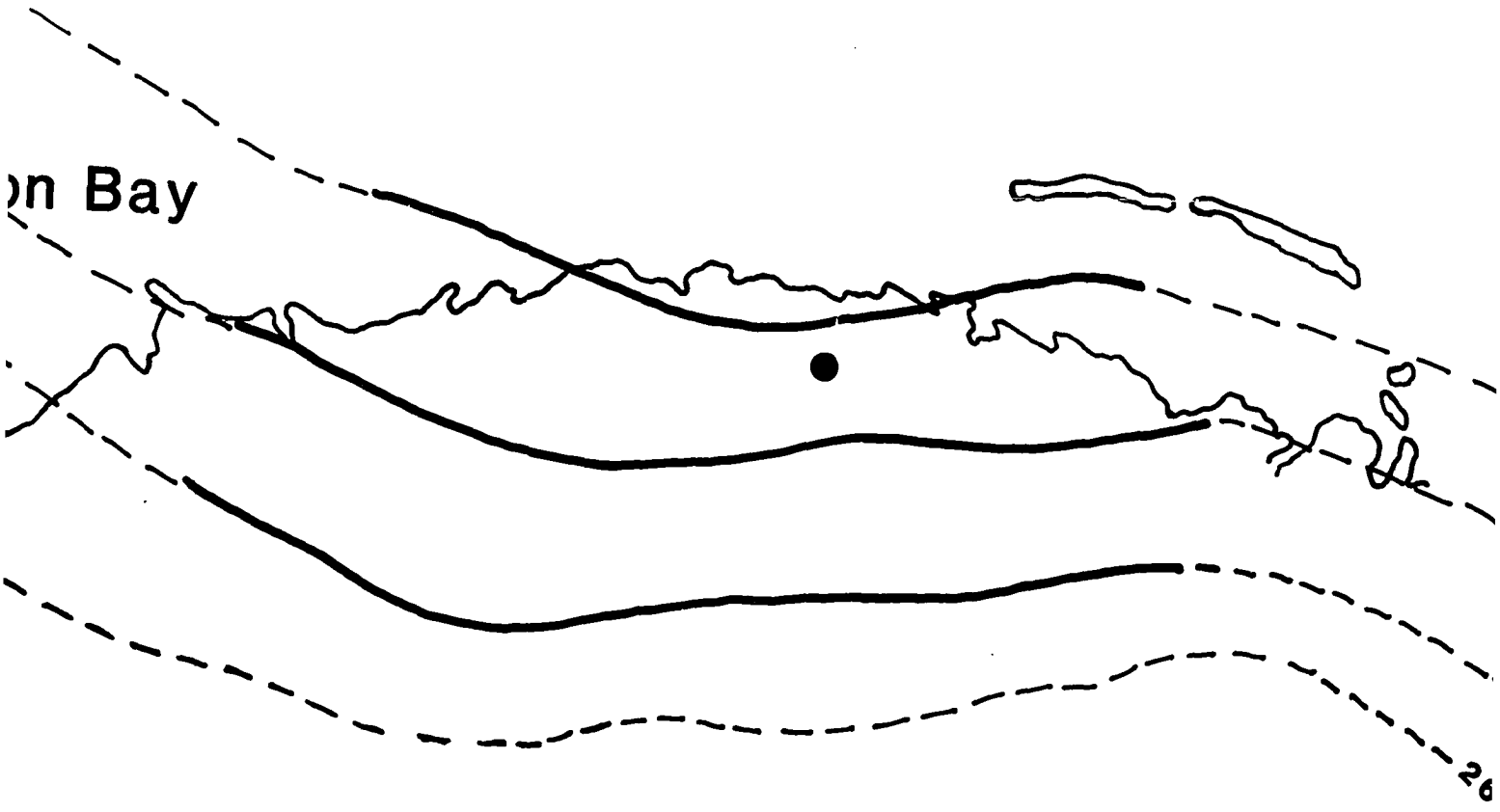

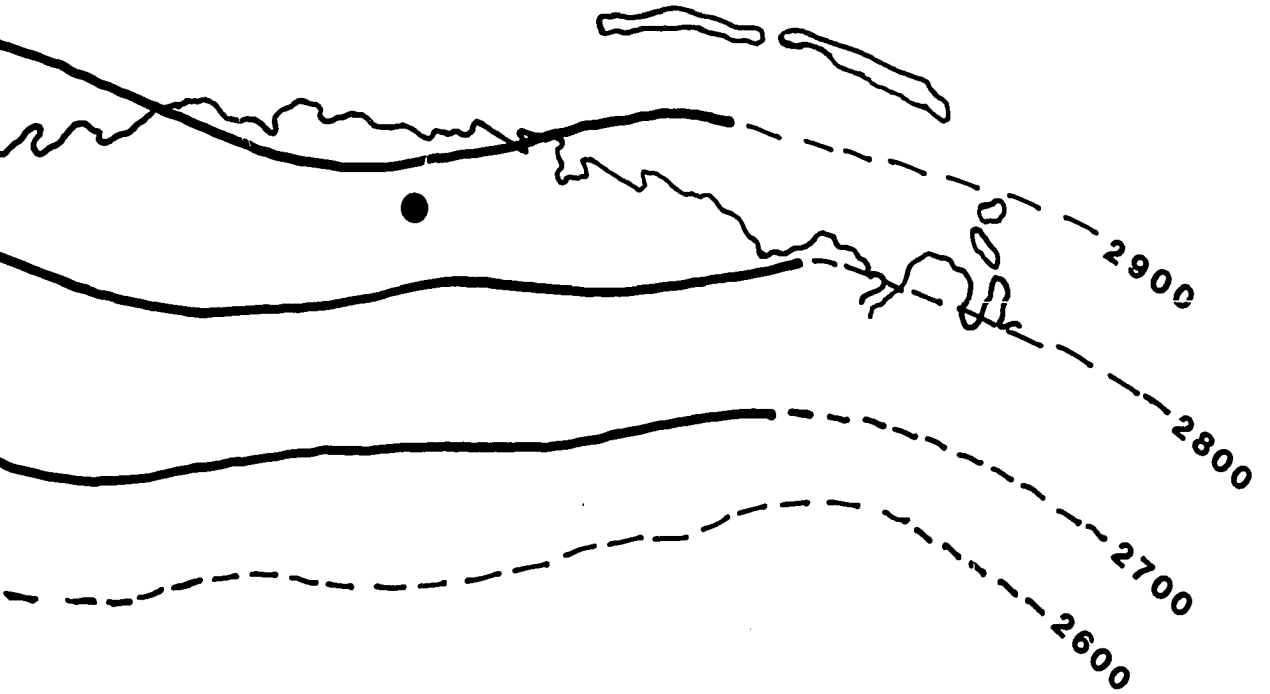

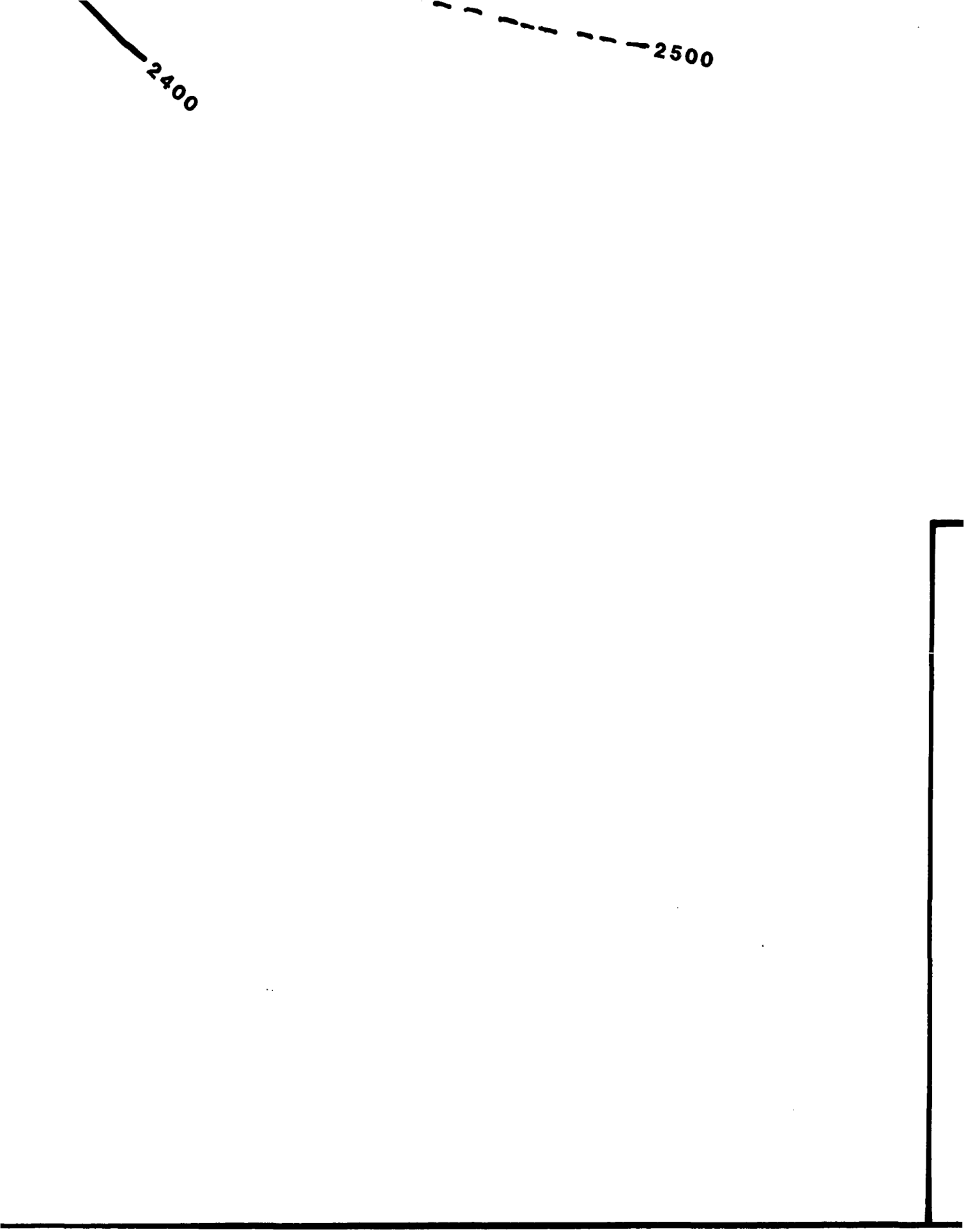

PLATE 4

MAPS OF DEPTH TO HORIZON 6 & 12

contour interval:100 feet

Scale

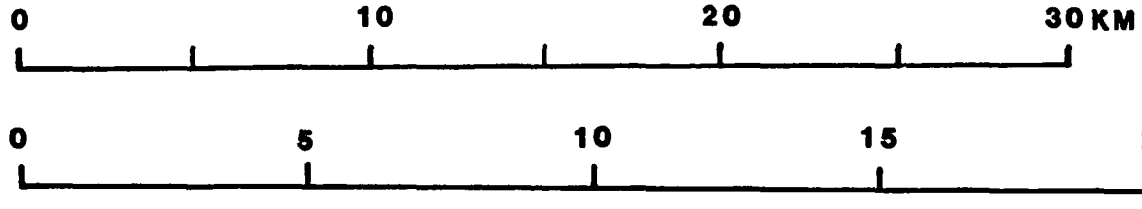

● **Data Point,, Well Location**

PLATE 4

PS OF DEPTH TO HORIZON 6 & 12

contour interval:100 feet

ale

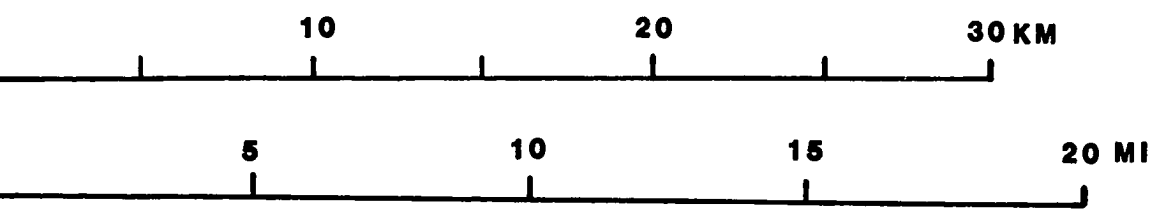

Data Point,, Well Location

PLATE 4

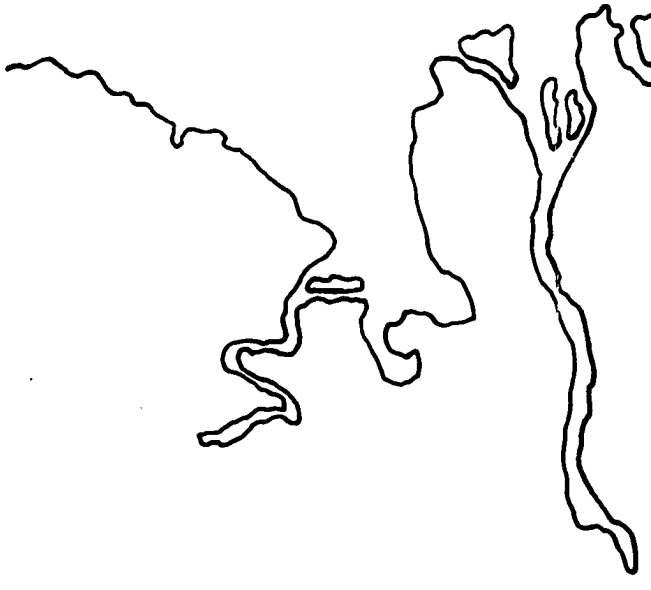

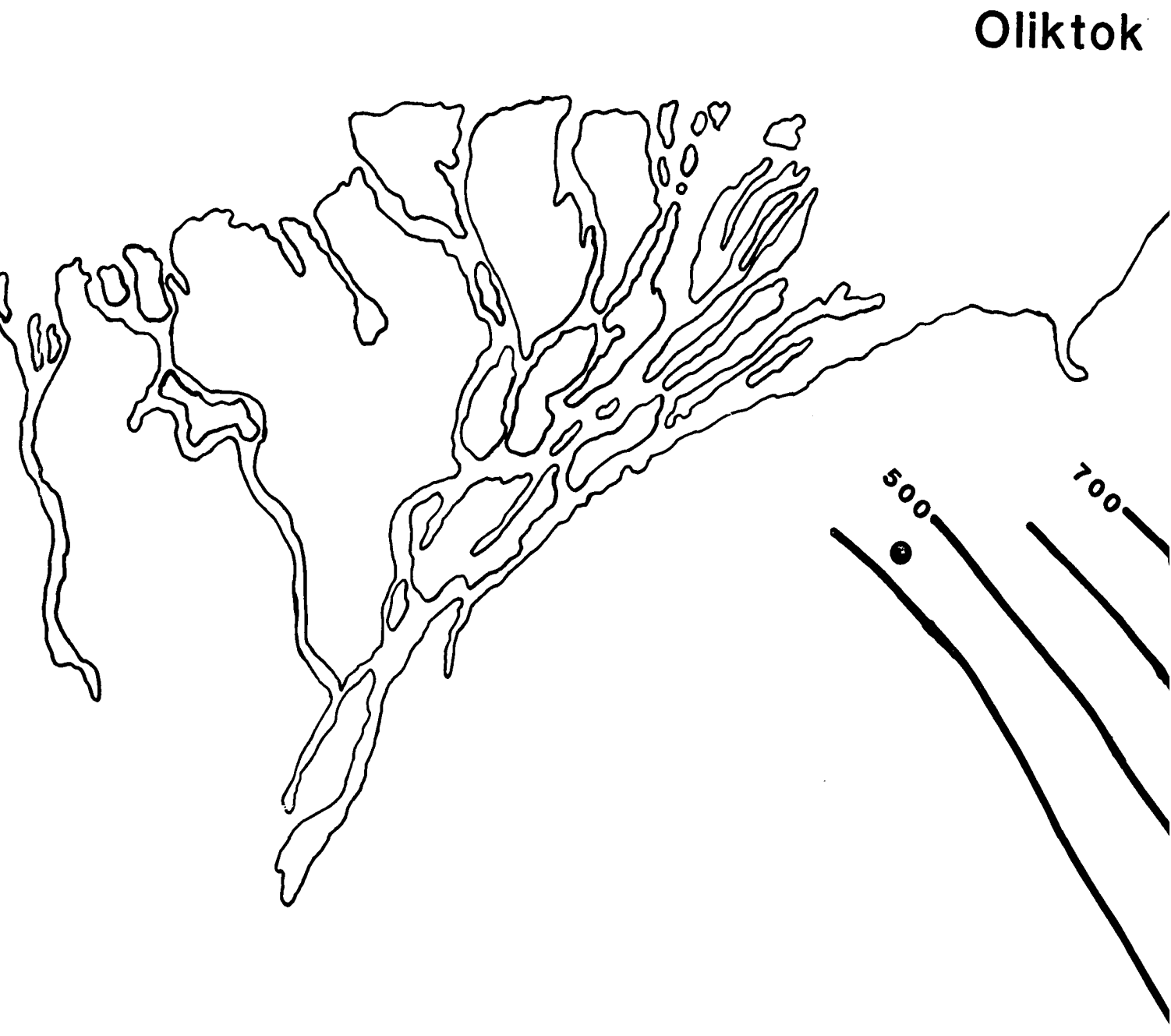

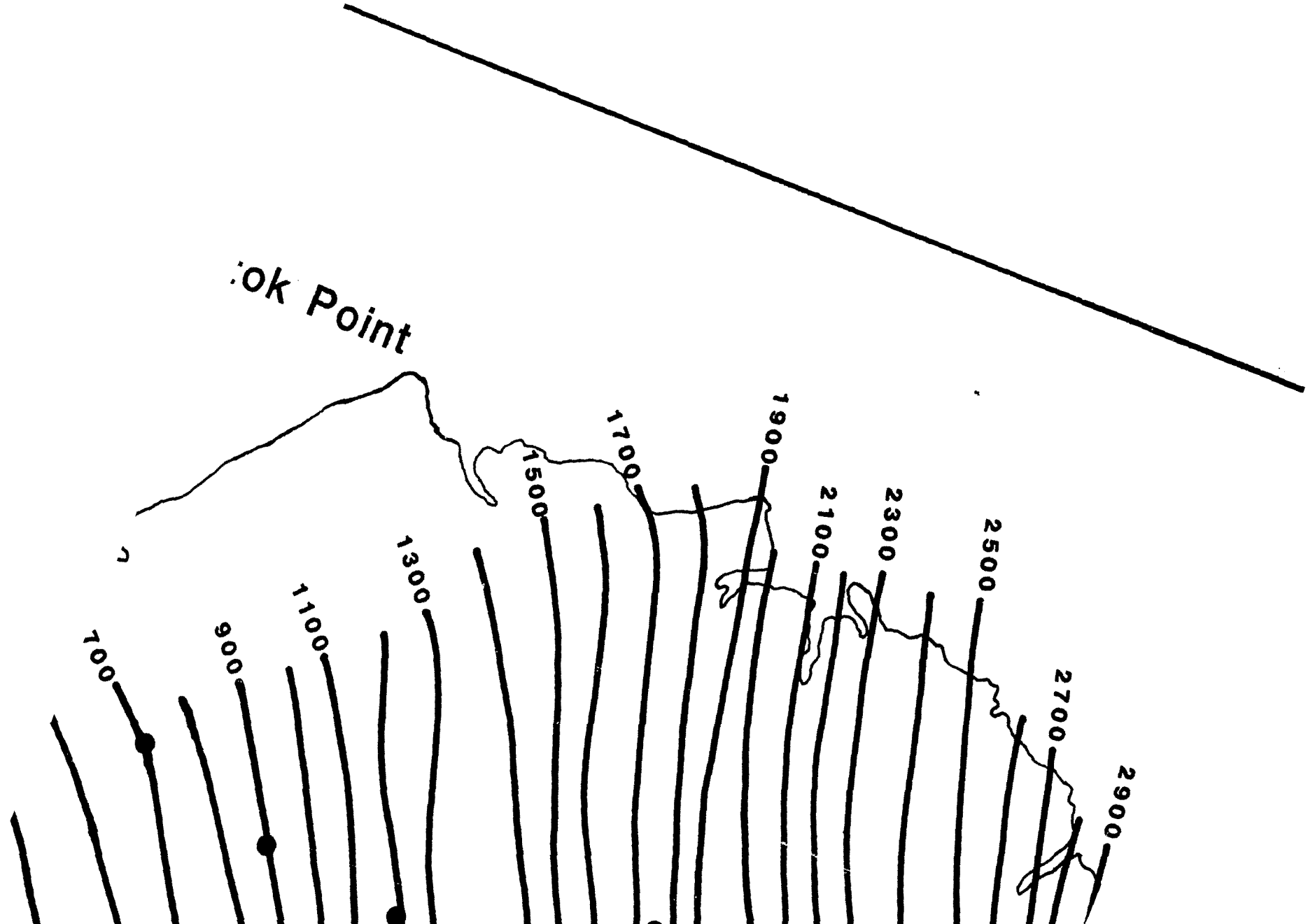
:ok Point
700
900
1100
1300
1500
1700
1900
2100
2300
2500
2700
2900

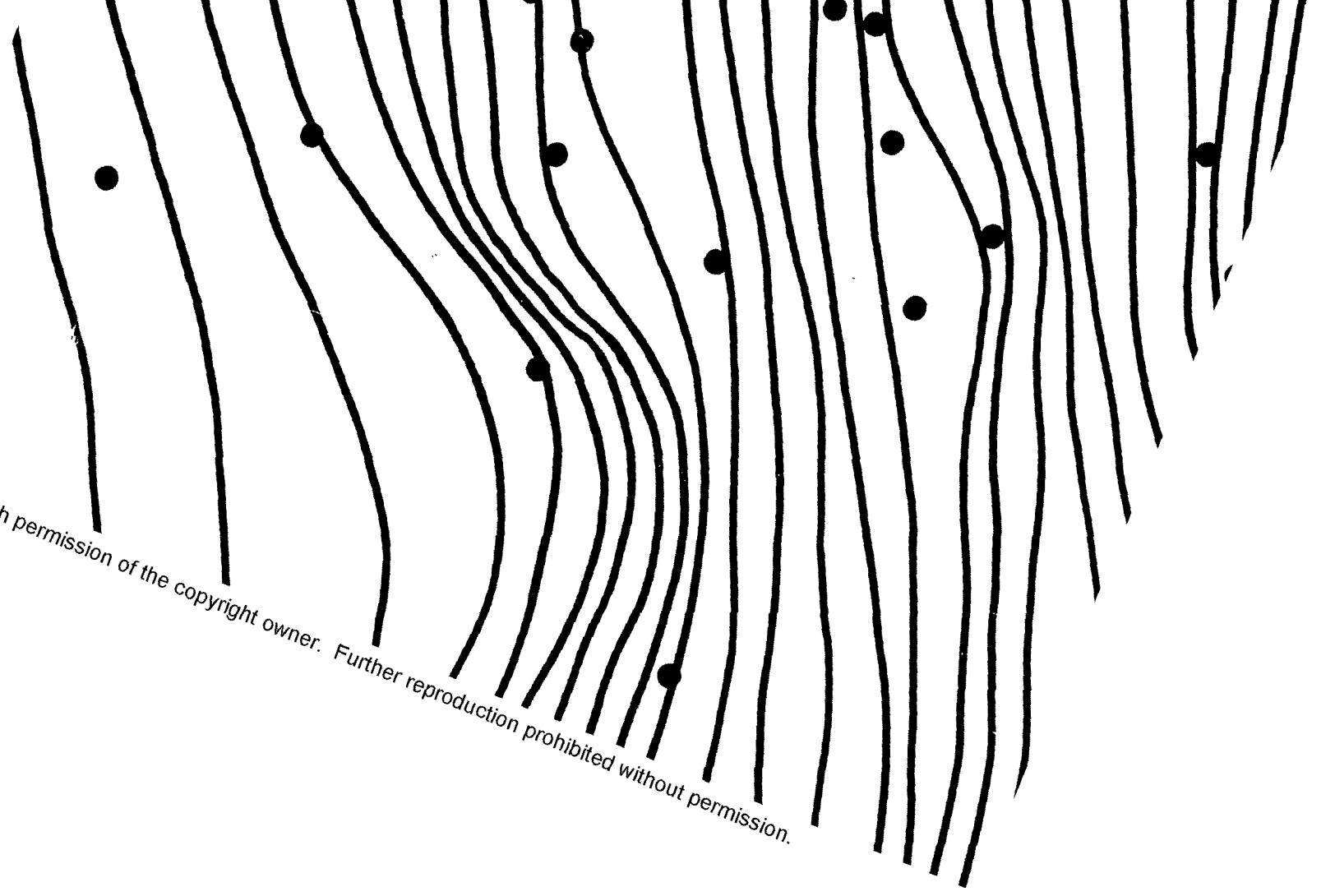

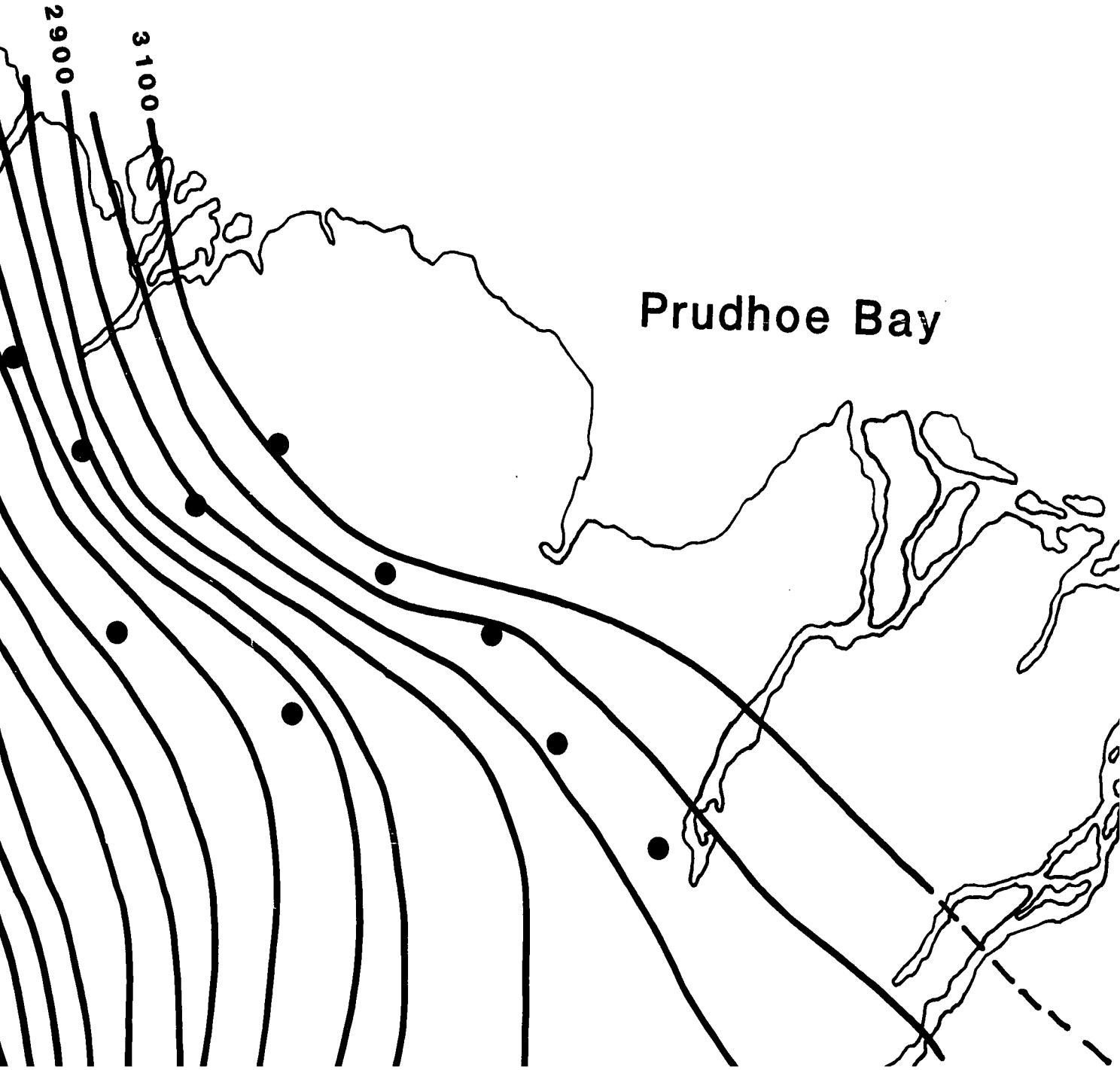

ARCTIC

C OCEAN

kelson Bay

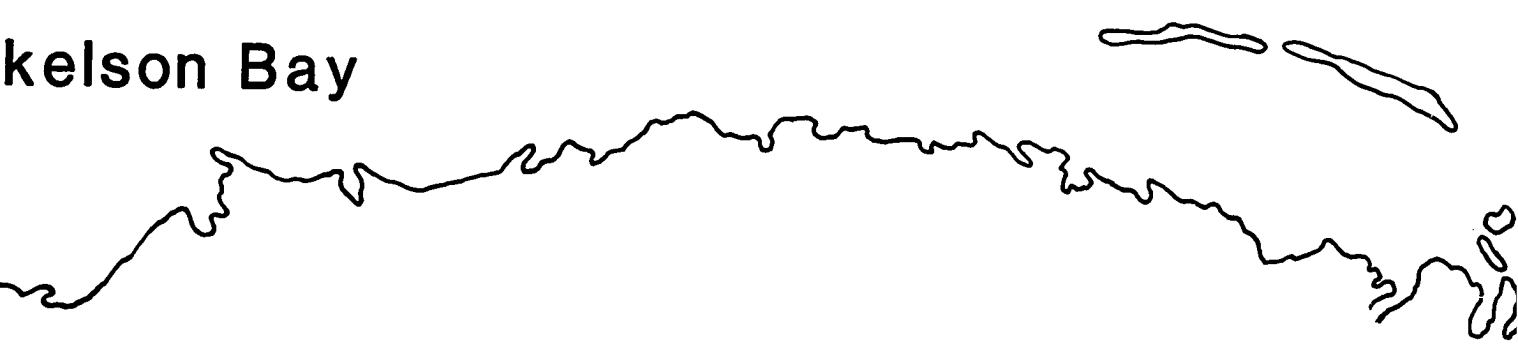

EAN

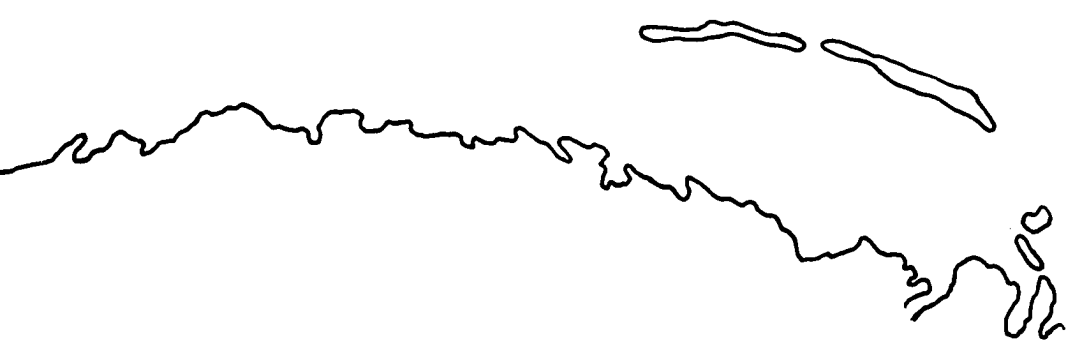

HORIZON 15

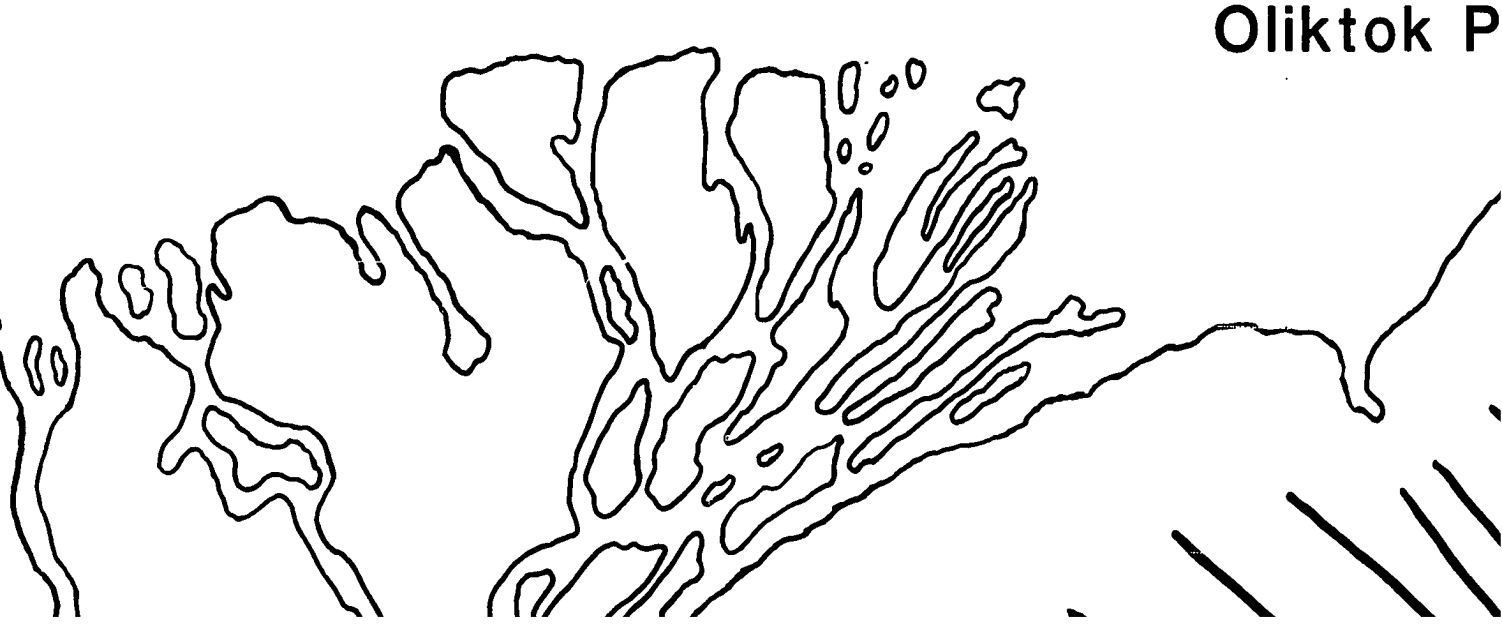

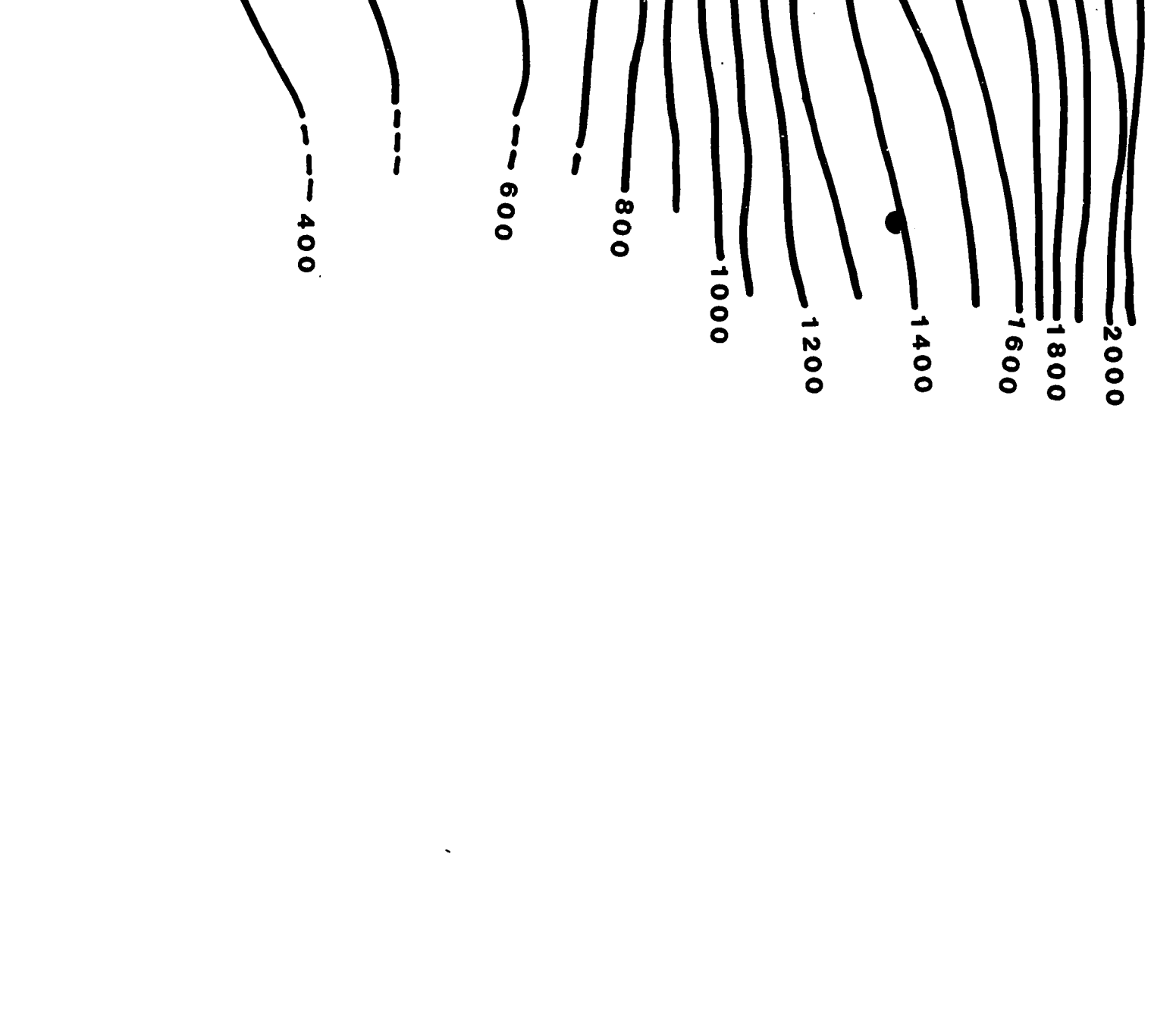

ok Point

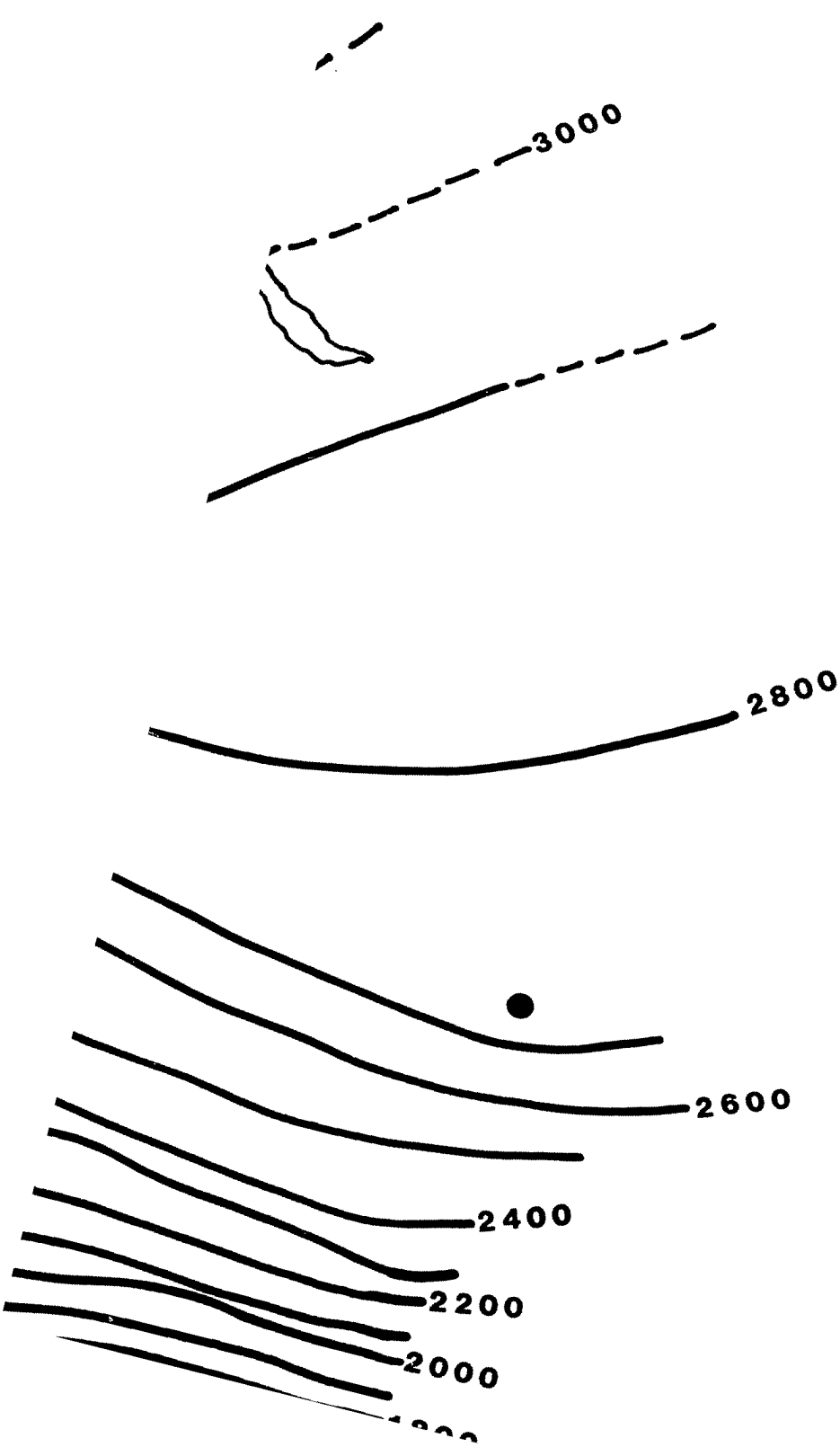
3000
2800
2600
2400
2200
2000

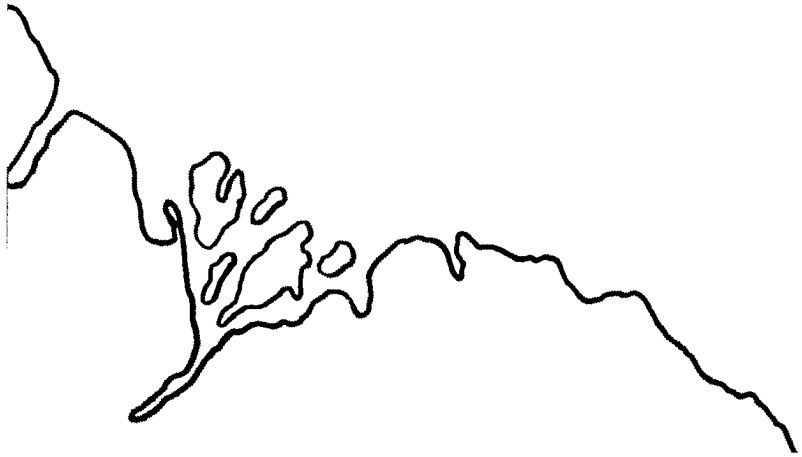

Prudhoe Bay

ARCTIC OCEAN

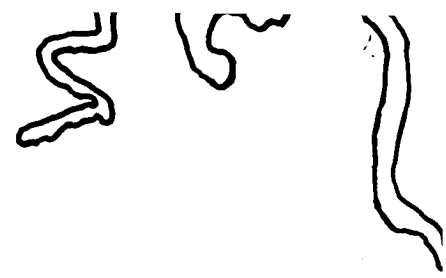

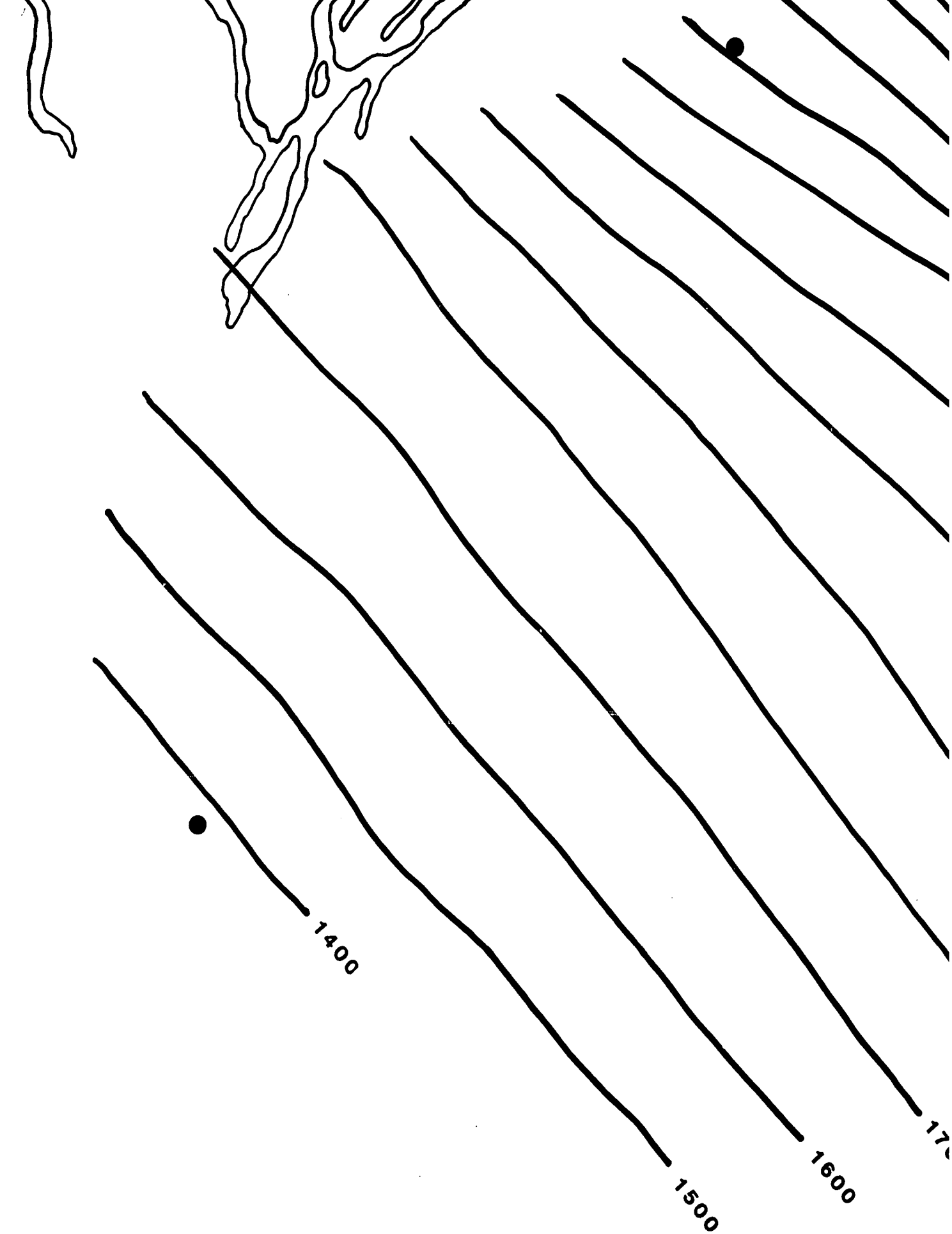

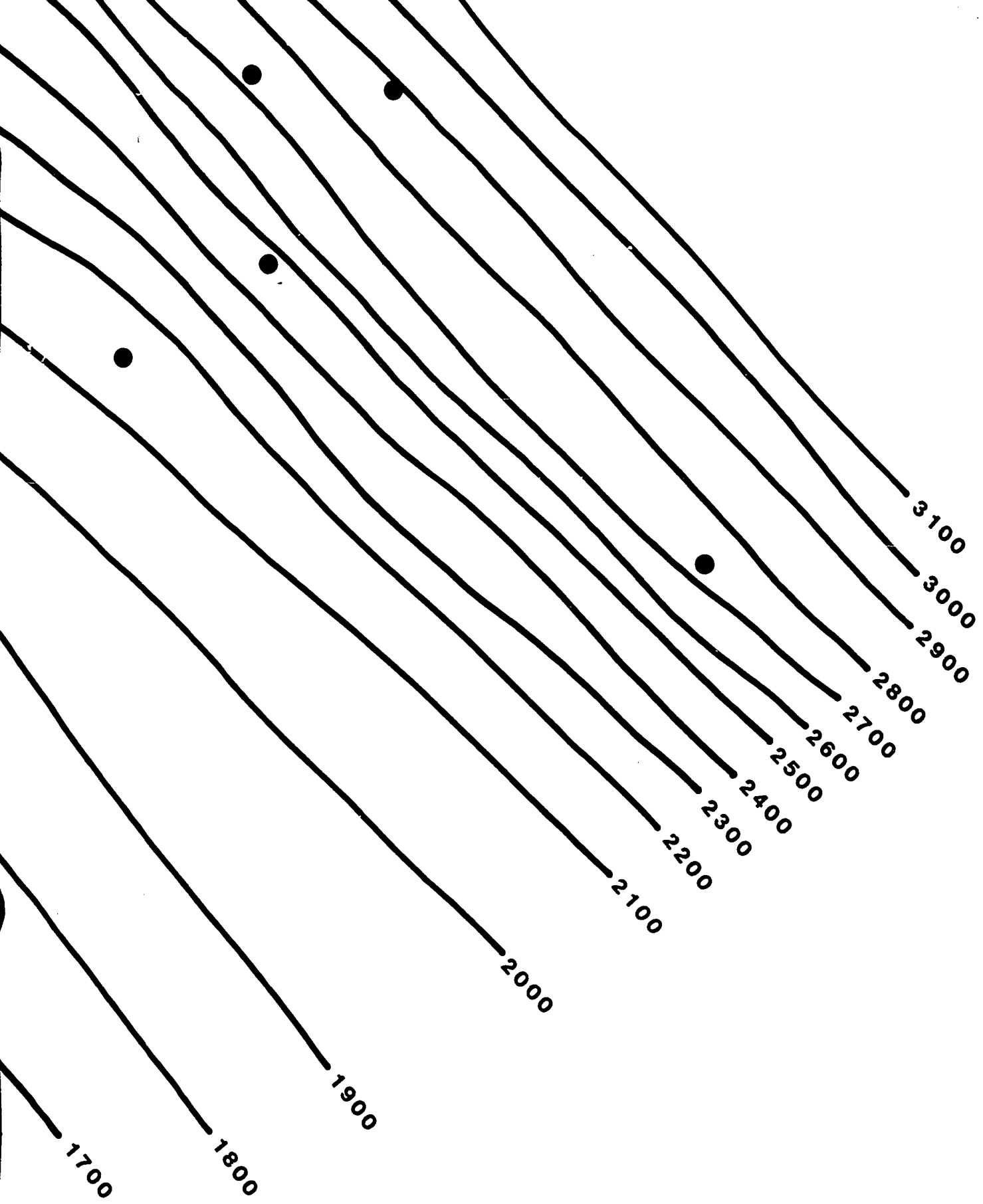

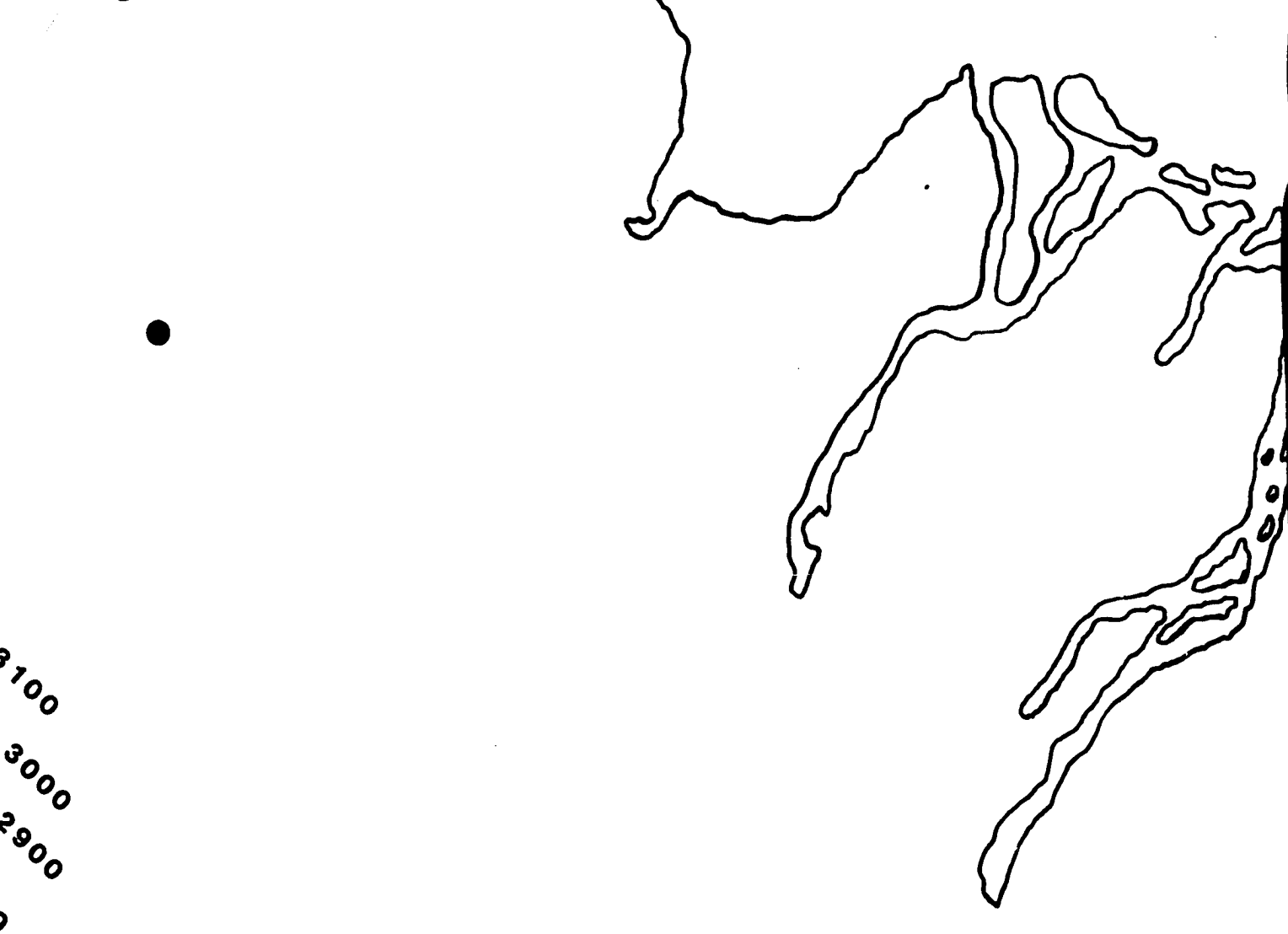

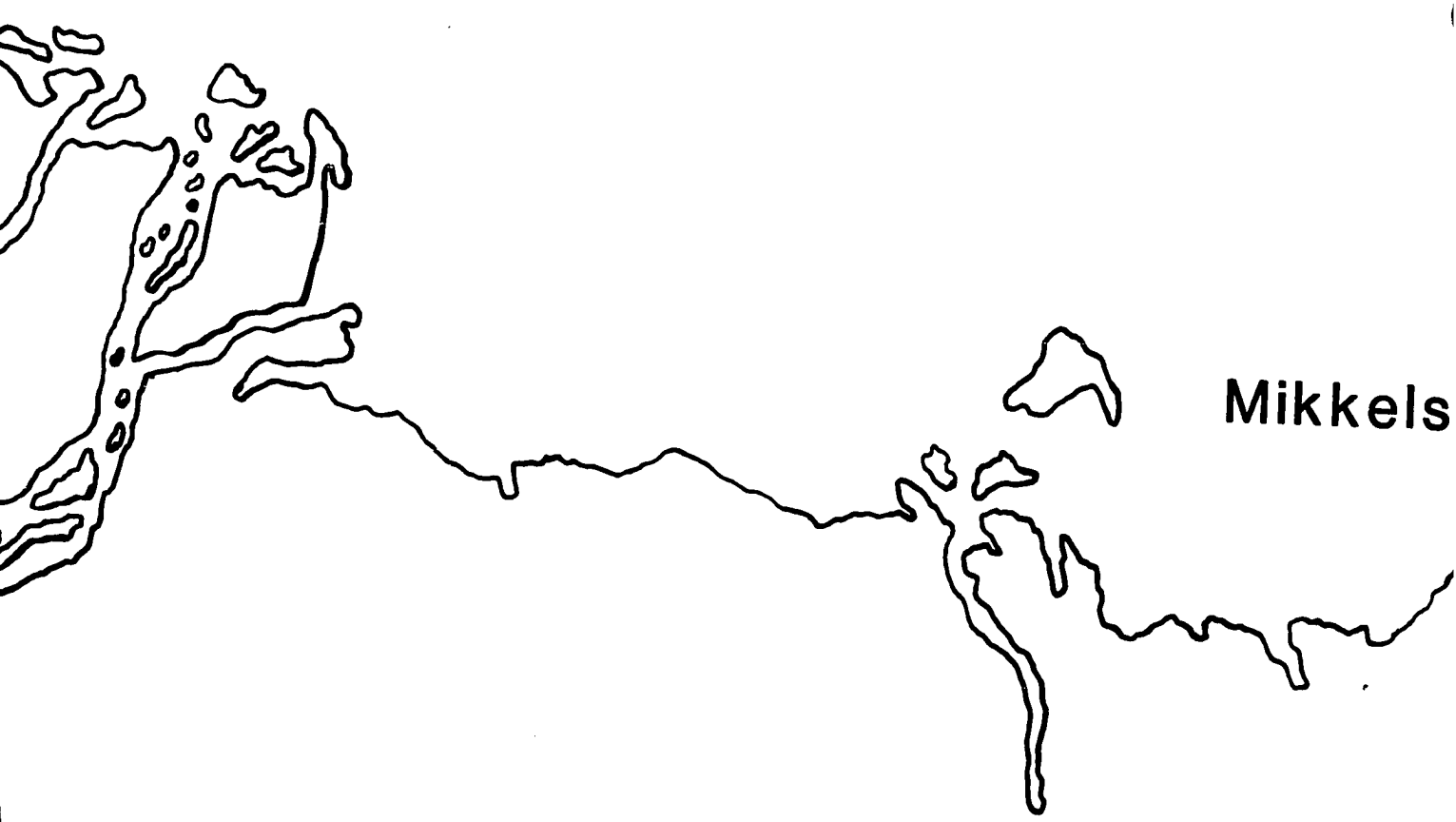

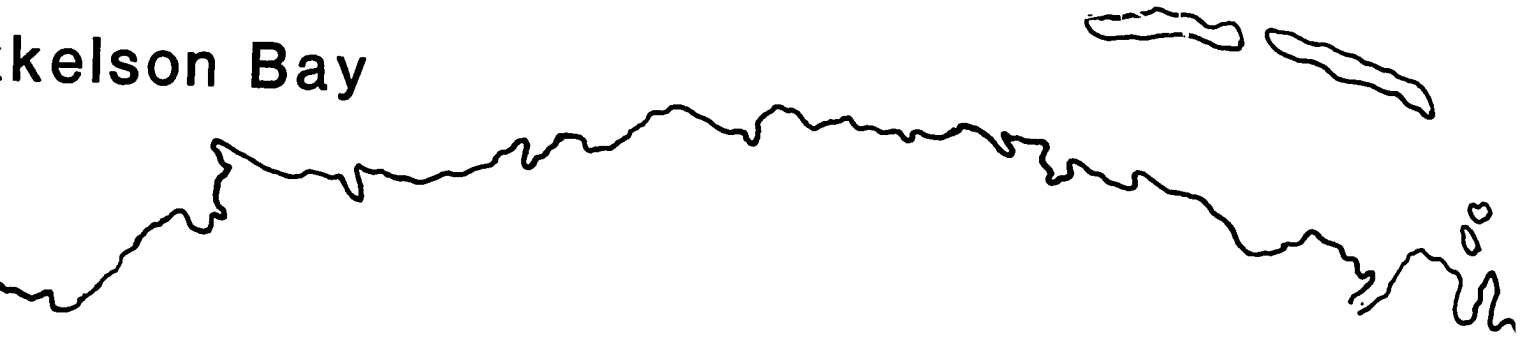

HOR

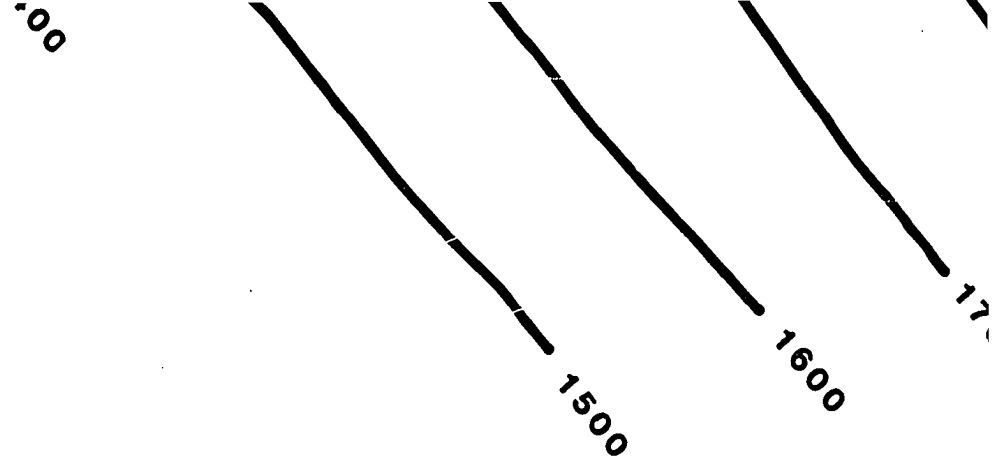

HORIZON 21

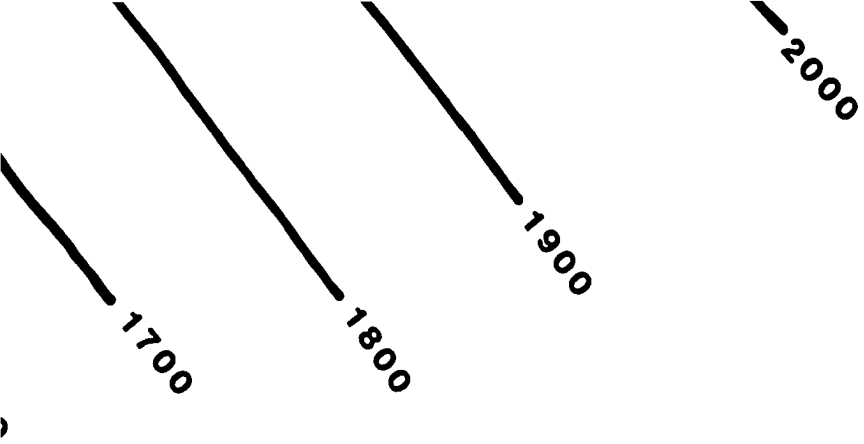

PLATE 5

MAPS OF DEPTH TO HORIZON 15 &

contour interval:100 feet

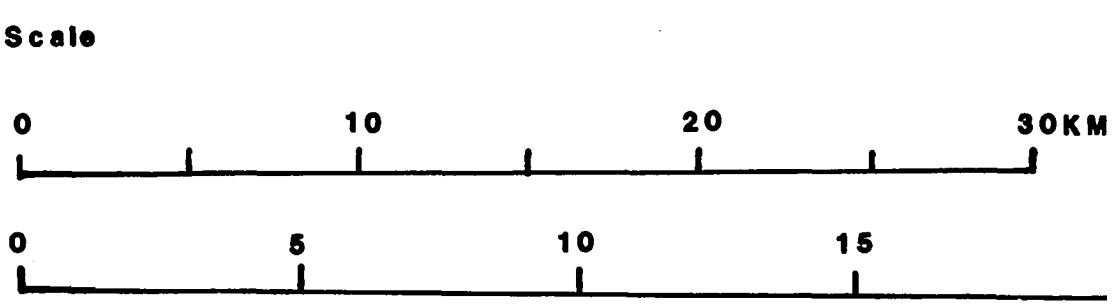

● Data Point, Well Location

PLATE 5

'S OF DEPTH TO HORIZON 15 & 21

contour interval:100 feet

ale

10 20 30KM

5 10 15 20MI

Data Point, Well Location

PLATE 5

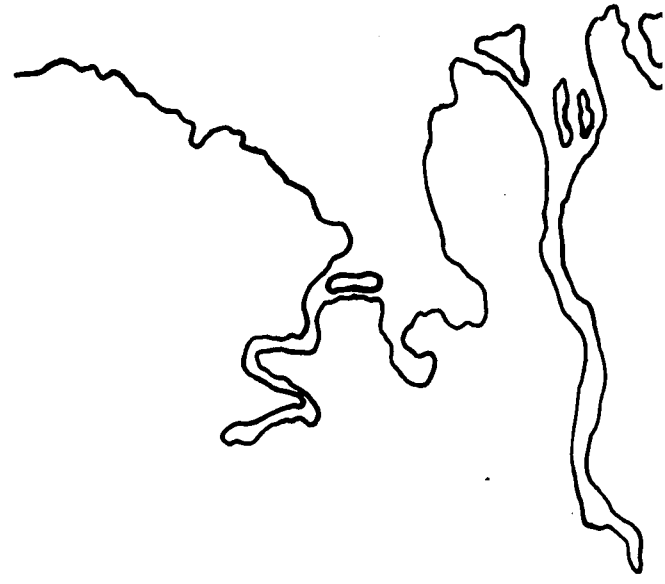

Oliktok F

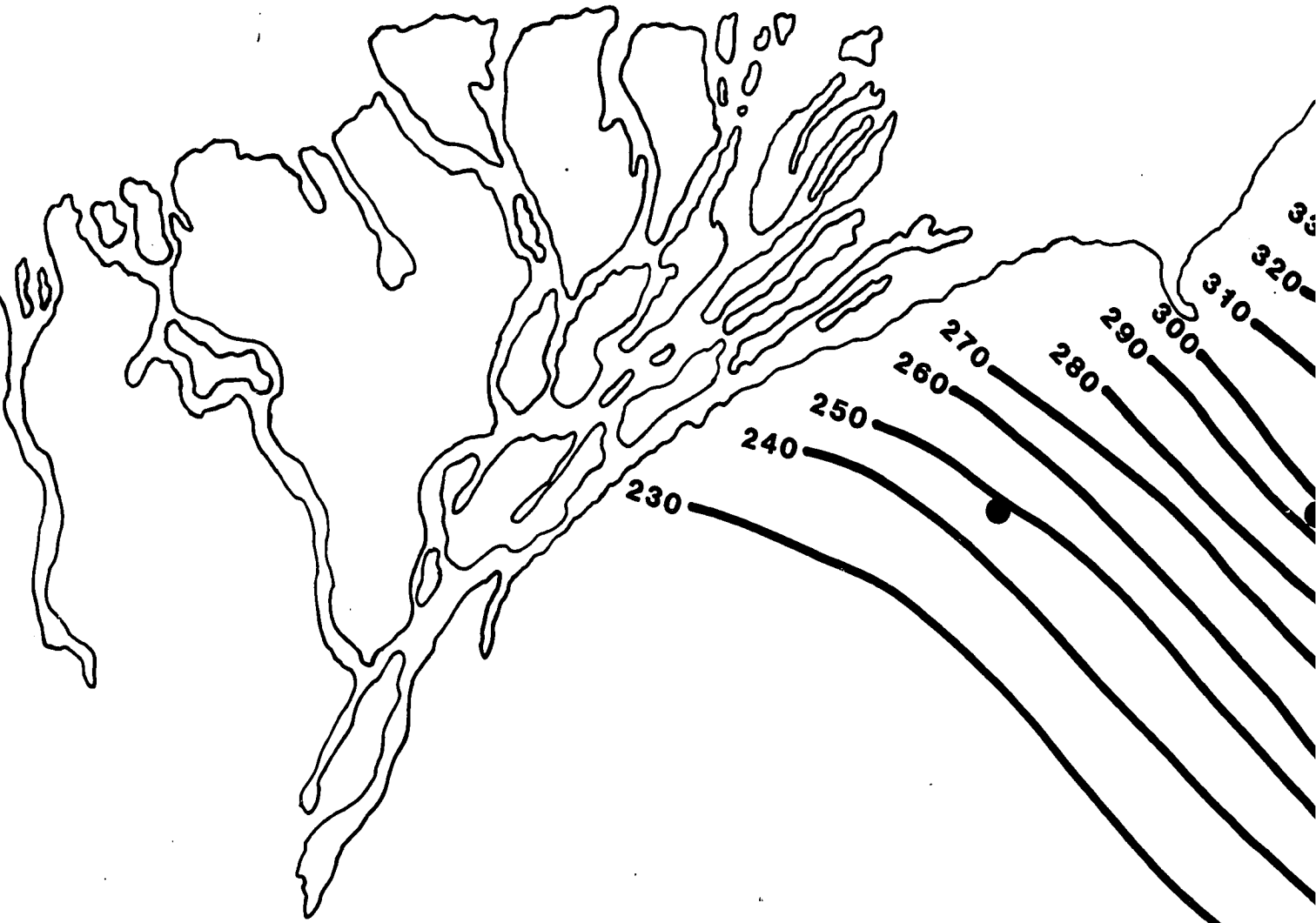

UNIT R

tok Point

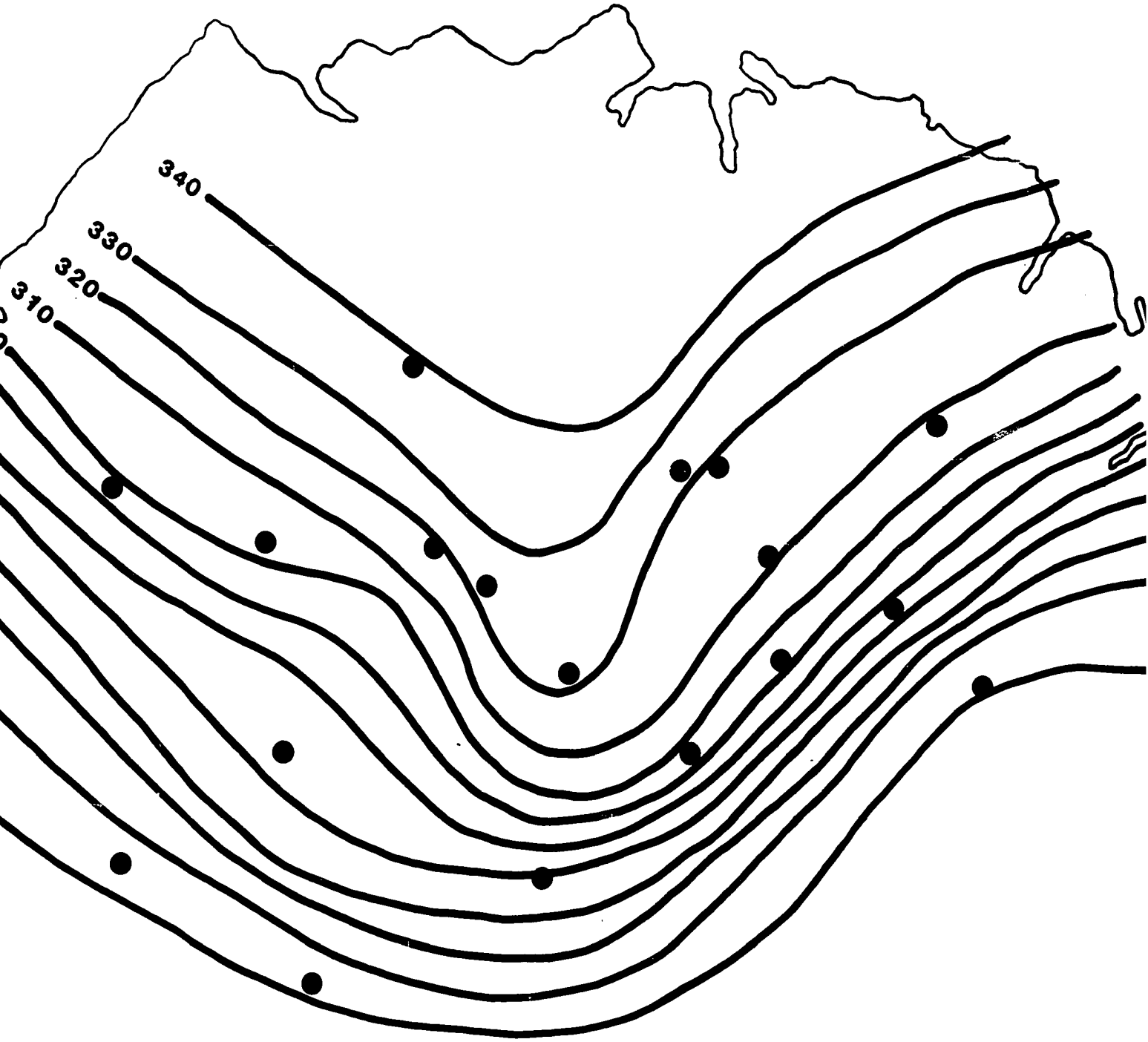

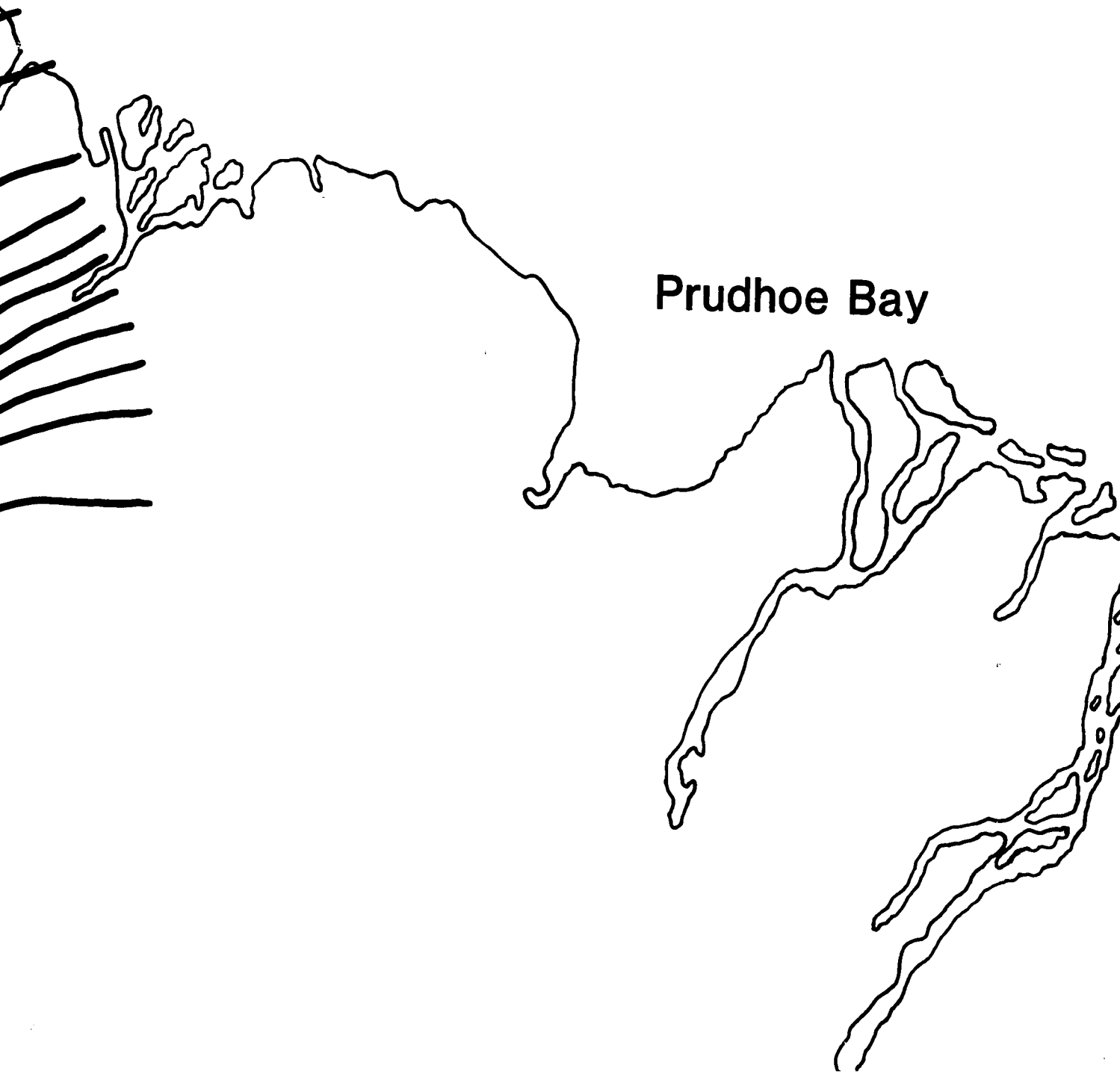

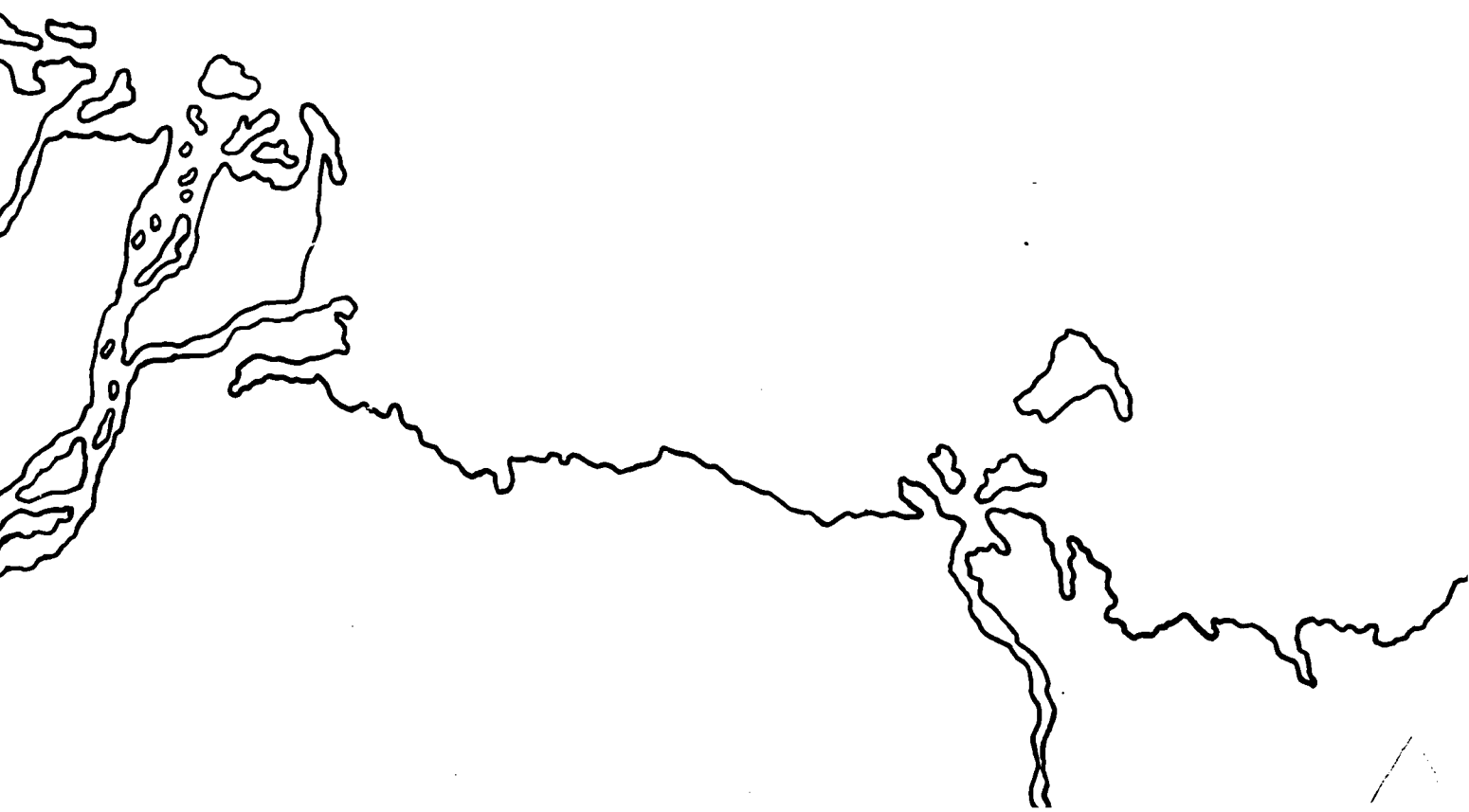

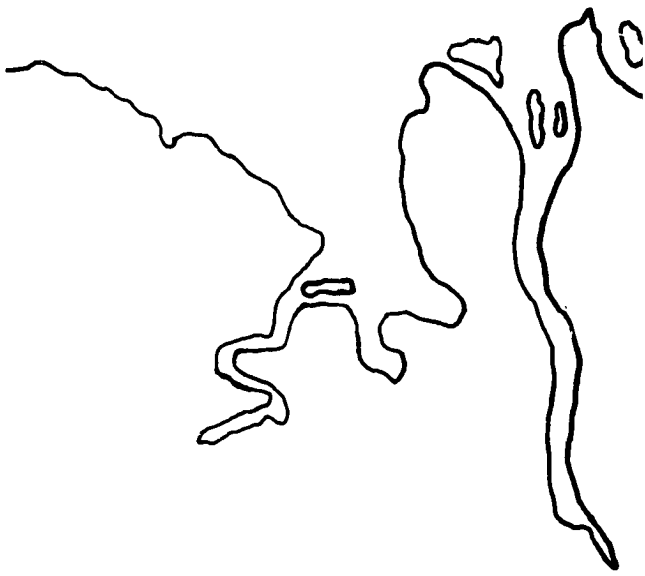

Oliktok

UNIT Q

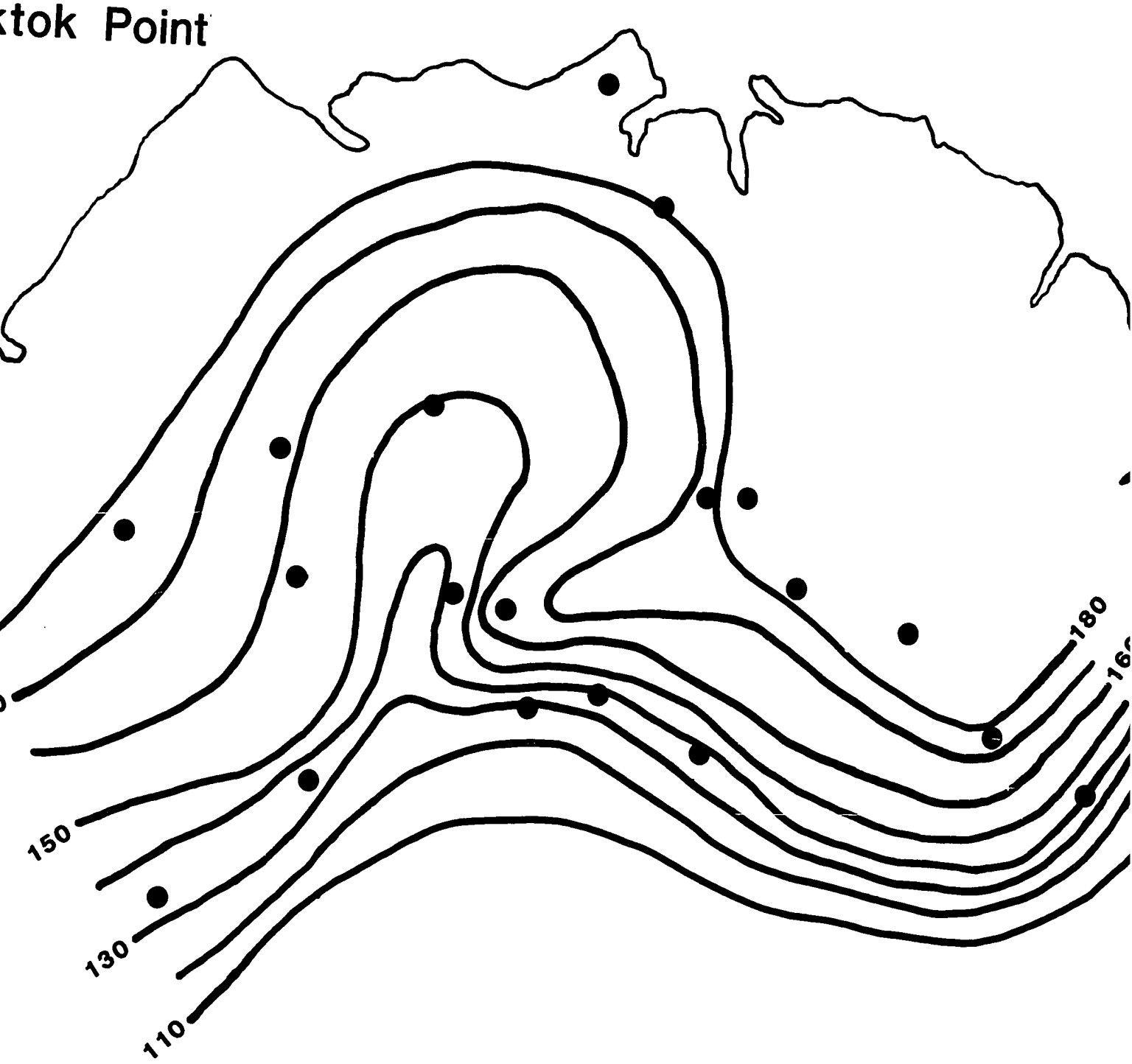

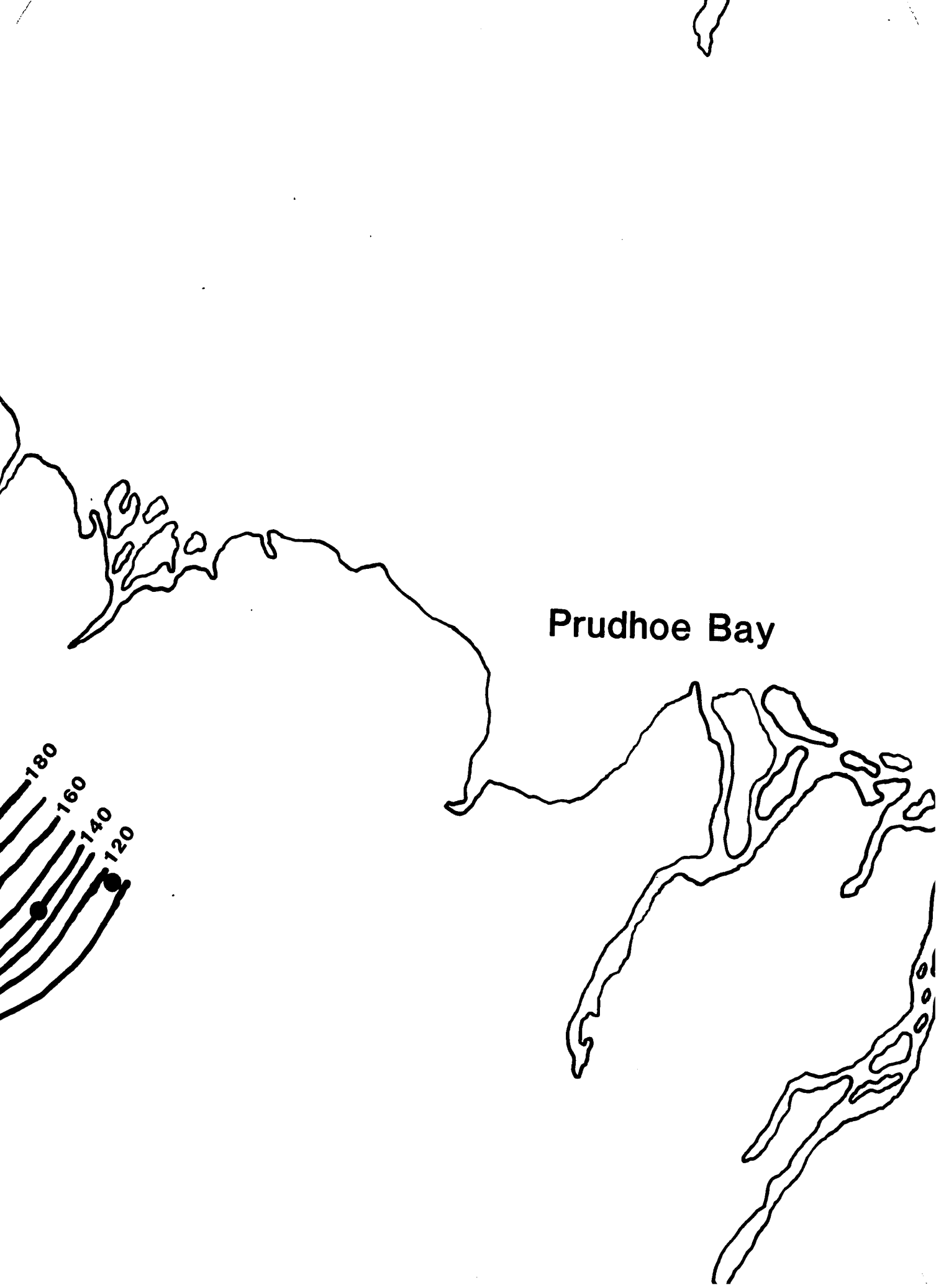

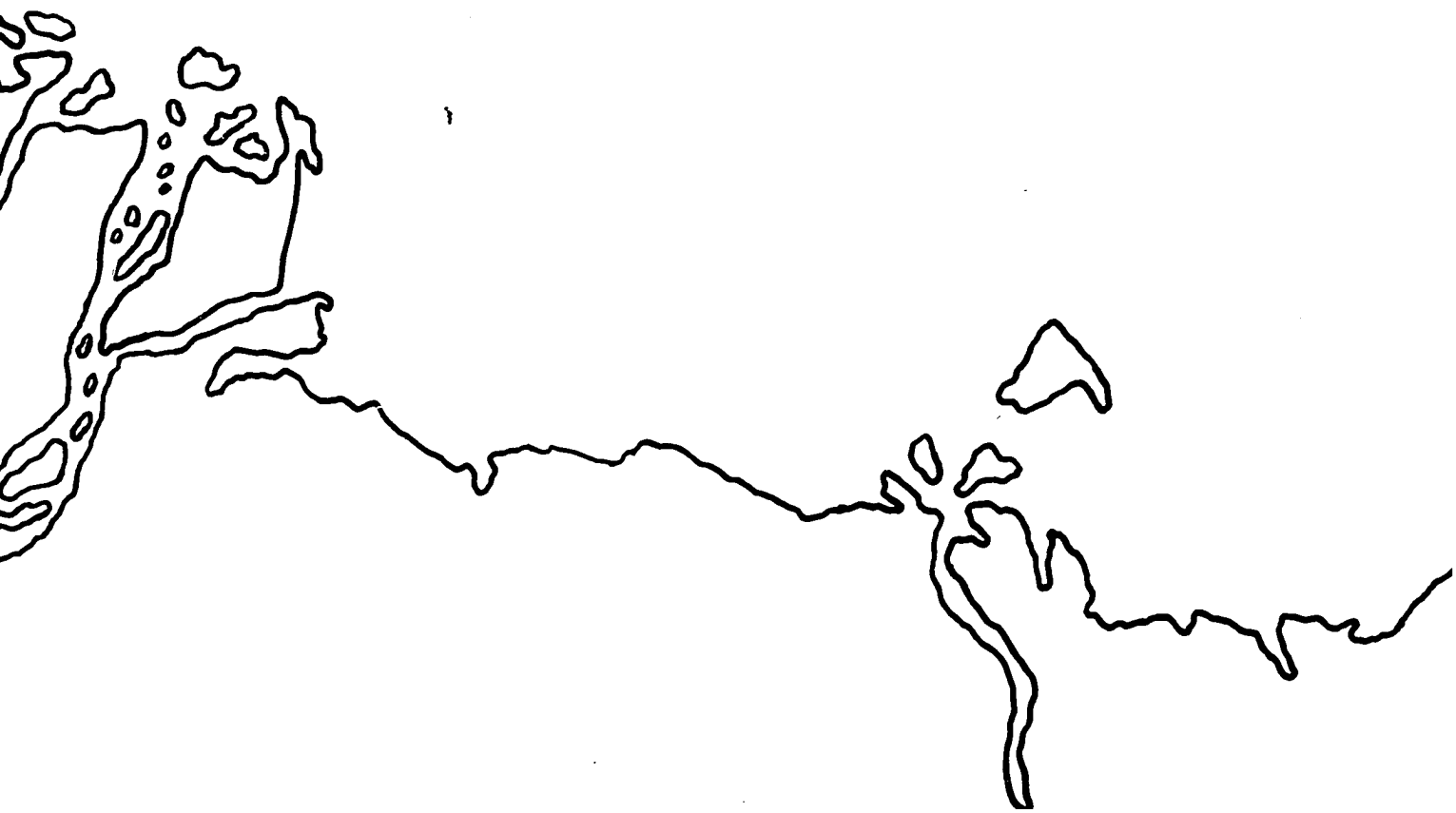

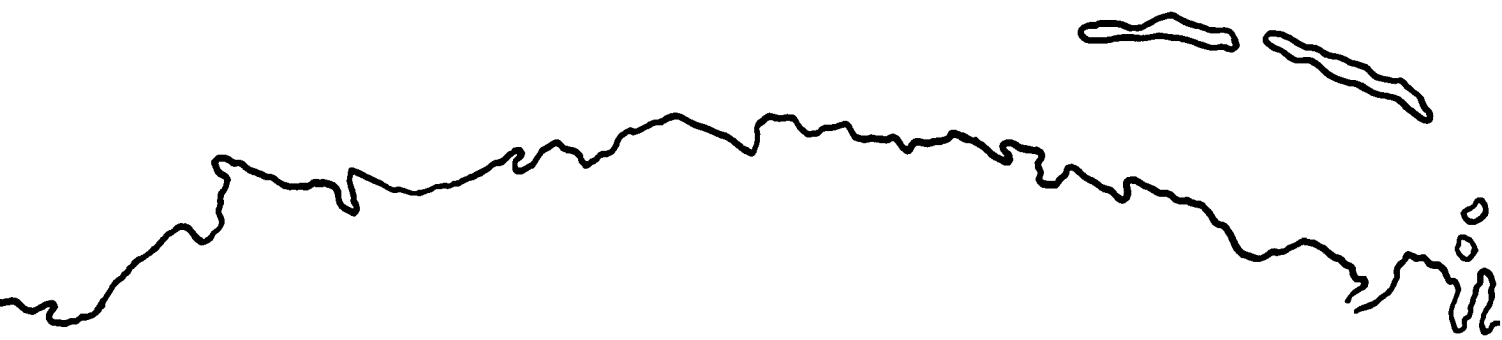

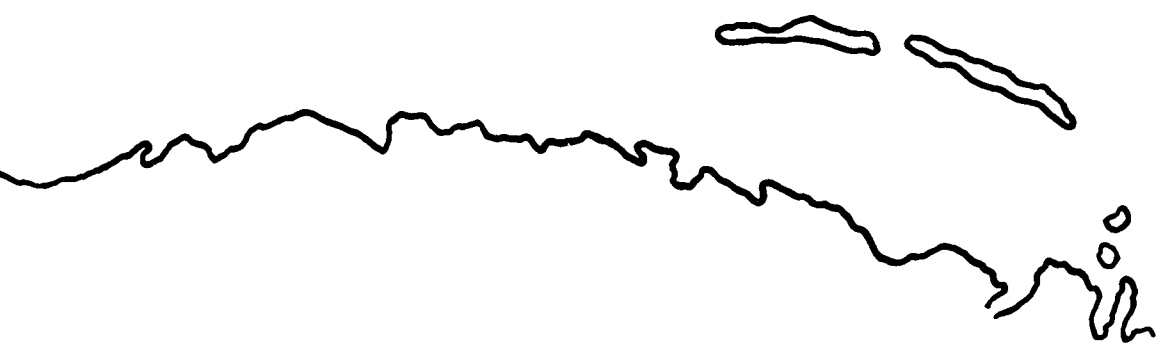

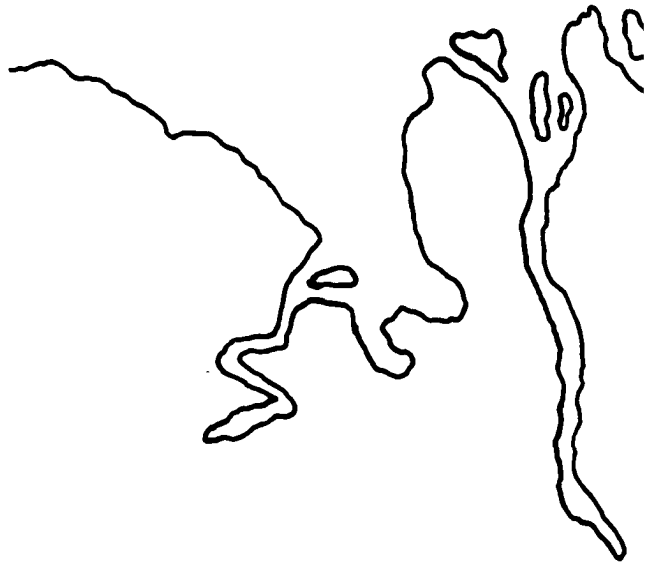

Oliktok I

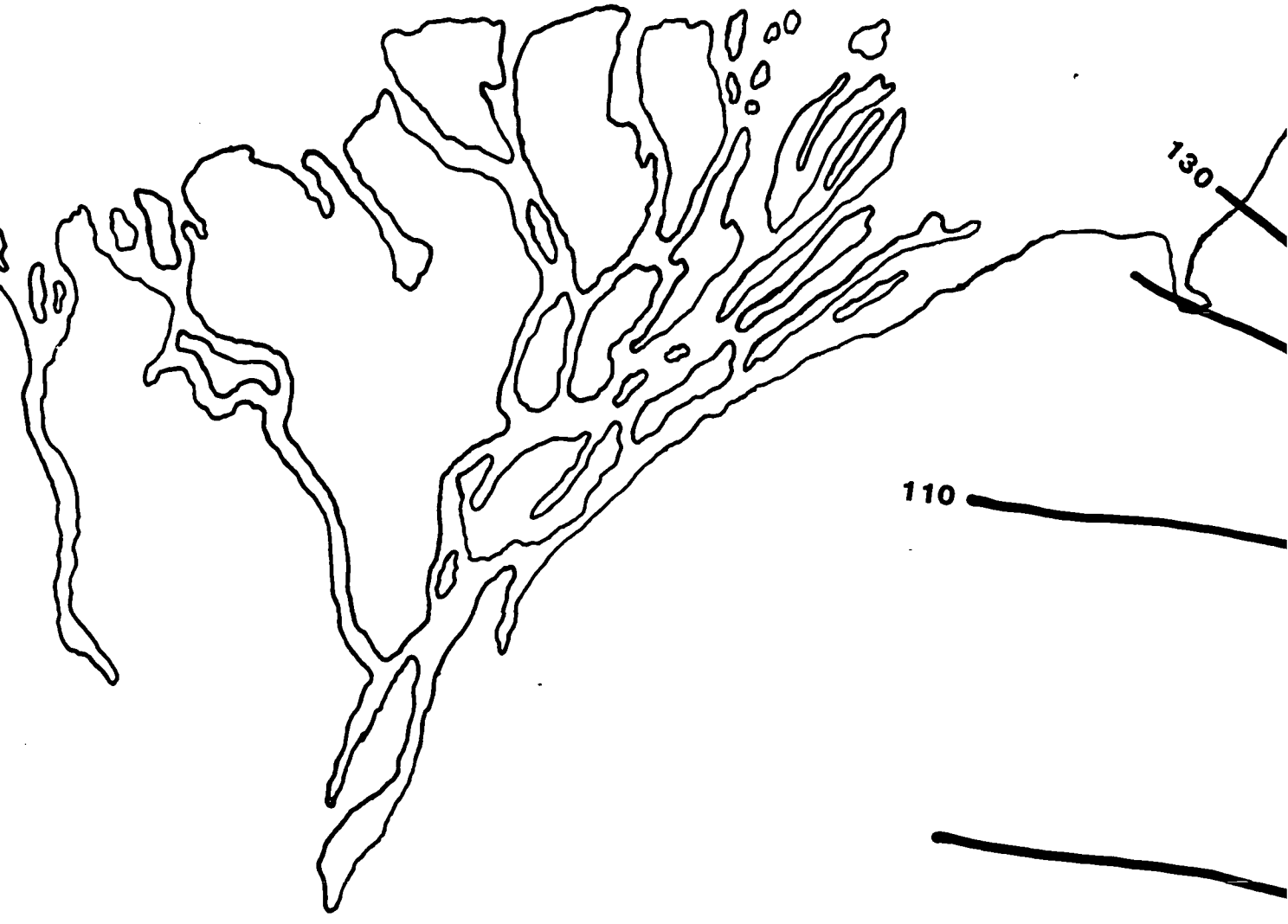

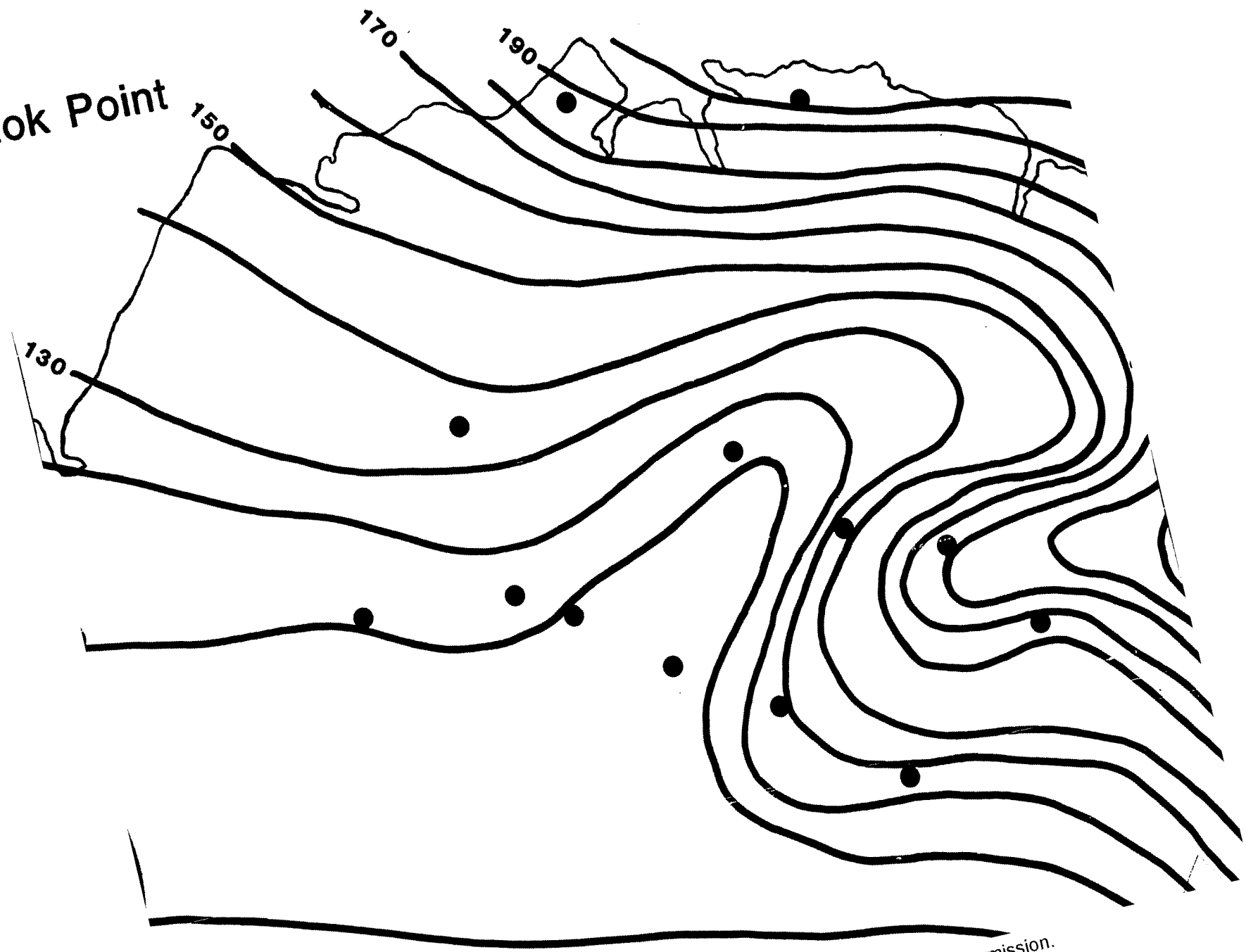

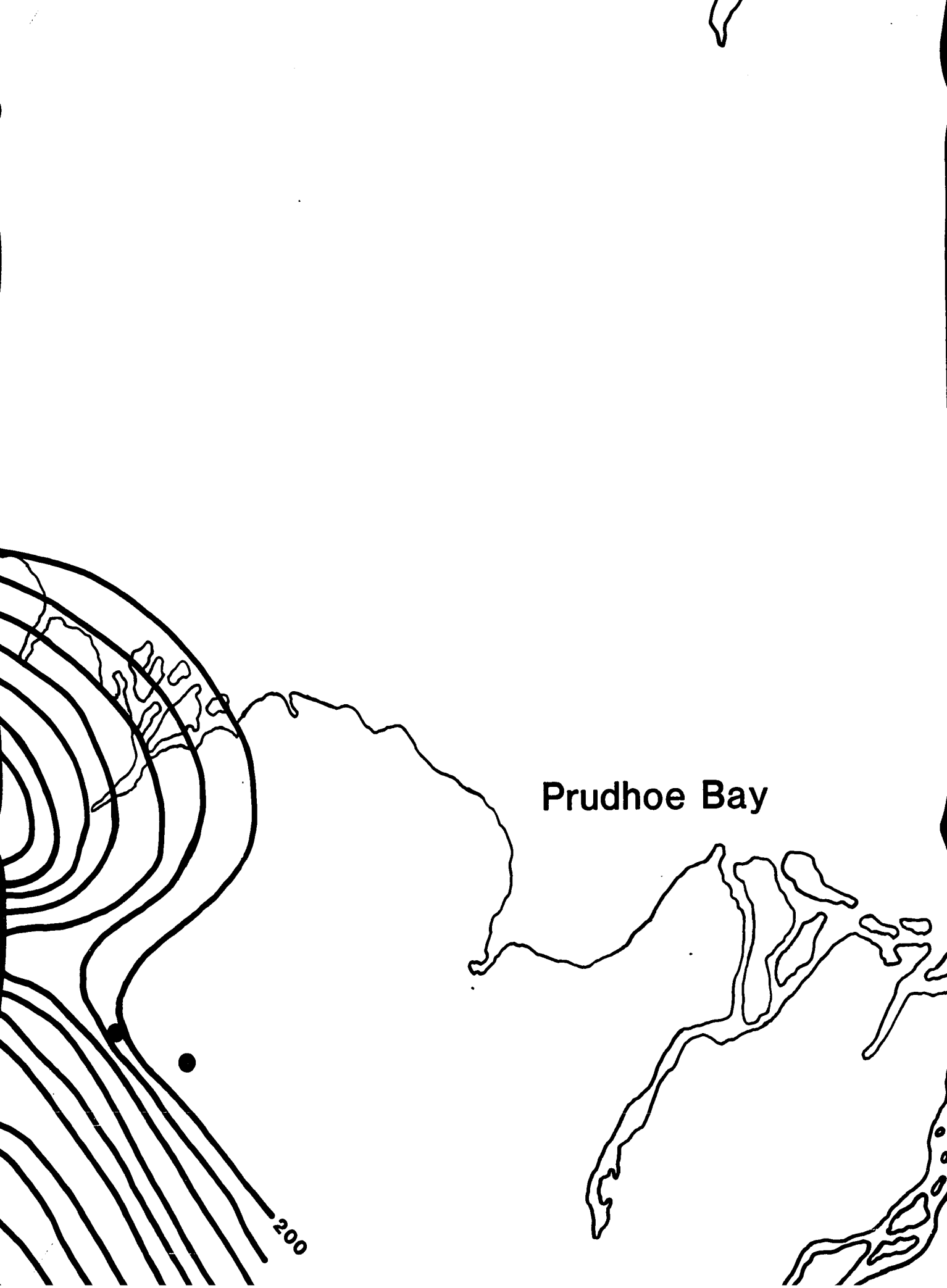

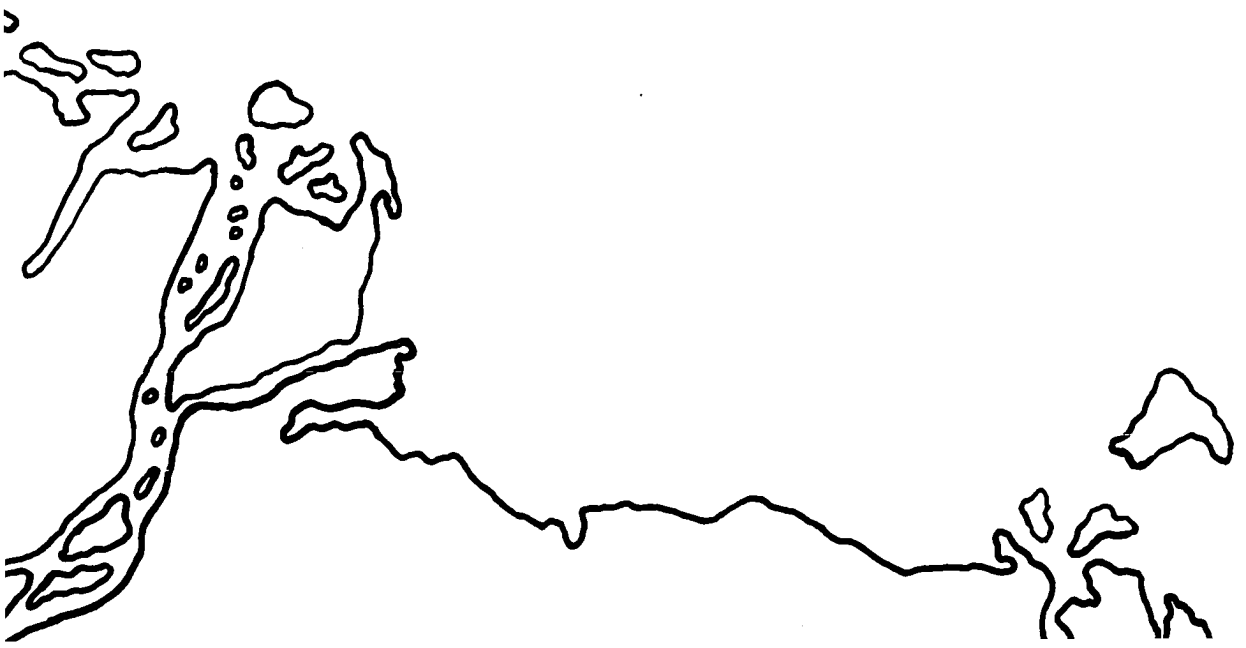

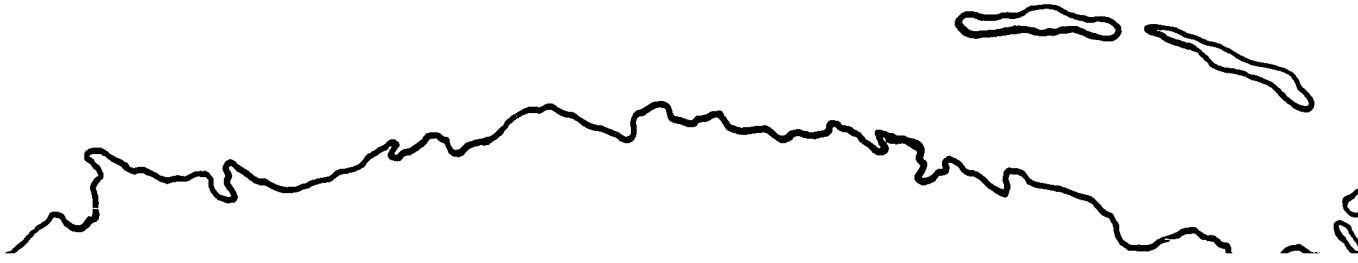

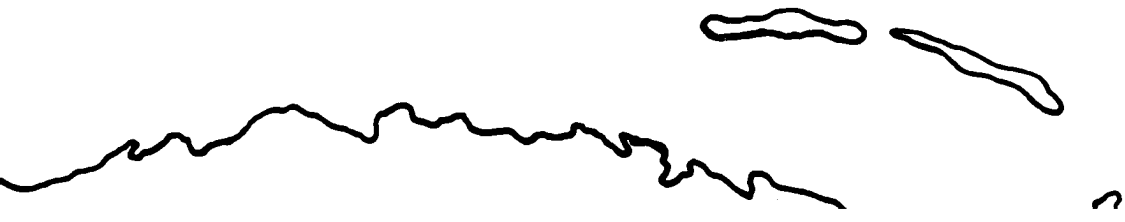

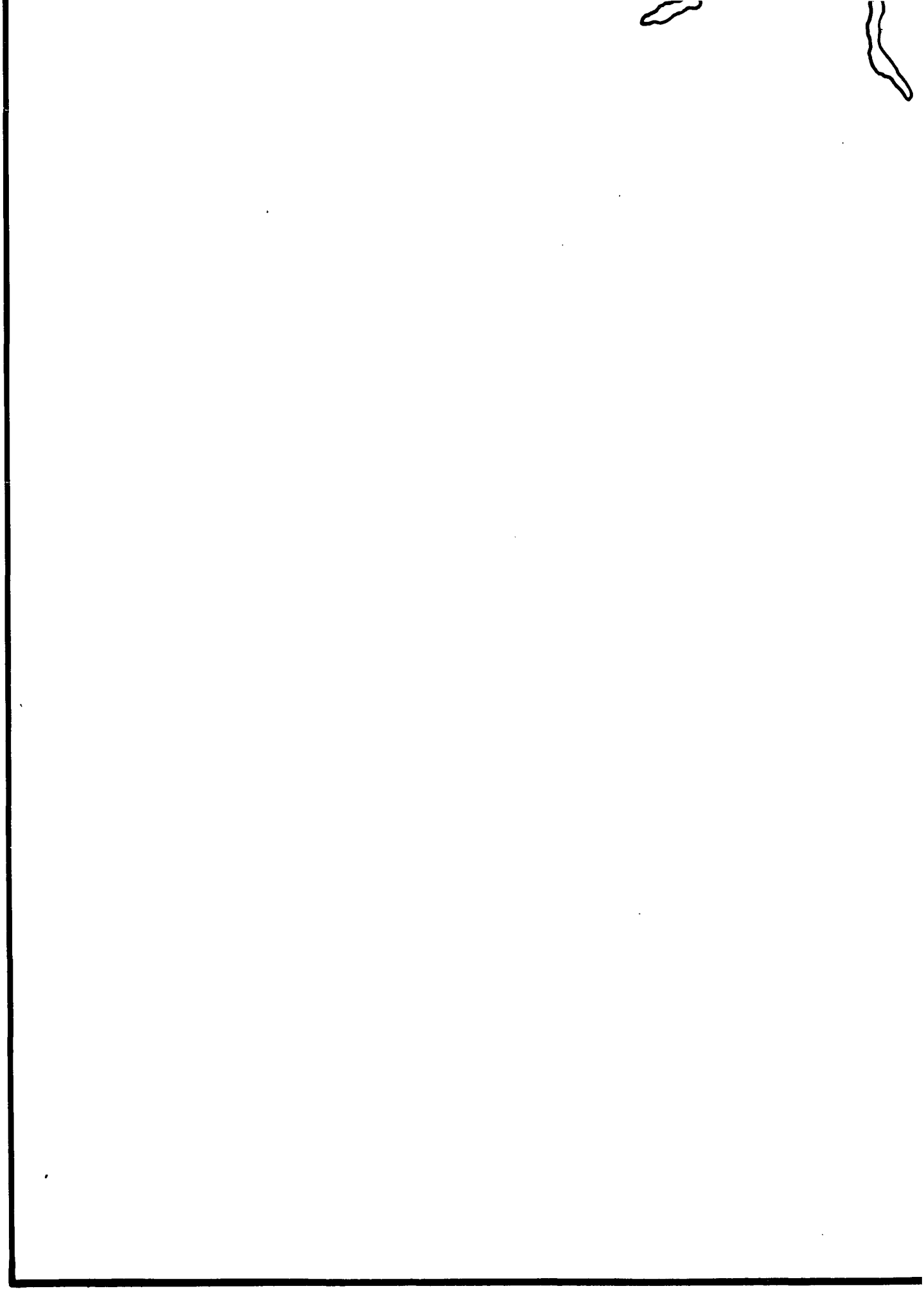

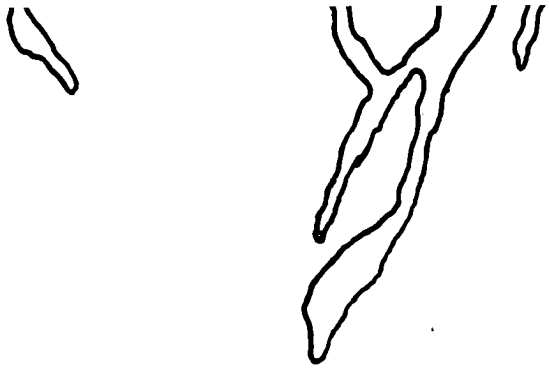

UNIT P

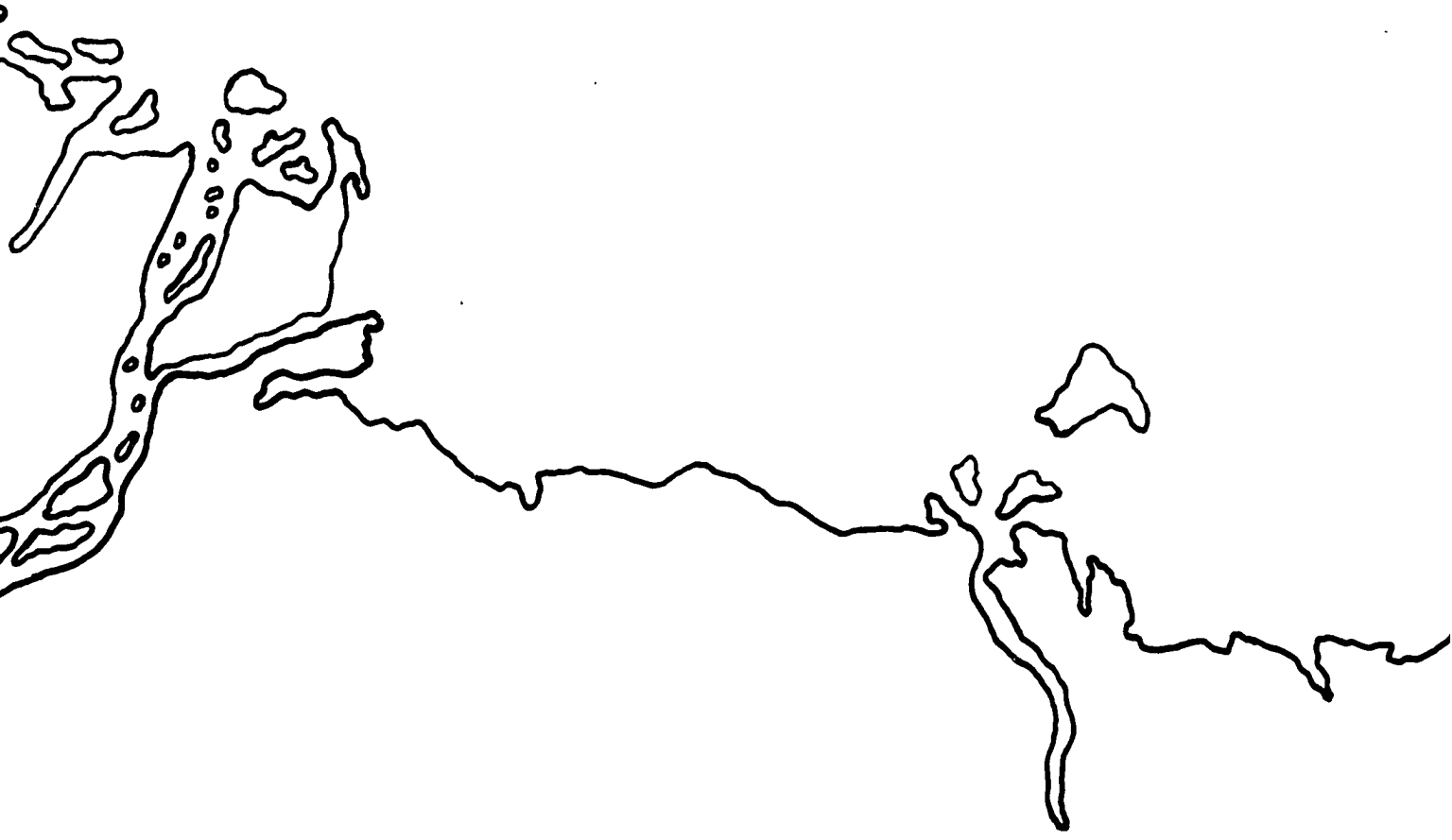

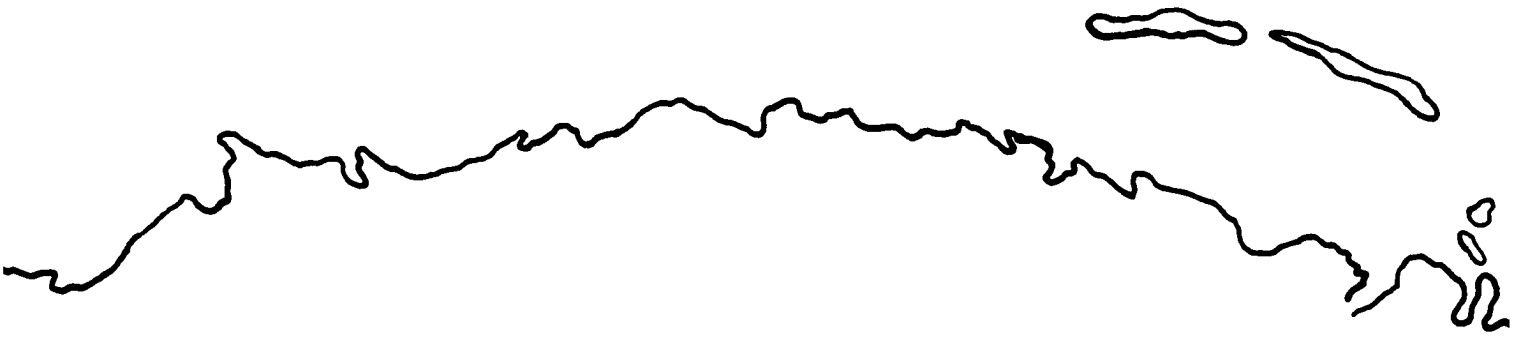

PLATE 6

ISOPACH MAPS OF UNITS P, Q & I

contour: interval:10 feet

Scale

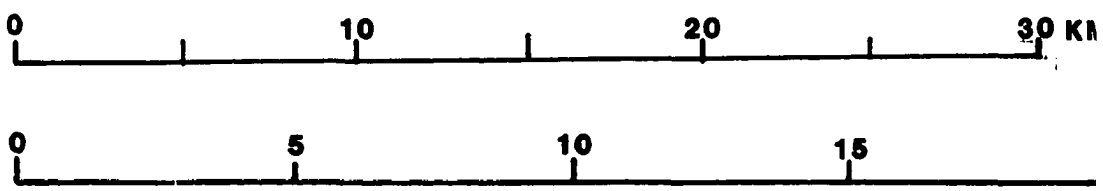

● Data Point, Well Location

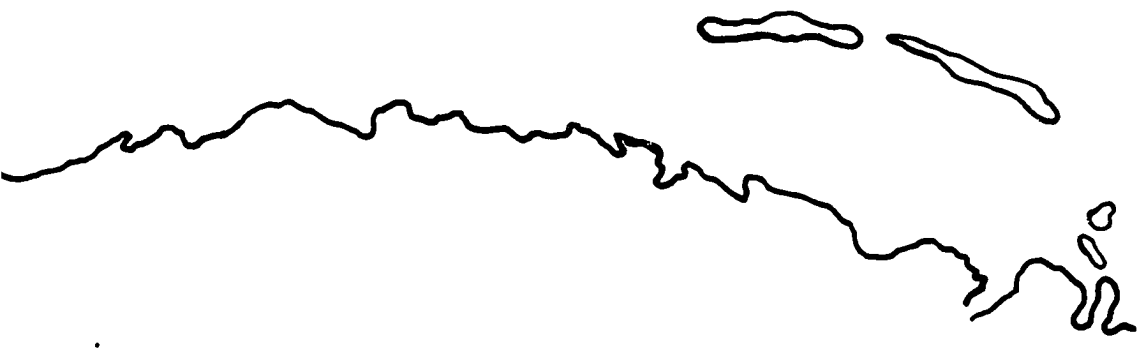

PLATE 6

ISOPACH MAPS OF UNITS P, Q & R

contour: interval: 10 feet

Scale

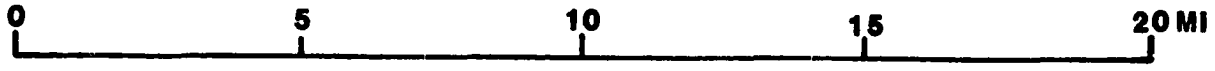

● **Data Point, Well Location**

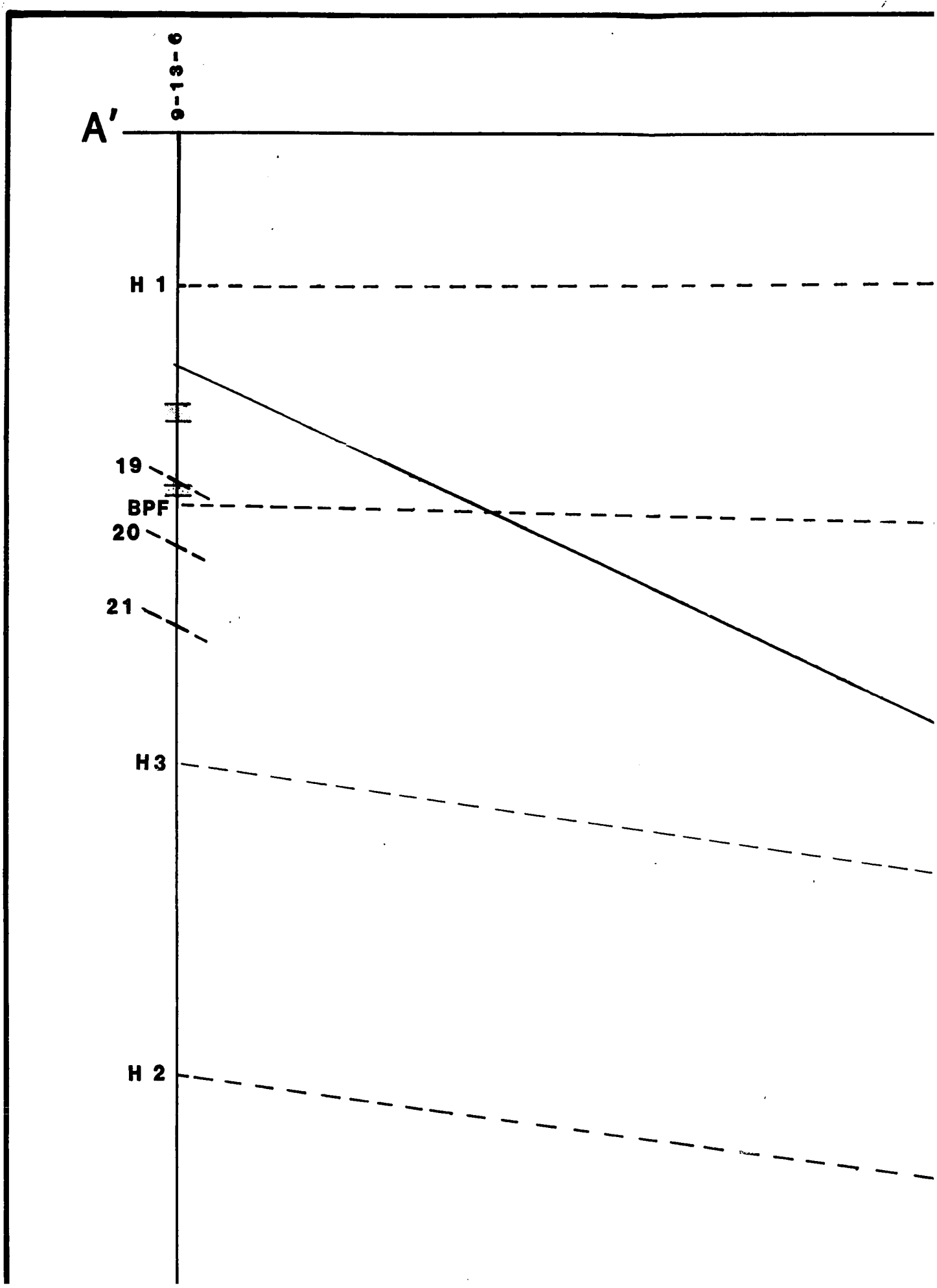

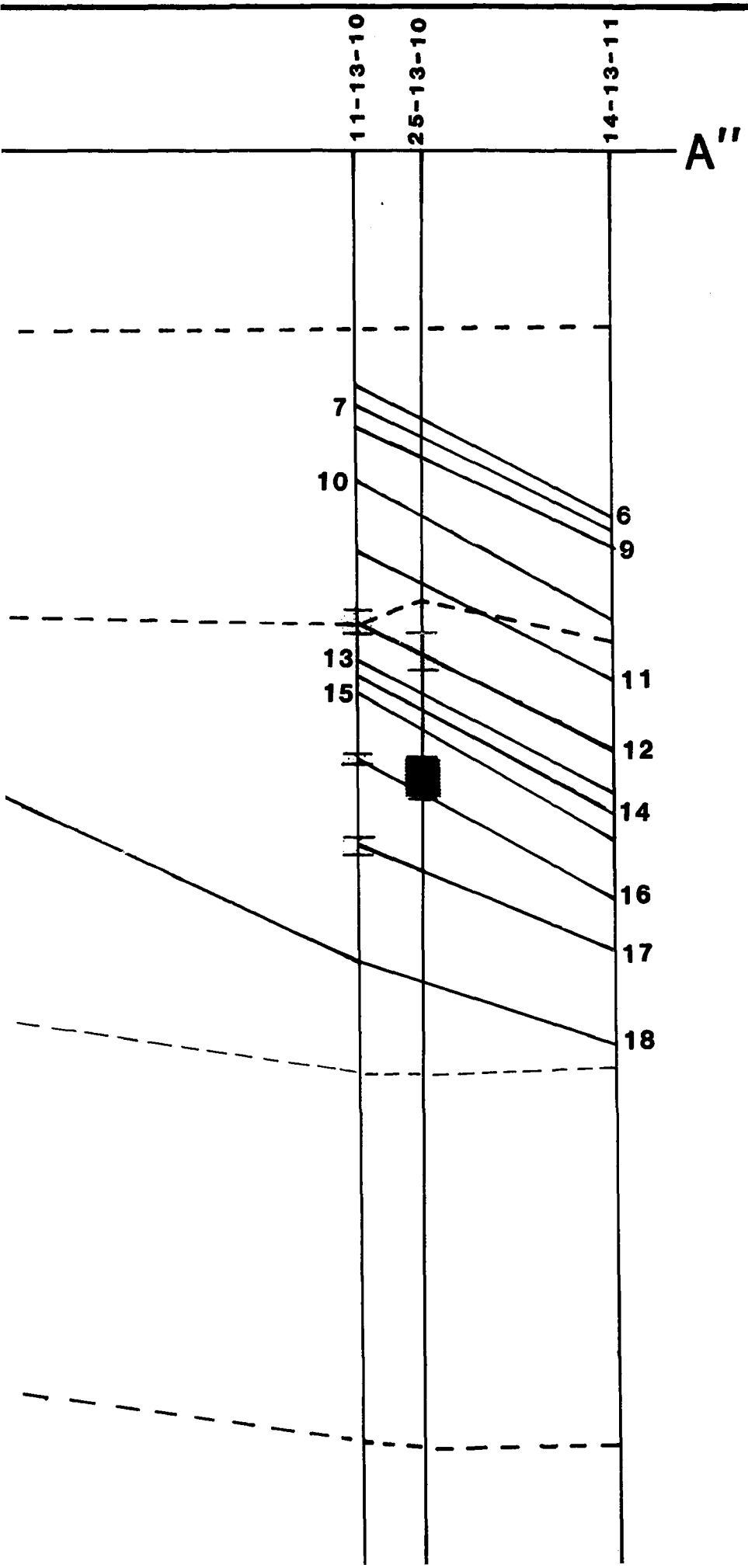

PLA

A'A''

CROSS S

Showing Hydrate Occurrences

Key:

11-12-13 Location

High Concentration

intermediate

Low Concentration

H 1 Upper Hydrate Stab

H 2 Lower Hydrate Stabi (with no geothe gradient cha

H3 Lower Hydrate S Boundary (with geotherma change at BI

BPF Base of the Per

Horizontal

0 10

0 5

PLATE 7

A'A''-G'G''

SS SECTIONS

rrences and Degree of Hydrate Saturation

ion

ntration

e

ntration

te Stability Boundary

te Stability Boundary
geothermal
nt change at BPF)

lrate Stabiiity
ary
thermal gradient
e at BPF)

he Permafrost

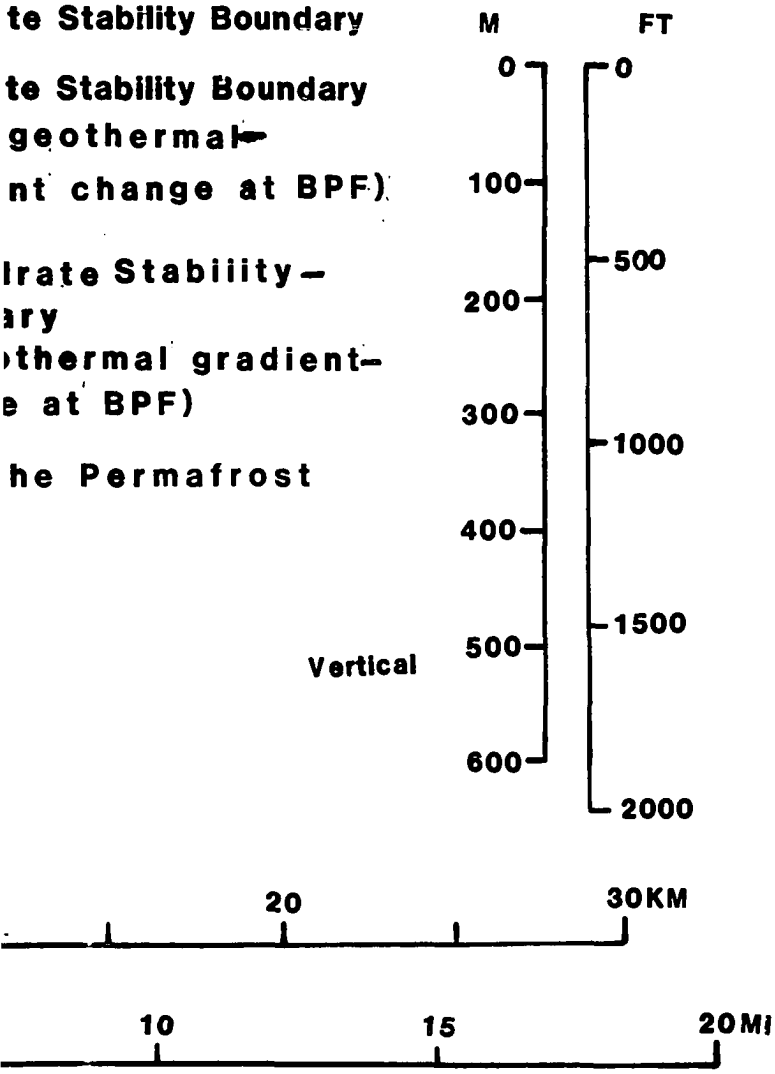

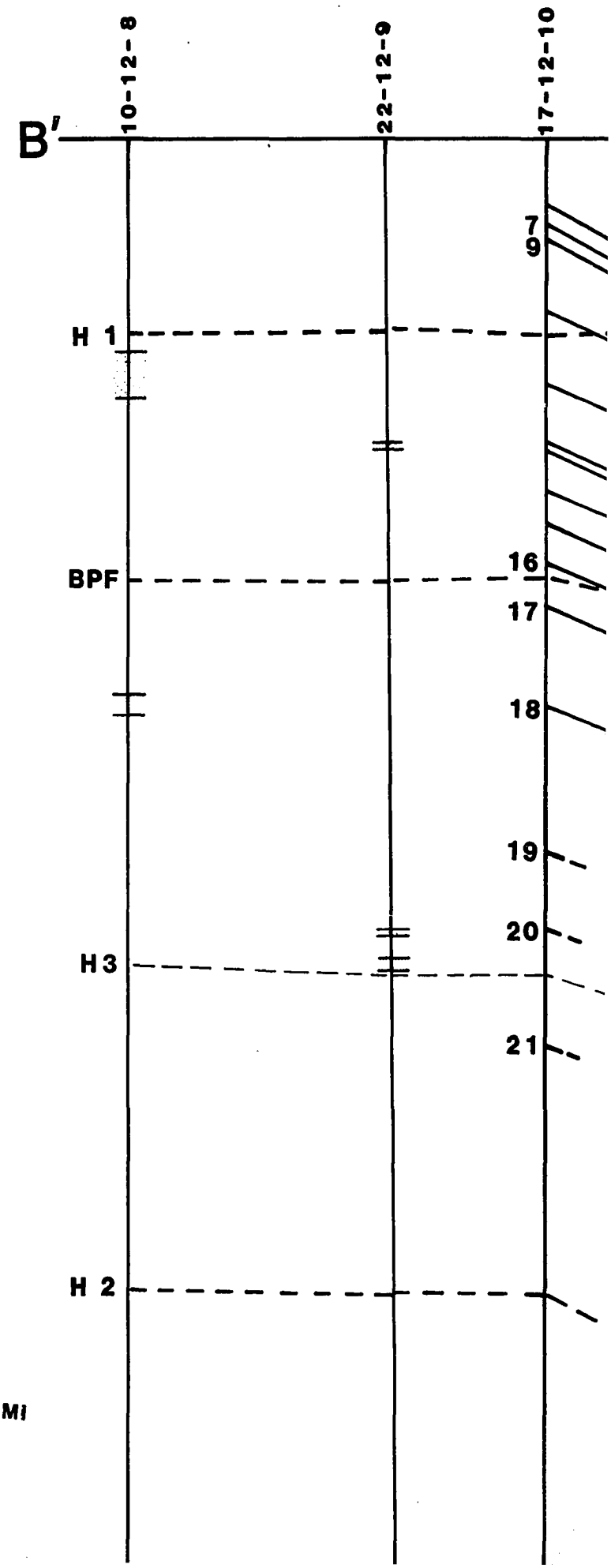

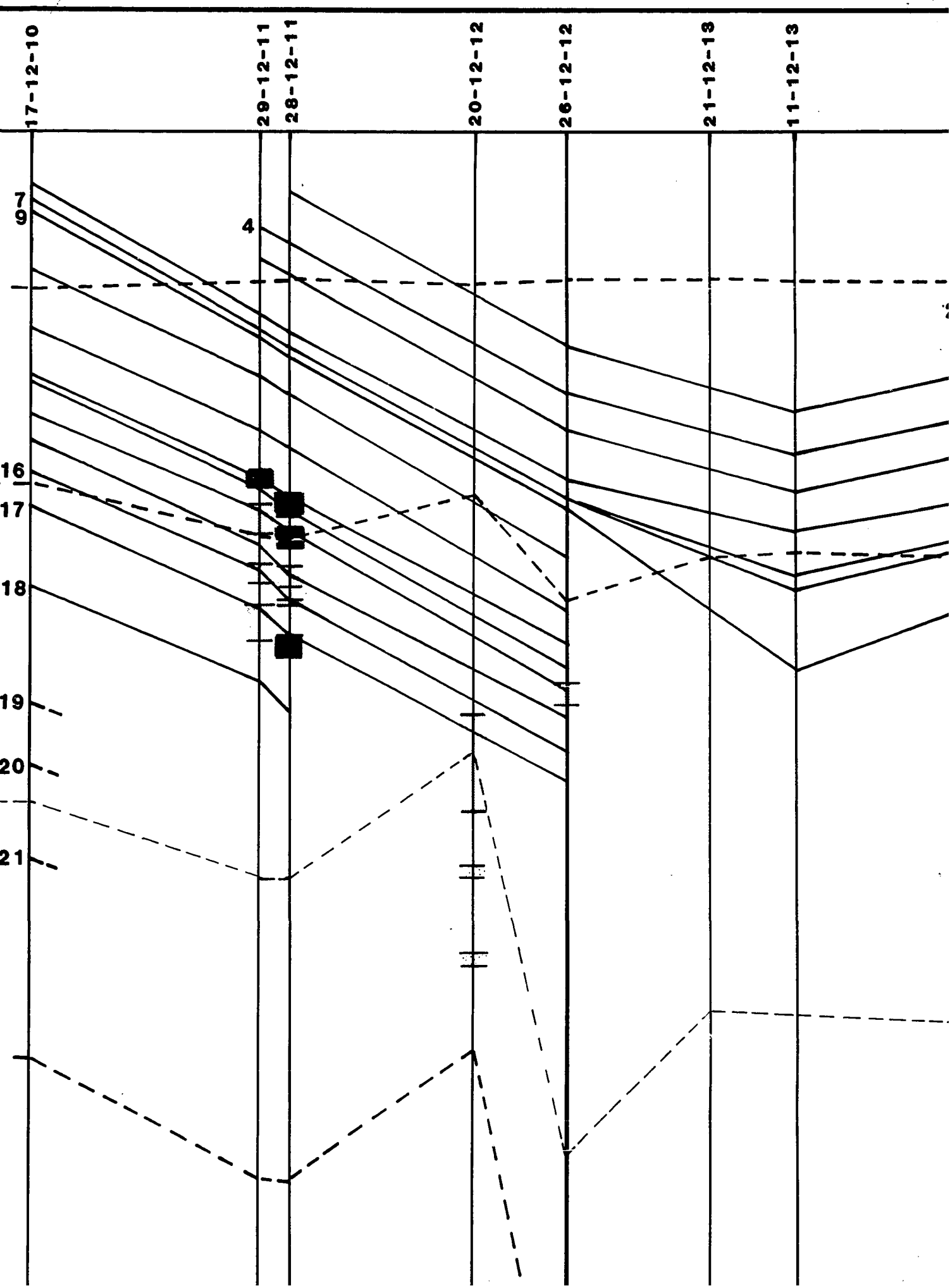

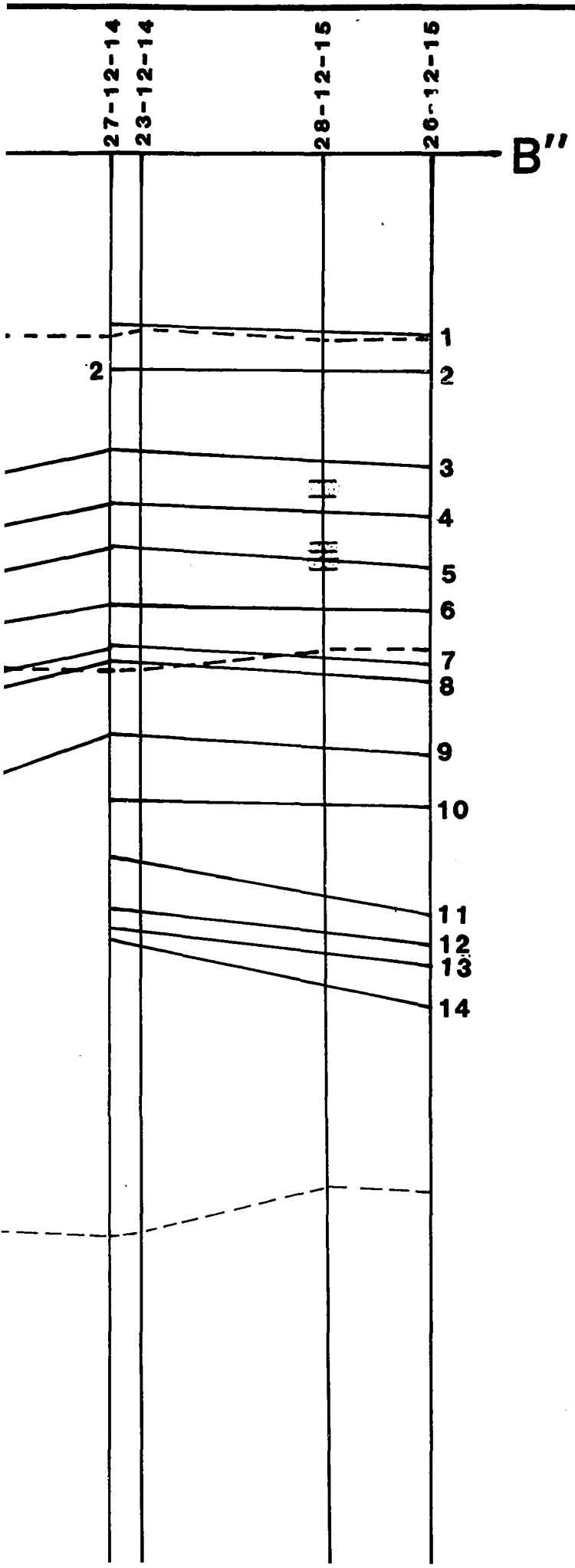

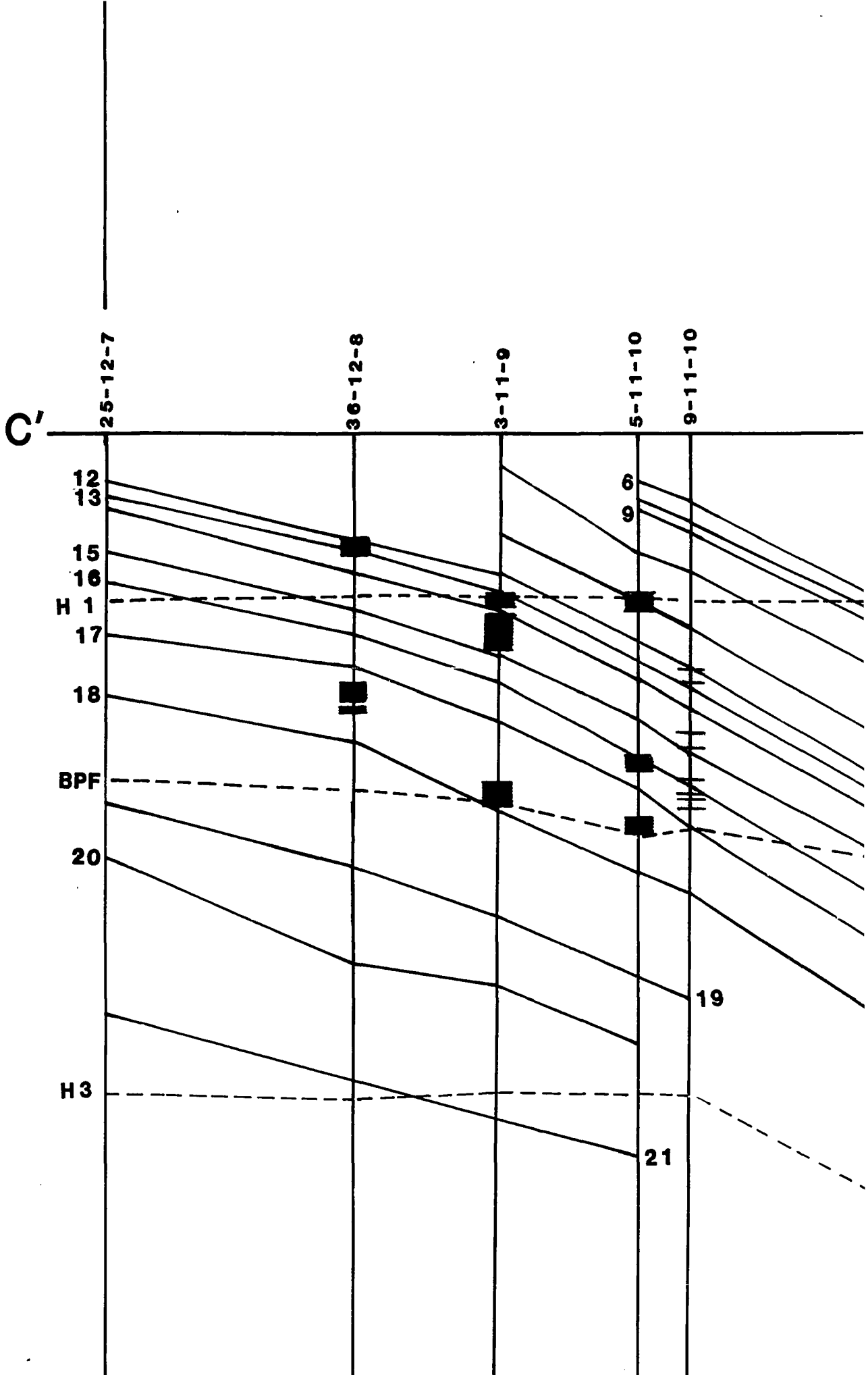

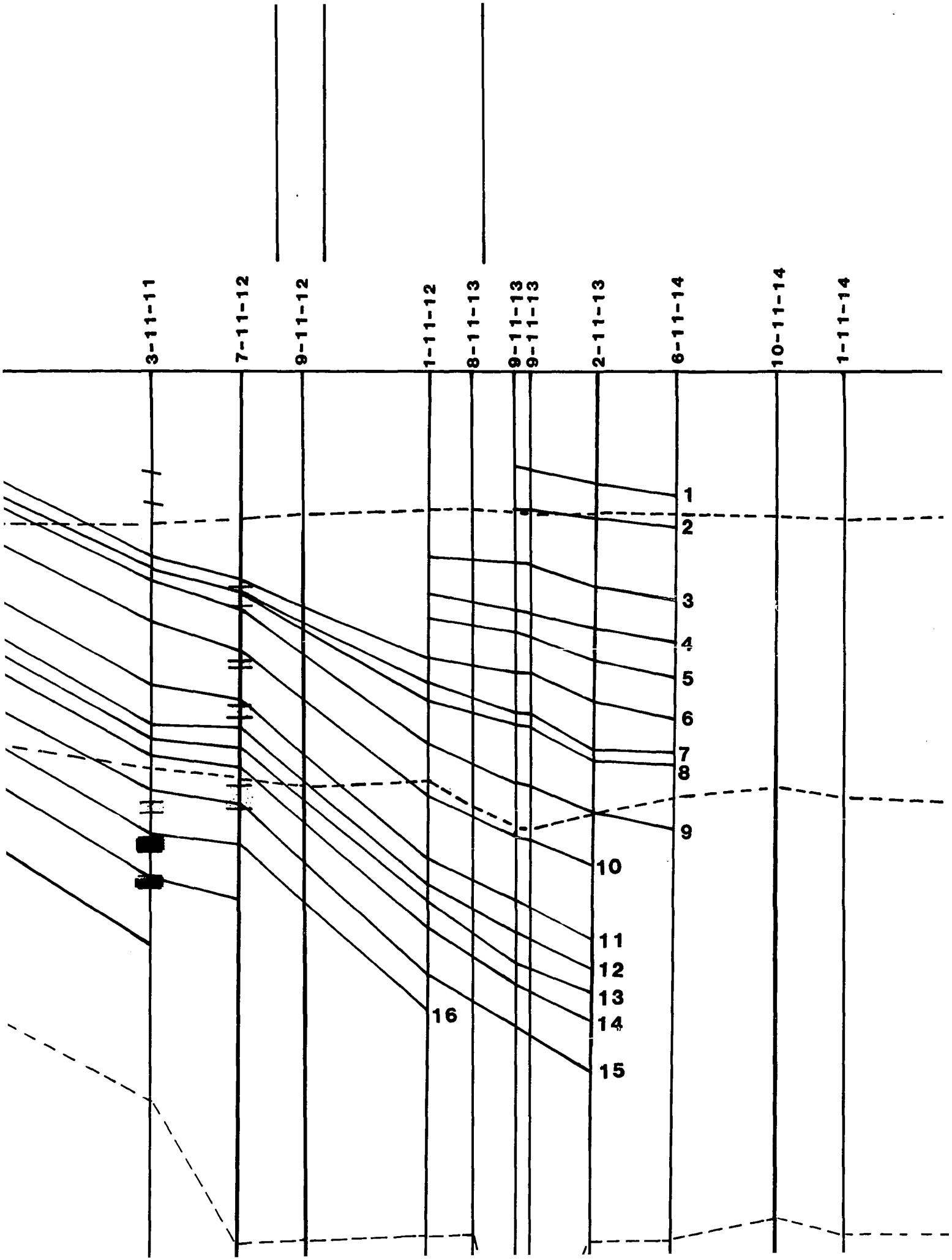

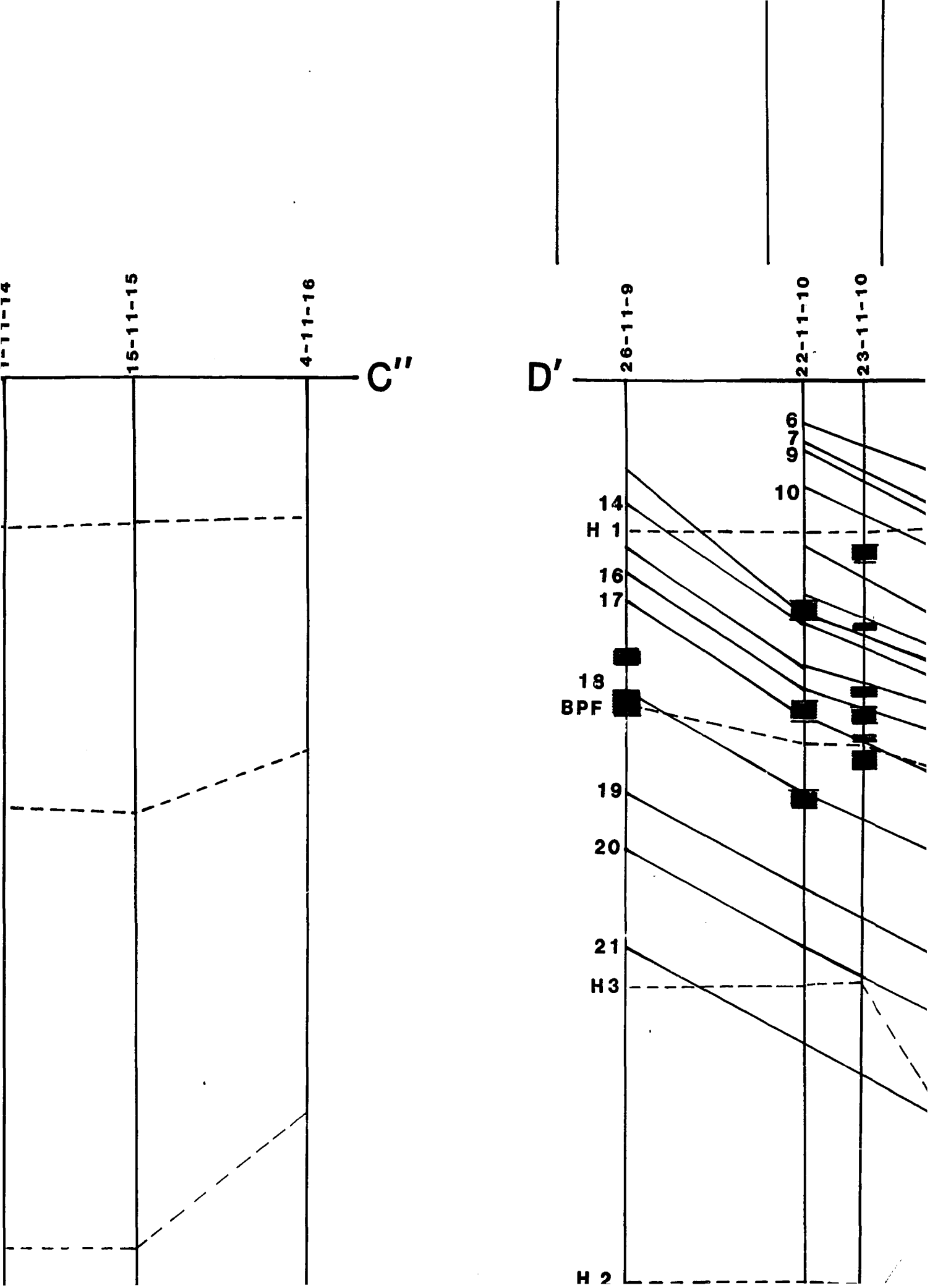

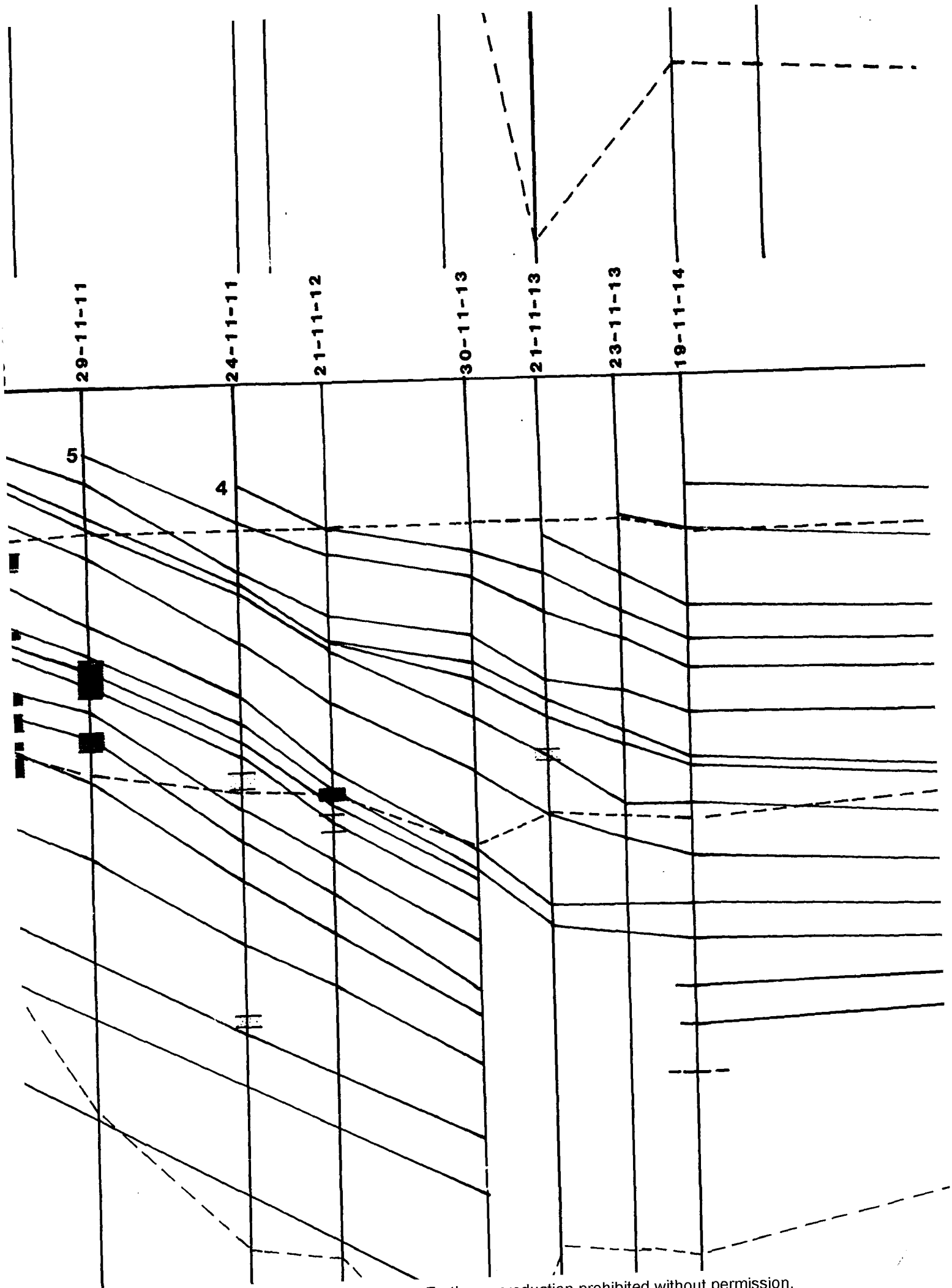

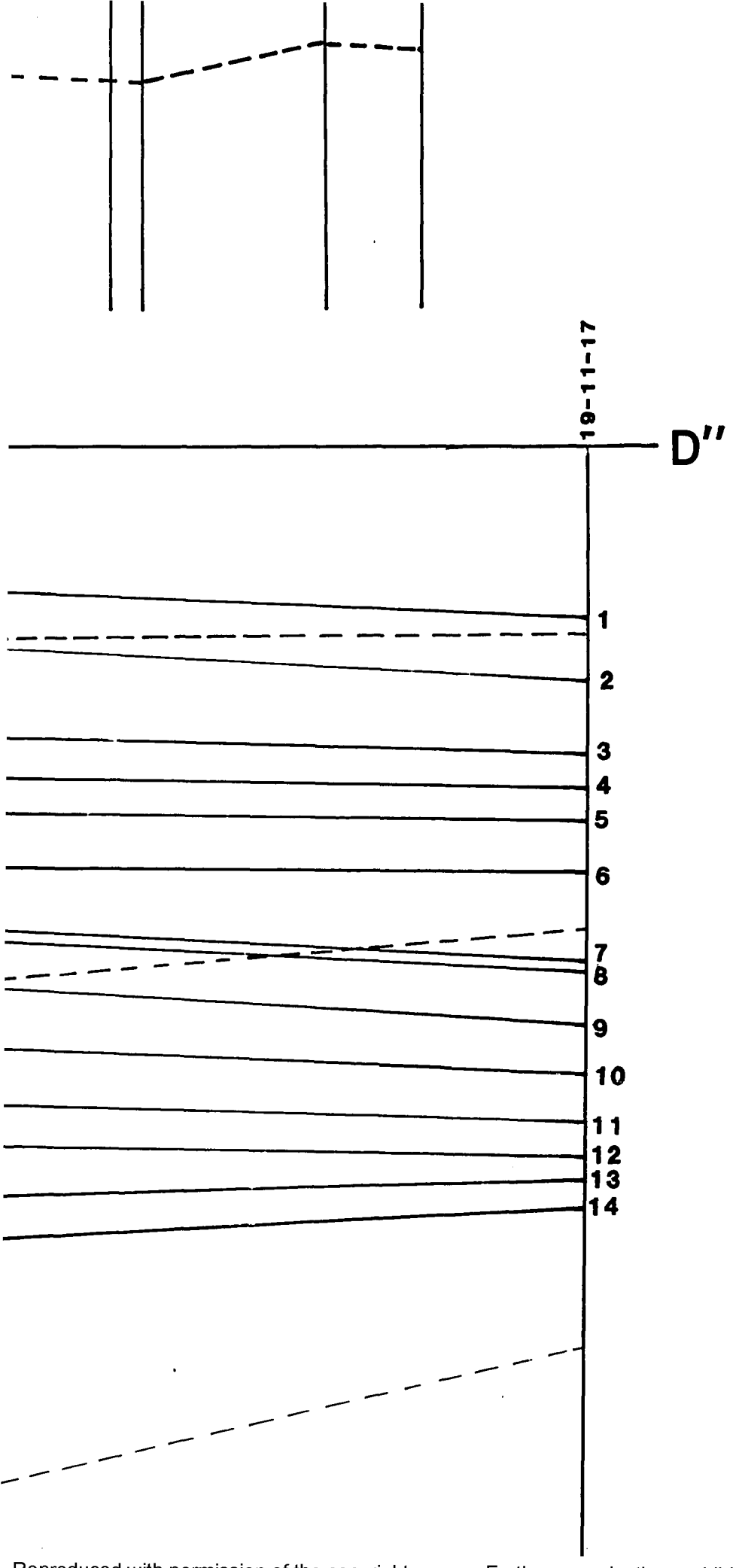

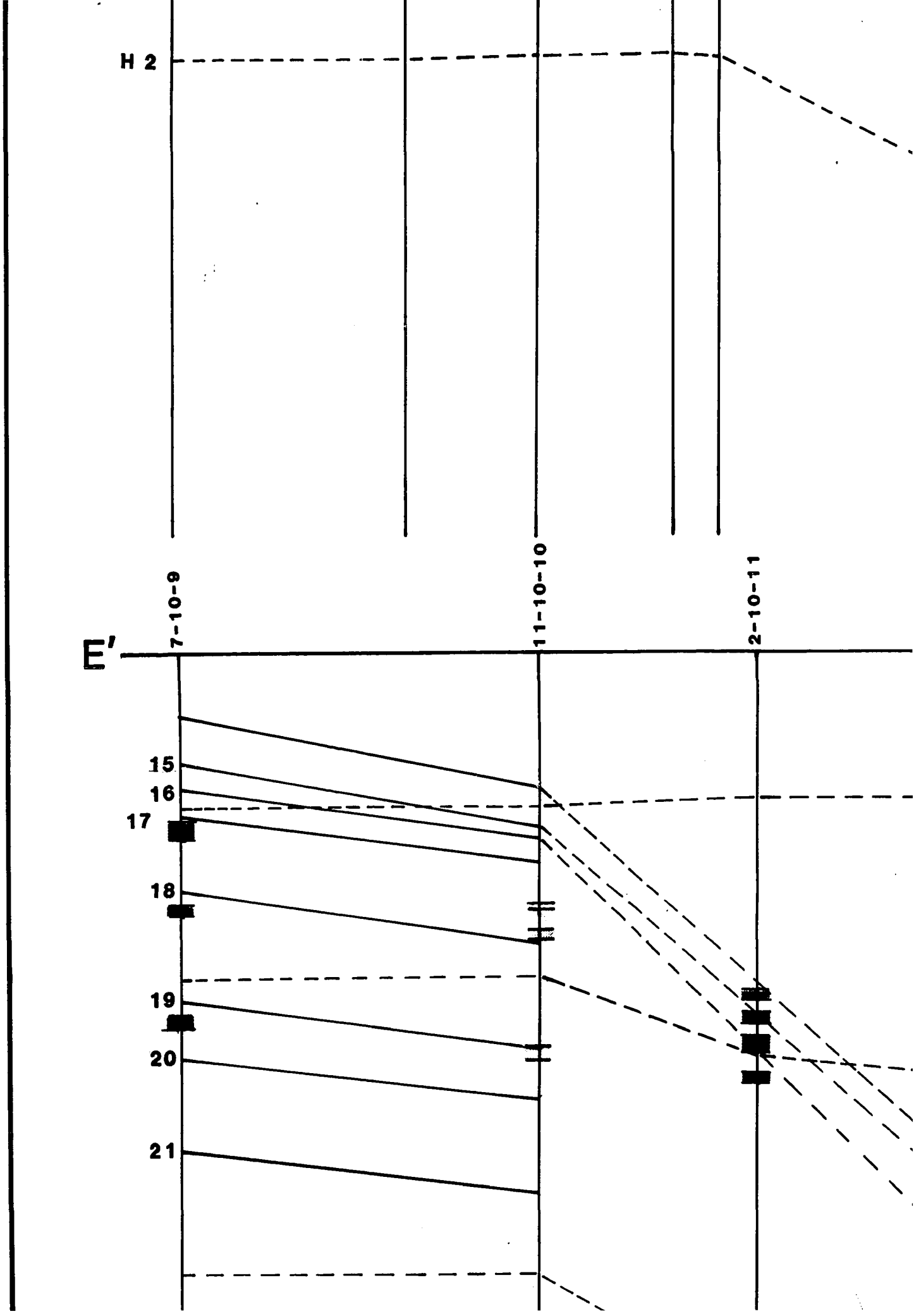

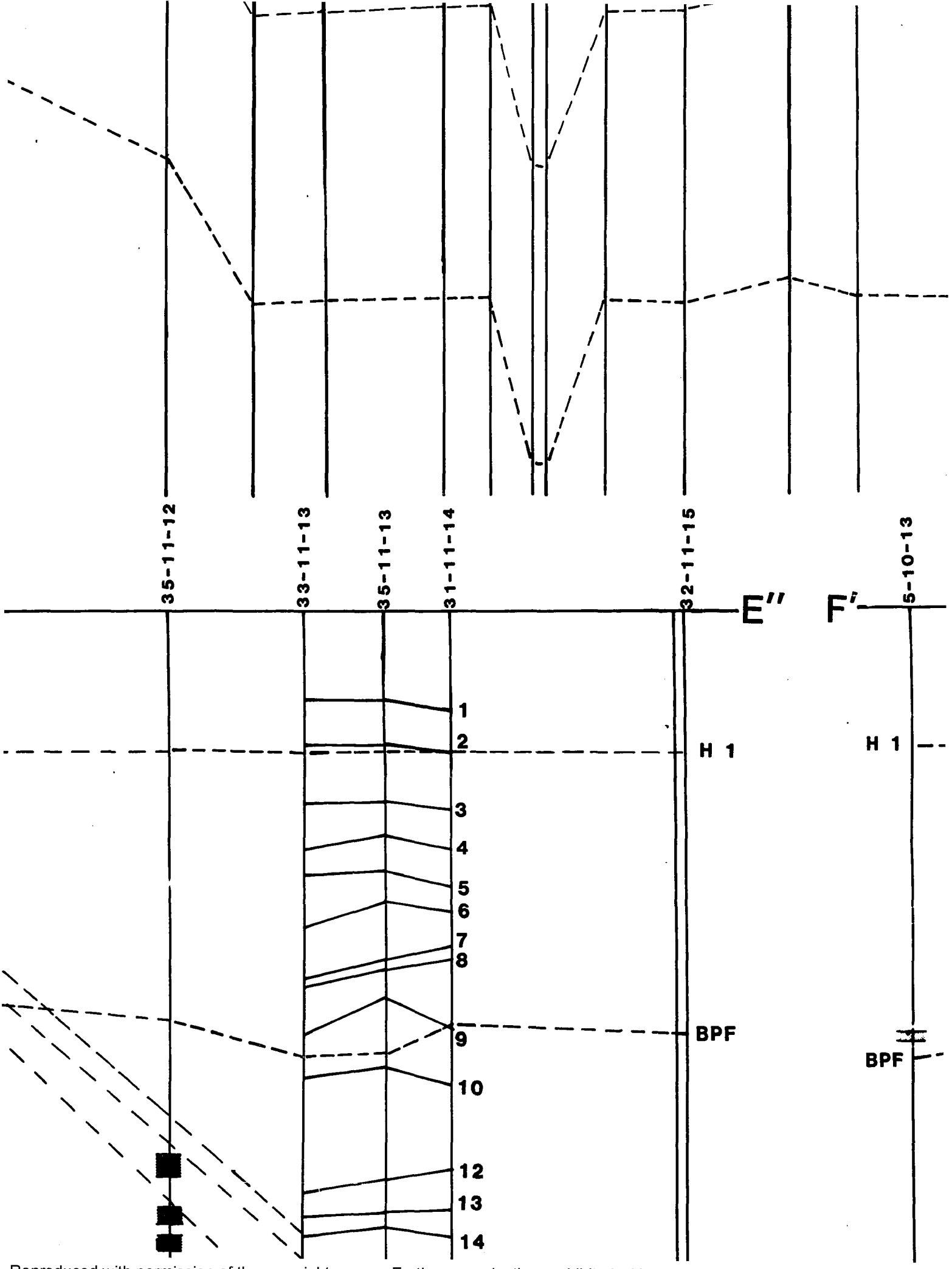

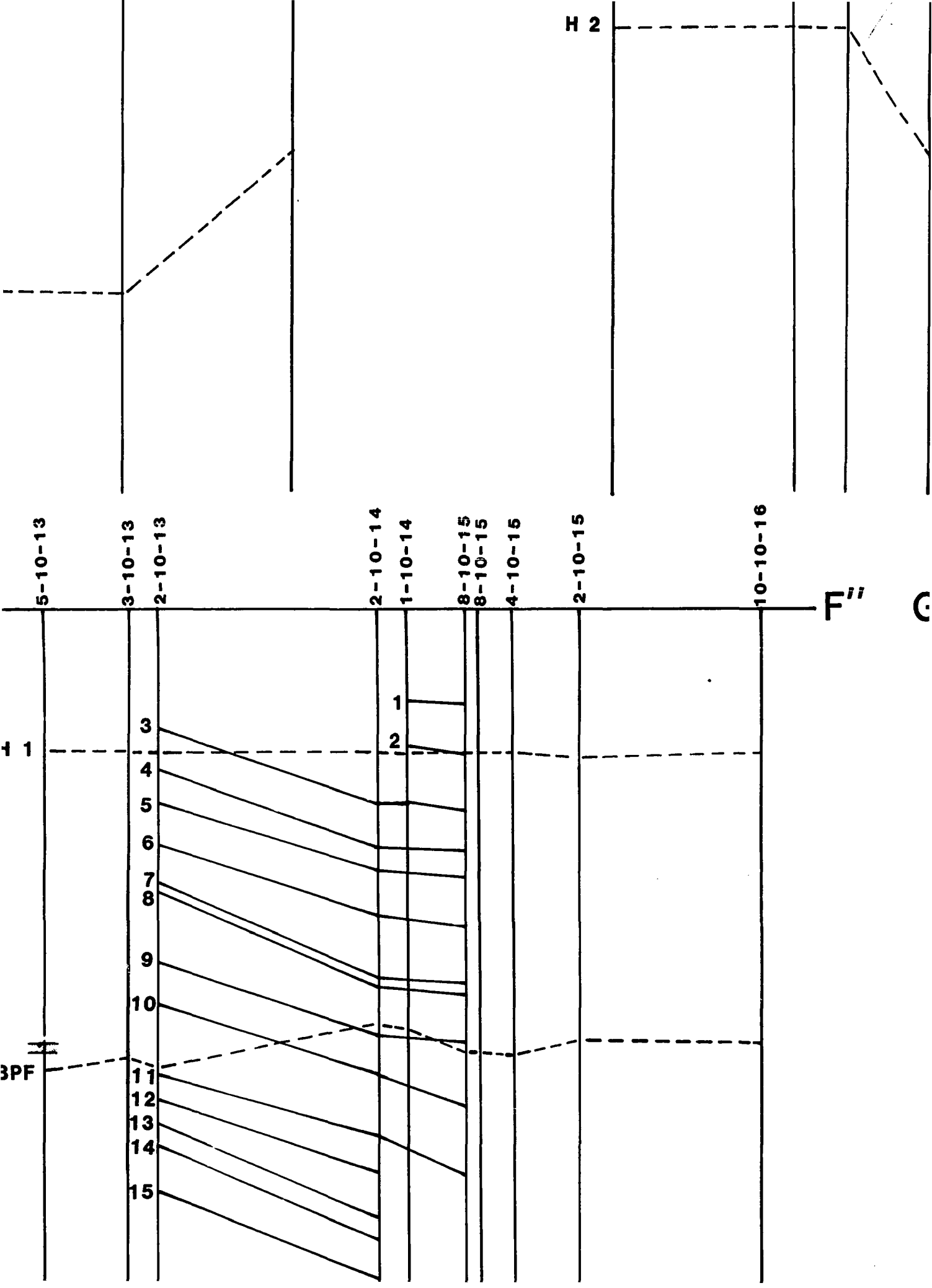

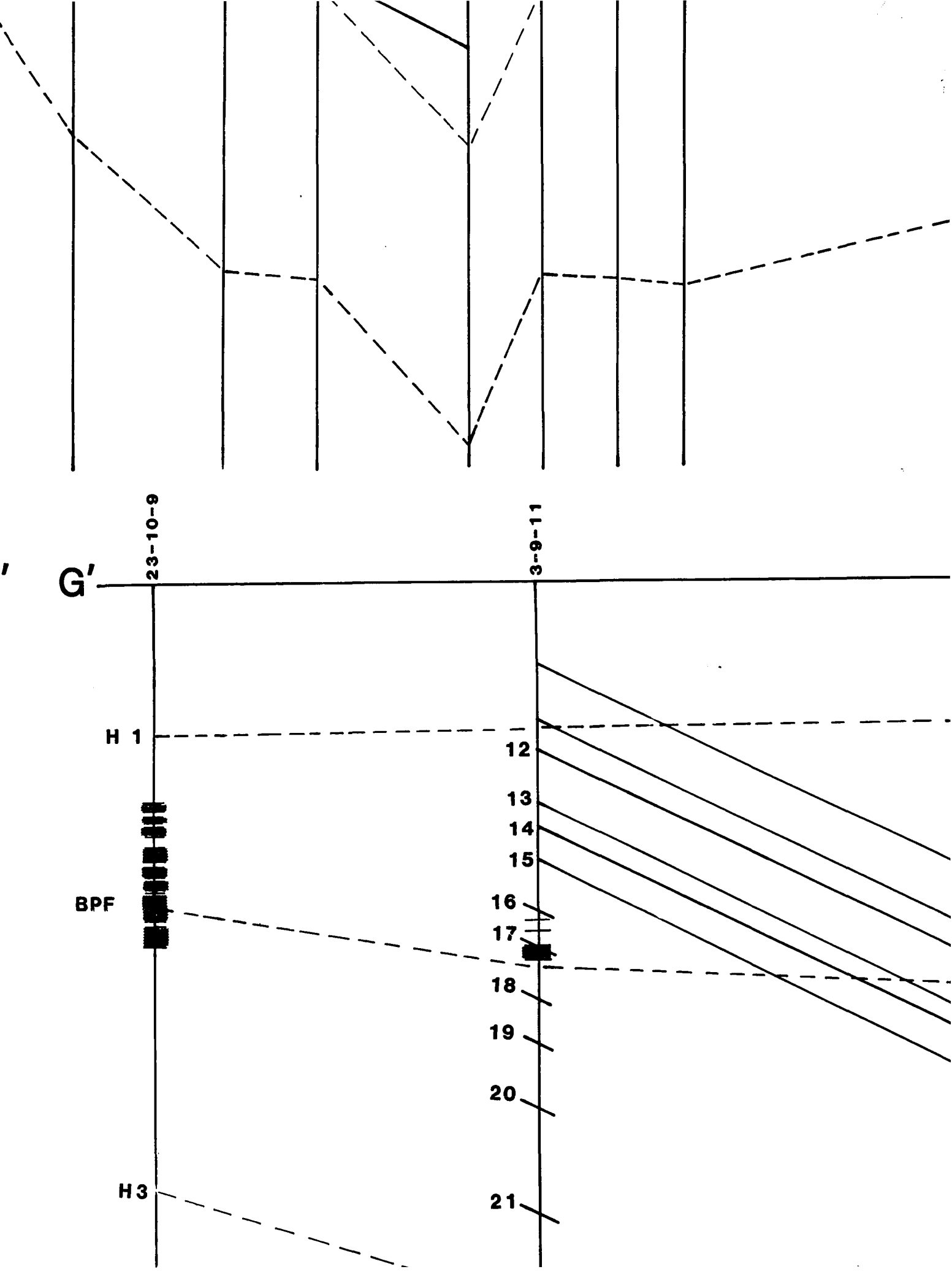

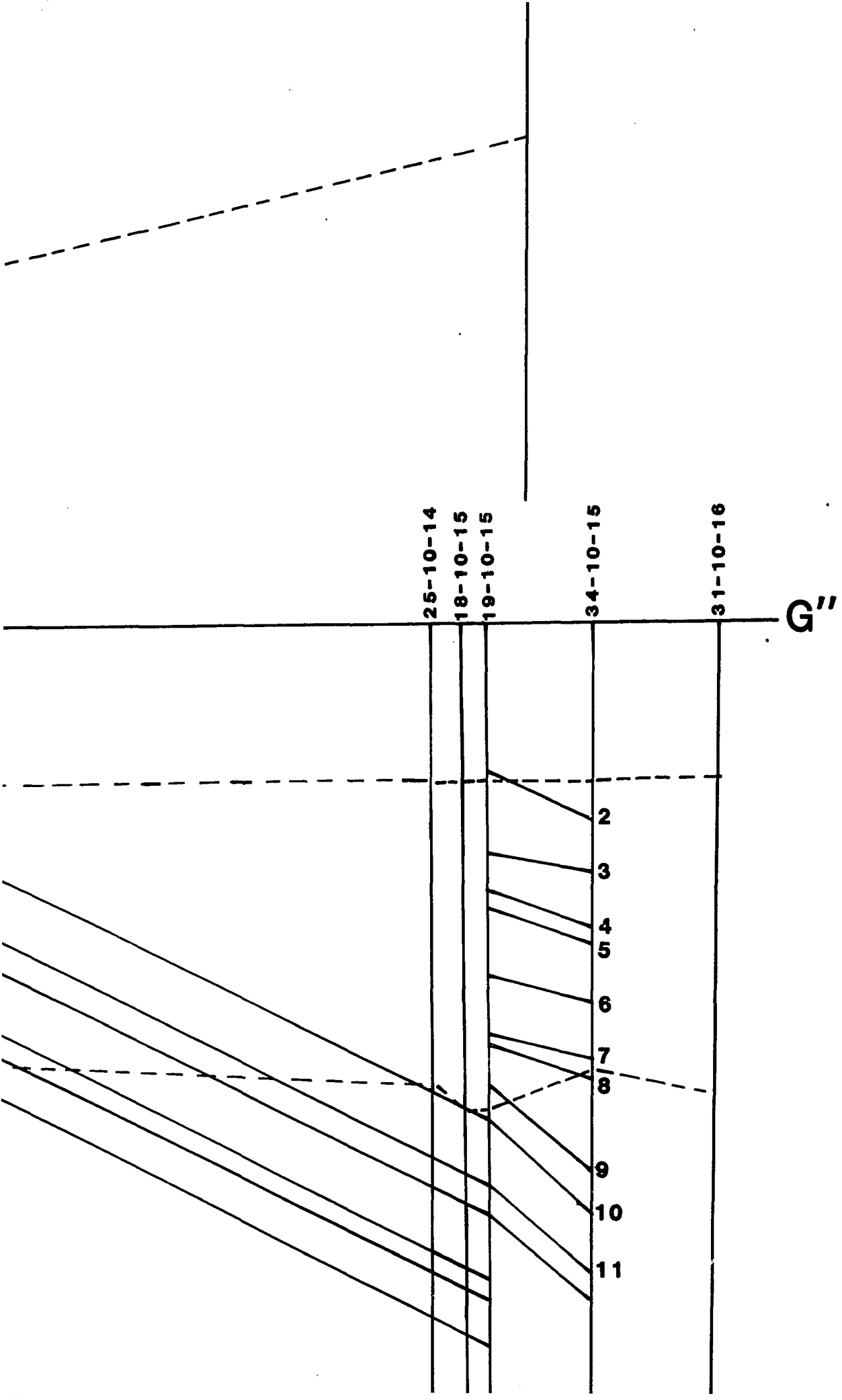

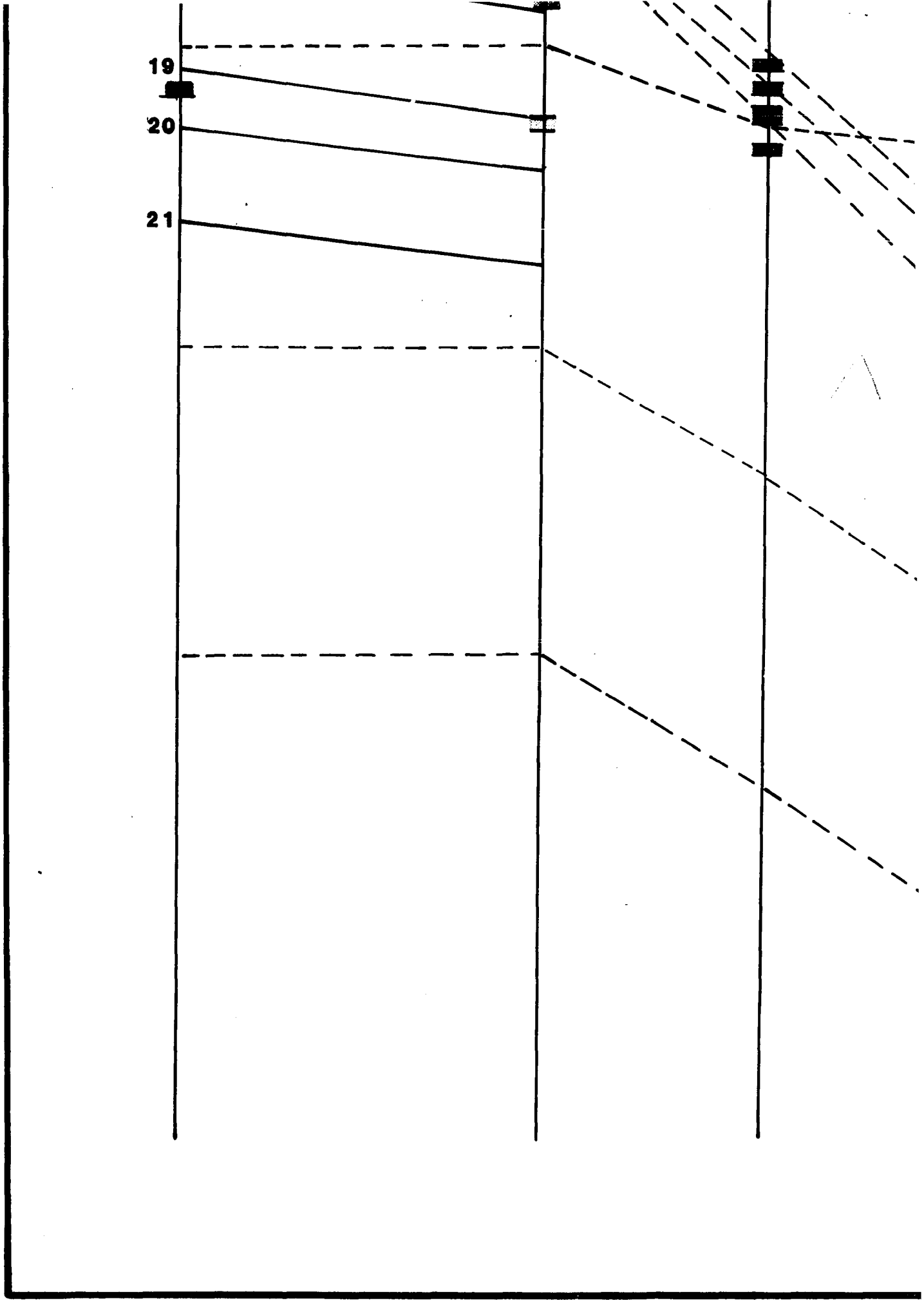

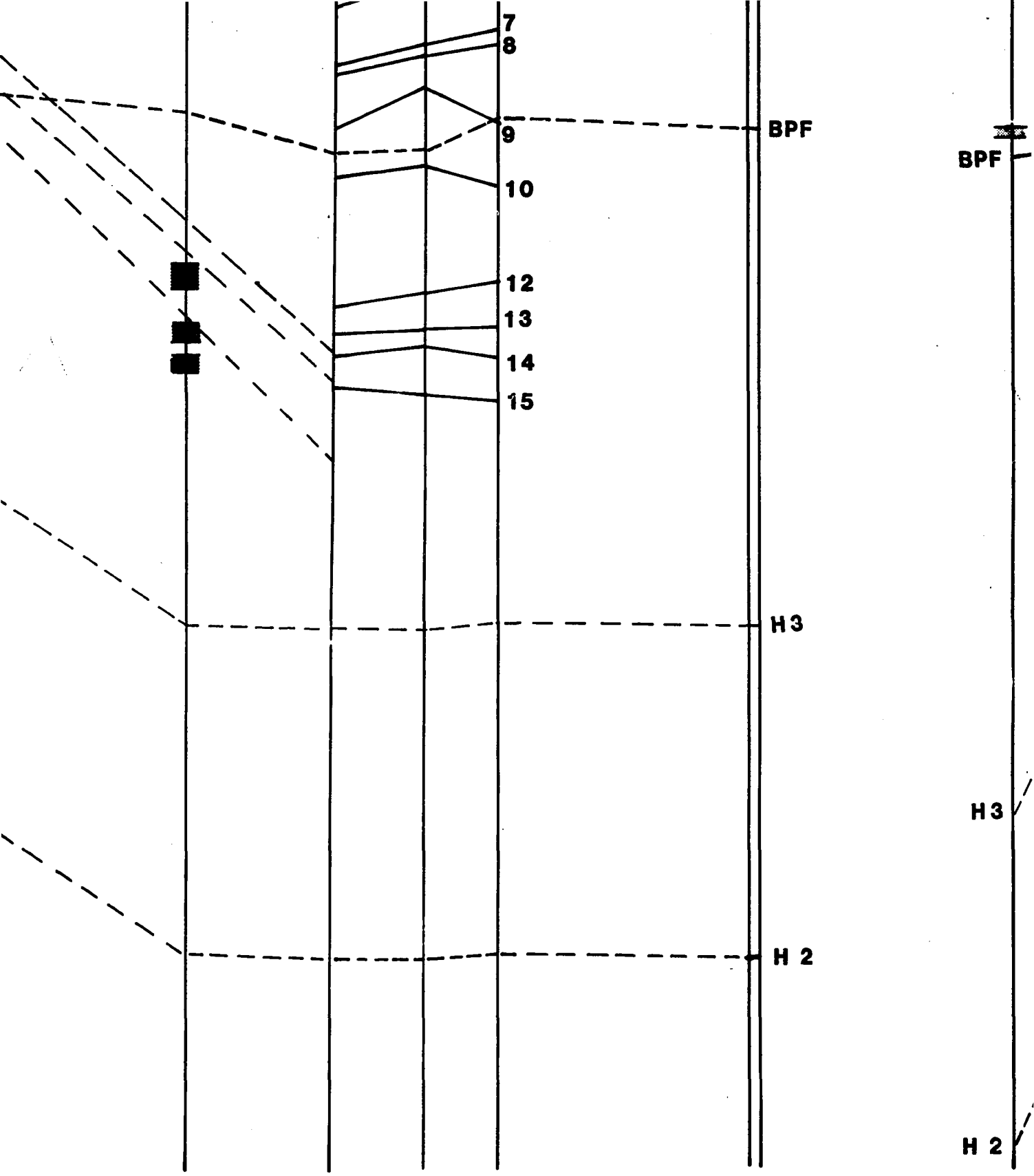

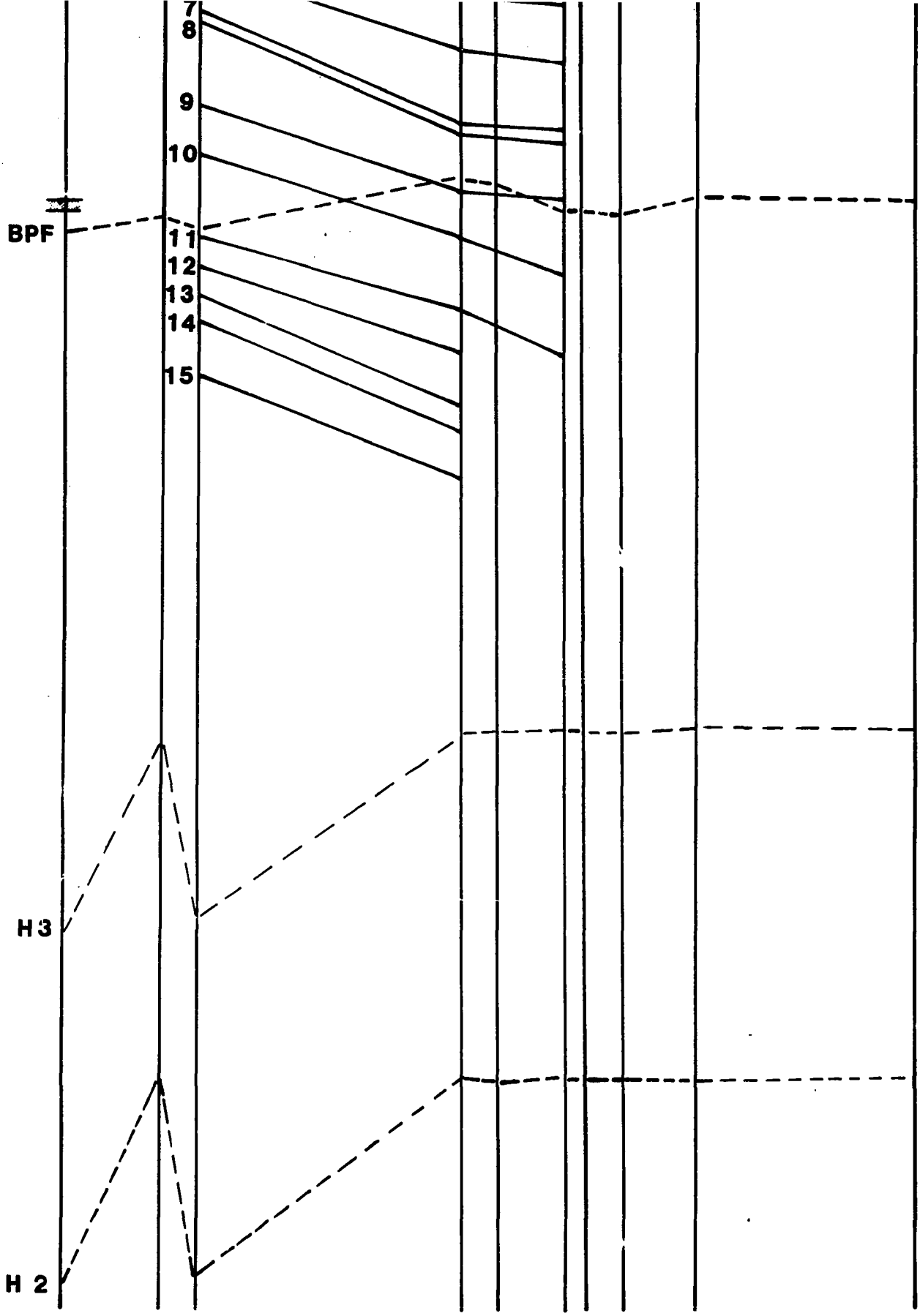

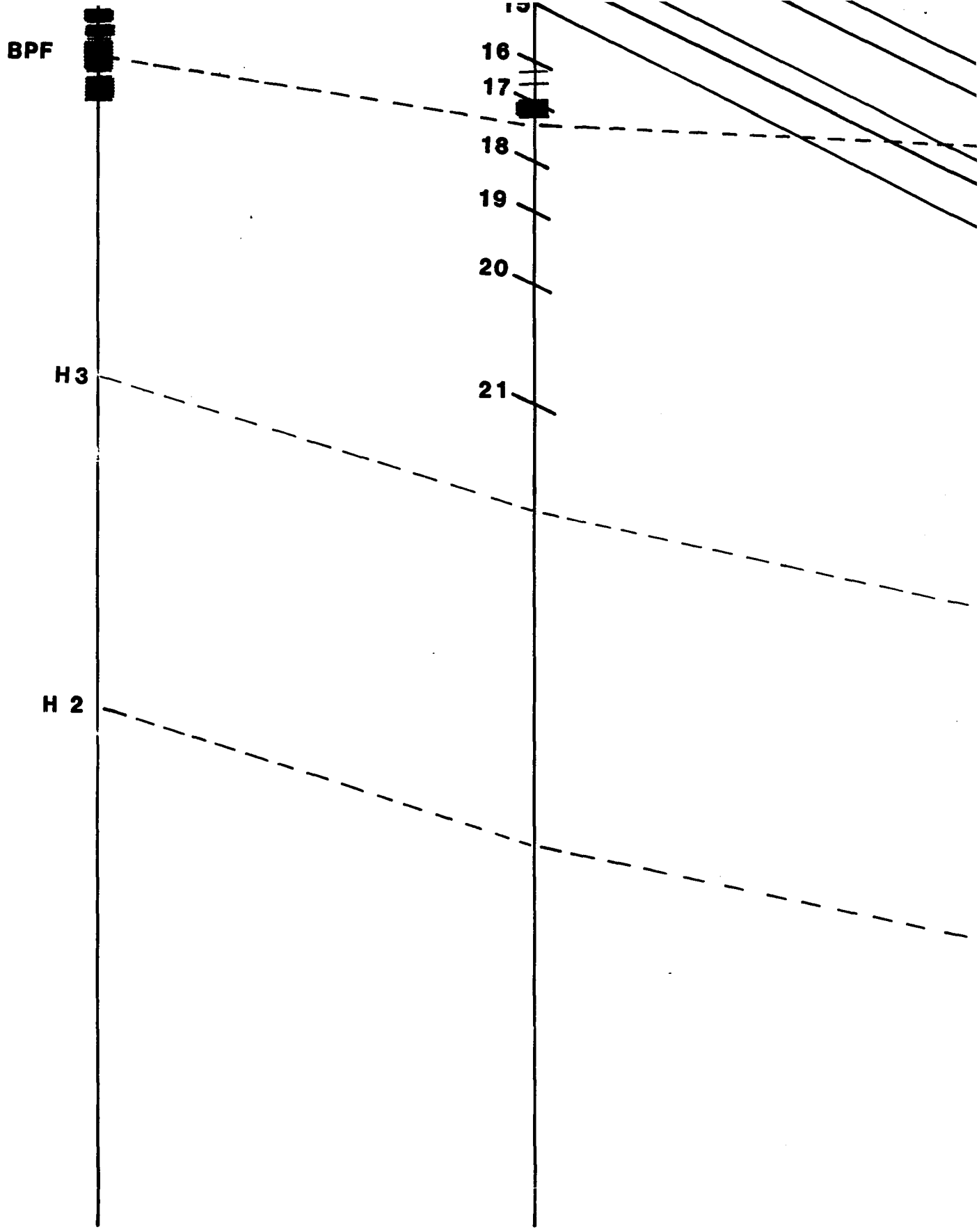

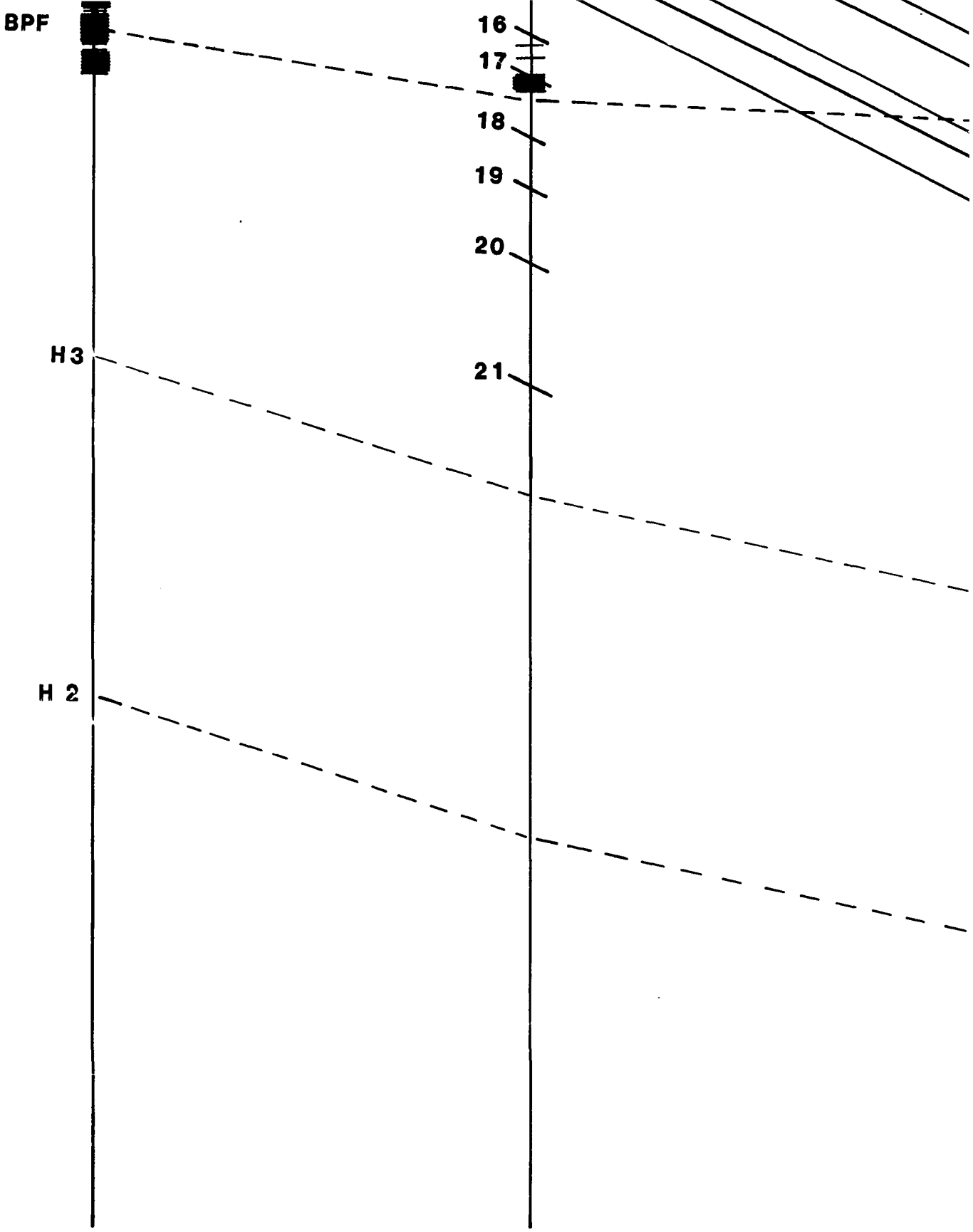

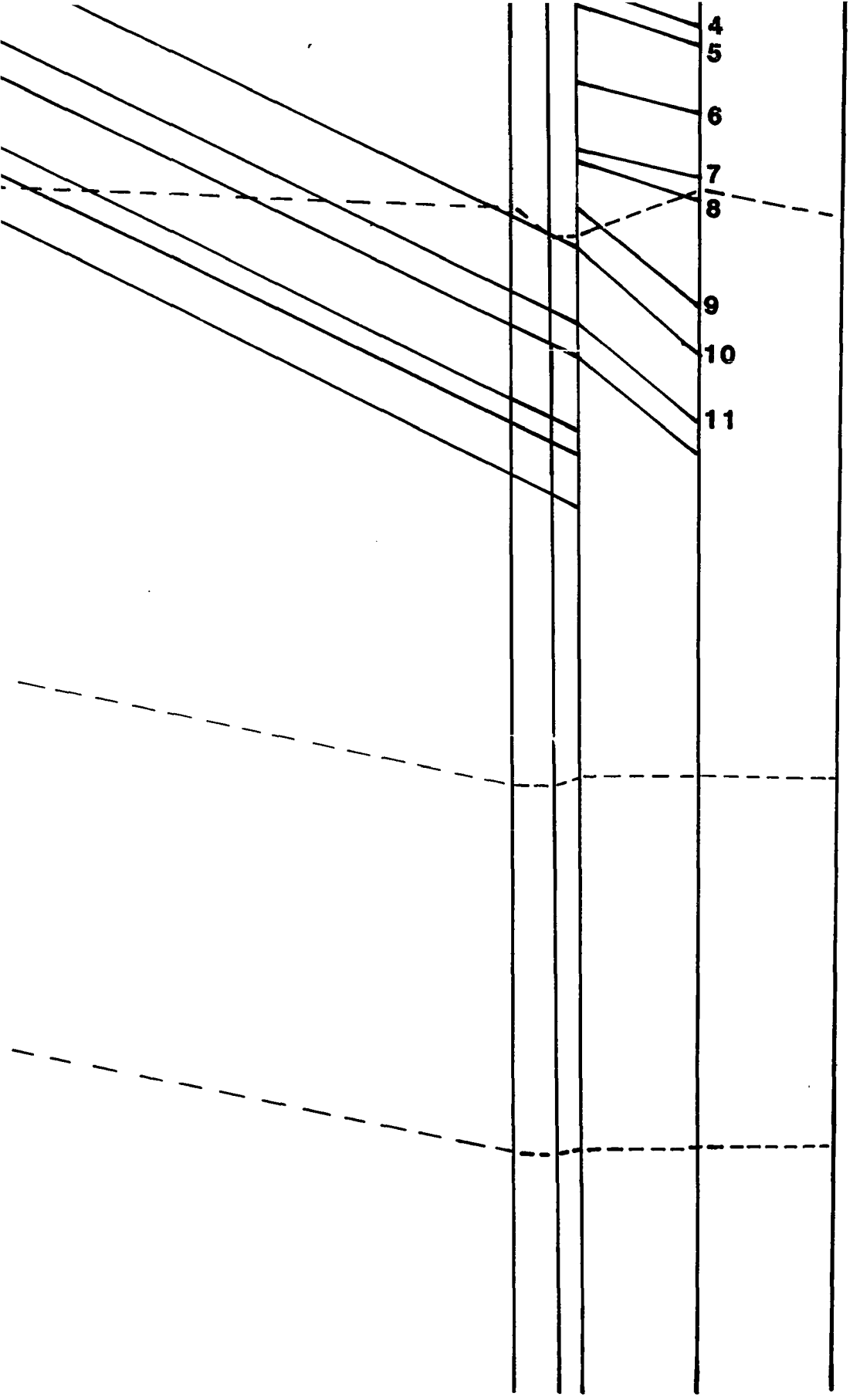

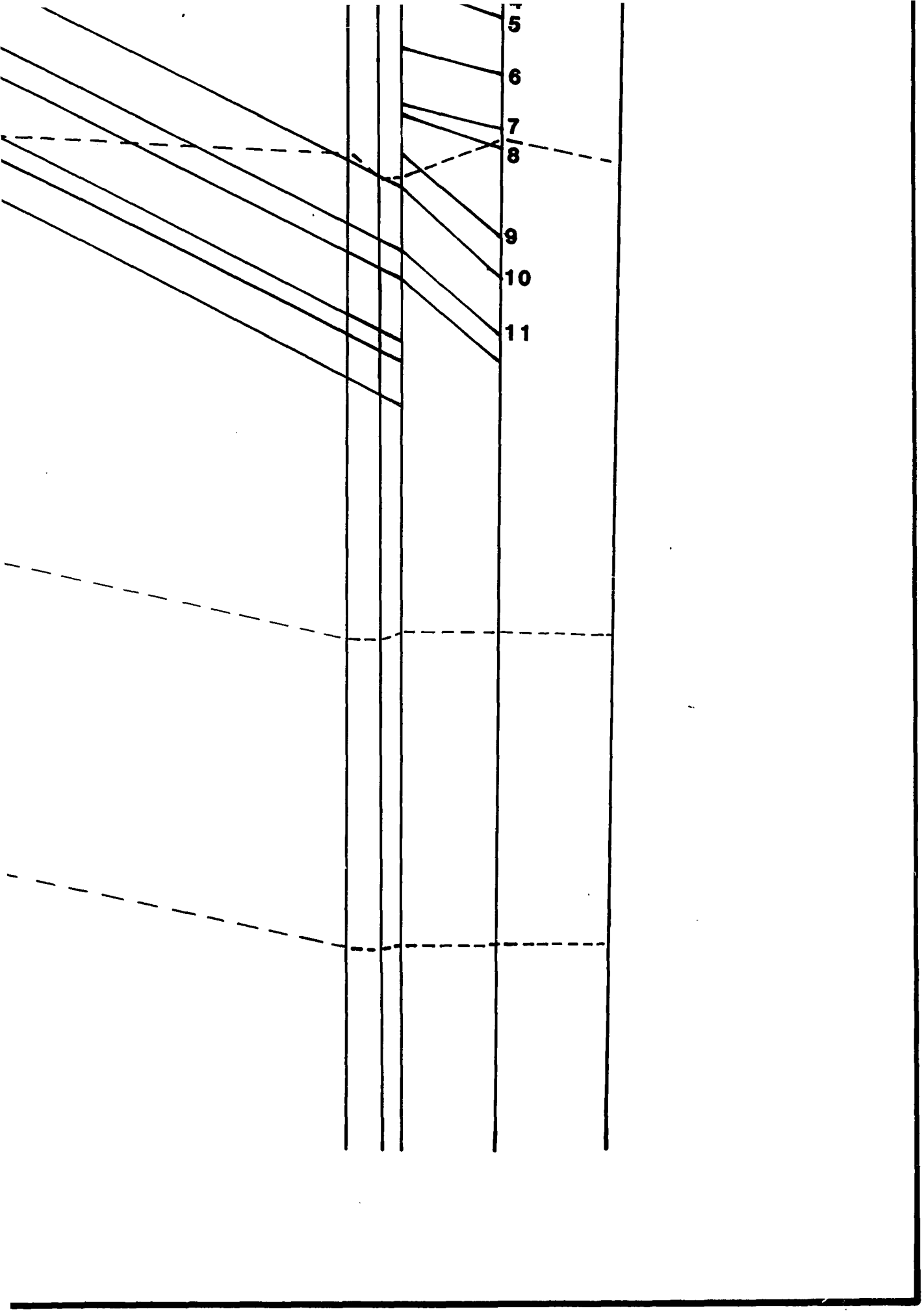

PLATE 7

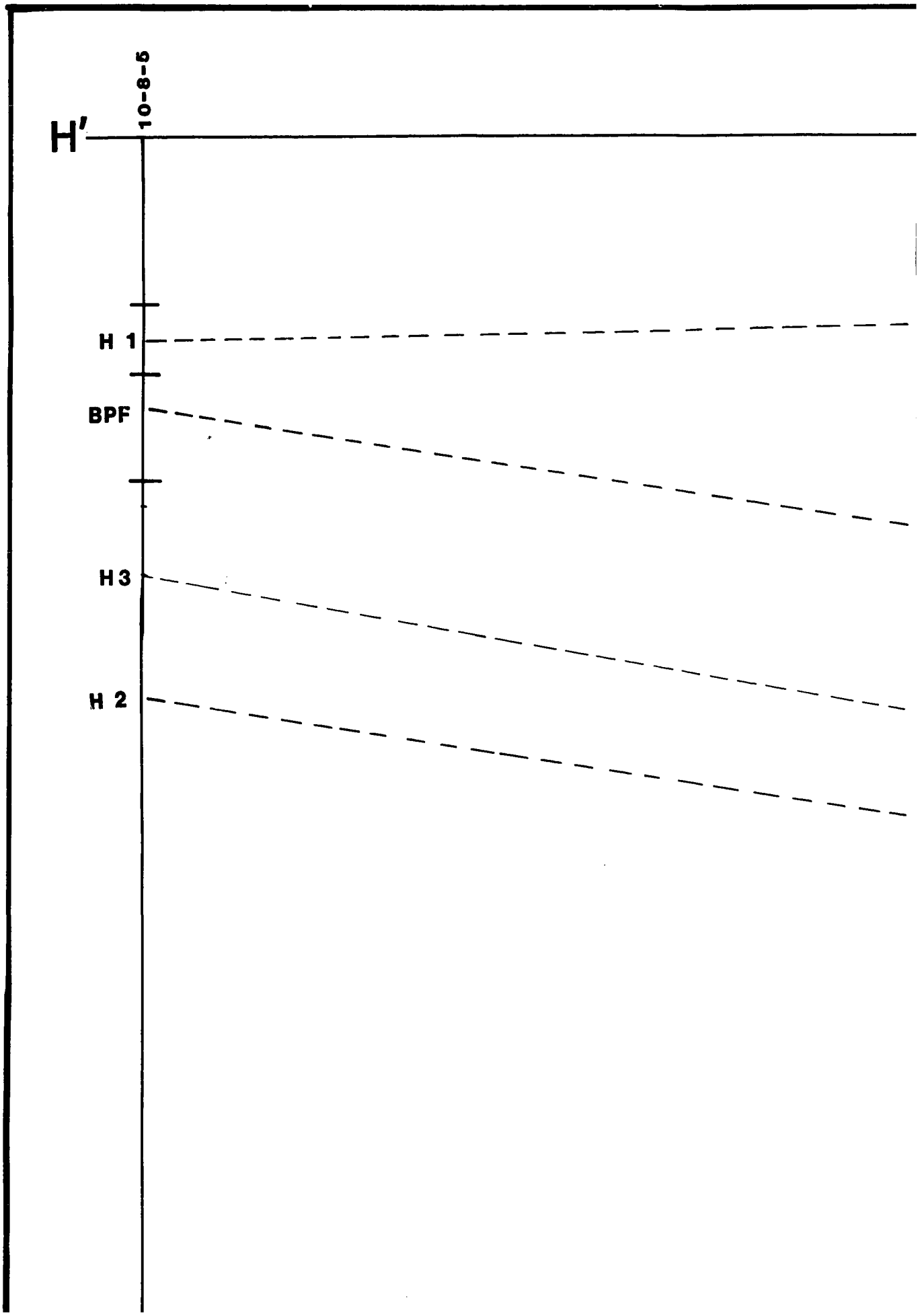

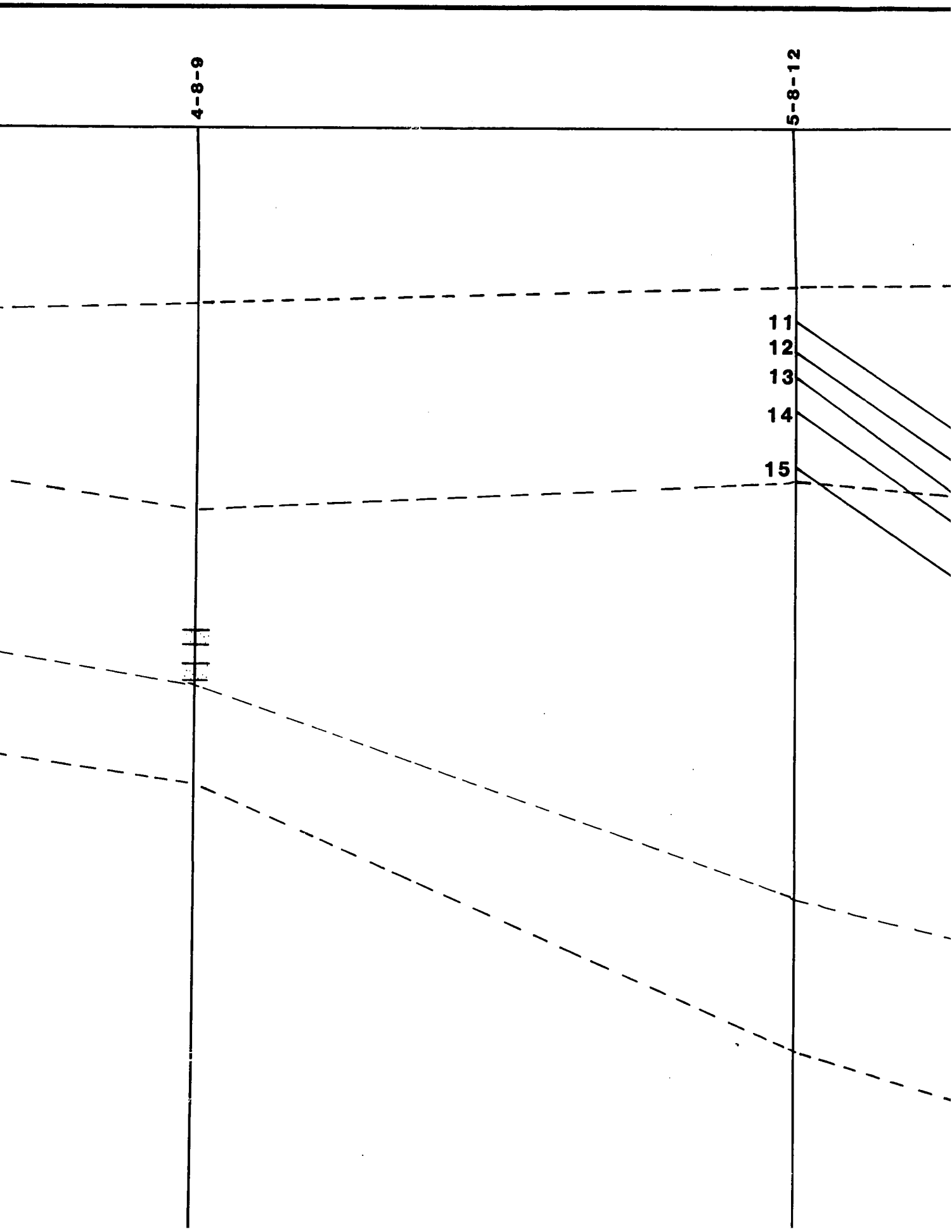

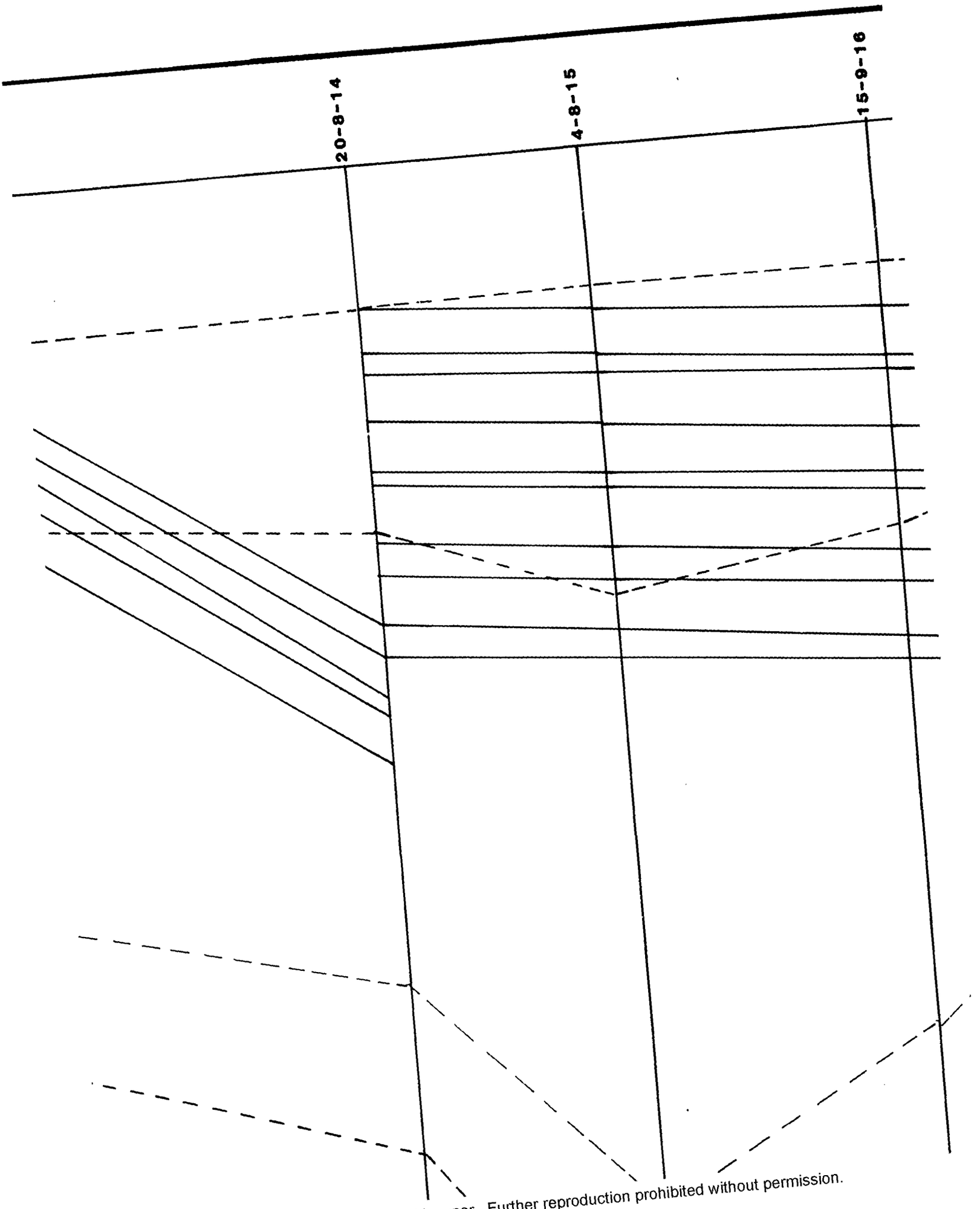

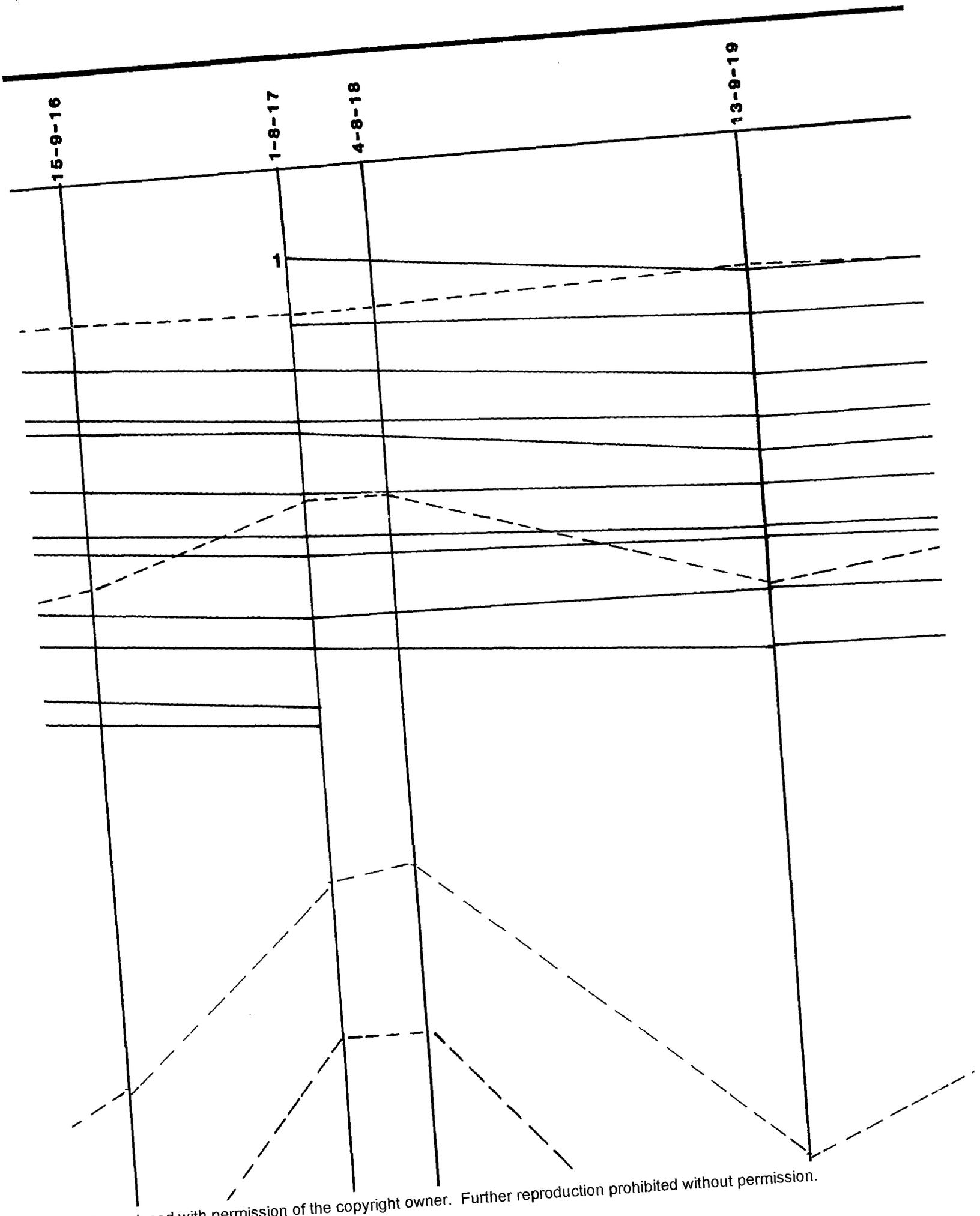

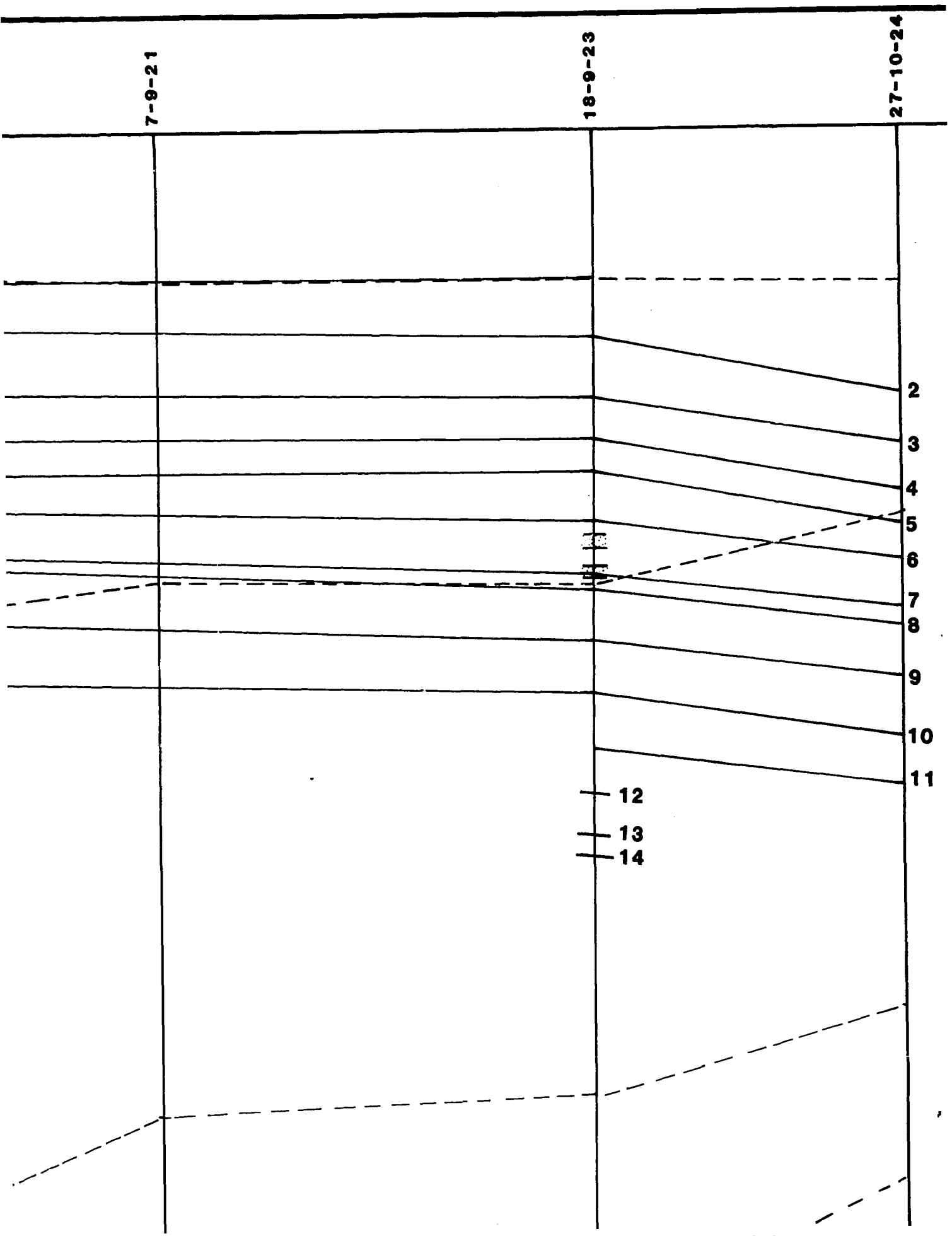

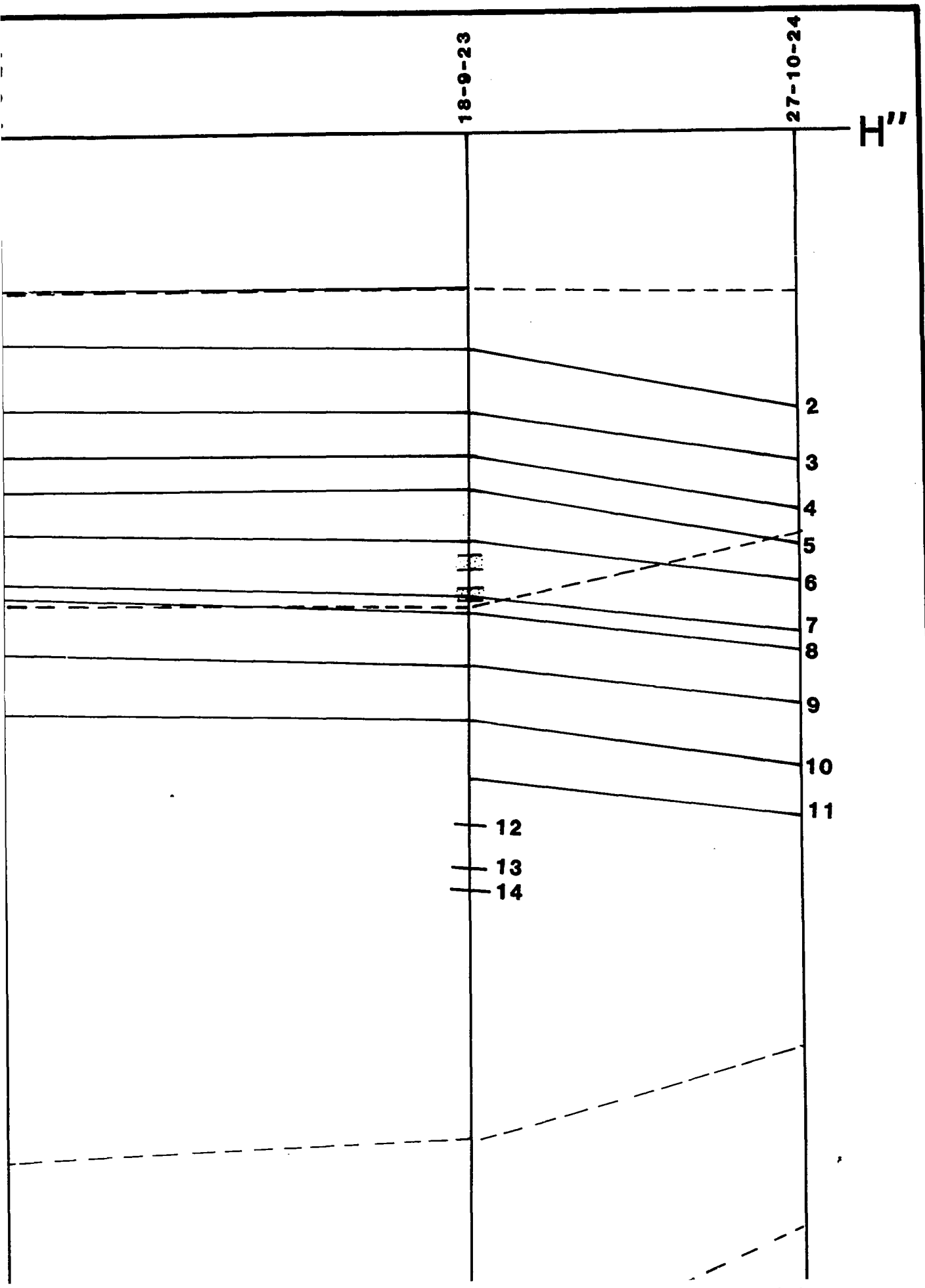

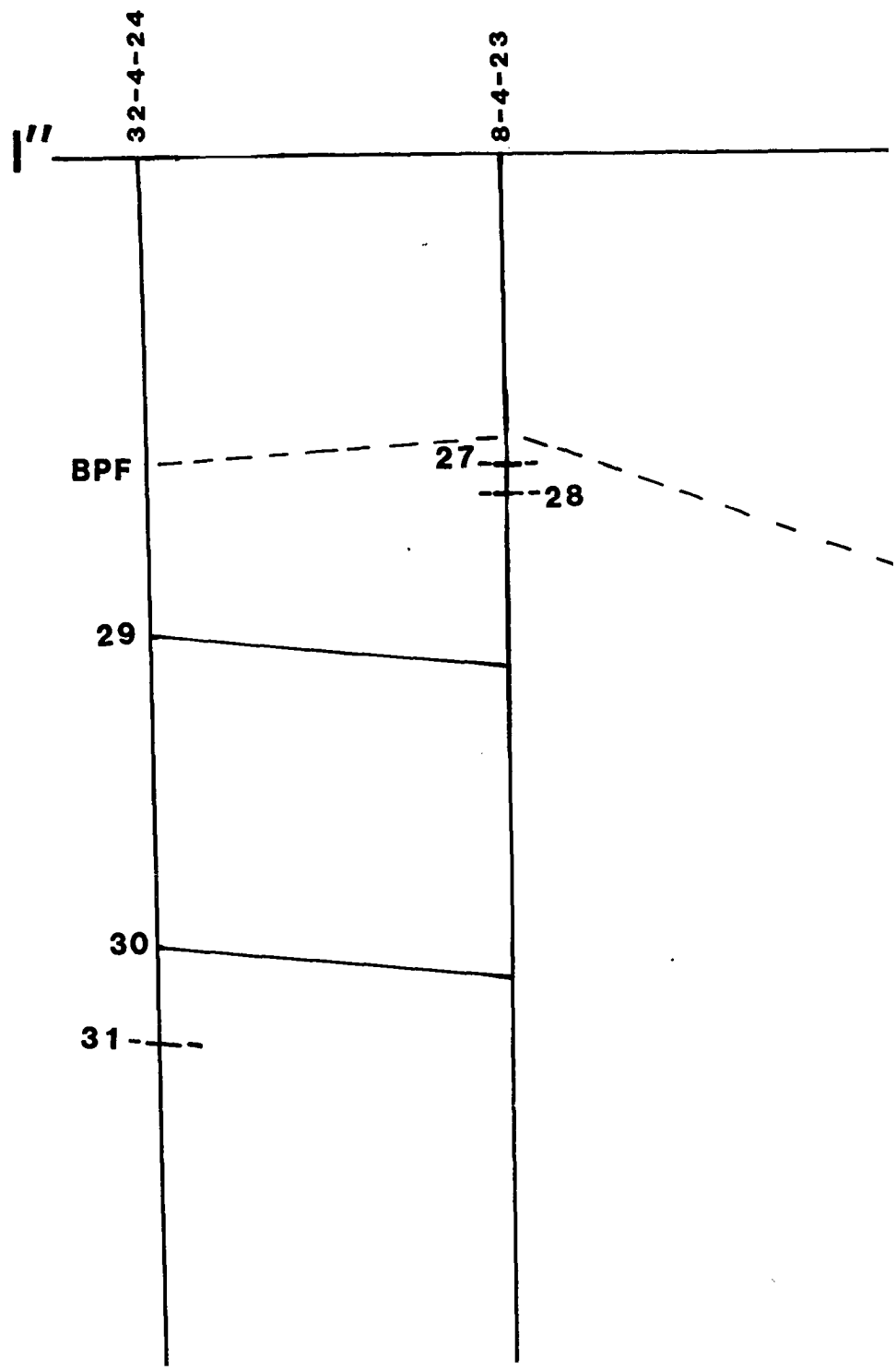

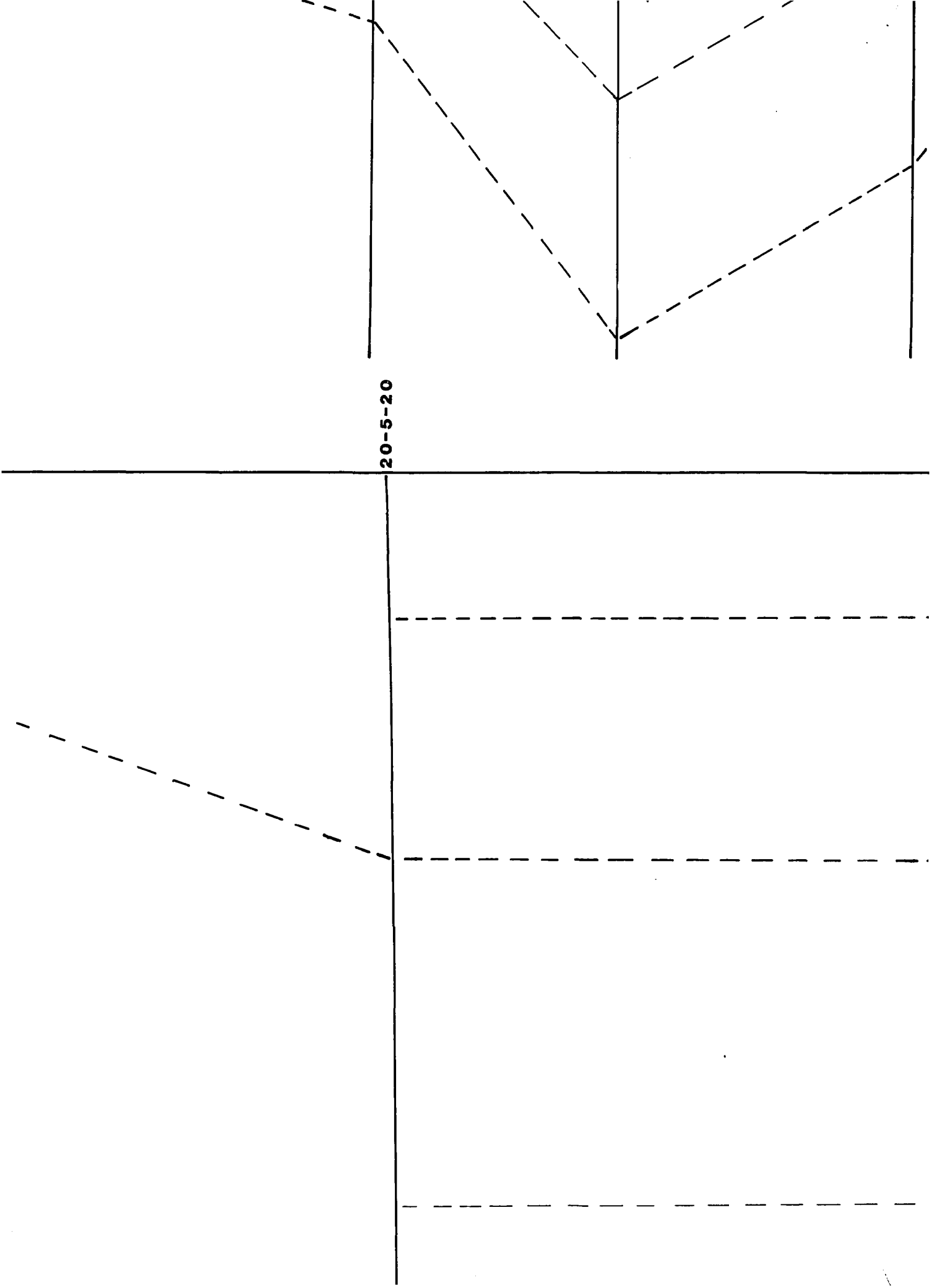

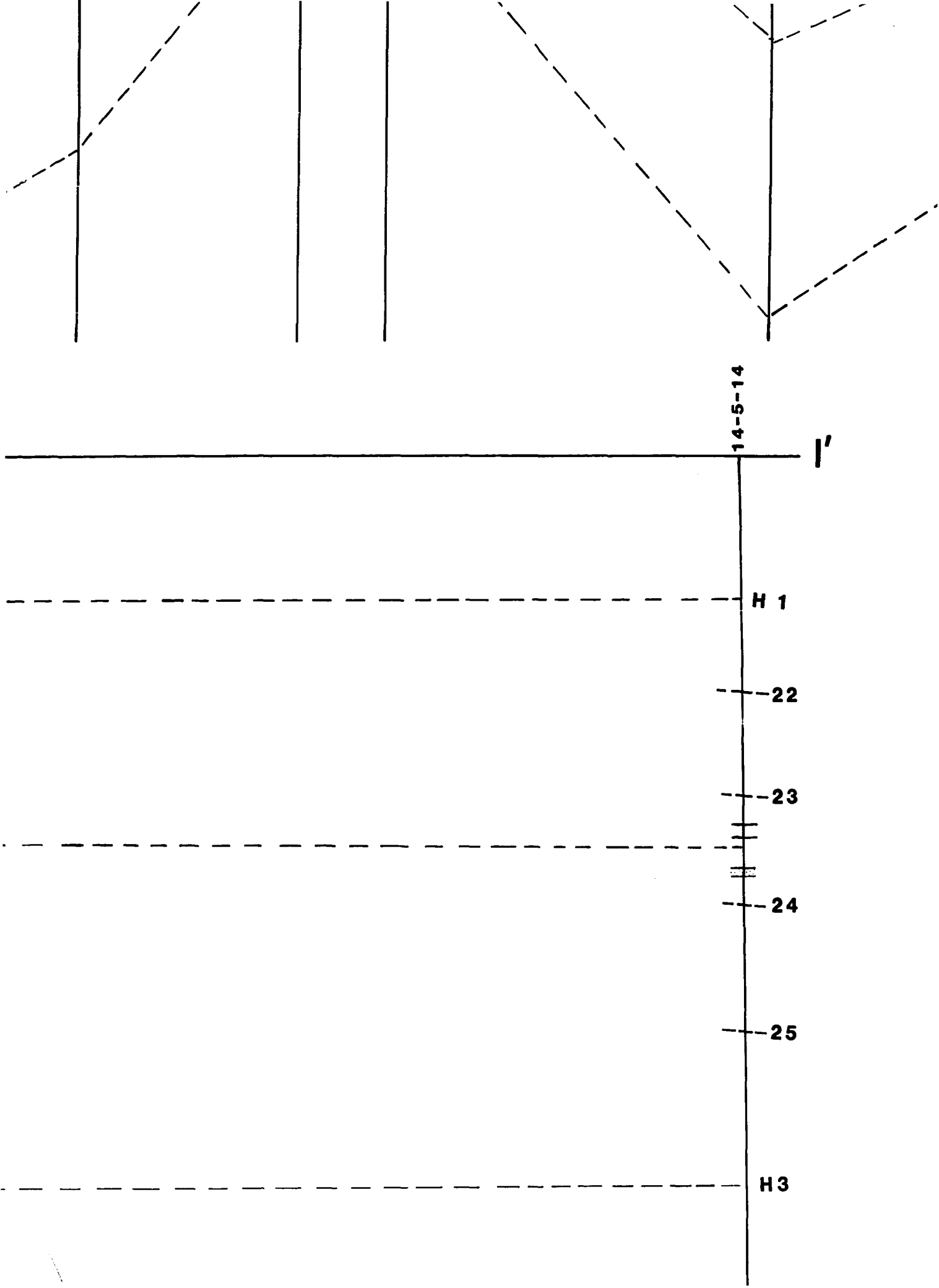

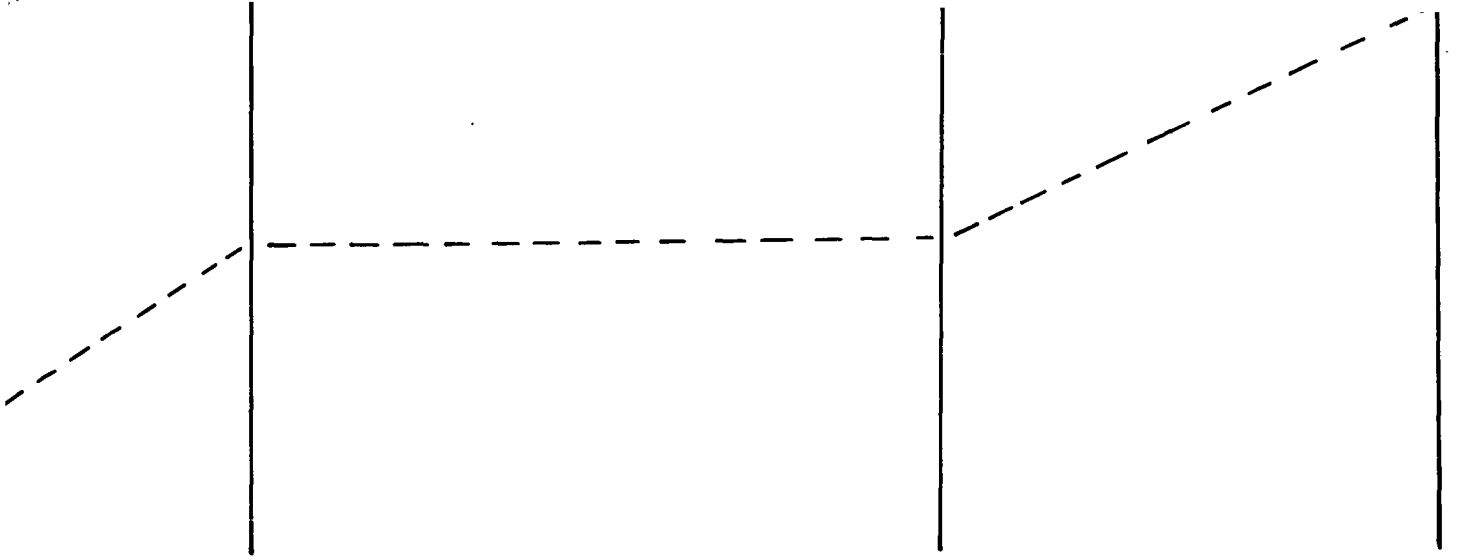

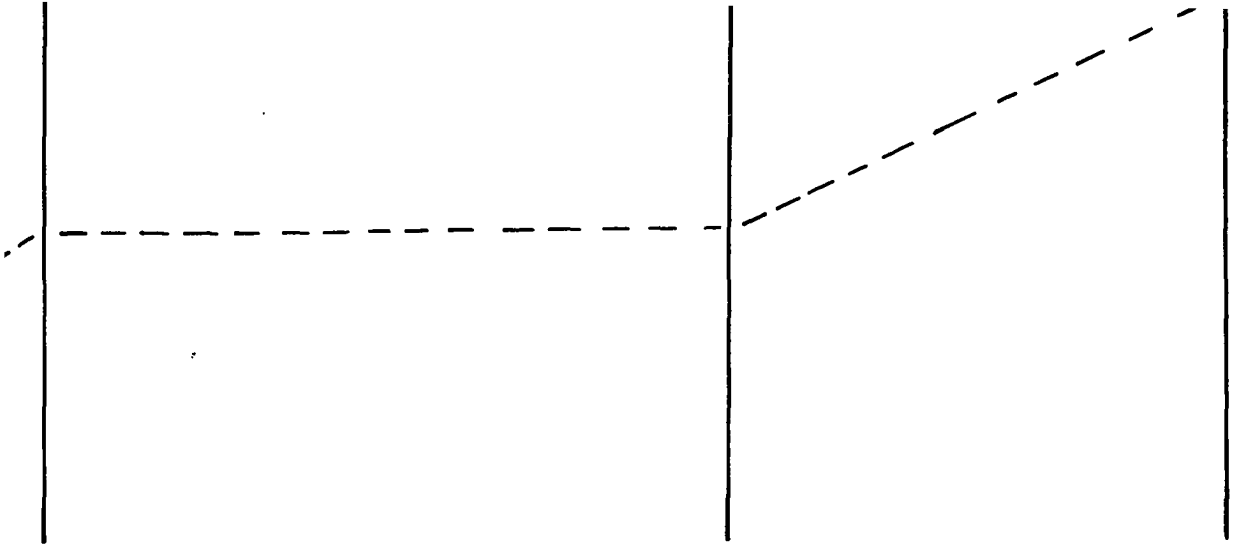

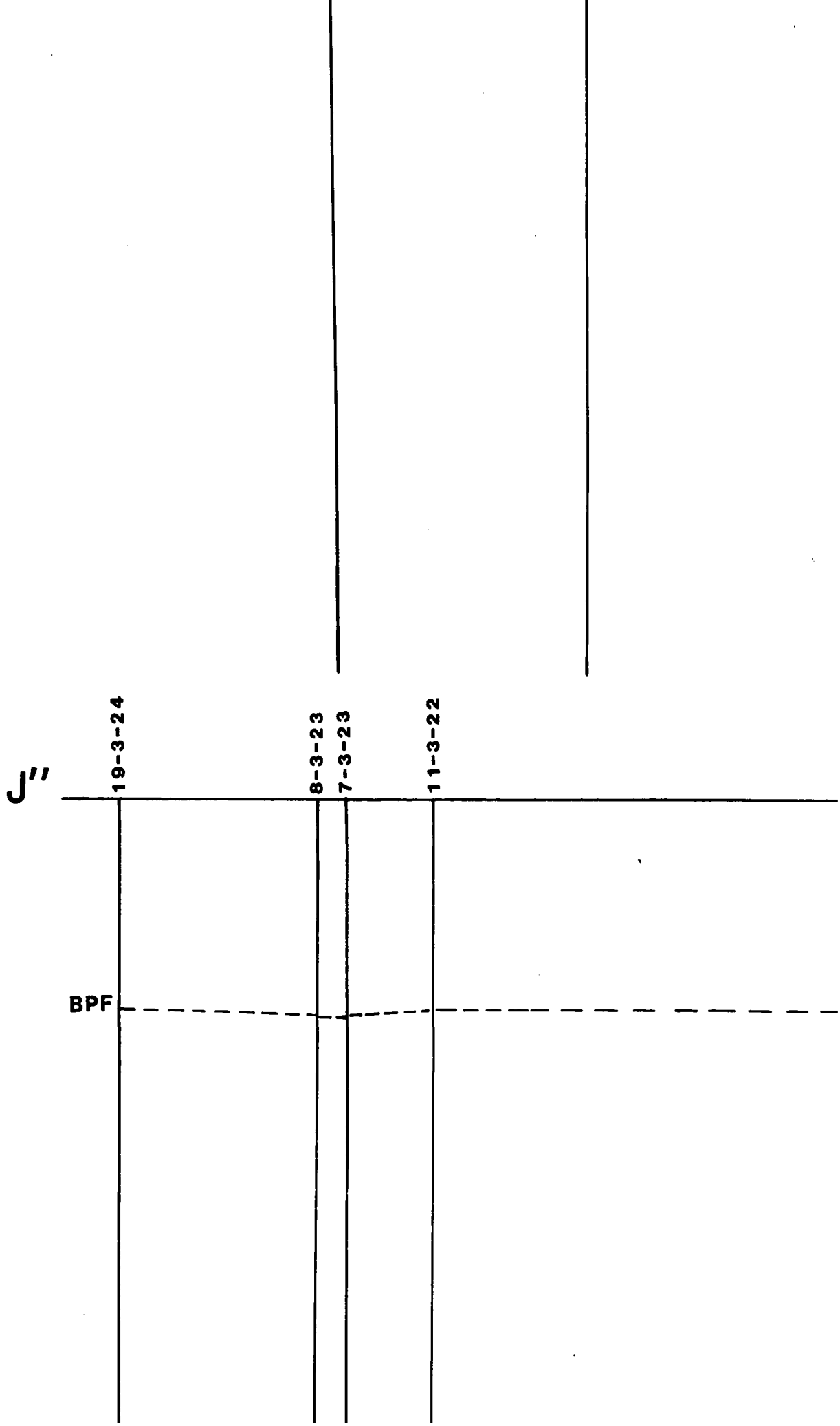

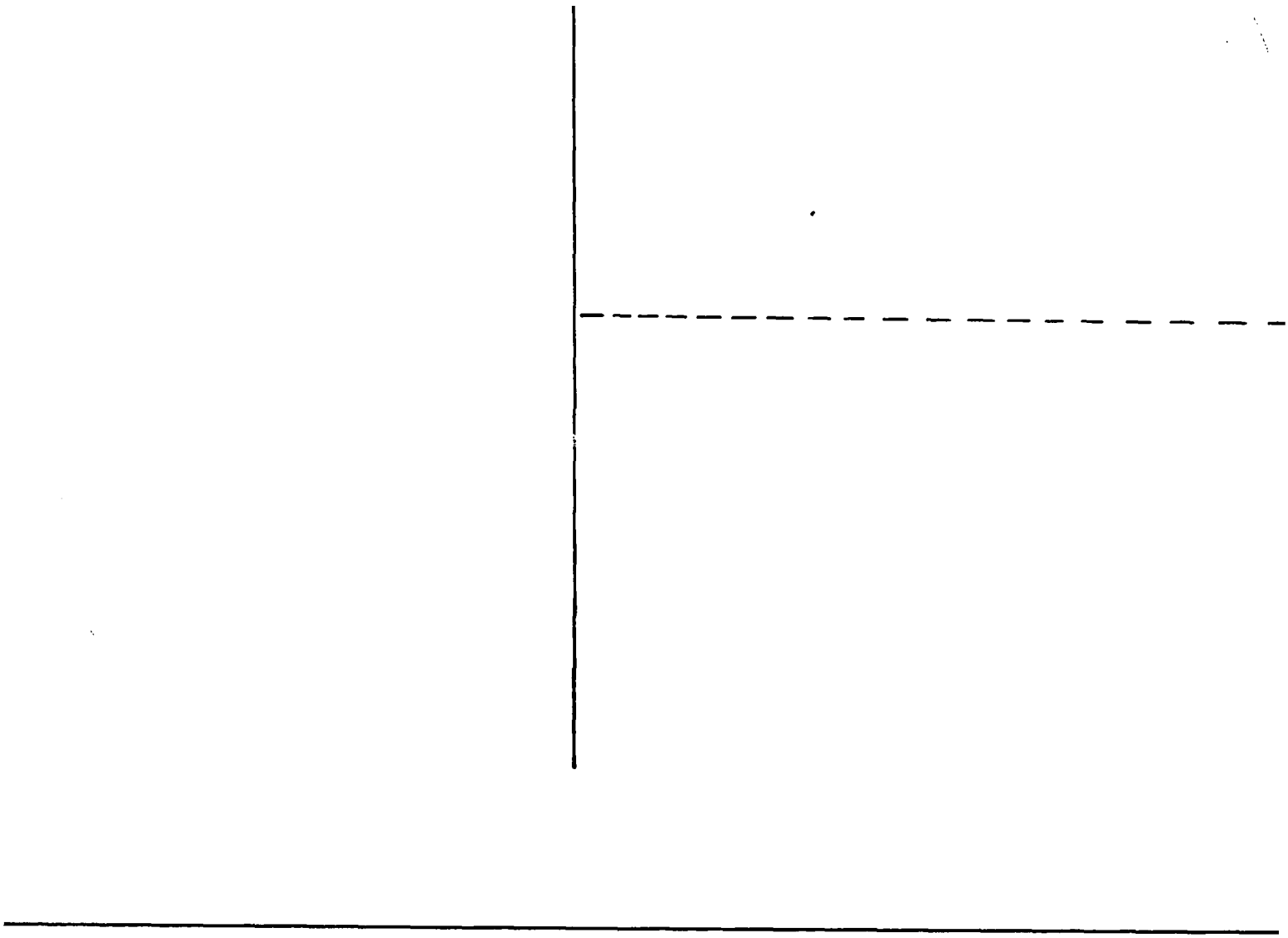

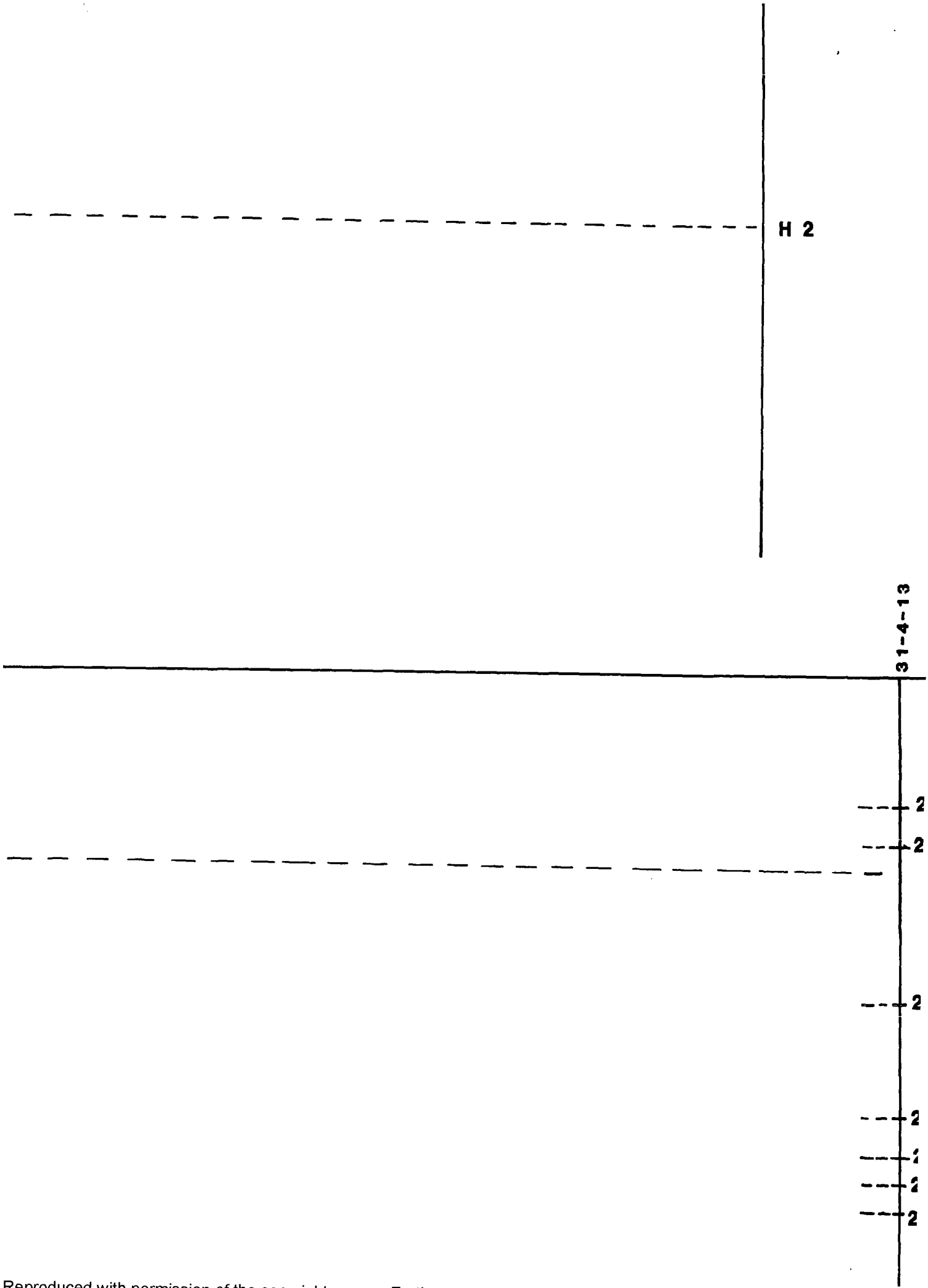

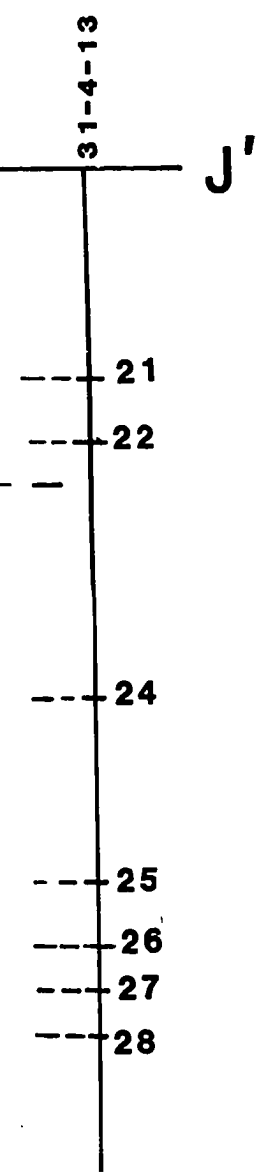

PLATE 8

H'H''-J'J''

CROSS SECTIONS

Showing Hydrate Occurrences and Degree of Hydrate Saturation

Key:

11-12-13 Location

High Concentration

Intermediate

Low Concentration

PLATE 8

H'H''-J'J''

CROSS SECTIONS

Showing Hydrate Occurrences and Degree of Hydrate Saturation

Key:

11-12-13 Location

High Concentration

Intermediate

Low Concentration

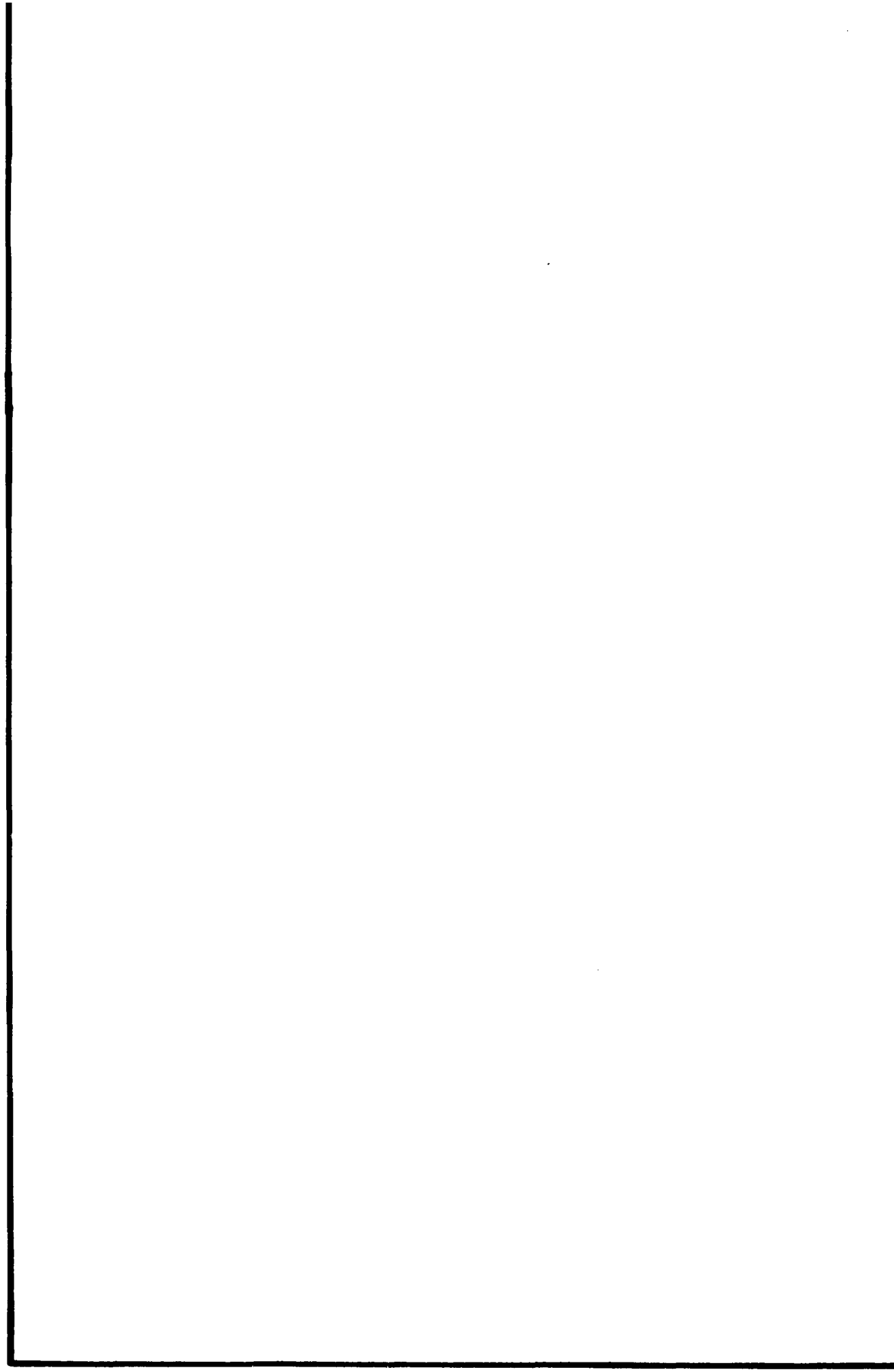

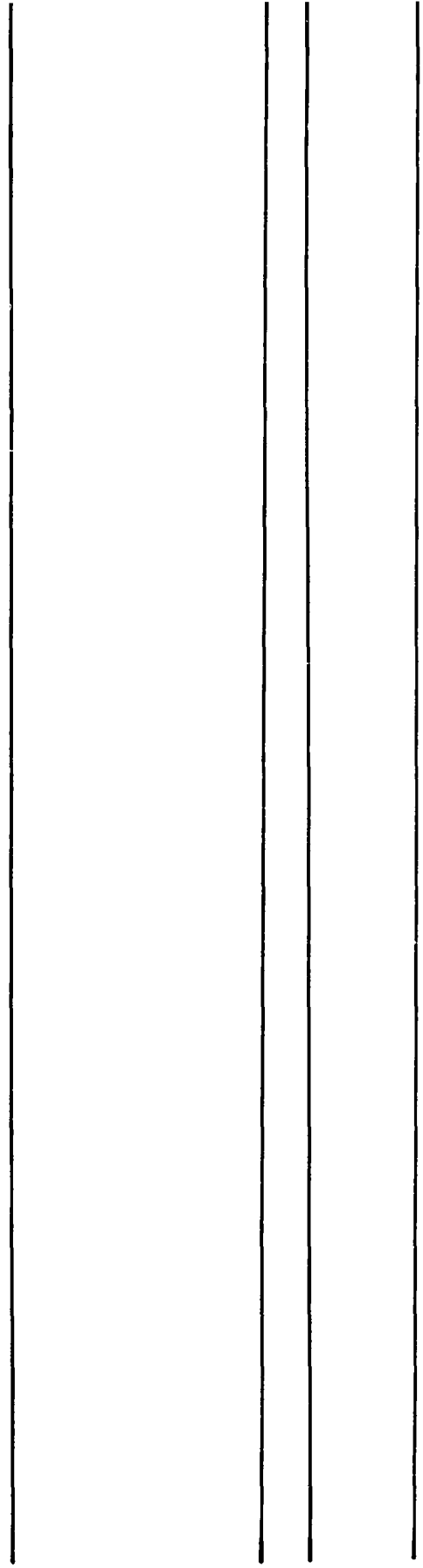

CROSS SECTIONS

Showing Hydrate Occurrences and Degree of Hydrate Saturation

24

25

26

27

28

Key:

11-12-13 Location

High Concentration

Intermediate

Low Concentration

H 1 Upper Hydrate Stability Boundary

H 2 Lower Hydrate Stability Boundary (with no geothermal-gradient change at BPF)

H3 Lower Hydrate Stability-Boundary (with geothermal gradient-change at BPF)

BPF Base of the Permafrost

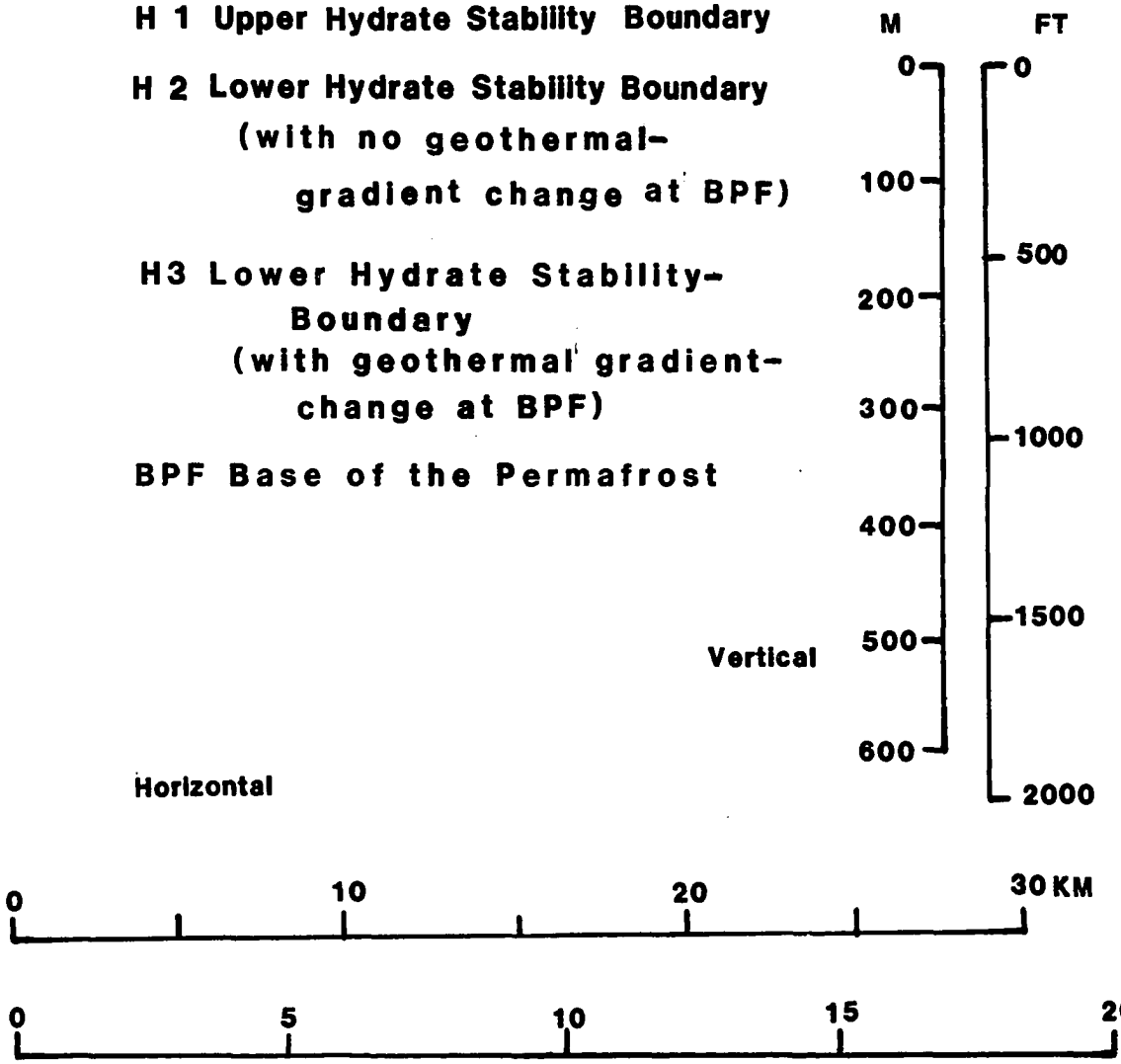

Showing Hydrate Occurrences and Degree of Hydrate Saturation

Key:

11-12-13 Location

High Concentration

Intermediate

Low Concentration

H 1 Upper Hydrate Stability Boundary

H 2 Lower Hydrate Stability Boundary (with no geothermal-gradient change at BPF)

H3 Lower Hydrate Stability-Boundary (with geothermal gradient-change at BPF)

BPF Base of the Permafrost

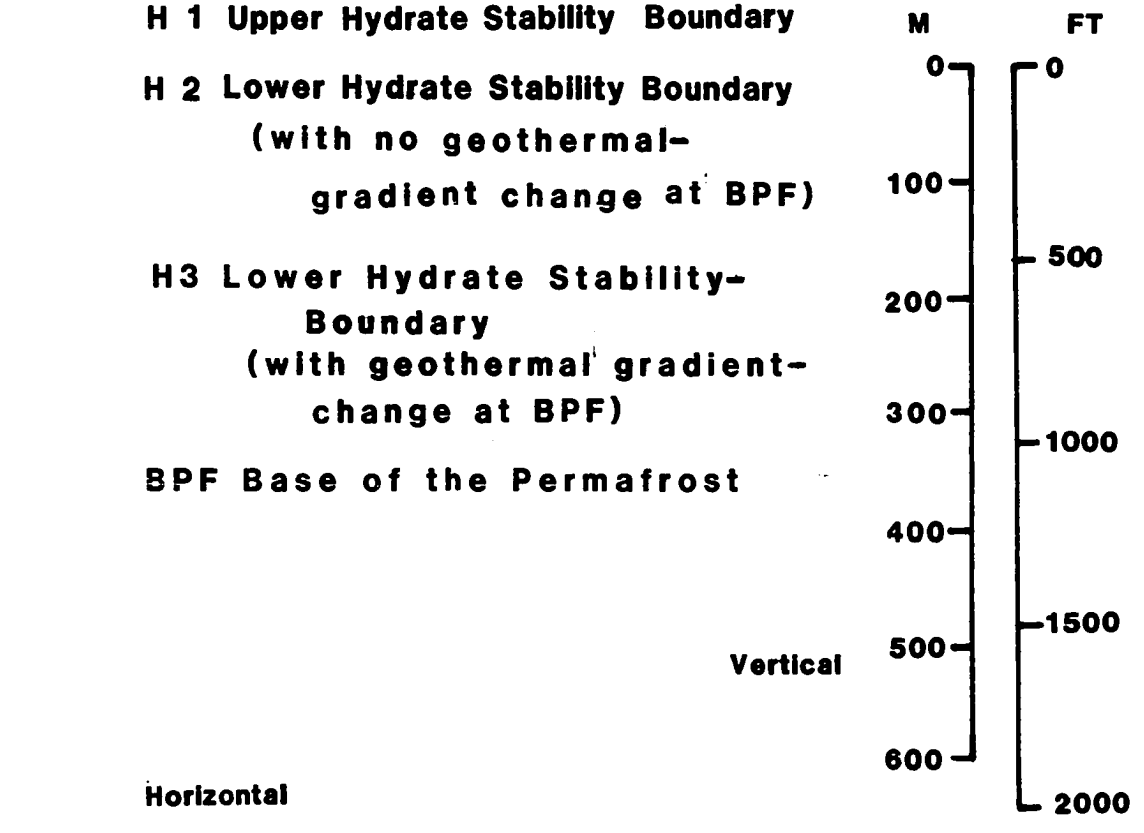

Horizontal

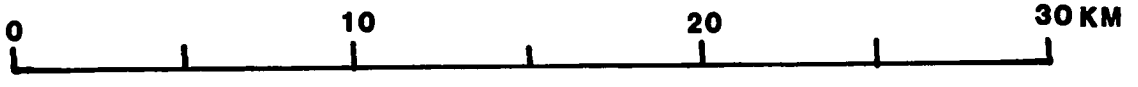

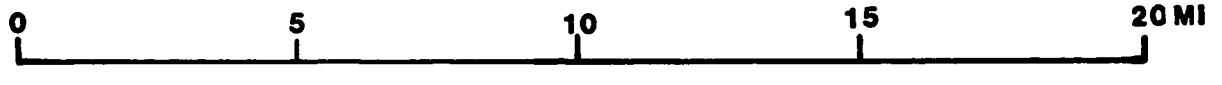

PLATE 8

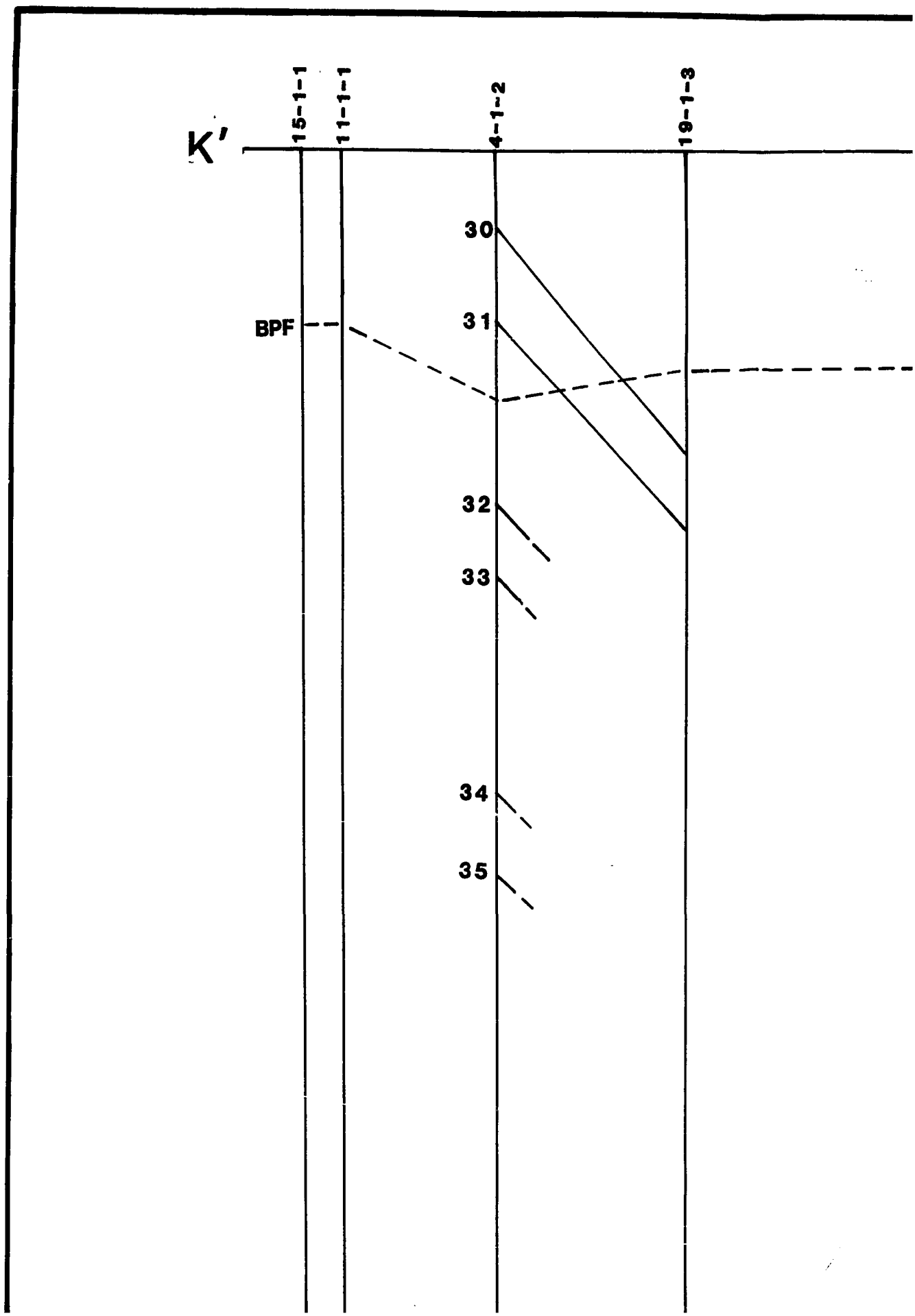

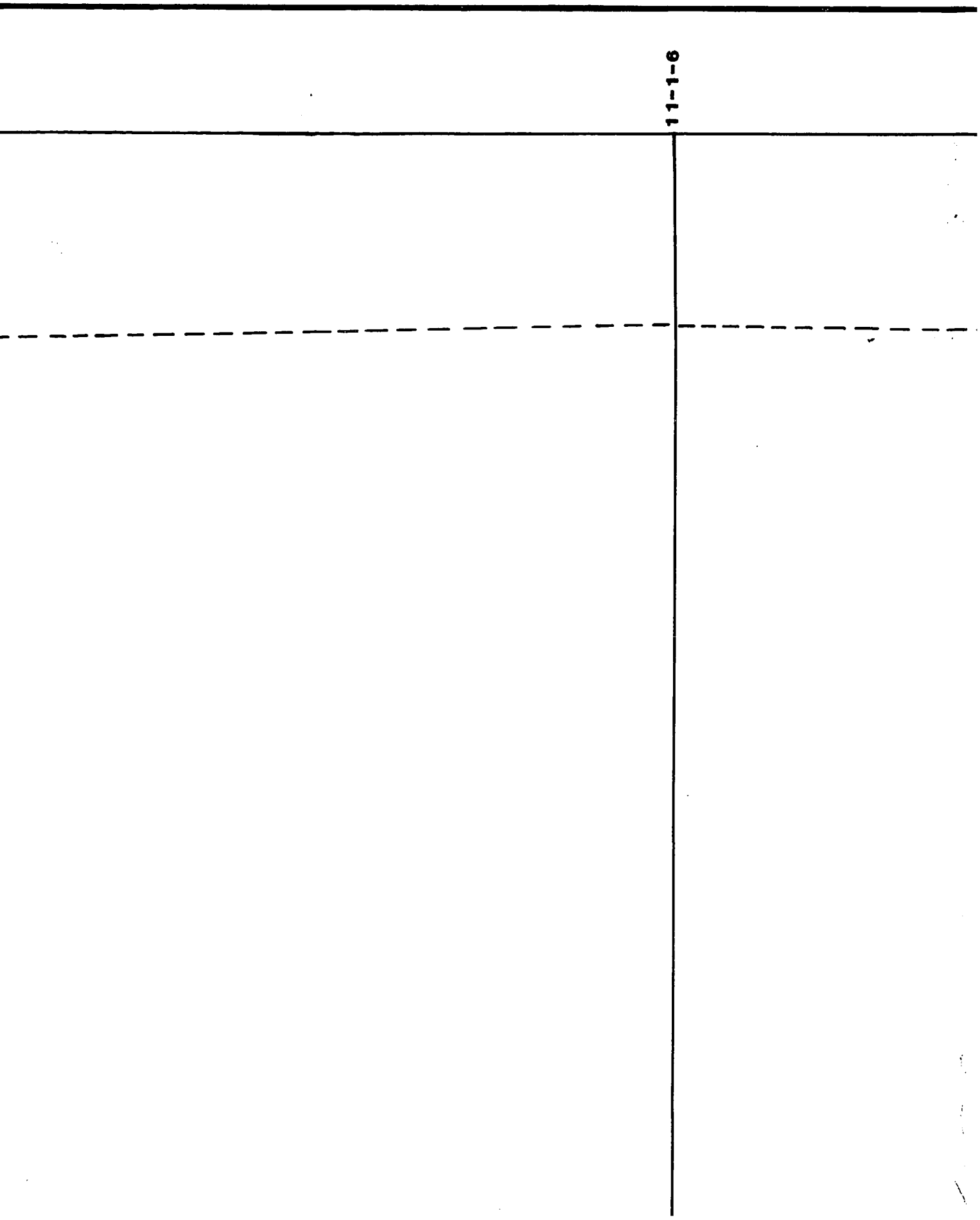

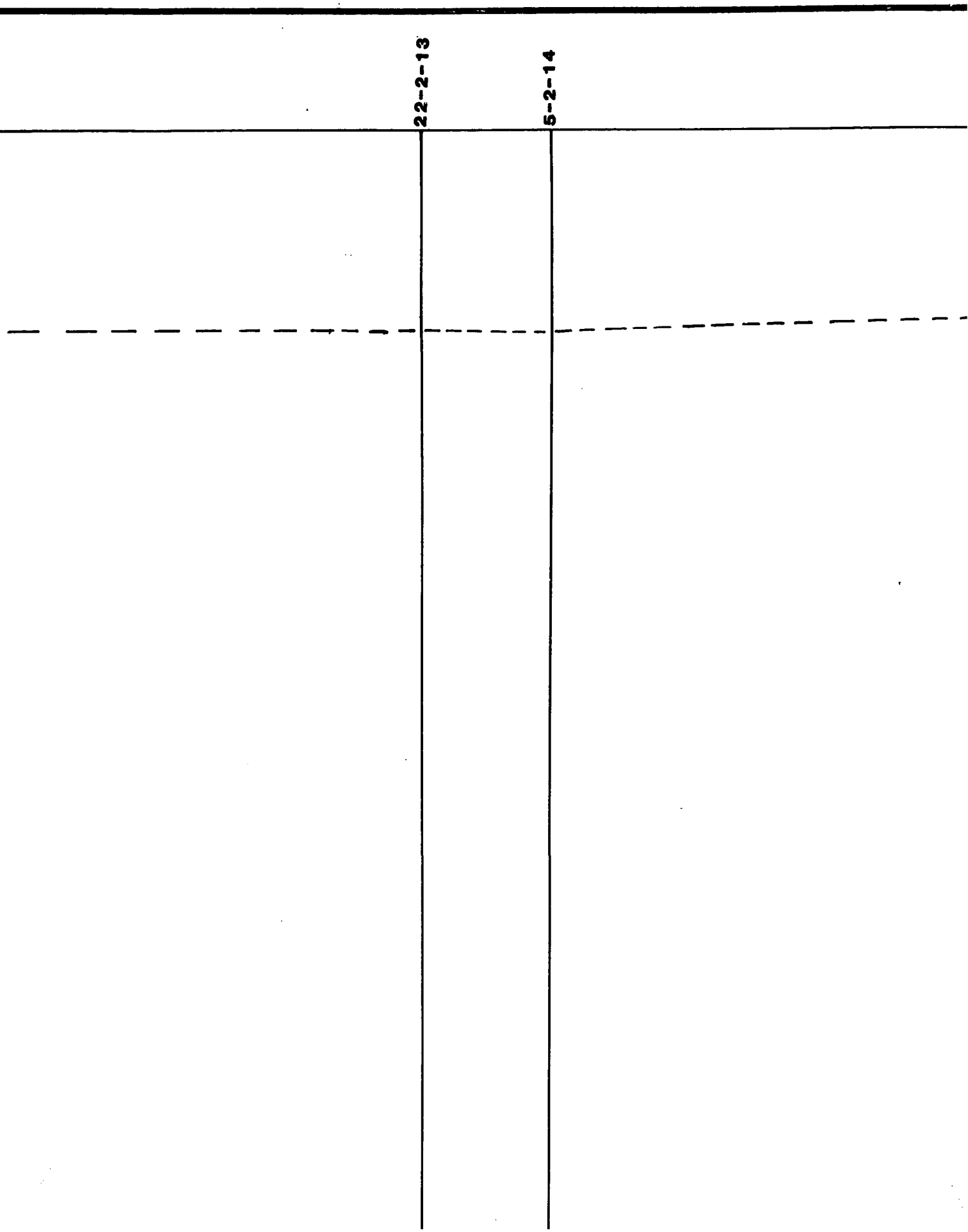

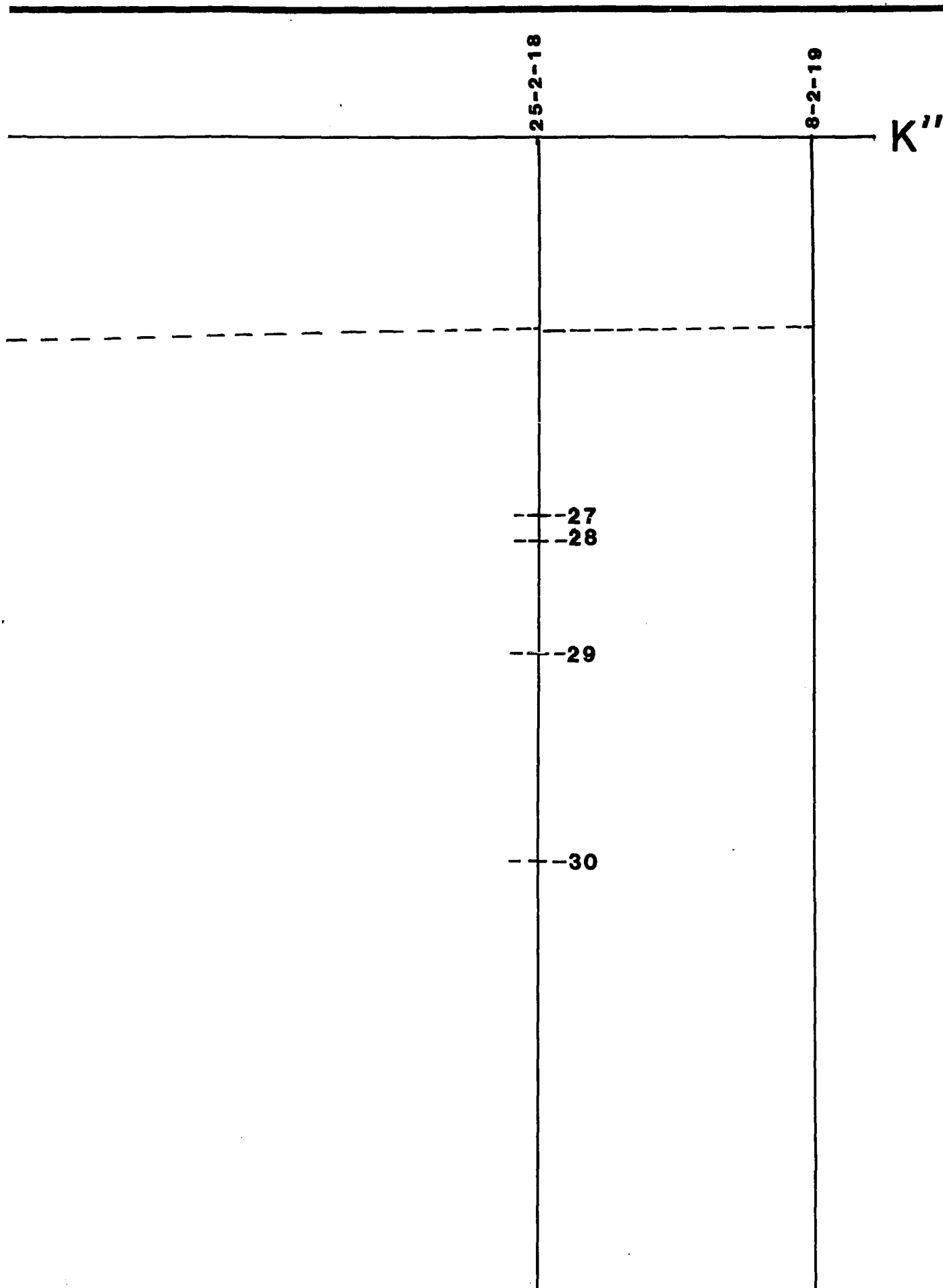

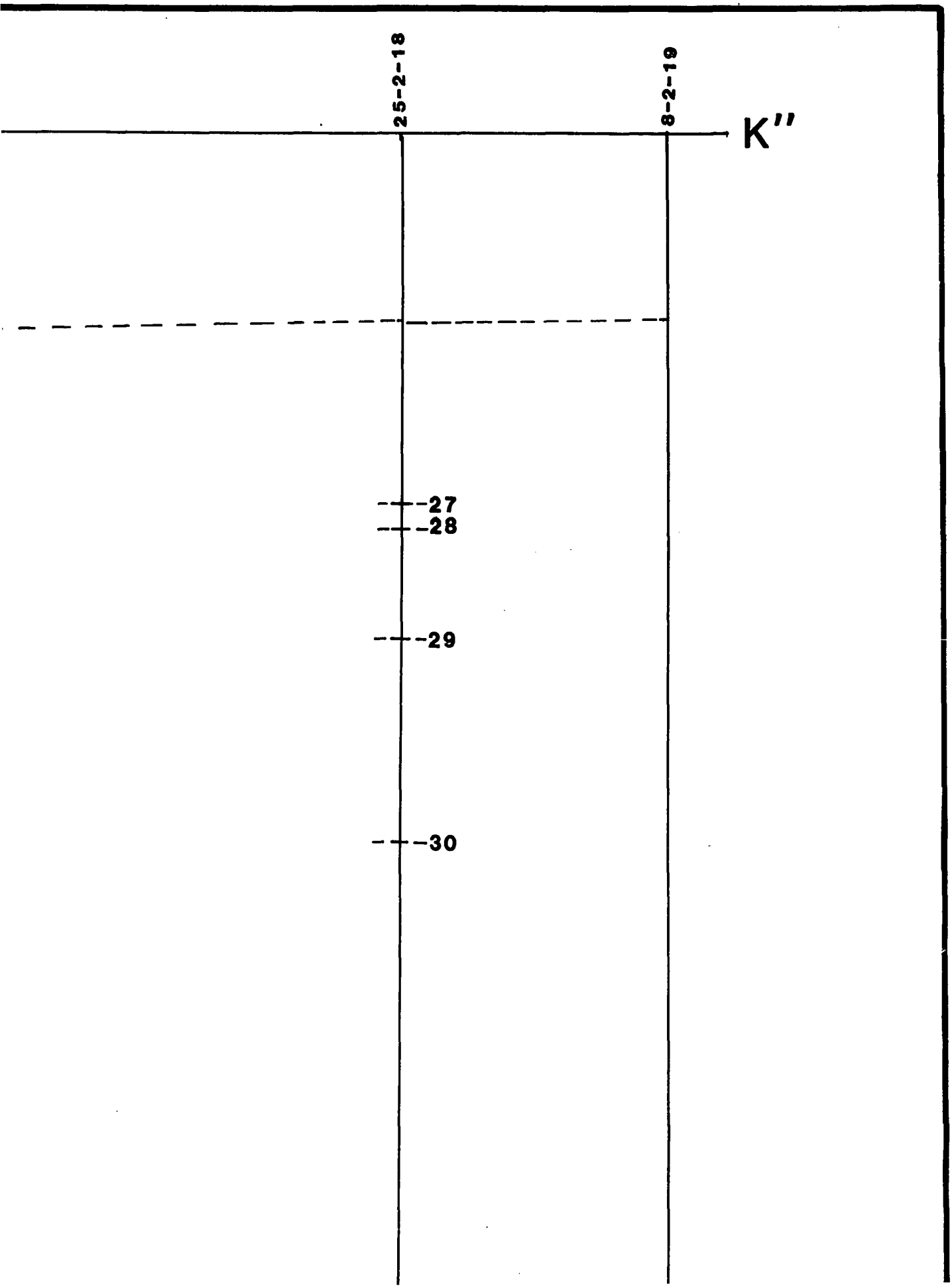

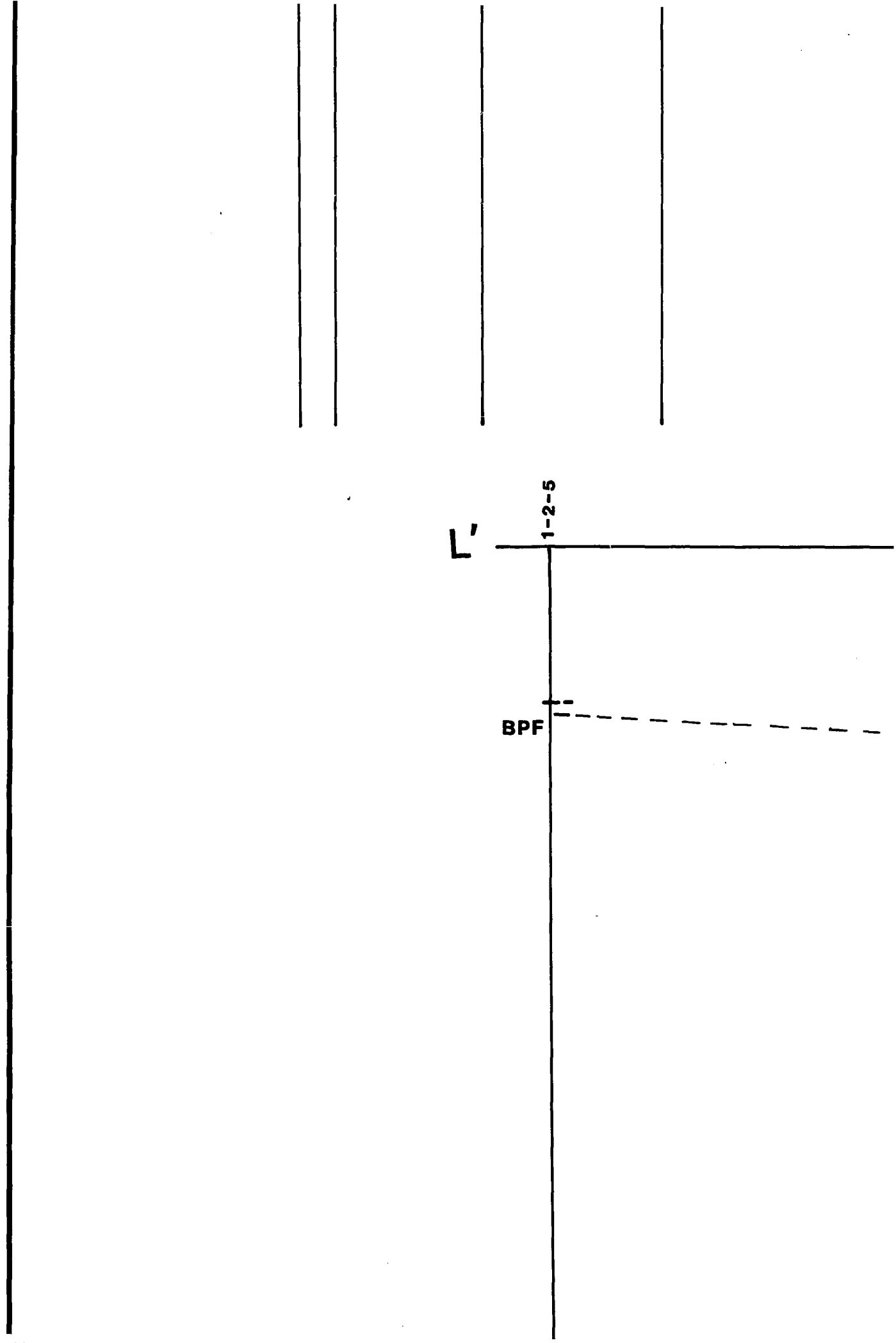

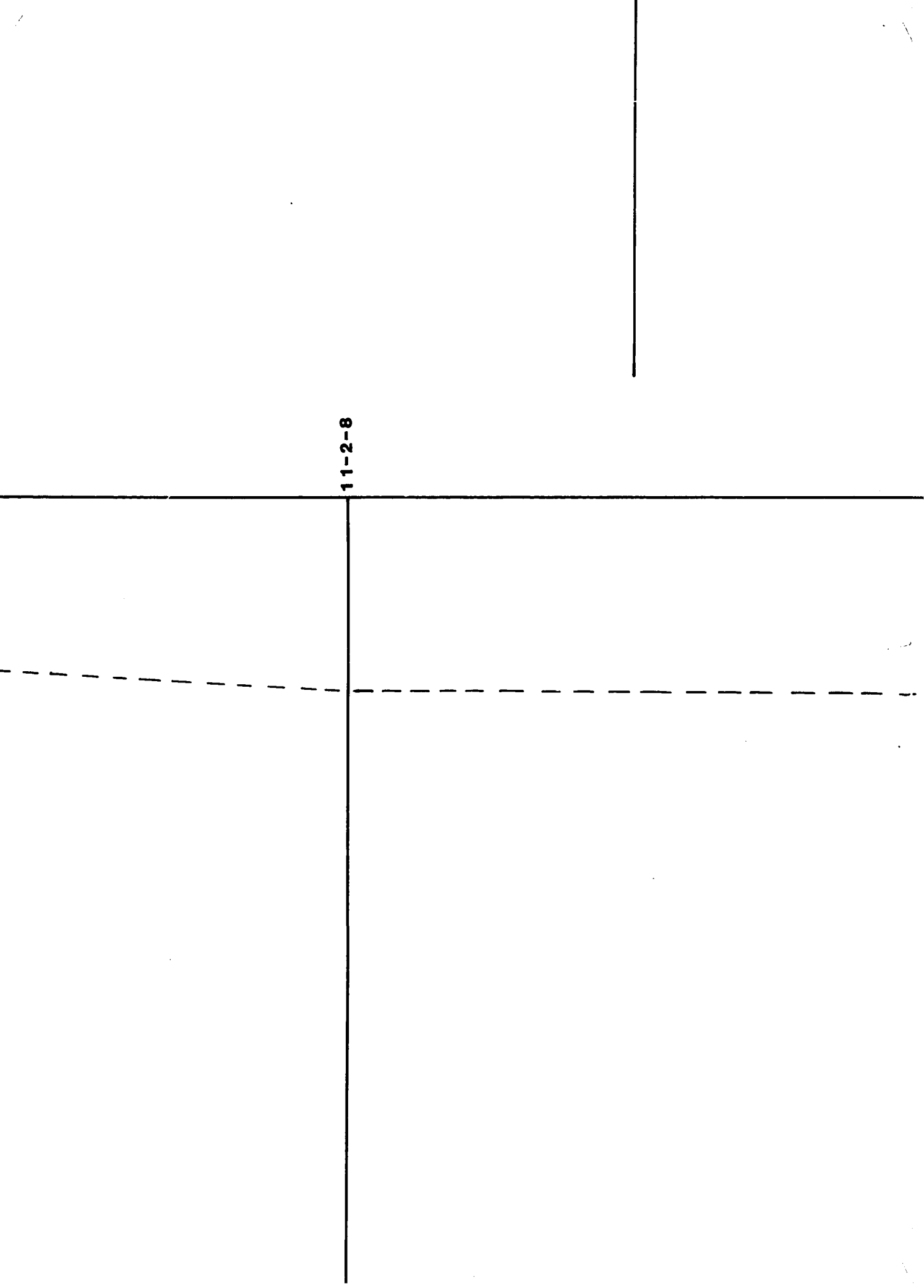

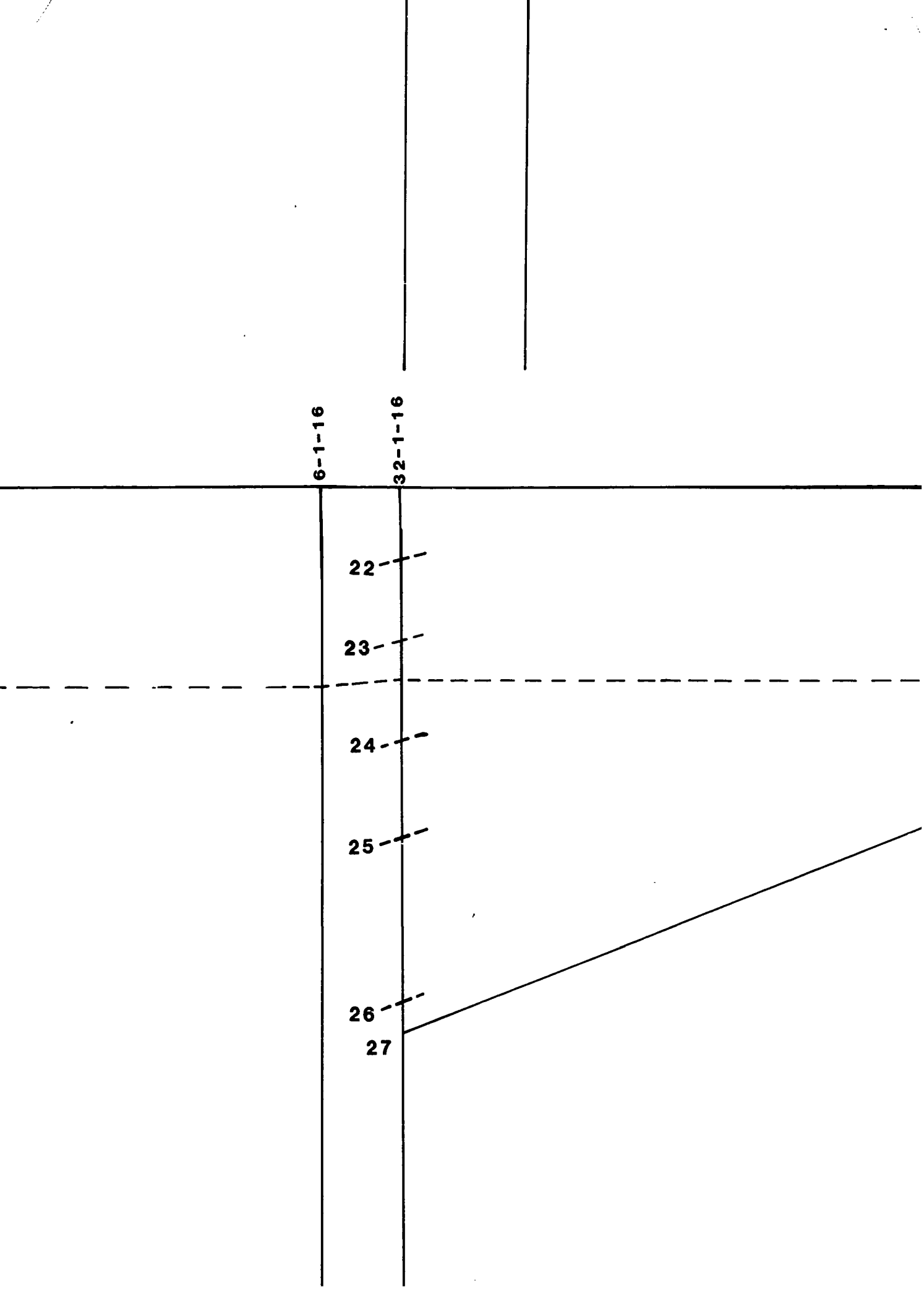

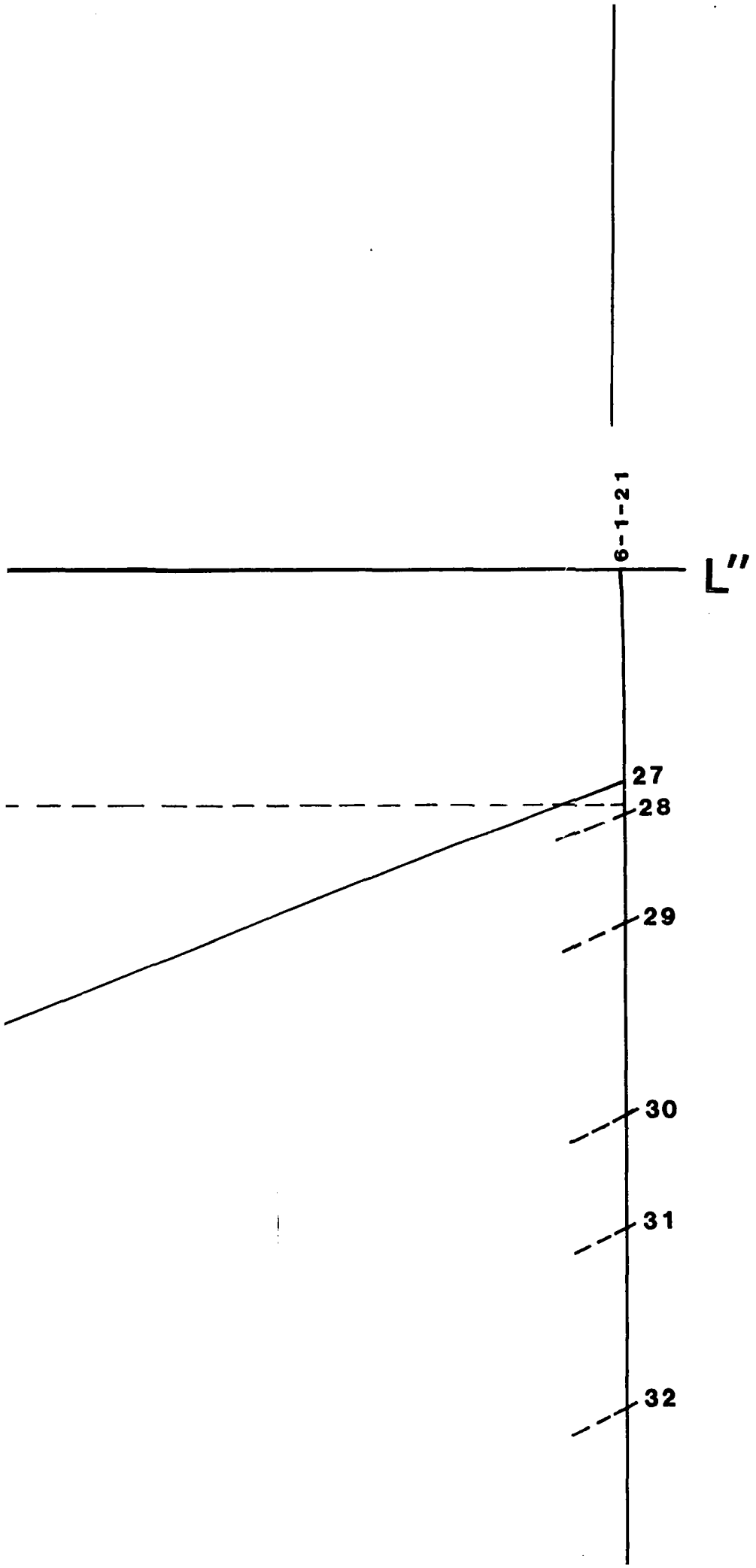

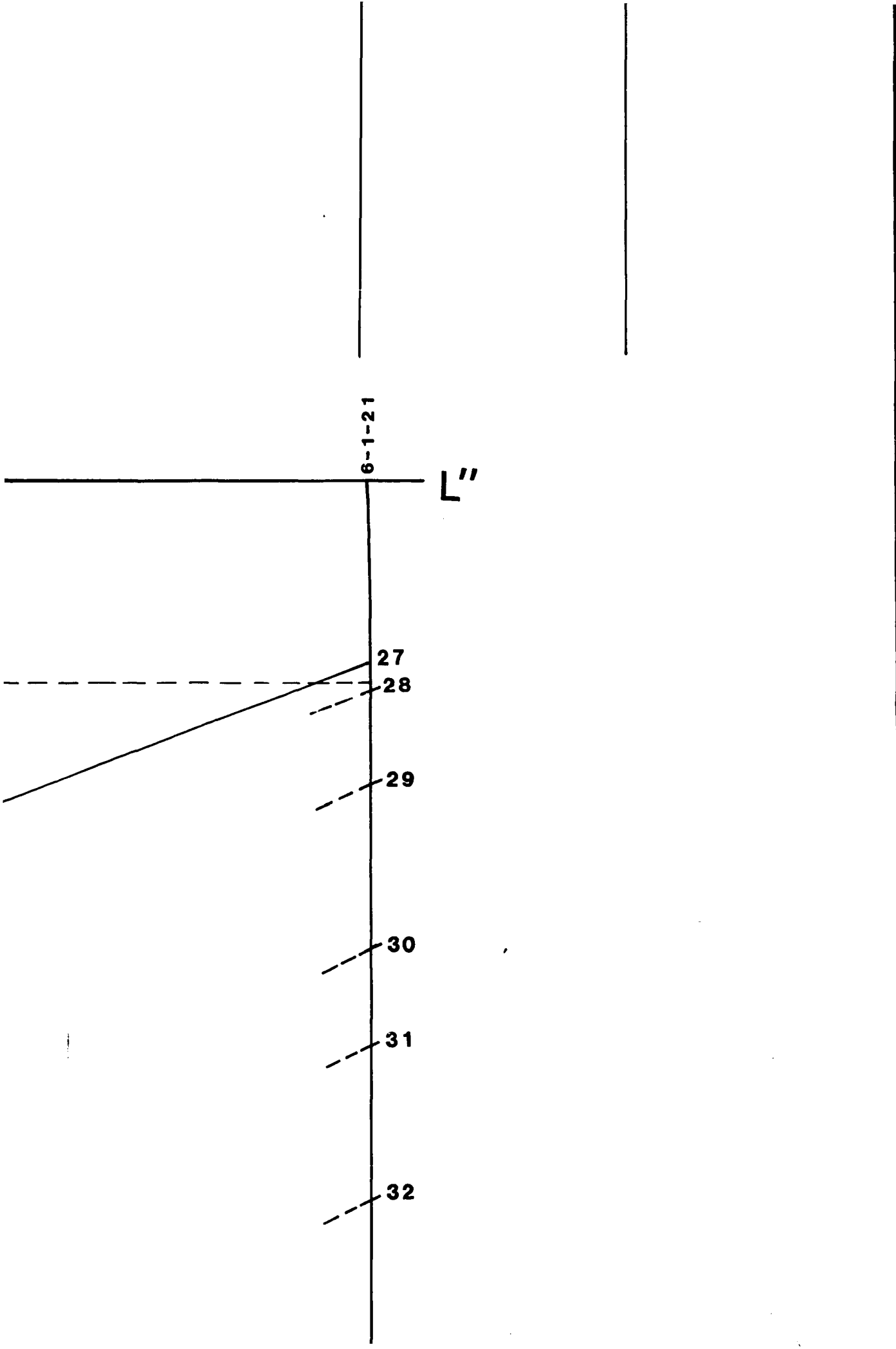

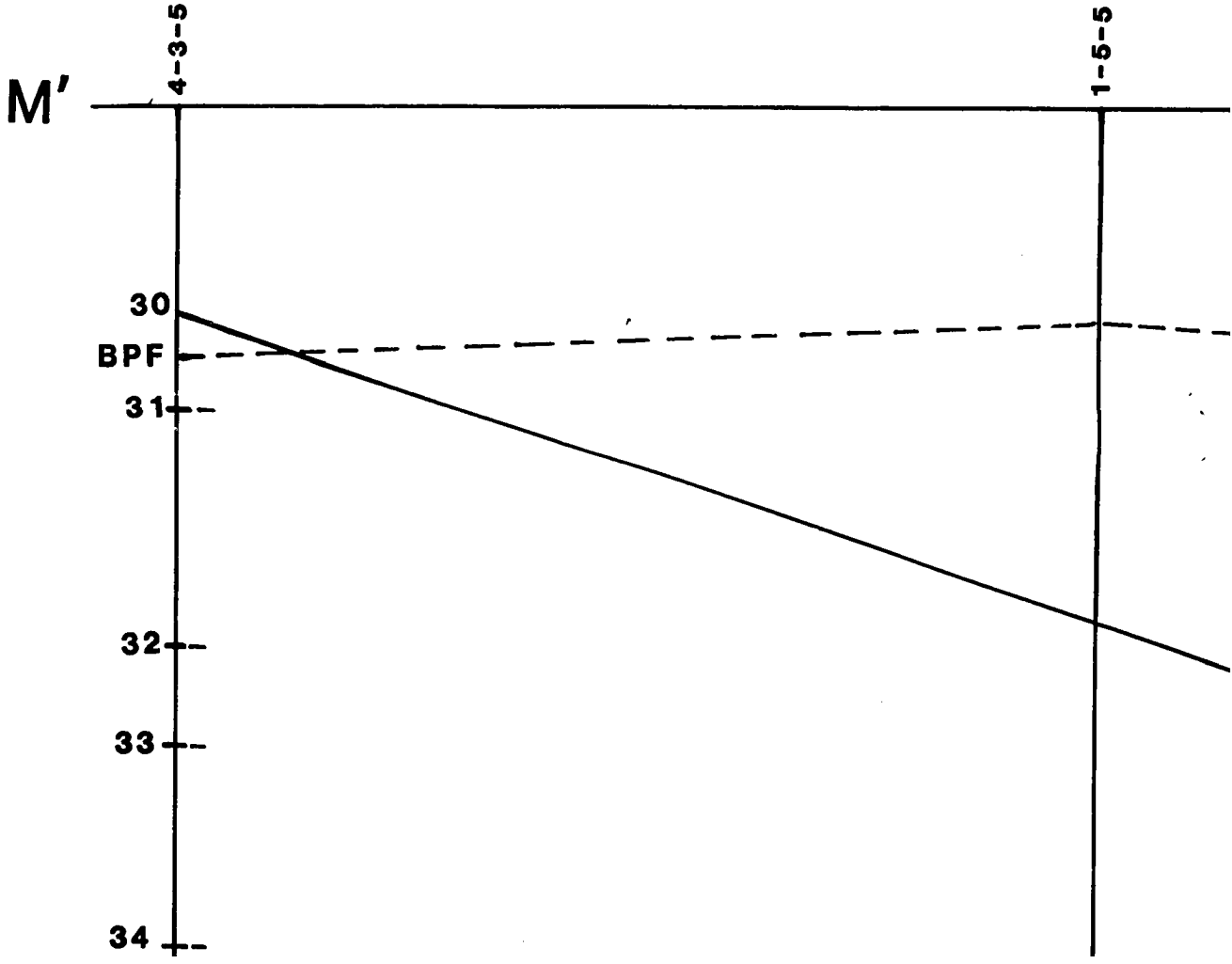

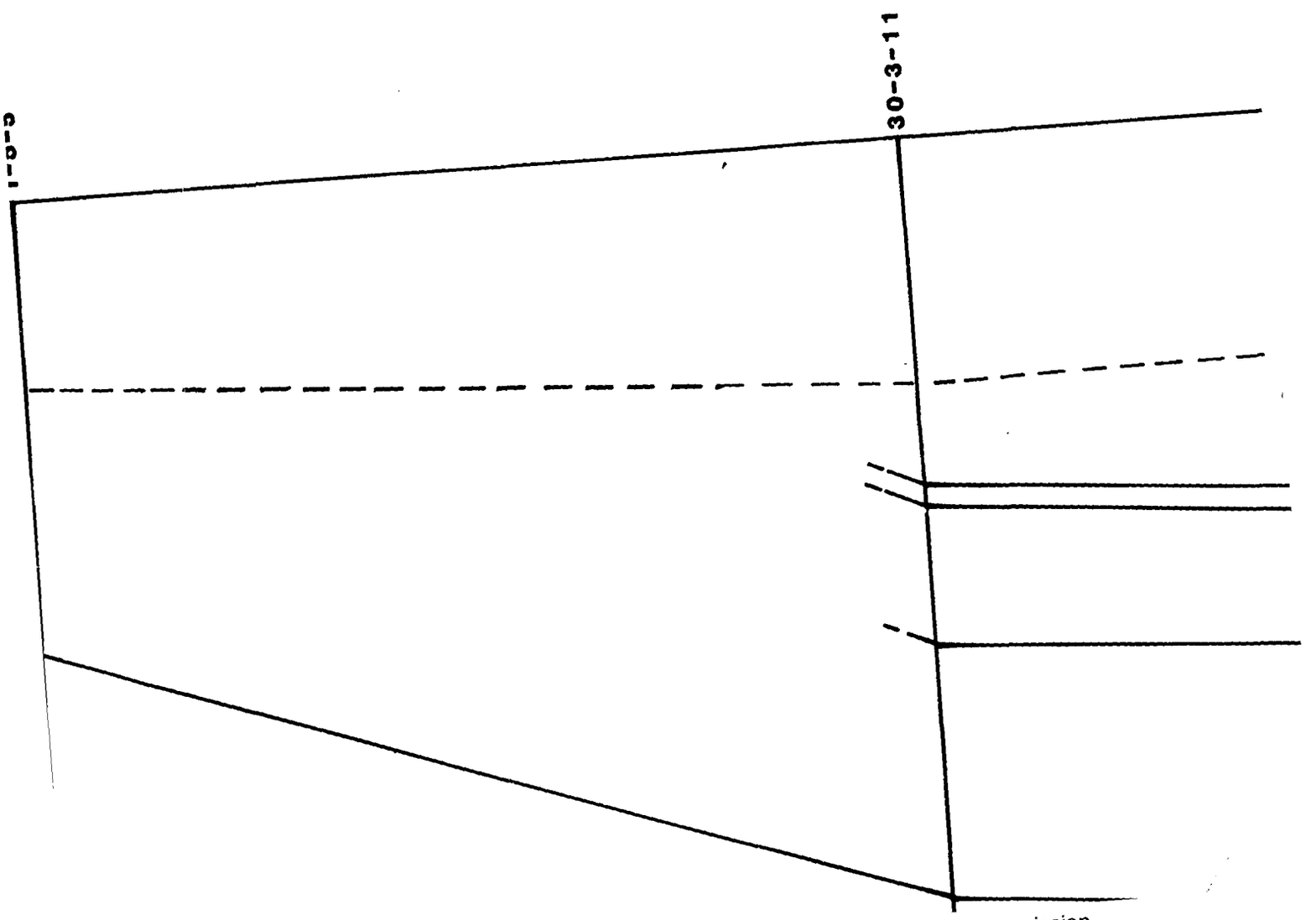

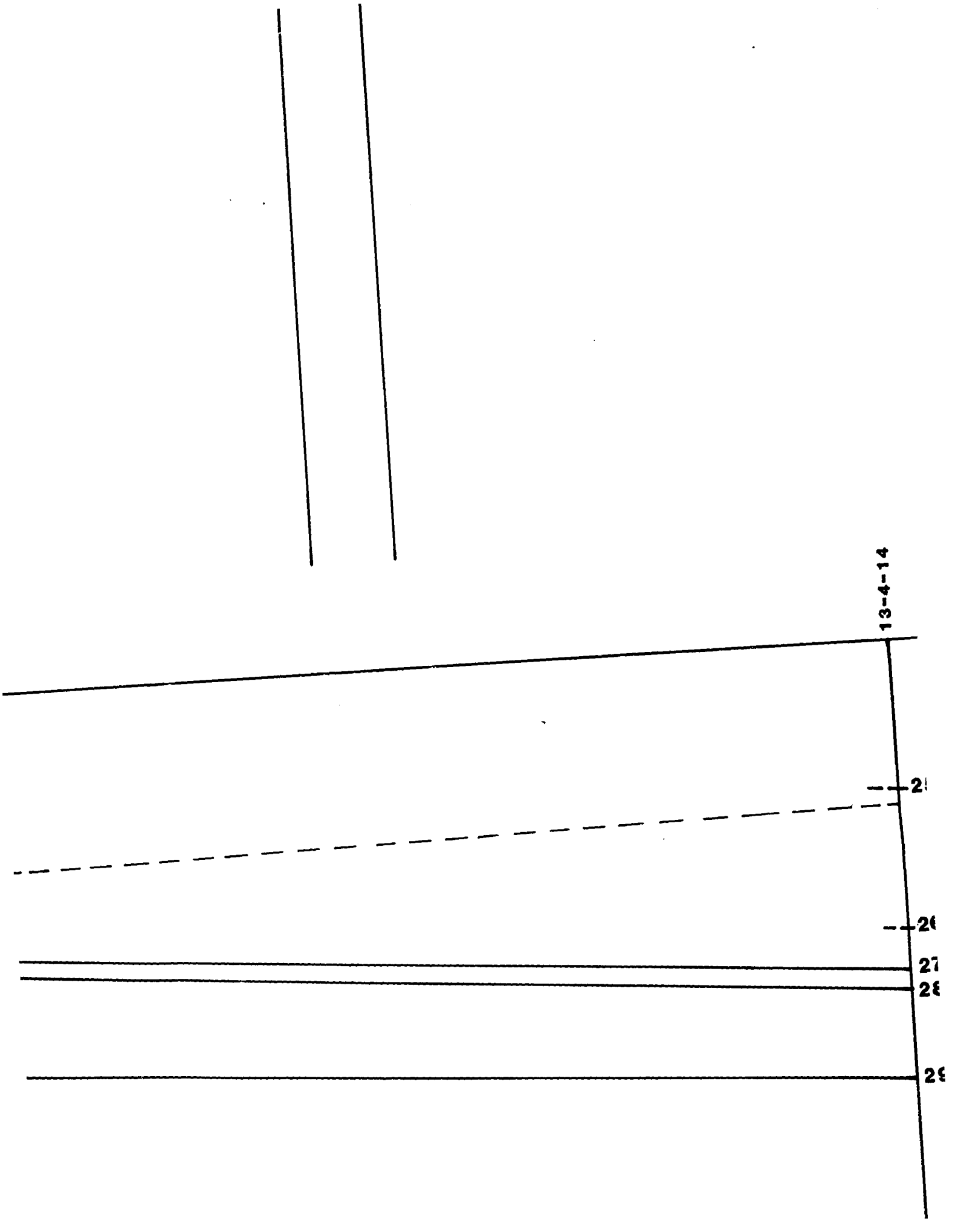

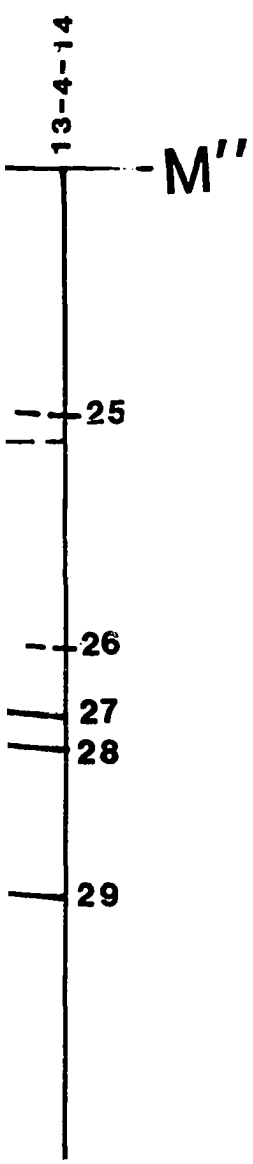

PLATE 9

K'K''-M'M''

CROSS SECTIONS

Showing Hydrate Occurrences and Degree of Hydrate Saturation

Key:

11-12-13 Location

High Concentration

Intermediate

Low Concentration

PLATE 9

K'K''-M'M''

CROSS SECTIONS

Showing Hydrate Occurrences and Degree of Hydrate Saturation

Key:

11-12-13 Location

High Concentration

Intermediate

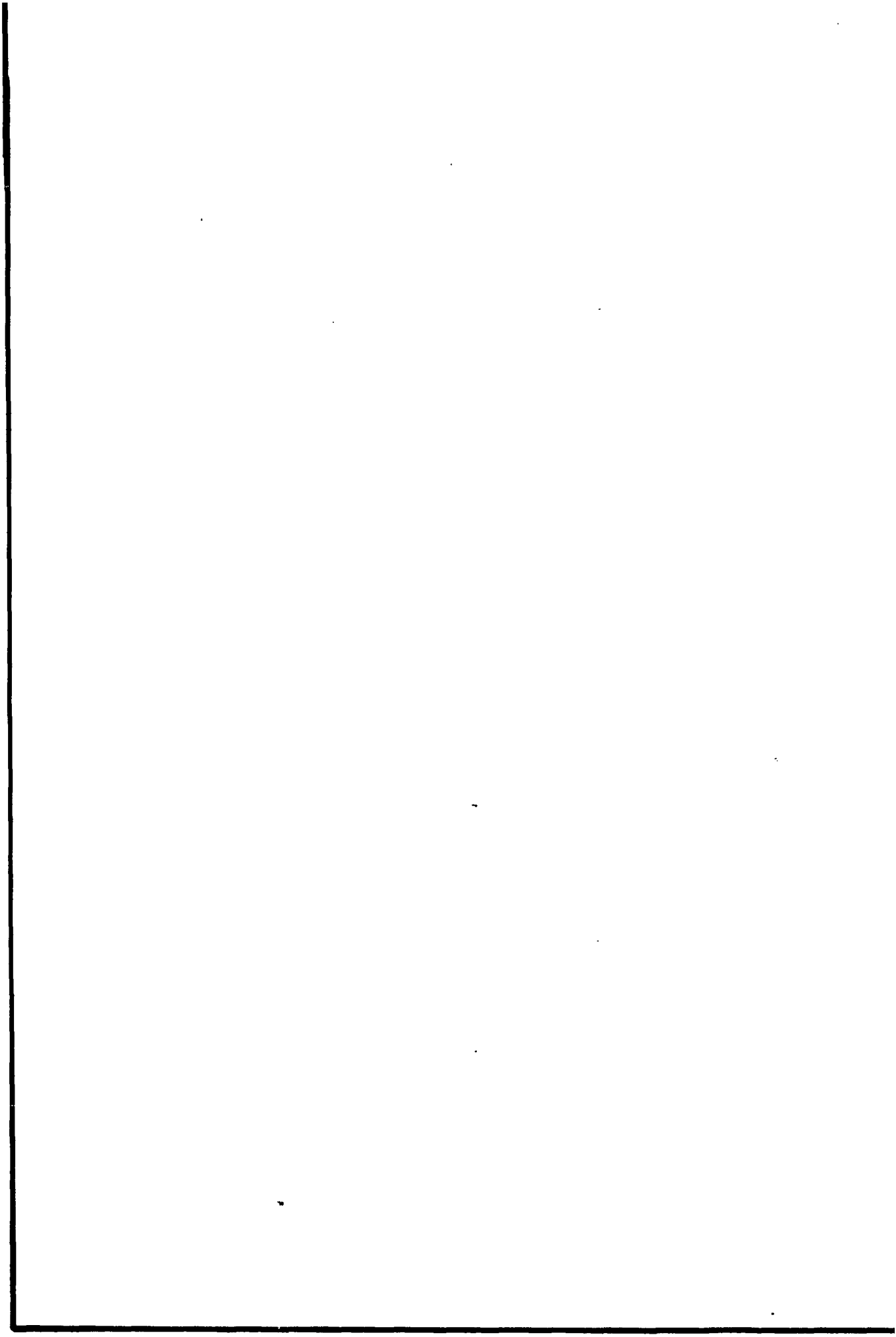

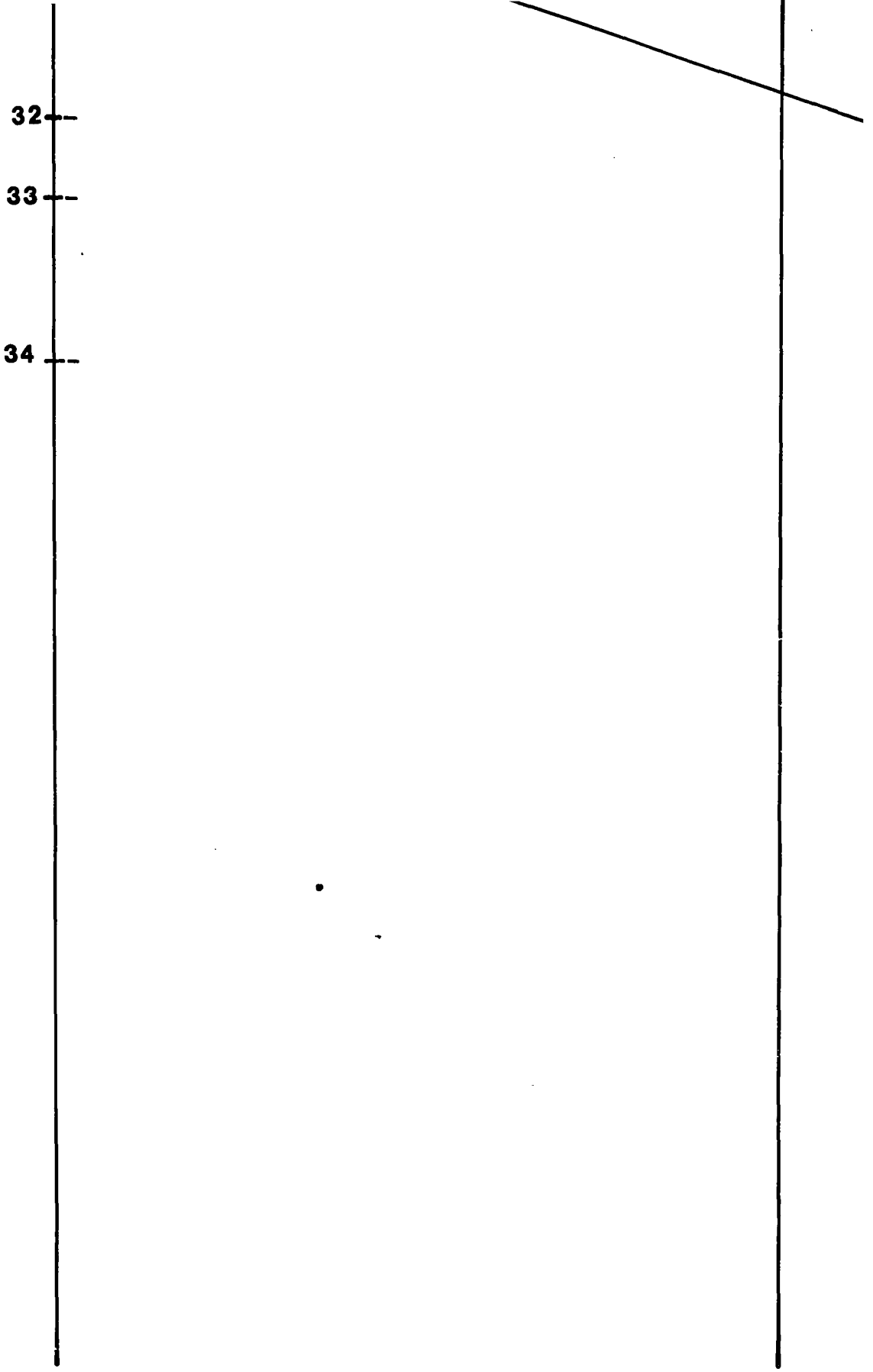

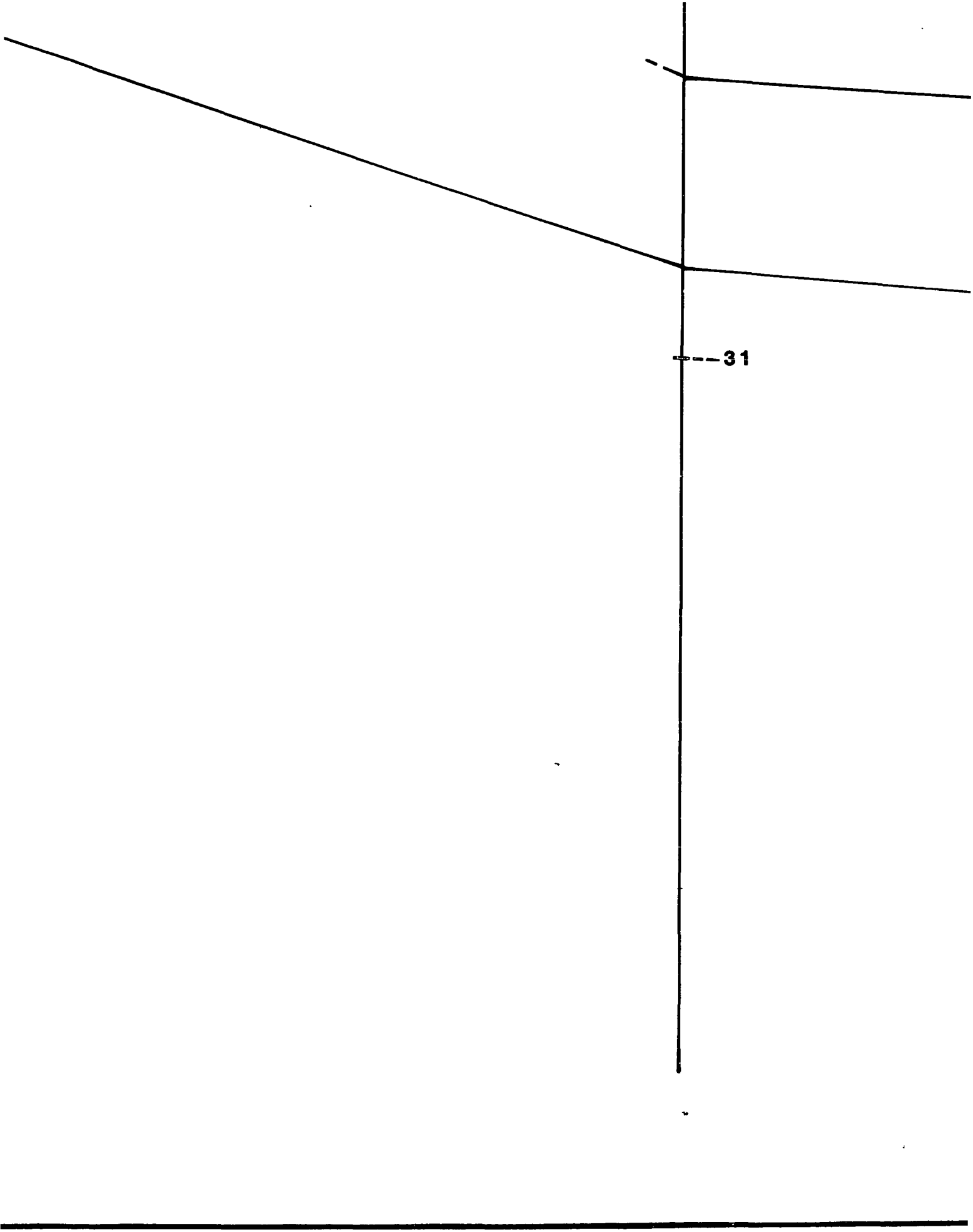

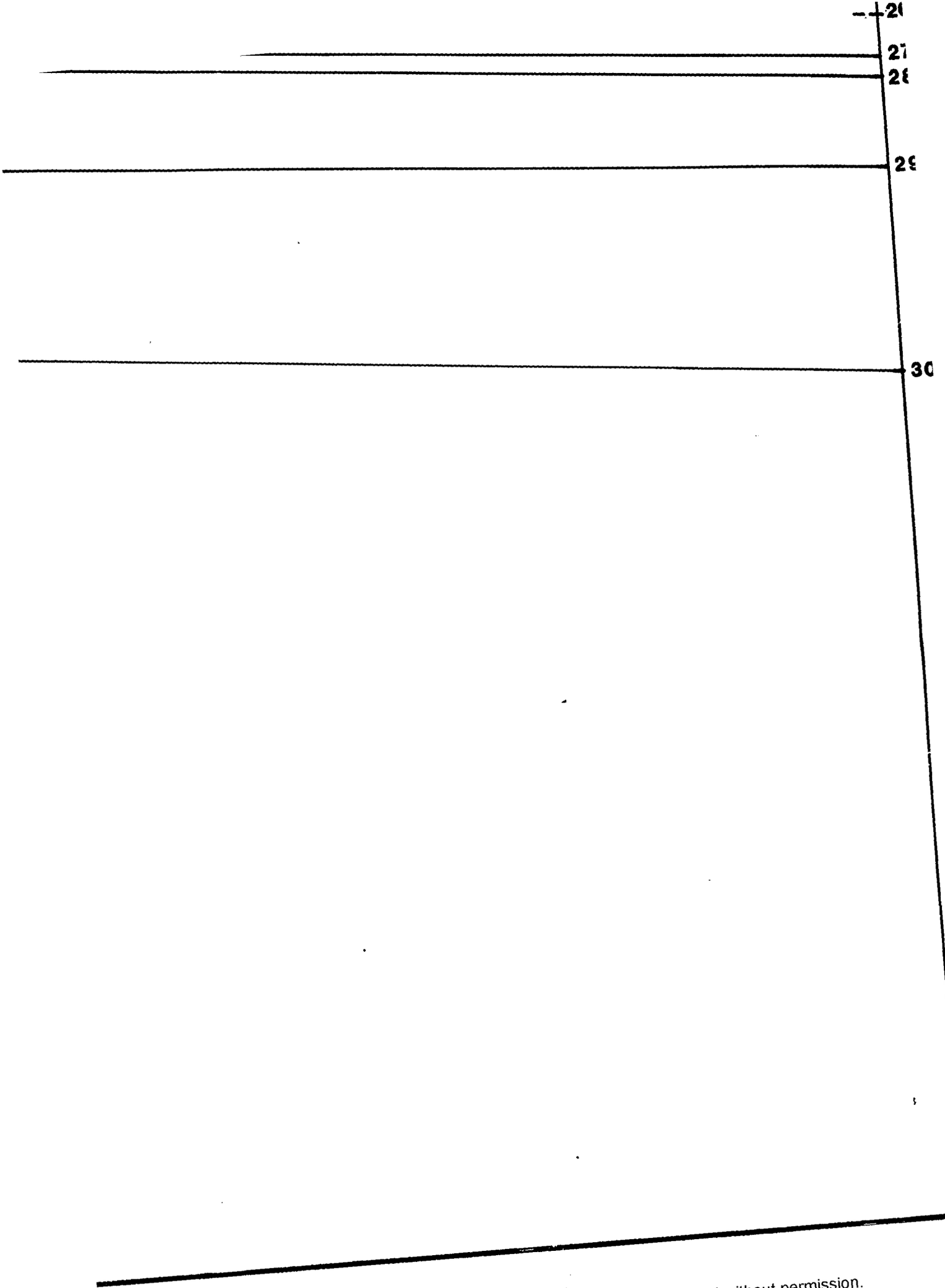

K'K''-M'M''

CROSS SECTIONS

Showing Hydrate Occurrences and Degree of Hydrate Saturation

26

27

28

29

30

Key:

11-12-13 Location

High Concentration

Intermediate

Low Concentration

H 1 Upper Hydrate Stability Boundary

H 2 Lower Hydrate Stability Boundary (with no geothermal-gradient change at BPF)

H3 Lower Hydrate Stability-Boundary (with geothermal gradient-change at BPF)

BPF Base of the Permafrost

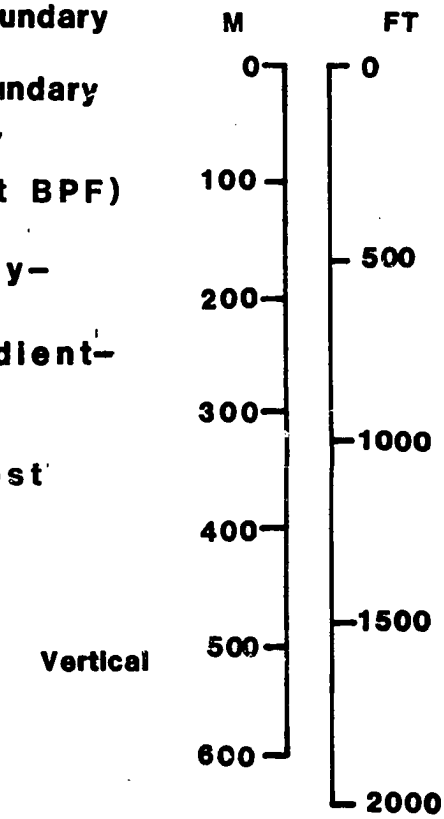

Horizontal

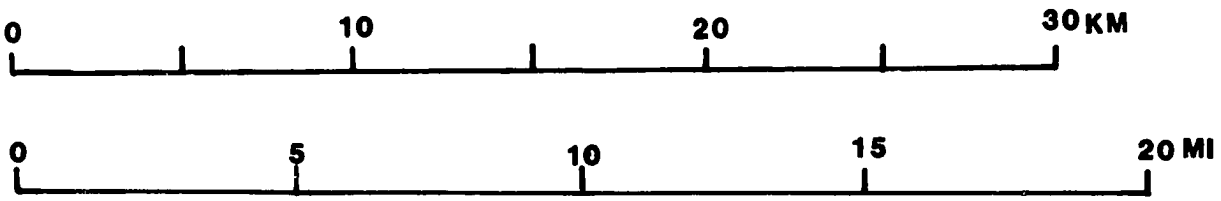

CROSS SECTIONS

Showing Hydrate Occurrences and Degree of Hydrate Saturation

Key:

11-12-13 Location

High Concentration

Intermediate

Low Concentration

H 1 Upper Hydrate Stability Boundary

H 2 Lower Hydrate Stability Boundary (with no geothermal-gradient change at BPF)

H3 Lower Hydrate Stability-Boundary (with geothermal gradient-change at BPF)

BPF Base of the Permafrost

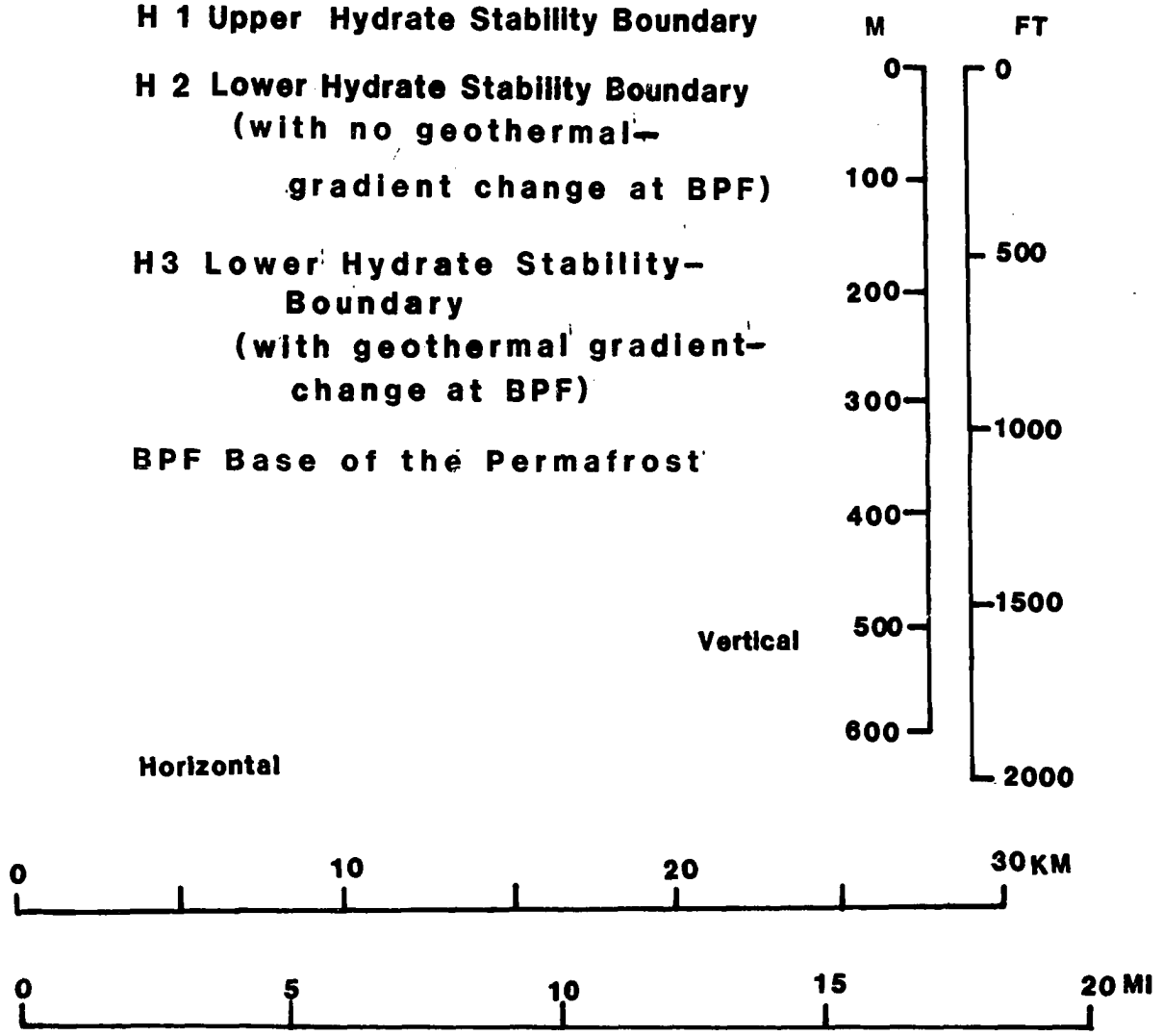

PLATE 9